



Trinity College Dublin
Coláiste na Tríonóide, Baile Átha Cliath
The University of Dublin

**Defining the role of ROR α in the
functionality of distinct immune cell
populations**

A thesis submitted to Trinity College Dublin, University of
Dublin, as requirement for the degree of Doctor in
Philosophy (PhD) in Clinical Medicine

2021

Joseph Roberts B.Sc (Hons) M.Sc

Under the supervision and direction of

**Professor Padraic Fallon &
Dr Emily Hams**

School of Medicine

Declaration of Authorship

This thesis is submitted by the undersigned to the Trinity College Dublin for the examination of a Doctorate in Philosophy. The work herein is entirely my own and has not been submitted as an exercise for a degree in any other university. The library at Trinity College Dublin has my permission to lend or copy this thesis upon request.

Joseph Roberts

Acknowledgments

I would sincerely like to thank my supervisors, Professor Padraic Fallon and Dr Emily Hams, for their continuous support, mentoring and for always intellectually challenging me. Thank you for your creativity, leadership and accessibility. It has been an honour to learn from both of you and this thesis would not have been possible without your expertise, guidance and encouragement. I am forever grateful.

Thank you to all my lab colleagues, past and present, especially Ciara Byrne, Aoife Yeow, Silvia Talavera, Heike Hawerkamp, Anne Chevalier and Keelin O'Shanahan. You have all been a big part of my PhD and made those long lab days enjoyable! This chapter of my life has been greatly enhanced by knowing you all, so for that, we will be friends for life.

I would also like to thank Science Foundation Ireland who financially supported this research, without this support my PhD would not have been possible.

To my family, Mum (Lyn), Dad (Chris), Nanny (Rosemary), Grandad (William), Christopher, Louise and Carolyn and not forgetting my aunt, uncle, cousins, nieces and nephews, you have all been there on this journey with me from afar. You have encouraged and believed in me to fulfil my dream of pursuing a career in science. From day one until now, thank you for your constant support and unconditional love!

To the Hogan family, especially Margaret Hogan, you have made Ireland feel like home. I really appreciate your love and interest in my scientific endeavours.

Finally, thank you to my fiancé, Aisling. I could not have done this without your love and support. In good times and bad times, you were always there for me. You have been the rock by my side for the last 7 years, I look forward to our future!

Summary

Parasitic helminths infect over 1.5 billion people globally and are capable of causing death. Helminth infected individuals also experience signs of malnutrition, anaemia, diarrhoea, cognitive dysfunction, vitamin deficiencies and growth retardation, therefore, they cause a significant problem worldwide. Helminth infections elicit a type 2 immune response characterised by innate (ILC2s, eosinophils and M2 macrophages) and adaptive (Th2) immune cells. However, an uncontrolled type 2 immune response leads to the development of allergic disorders such as asthma, which affects over 300 million people globally. Therefore, a full understanding of a type 2 immune response may provide a therapeutic benefit for helminth infections and allergic disorders. The transcription factor Retinoic acid-related Orphan Receptor (ROR)- α has roles in cerebellar development, metabolism, circadian rhythm and inflammatory responses. ROR α is also required for the cellular development such as Th17 cells and group 2 innate lymphoid cells (ILC2). The identification that ROR α was important for the development of ILC2 cells was discovered using the type 2 inducing helminth *N. brasiliensis*. Recently, there is accumulating evidence for a role of *Rora* in Th2 cells during inflammation. Therefore, the aims of this study were to investigate the role of other ROR α -expressing cells in immune responses to *N. brasiliensis* infection and HDM challenge, with particular focus on the development of lung Th2 cells.

Infecting *Rora*^{sg/sg} mice, which have a natural mutation in the gene encoding *Rora* resulting in a non-functional protein, with *N. brasiliensis* developed an altered type 2 immune response, characterised by a higher worm count in the small intestine and reduced lung ILC2s compared to WT mice. Interestingly, *Rora*^{sg/sg} mice also have a reduced frequency of lung CD4 T cells, GATA3⁺CD4 T (Th2) cells and eosinophils following *N. brasiliensis* infection. To expand on these findings, *Rora*^{sg/sg} mice were used to generate *Rora*^{sg/sg} BM chimera mice to explore the role of *Rora* in cells from hematopoietic versus non-hematopoietic origin. *Rora*^{sg/sg} BM chimera mice had a delayed *N. brasiliensis* expulsion and also had a reduced frequency of lung ILC2s, CD4 T cell, GATA3⁺CD4 T (Th2) cells and eosinophils following *N. brasiliensis* infection. Therefore, indicating that in addition to its known role in ILC2 development, ROR α has a role in Th2 and eosinophil development. Furthermore, generating a *Rora* reporter mouse

allowed for the identification of *Rora* expressing cells by flow cytometry. Notably, following *N. brasiliensis* infection, there was an increase in *Rora* expressing CD4 T cell, GATA3⁺CD4 T (Th2) cells in the lung. There was also an association of *Rora* expressing CD4 T cells with T_{EM}, activation and tissue-resident CD4 T cells in the lungs, indicating a role for ROR α in Th2 cell development and activation following *N. brasiliensis* infection. To expand on these observations, the Cre-Lox recombination technology was used to generate *Rora*^{fl/fl}*CD4Cre* and *Rora*^{fl/fl}*Il7raCre* mice, which have *Rora* deleted from CD4 and *Il7ra* expressing cells, respectively. As previously shown, *Rora*^{fl/fl}*Il7raCre* mice had reduced ILC2s and a delayed worm expulsion, whilst *Rora*^{fl/fl}*CD4Cre* mice had comparable frequency of lung ILC2s and worm expulsion. Interestingly, however, it was also observed that *Rora*^{fl/fl}*CD4Cre* mice had a reduced frequency of lung GATA3⁺CD4 T cells following *N. brasiliensis* infection. Therefore, indicating that *Rora* has a role in GATA3⁺CD4 T cells, independent of ILC2s. To further corroborate the findings generated following *N. brasiliensis* infection, HDM challenge was used as a non-worm immunity model which induces lung inflammation. Notably, both *Rora*^{sg/sg} and *Rora*^{fl/fl}*CD4Cre* mice had reduced frequency of lung GATA3⁺CD4 T cells following HDM challenge. Whilst the *Rora* reporter mice had an increase in frequency of *Rora* expressing GATA3⁺CD4 T cells and activated CD4 T cells following HDM challenge. Furthermore, in support of the *in vivo* results, *in vitro* analysis revealed that naïve CD4 T cells isolated from both *Rora*^{sg/sg} and *Rora*^{fl/fl}*CD4Cre* had reduced ability to polarise towards GATA3⁺CD4 T cells. Therefore, providing further evidence of a role for *Rora* in Th2 cell development.

The findings of the present study identify a role for the transcription factor ROR α in activation and development of Th2 cells during type 2 inflammation. Therefore, this may provide possible therapeutic benefit for targeting *Rora* in helminth infections or allergic disorders such as asthma.

Publications

Hams E, **Roberts J**, Bermingham R and Fallon PG (2021). Functions for Retinoic Acid-Related Orphan Receptor Alpha (ROR α) in the Activation of Macrophages During Lipopolysaccharide-Induced Septic Shock. *Front. Immunol.* 12:647329. doi:10.3389/fimmu.2021.647329

Hams E, **Roberts J**, Bermingham R, Hogan AE, O'Shea D, O'Neill L and Fallon PG (2020). Role for Retinoic Acid-Related Orphan Receptor Alpha (ROR α) Expressing Macrophages in Diet-Induced Obesity. *Front. Immunol.* 11:1966. doi: 10.3389/fimmu.2020.01966

Roberts, J., Fallon, P. & Hams, E. 2019. The pivotal role of macrophages in metabolic distress. In: BHAT, D. K. H. (ed.) *Macrophage at The Crossroads of Innate and Adaptive Immunity*. IntechOpen. DOI: 10.5772/intechopen.86474.

List of abbreviations used

AAM	Alternatively activated macrophage
AD	Atopic dermatitis
AF	Activation function
APC	Antigen presenting cells
APC	Allophycocyanin fluorophore
ASD	Autism spectrum disorder
ATM	Adipose tissue macrophages
BAL	Bronchoalveolar lavage
BCL	B Cell lymphoma
BM	Bone marrow
BMAL	Brain and muscle ARNT-like
BP	Base pair
BSA	Bovine Serum Albumin
CAM	Classically activated macrophage
CD	Cluster of differentiation
CLOCK	Circadian locomotor output cycles kaput
CLP	Common lymphoid progenitor
CMP	Common myeloid progenitor
Cy5/7	CyChrome 5/ CyChrome 7
DAMP	Damage-associated molecular patterns
DBD	DNA binding domain
DC	Dendritic cells
DMSO	Dimethyl sulfoxide
EAE	Experimental autoimmune encephalomyelitis
EDTA	Ethylenediaminetetraacetic acid
ELISA	Enzyme-linked immunosorbent assay
EOMES	Eomesodermin
FACS	Fluorescence-activated cell sorting
FBS	Fetal bovine serum
FITC	Fluorescein isothiocyanate
FMO	Fluorescence minus one

FRT	FLP recognition target
FSC	Forward scatter
GM-CSF	Granulocyte macrophage colony stimulating factor
GMP	Granulocyte/macrophage progenitors
GWAS	Genome-wide association study
HDM	House dust mite
Het	Heterozygous
HFD	High fat diet
Hom	Homozygous
HSC	Haematopoietic stem cell
ICOS	Inducible T cell costimulator
IFN	Interferon
Ig	Immunoglobulin
IL	Interleukin
ILC	Innate lymphoid cell
ILCP	Innate lymphoid cell progenitor.
IRF	Interferon regulatory factor
JAK	Janus kinase
KC	Kupffer cells
KLRG1	Killer-cell lectin like receptor G1
Loxp	Locus of X-over P1
LPS	Lipopolysaccharide
LT	Lymphoid tissue
MACS	Magnetic-activated cell sorting
MC	Mast cell
MEP	Megakaryocyte/erythrocyte progenitors
MFI	Median fluorescence intensity
MHC	Major histocompatibility complex
mLN	Mediastinal lymph nodes
MLN	Mesenteric lymph node
mRNA	Messenger RNA
MW	Molecular weight
N.b	Nippostrongylus brasiliensis

NbES	Nippostrongylus brasiliensis excretory-secretory proteins
NEO	Neomycin
NF	Nuclear factor
NK	Natural killer
NLT	Non-lymphoid tissue
NR	Nuclear receptor
OVA	Ovalbumin
PAMP	Pathogen associated molecular pattern
PBS	Phosphate buffered saline
PCR	Polymerase chain reaction
PD1	Programmed cell death protein-1
PE	Phyoerythrin
PerCP	Peridinin chlorophyll protein
PFA	Paraformaldehyde
PMA	Phorbol myristate acetate
PRR	Pattern recognition receptors
PTSD	Post-traumatic stress disorder
ROR	Retinoic acid receptor-related orphan receptor
RPMI	Roswell Park Memorial Institute medium
RWP	Ragweed pollen
SC	Subcutaneous
SCA	Stem cell antigen
scRT-PCR	Single-cell reverse transcription polymerase chain reaction
SNP	Single nucleotide polymorphisms
SOCS3	Suppressors of cytokine signalling 3
SSC	Side scatter
STAT	Signal transducer and activator of transcription
T _{CM}	Central memory T cells
TCR	T cell receptor
T _{EM}	Effector memory T cells
TF	Transcription factor
TGF	Transforming growth factor
Th	T helper

TLR	Toll-like receptor
T _N	Naïve T cell
TNF	Tumour necrosis factor
Treg	Regulator T cell
T _{RM}	T resident memory
TSLP	Thymic stromal lymphopietin
tSNE	t-distributed stochastic neighbour embedding
VCU	Villus crypt unit
WT	Wild type
YFP	Yellow fluorescent protein

Table of Contents

Declaration of Authorship	i
Acknowledgments	ii
Summary	iii
Publications	v
List of abbreviations used	vi
Chapter 1	2
1.1 The immune system	2
1.2 The hierarchical structure of cells in the murine immune system	2
1.3 The innate immune system	3
1.4 The adaptive immune system	3
1.5 Cells of the immune system	4
1.5.1 Myeloid cells	4
1.5.1.1 Neutrophils	4
1.5.1.2 Monocytes	5
1.5.1.3 Macrophages.....	5
1.5.1.4 Eosinophils	6
1.5.1.5 Dendritic Cells (DC).....	7
1.5.1.6 Mast cells (MC)	7
1.5.1.7 Basophils	8
1.5.2 Lymphoid cells.....	8
1.5.2.1 T lymphocytes	8
1.5.2.1.1 CD4 T (helper) cells.....	9
1.5.2.1.2 Regulatory T cells (Tregs)	11
1.5.2.1.3 Th2 cells.....	11
1.5.2.1.4 CD8 (cytotoxic) T cells.....	13
1.5.2.2 B lymphocytes	13
1.5.2.3 Innate lymphoid cells (ILC).....	14
1.5.2.3.1 Innate lymphoid cells 2 (ILC2).....	14
1.5.2.4 Natural killer (NK) cells	15
1.6 Helminths	16
1.7 The type 2 immune response	17
1.8 Retinoic acid receptor-related orphan receptor alpha (RORα)	20
1.8.1 Nuclear receptors	20
1.8.2 ROR α background and structure	21
1.8.3 Functions of ROR α	22
1.8.4 ROR α mechanism of action	22
1.8.5 <i>Rora</i> natural mutant mouse - <i>Staggerer</i> (<i>Rora</i> ^{sg/sg}) mice.....	23
1.8.6 ROR α expression	25
1.8.7 Sex difference in <i>RORA/Rora</i> expression	28
1.8.8 ROR α endogenous ligands.....	28
1.8.9 ROR α and inflammation	30
1.8.10 ROR α and type 2 immunity.....	31
1.8.11 ROR α and asthma.....	31
1.8.12 ROR α and cancer.....	33
1.8.13 ROR α and the circadian rhythm	34
1.8.14 ROR α in metabolism	36
1.8.15 ROR α in cerebellum development	37
1.8.16 ROR α and neuropsychiatric disorders.....	37
1.8.17 ROR α and cellular development	38

1.8.17.1	ROR α and macrophages	38
1.8.17.2	ROR α and ILC2s cells	39
1.8.17.3	ROR α and ILC3 cells	40
1.8.17.4	ROR α and Th17 Cells	40
1.8.17.5	ROR α and Tregs cells.....	41
1.8.17.6	ROR α and Th2 Cells	41
1.9	Thesis objectives.....	43
2	Chapter 2 Materials and Methods	46
2.1	Mice.....	46
2.1.1	<i>B6.C3(Cg)-Rorasg/J</i> Mice	46
2.1.2	<i>RoraCre</i> mice.....	47
2.1.3	<i>B6.129X1-Gt(ROSA)26Sor^{tm(EYFP)Cos/J}</i> Mice	49
2.1.4	<i>Rora^{fl/fl}</i> Mice.....	50
2.1.5	<i>Tg(Cd4-cre)1Cwi/BfluJ</i> Mice	52
2.1.6	<i>Il7raCre</i> Mice	53
2.1.7	<i>B6.SJL-Ptprc^aPeprc^b/BoyJ</i> Mice	54
2.2	Cre-LoxP system.....	54
2.3	Generation of the <i>Rora</i> reporter mouse.....	55
2.3.1	<i>Rora</i> reporter Mice	55
2.4	Generation of conditional <i>Rora</i> knock-out mice	56
2.4.1	<i>Rora^{fl/fl}CD4Cre</i> Mice	56
2.4.2	<i>Rora^{fl/fl}Il7raCre</i> Mice	57
2.5	Isolation of bone marrow (BM) cells.....	58
2.6	BM Chimera Generation	58
2.7	Genotyping and identification of mouse strains.....	62
2.7.1	Mice Ear Lysis	62
2.7.2	Polymerase Chain Reaction (PCR)	62
2.7.3	Agarose gel electrophoresis	63
2.8	<i>In vivo</i> models.....	63
2.8.1	<i>Nippostrongylus brasiliensis (Nb)</i> lifecycle	63
2.8.2	Lifecycle of <i>N. brasiliensis</i> in the rat	64
2.8.3	<i>N. brasiliensis</i> larvae recovery and counting	66
2.8.4	<i>N. brasiliensis</i> infection of mice	67
2.8.5	Adult (L5) <i>N. brasiliensis</i> counting in murine small intestine	70
2.8.6	<i>N. brasiliensis</i> egg counts in the faeces	71
2.8.7	House dust mite (HDM).....	72
2.9	Murine tissue dissection and processing.....	73
2.9.1	Lung isolation and generation of a single cell suspension	73
2.9.2	Spleen, thymus and mesenteric lymph node (MLN) isolation and single cells suspension	74
2.10	Cell counting	74
2.11	RNA extraction	74
2.12	Complementary DNA (cDNA) synthesis.....	76
2.13	Quantitative PCR (qPCR)	76
2.14	Flow-cytometric staining.....	78
2.14.1	Surface markers staining	78
2.14.2	Intracellular (nuclear) staining	79
2.15	Flow-cytometric analysis.....	81
2.16	Fluorescence activated cell sorting (FACS).....	83

2.17	CD4 ⁺ T cell isolation	84
2.18	Naïve CD4 T cell isolation	85
2.19	<i>In vitro</i> CD4 T cell polarisation.....	86
2.20	Enzyme-linked immunosorbent assay (ELISA)	88
2.20.1	Cytokine ELISA	88
2.20.2	Total IgE ELISA	89
2.21	Whole blood collection and serum isolation	89
2.22	Cell culture stimulation	89
2.23	Histology	90
2.23.1	Tissue fixation	90
2.23.2	Tissue dehydration.....	90
2.23.3	Tissue embedding and sectioning.....	90
2.23.4	Histology staining.....	91
2.23.5	Histology scoring	92
2.24	Statistical analysis	93
3	Chapter 3.....	95
3.1	Introduction.....	95
3.2	Chapter Objectives	96
3.3	Results	97
3.3.1	Determining the role of the transcription factor ROR α in <i>N. brasiliensis</i> infection using <i>Rora</i> ^{sg/sg} mice	97
3.3.1.1	<i>Rora</i> ^{sg/sg} mice have a higher <i>N. brasiliensis</i> count in small intestine at day 7 post-infection, compared to WT mice	97
3.3.1.2	<i>Rora</i> ^{sg/sg} mice have reduced goblet cells in the small intestine compared to WT mice following to <i>N. brasiliensis</i> infection.....	99
3.3.1.3	<i>Rora</i> ^{sg/sg} mice have a reduced frequency of lung ILC2s compared to WT mice in both uninfected condition and following <i>N. brasiliensis</i> infection	101
3.3.1.4	<i>Rora</i> ^{sg/sg} mice have reduced frequency of lung CD4 T cells compared to WT mice following <i>N. brasiliensis</i> infection.....	103
3.3.1.5	<i>Rora</i> ^{sg/sg} mice have a reduced frequency of lung GATA3 ⁺ CD4 T cells compared to WT mice in response to <i>N. brasiliensis</i> infection	105
3.3.1.6	<i>Rora</i> ^{sg/sg} mice have reduced frequency of GATA3 ⁺ CD4 T cell in the mesenteric lymph node (MLN) compared to WT mice following <i>N. brasiliensis</i> infection.....	107
3.3.1.7	<i>Rora</i> ^{sg/sg} mice have a reduced frequency of lung eosinophils in response to <i>N. brasiliensis</i> infection compared to WT mice	109
3.3.2	Determining the role of the transcription factor ROR α in response to <i>N. brasiliensis</i> infection by generating and utilising <i>Rora</i> ^{sg/sg} bone marrow (BM) chimera mice.....	111
3.3.2.1	<i>Rora</i> ^{sg/sg} BM chimera mice have a delayed <i>N. brasiliensis</i> expulsion compared to WT BM chimera mice	112
3.3.2.2	<i>Rora</i> ^{sg/sg} BM chimera mice have a reduced small intestine goblet cells at days 5 and 7 post <i>N. brasiliensis</i> compared to WT BM chimera mice	114
3.3.2.3	<i>Rora</i> ^{sg/sg} BM chimera mice have an altered serum IgE compared to WT BM chimera mice following <i>N. brasiliensis</i> infection.....	116
3.3.2.4	<i>Rora</i> ^{sg/sg} BM chimera mice MLN cells have delayed T cell type 2 cytokine (IL-4, IL-5 and IL-13) secretion following <i>N. brasiliensis</i> infection	118
3.3.2.5	<i>Rora</i> ^{sg/sg} BM chimera mice have increase <i>N. brasiliensis</i> count in primary and secondary <i>N. brasiliensis</i> infection compared to WT BM chimera mice	120
3.3.2.6	<i>Rora</i> ^{sg/sg} BM chimera mice have a reduced frequency of lung ILC2s following <i>N. brasiliensis</i> infection compared to WT BM chimera mice	122
3.3.2.7	<i>Rora</i> ^{sg/sg} BM chimera mice have reduced lung CD4 T cells following <i>N. brasiliensis</i> infection compared to WT BM chimera mice	124
3.3.2.8	<i>Rora</i> ^{sg/sg} BM chimera mice have reduced lung GATA3 ⁺ CD4 T cells following <i>N. brasiliensis</i> infection.....	127

3.3.2.9	<i>Rora</i> ^{sg/sg} BM chimera mice have reduced lung eosinophils following <i>N. brasiliensis</i> infection	130
3.3.3	Determining the <i>in vitro</i> CD4 T cell polarisation of <i>Rora</i> ^{sg/sg} naïve CD4 T cells	132
3.3.3.1	Naïve CD4 T cells isolated from <i>Rora</i> ^{sg/sg} mice have reduced <i>in vitro</i> polarisation towards GATA3 ⁺ and Rorγ ⁺ compared to WT mice naïve CD4 T cells	132
3.4	Discussion	134
4	Chapter 4	142
4.1	Introduction	142
4.2	Chapter Objectives	143
4.3	Results	144
4.3.1	Generation of <i>Rora</i> ^{Cre/Cre} <i>Rosa</i> ^{YFP/YFP} mice	144
4.3.2	<i>Rora</i> ^{Cre/Cre} <i>Rosa</i> ^{YFP/YFP} mice have highest frequency of YFP ⁺ CD45 cells	145
4.3.3	YFP ⁺ expressing CD45 cells are <i>Rora</i> expressing cells	147
4.3.4	ILC2s express <i>Rora</i> -YFP	148
4.3.5	tSNE clustering of <i>Rora</i> -YFP expressing CD45 ⁺ cells	151
4.3.6	<i>Rora</i> -YFP expressing lung CD4 T cells	153
4.3.7	<i>Rora</i> -YFP expressing CD4 T cells express <i>Rora</i> mRNA	155
4.3.8	<i>Rora</i> reporter mice had a comparable type 2 immune response to control mice following <i>N. brasiliensis</i> infection	157
4.3.9	Identification of lung <i>Rora</i> -YFP expressing CD45 ⁺ cells following <i>N. brasiliensis</i> infection	159
4.3.10	Increased expression of transcription factors (<i>Gata3</i> , <i>Foxp3</i> and <i>Rora</i>) in CD4 T cells following <i>N. brasiliensis</i> infection	161
4.3.11	Increase in <i>Rora</i> -expressing lung CD4 T cells following <i>N. brasiliensis</i> infection	162
4.3.12	Increase in frequency of lung <i>Rora</i> -expressing GATA3 ⁺ CD4 T cells following <i>N. brasiliensis</i> infection	164
4.3.13	<i>Rora</i> is expressed by activated CD4 T cells	167
4.3.14	<i>Rora</i> is associated with lung effector memory CD4 T (T _{EM}) cells	169
4.3.15	Increase in <i>Rora</i> expressing CD69 ⁺ and CD103 ⁺ CD4 T cells following <i>N. brasiliensis</i> infection	171
4.3.16	Increase in frequency of <i>Rora</i> expressing CD4 T cells in the lung compared to MLN following <i>N. brasiliensis</i> infection	173
4.4	Discussion	174
5	Chapter 5	180
5.1	Introduction	180
5.2	Objectives	182
5.3	Results	183
5.3.1	<i>Rora</i> ^{fl/fl} <i>Il7ra</i> ^{Cre} mice have delayed <i>N. brasiliensis</i> expulsion	183
5.3.2	<i>Rora</i> ^{fl/fl} <i>CD4</i> ^{Cre} and <i>Rora</i> ^{fl/fl} <i>Il7ra</i> ^{Cre} mice had comparable small intestine goblet cells in uninfected and following <i>N. brasiliensis</i> infection	184
5.3.3	<i>Rora</i> ^{fl/fl} <i>Il7ra</i> ^{Cre} mice have reduced lung ILC2 cells, whilst <i>Rora</i> ^{fl/fl} <i>CD4</i> ^{Cre} mice have comparable frequency of lung ILC2s to WT mice	186
5.3.4	Identification of <i>Rora</i> expressing <i>Il7ra</i> (CD127) CD4 T cells and ILC2 populations	187
5.3.5	<i>Rora</i> ^{fl/fl} <i>CD4</i> ^{Cre} and <i>Rora</i> ^{fl/fl} <i>Il7ra</i> ^{Cre} mice have a reduced frequency of lung CD4 T cells compared to WT mice following <i>N. brasiliensis</i> infection	190
5.3.6	<i>Rora</i> ^{fl/fl} <i>CD4</i> ^{Cre} and <i>Rora</i> ^{fl/fl} <i>Il7ra</i> ^{Cre} mice have a reduced frequency of lung GATA3 ⁺ CD4 T cells compared to WT mice following <i>N. brasiliensis</i> infection	191
5.3.7	<i>Rora</i> ^{fl/fl} <i>CD4</i> ^{Cre} mice had comparable frequency of CD4 T cells in the whole blood with WT mice	193
5.3.8	<i>Rora</i> ^{fl/fl} <i>CD4</i> ^{Cre} mice have reduced frequency of lung GATA3 ⁺ CD4 T cells compared to <i>Rora</i> ^{fl/fl} mice in response to <i>N. brasiliensis</i> infection	195
5.3.9	<i>Rora</i> ^{fl/fl} <i>CD4</i> ^{Cre} mice have a reduced frequency of proliferating (Ki67 ⁺) lung GATA3 ⁺ CD4 T cells following <i>N. brasiliensis</i> infection compared to WT mice	197

5.3.10	<i>Rora^{fl/fl}CD4Cre</i> mice have reduced frequency of MLN GATA3 ⁺ CD4 T cells compared to <i>Rora^{fl/fl}</i> mice following <i>N. brasiliensis</i> infection	199
5.3.11	Naïve CD4 T cells isolated from <i>Rora^{fl/fl}CD4Cre</i> have reduced <i>in vitro</i> GATA3 ⁺ CD4 T cell polarisation compared to <i>Rora^{fl/fl}</i> naïve CD4 T cells	201
5.3.12	<i>Rora^{fl/fl}Il7raCre</i> mice have reduced frequency of lung eosinophils, whilst <i>Rora^{fl/fl}CD4Cre</i> mice had comparable lung eosinophils with WT mice following <i>N. brasiliensis</i> infection	203
5.3.13	WT, <i>Rora^{fl/fl}Il7raCre</i> and <i>Rora^{fl/fl}CD4Cre</i> mice had comparable frequency of lung M2 macrophages in uninfected mice and following <i>N. brasiliensis</i> infection	206
5.3.14	WT, <i>Rora^{fl/fl}Il7raCre</i> and <i>Rora^{fl/fl}CD4Cre</i> mice had comparable frequency of lung neutrophils in uninfected conditions and following <i>N. brasiliensis</i> infection	208
5.3.15	<i>Rora^{fl/fl}CD4Cre</i> mice had comparable serum IgE with <i>Rora^{fl/fl}</i> mice	209
5.4	Discussion	211
6	Chapter 6.....	216
6.1	Introduction.....	216
6.2	Chapter Objectives	217
6.3	Results.....	218
6.3.1	Determining the role of the transcription factor ROR α in lung immune cells in the HDM mouse model using <i>Rora^{sg/sg}</i> mice	218
6.3.1.1	<i>Rora^{sg/sg}</i> mice have a reduced frequency of lung GATA3 ⁺ and Ror γ ⁺ CD4 T cells in response to HDM challenge compared to WT mice	218
6.3.1.2	<i>Rora^{sg/sg}</i> mice have reduced frequency of lung eosinophils in response to HDM challenge compared to WT mice	220
6.3.2	Determining the role of the transcription factor ROR α in the lung immune cells in the HDM mouse model using <i>Rora</i> reporter mice.....	222
6.3.2.1	Increase in <i>Rora</i> expressing lung CD4 T cells following HDM	222
6.3.2.2	Increase in <i>Rora</i> expressing lung GATA3 ⁺ and Foxp3 ⁺ CD4 T cells following HDM challenge	223
6.3.2.3	<i>Rora</i> expressing lung CD4 T cells are associated T _{EM} CD4 T cells	226
6.3.2.4	Increase in <i>Rora</i> expressing CD69 ⁺ and CD103 ⁺ CD4 T cells in the lungs following HDM challenge.....	228
6.3.3	Determining the role of the transcription factor ROR α in lung immune cells in the HDM mouse model using <i>Rora</i> conditional deleter mice	230
6.3.3.1	<i>Rora^{fl/fl}CD4Cre</i> and <i>Rora^{fl/fl}Il7raCre</i> mice have reduced lung CD4 ⁺ T cell subsets compared to WT mice in response to HDM challenge	230
6.3.3.2	<i>Rora^{fl/fl}Il7raCre</i> mice have reduced lung eosinophils in response to HDM challenge	232
6.4	Discussion	234
7	Discussion and future directions.....	238
	Appendices	253
7.1	Appendix I	253
7.2	Appendix II.....	254
7.3	Appendix III	256
7.4	Appendix IV	257
8	References	259

Chapter 1

Introduction

Chapter 1

1.1 The immune system

The immune system is a highly specialised, adaptive, and sensitive system that comprises of a network of organs, cells, and cell products, that work in synchronicity to maintain homeostasis. The immune system provides a defence mechanism against infectious agents such as helminths, bacteria, viruses, fungus, protozoans and infected or malignant cells. However, an uncontrolled immune response may result in an excessive inflammatory response leading to autoimmunity or atopic diseases, such as asthma. Whilst an excessive anti-inflammatory response may allow tumour evasion of the immune system and promote its progression. Therefore, the immune system is in a delicate balance maintaining homeostasis.

1.2 The hierarchical structure of cells in the murine immune system

All circulating immune cells of the immune system originate from bone marrow (BM) and differentiate from pluripotent hematopoietic stem cells (HSC). HSCs differentiate into one of two progenitor cells, the common lymphoid progenitor (CLP) or the common myeloid progenitor (CMP). The CLPs cells give rise to the T lymphocytes, B lymphocytes, natural killer cells (NK cells) and innate lymphoid cells (ILC). Whilst the CMPs differentiate into megakaryocyte/erythrocyte progenitors (MEP) and granulocyte/macrophage progenitors (GMP). MEPs then differentiate into either megakaryocyte or proerythroblasts which gives rise to platelets and erythrocytes, respectively. Whilst GMPs give rise to neutrophils, eosinophils, basophils, dendritic cells, mast cells and monocytes/macrophages (**Figure 1.1**) (Seita and Weissman, 2010). These cells make up the immune system and can be broadly categorised into two systems, the innate (**Section 1.3**) and the adaptive (**Section 1.4**) immune system.

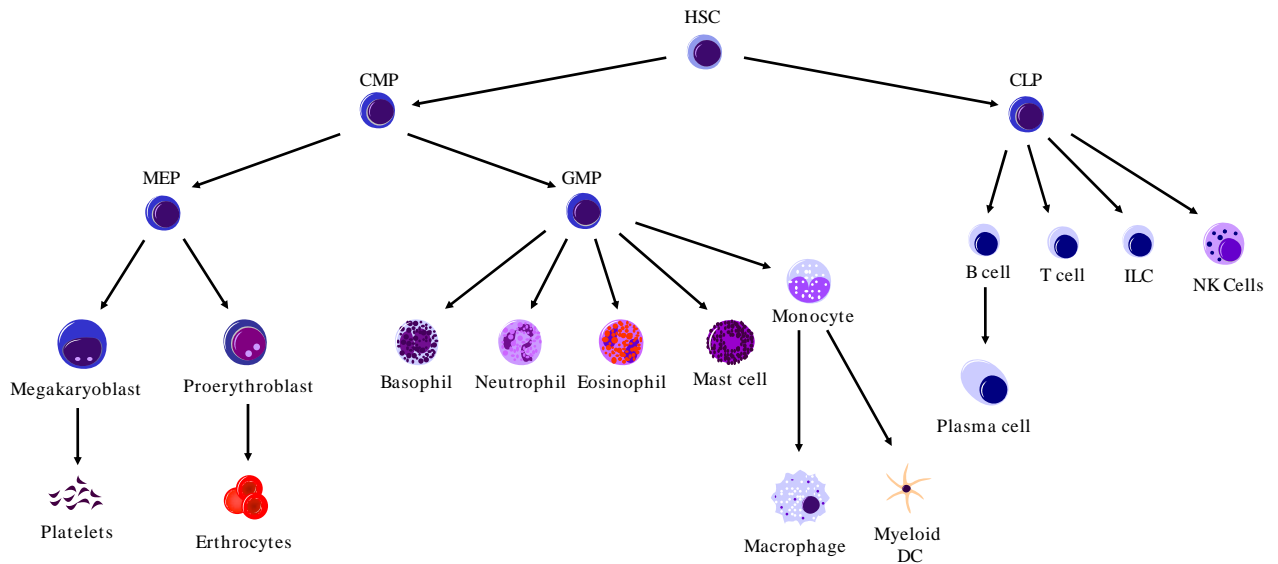


Figure 1.1: Hierarchical structure of mouse haematopoietic system.

1.3 The innate immune system

The innate immune system is the first line of immunological defence and comprises of both cells that rapidly respond to pathogens without prior exposure to the antigen, and barriers to prevent pathogen entry such as physical, chemical and microbiological. Innate immunity is non-specific and relatively short lived, with no long-term immunological memory. The innate immune system recognises pathogen associated molecular patterns (PAMPs) and damage associated molecular patterns (DAMPs), through pattern recognition receptors (PRRs) on cells, which triggers downstream signalling pathways leading to an immune response. The innate immune response consists of both cellular and humoral components. The main cells of the innate immune system are innate lymphoid cells (ILCs), neutrophils, eosinophils, basophils, mast cells, monocytes, macrophages, dendritic cells (DCs) and natural killer (NK) cells (**Section 1.5**). Whilst the humoral innate immune system consists of complement proteins, C-reactive proteins, coagulation factors and natural antibodies.

1.4 The adaptive immune system

The adaptive immune system refers to a pathogen-specific immune response. In contrast to the innate immune system, the adaptive immune system is specific and relies on unique

antigen specificity mediated by T and B lymphocytes (**Section 1.5**). The adaptive immune system relies on pathogens being captured and presented by antigen presenting cells (APCs), such as dendritic cells and macrophages. These APCs migrate to lymphoid tissues and present the digested antigens on major histocompatibility complex (MHC) molecules on the surface of the APCs to T cells, resulting in lymphocyte activation and clonal expansion. B cells make antibodies as both membrane bound receptors and secreted molecules that can recognise antigens. As the adaptive immune response relies on APCs, it takes several days to mount an effective response on primary infection. However, a defining feature of the adaptive immune system is immunological memory. This improves the immunological response upon encounter of the same pathogen. The adaptive immune response can be categorised into two compartments, the cell-mediated immune response, which is governed by T lymphocytes, and the humoral response, which is mediated by B lymphocytes against antigens outside the cells in the blood and body fluid.

1.5 Cells of the immune system

1.5.1 Myeloid cells

1.5.1.1 Neutrophils

Neutrophils are granulocytes that form part of the innate immune system. They are the most abundant immune cell (50-70% circulating leukocytes) with $\sim 10^7$ and $\sim 10^{11}$ produced in the bone marrow each day in mice and humans, respectively (Ng et al., 2019). Neutrophils can be identified by their lobulated nucleus and by expression of the surface markers cluster of differentiation (CD)11b and Ly6G (Misharin et al., 2013). During inflammation, neutrophils are one of the first immune cells to respond, and are recruited following secretion of Interleukin (IL)-1 β , IL-6, IL-8 and Tumour Necrosis Factor (TNF)- α by tissue resident cells (Rosales, 2018). Neutrophils play a key role in the elimination of pathogens and once at the site of infection, neutrophils drive inflammation by recruitment of granulocytes, monocytes and T cells. Neutrophils have a short half-life of between 6-8 hours, but have the ability to damage healthy tissues, which occurs in inflammatory diseases such as rheumatoid arthritis, inflammatory bowel disease and

acute respiratory distress syndrome (Summers et al., 2010). Neutrophils have several mechanisms of actions, such as degranulation, phagocytosis and the generation of neutrophil extracellular traps (NETs). During helminth, infections neutrophils have been reported to kill the rodent hookworm *Nippostrongylus brasiliensis* in the lungs (Sutherland et al., 2014). However, neutrophilic inflammation leads to haemorrhage and acute lung injury (Allen and Sutherland, 2014). Therefore, the activation and recruitment of neutrophils needs to be tightly controlled.

1.5.1.2 Monocytes

Monocytes are myeloid cells that account for 5-7% of circulating leukocytes and have the ability to phagocytose, act as APCs, and secrete cytokines and chemokines in response to infection or injury. Once circulating monocytes are recruited into tissue they differentiate into macrophages or dendritic cells. Human monocytes can be defined by the expression of the CD14 and CD16, whilst murine monocytes can be identified by their expression of Ly6C and chemokine receptors CCR2 and CX3CR1 (Kawamura and Ohteki, 2018). Resident and circulating monocytes are derived from different origins, either from an embryonic precursor and maintained by self-proliferation and renewal (Yona et al., 2013, Hashimoto et al., 2013, Sieweke and Allen, 2013), or from circulating monocytes that can infiltrate the tissue, where they differentiate to an inflammatory or anti-inflammatory phenotype dependent upon the local cytokine and mediator milieu they are exposed to (Auffray et al., 2009).

1.5.1.3 Macrophages

Macrophages are innate immune cells that are extremely heterogenic in function and phenotype. They can phagocytose invading microorganisms and apoptotic cells, secrete cytokines and chemokines to recruit other immune cells, and act as APCs. Macrophages have historically been characterized into two phenotypes; M1 and M2. M1 macrophages are often defined as ‘classically activated’ and are generally pro-inflammatory in function, with a vital role in eliminating pathogens and virus-infected cells. M1 macrophages are activated by signals associated with infection such as Interferon (IFN)- γ as well as bacterial-derived products such lipopolysaccharide (LPS) and free fatty acids

(FFA). M1 macrophages can be identified by surface expression of F4/80 and CD11c with high levels of MHC-II, CD68, CD80 and CD86 costimulatory molecules in addition to release of TNF- α and inducible nitric oxide synthase (iNOS) (Galvan-Pena and O'Neill, 2014). Whereas, M2 macrophages, also termed 'alternatively activated macrophages' (AAM), are anti-inflammatory in function and promote tissue repair and wound healing (Roberts et al., 2019). These macrophages have important roles in response to type 2 immune response to helminth infections. M2 macrophages are activated by type 2 cytokines (IL-4 and IL-13) as well as by parasitic products (Roberts et al., 2019). M2 macrophages can be identified by expression of F4/80 and CD206. They also express genes encoding anti-inflammatory proteins such as *Chil3*, *Arg1* and *Il10* in mice (Lumeng et al., 2008).

1.5.1.4 Eosinophils

Eosinophils are granulocytes that are effector cells in a type 2 immune response, and provide protection against helminths, bacteria and viruses. However, uncontrolled inflammation and activation of eosinophils plays a significant role in diseases such as asthma (Rosenberg et al., 2013). In the steady state, eosinophils account for less than 5% circulating leukocytes and can be identified by their bilobed nuclei and large granules. In humans, eosinophils can be identified by surface markers IL-5R α , CC-chemokine receptor 3 (CCR3) and Siglec-8. Whilst in mice, eosinophils can be identified by expression of SiglecF, F4/80 and CD11b (Misharin et al., 2013). Eosinophil granules contain proteins such as eosinophil peroxidase, major basic protein, ribonucleases eosinophil cationic protein and eosinophil-derived neurotoxin, cytokines and growth factors. Mature eosinophils are released into the peripheral blood where they reside in tissues and have a relatively short half-life (approximately 18 hrs) (Steinbach et al., 1979). However, during inflammation, the function of eosinophils is to kill pathogens and secrete pro-inflammatory cytokines. IL-5 is a key cytokine involved in eosinophil activation, recruitment and survival. Th2 cells, ILC2s and to a lesser extent NK cells, NKT cells, mast cells and eosinophils are known to secrete IL-5 (Rosenberg et al., 2013). In addition, IL-4 and IL-13 along with chemoattractants eotaxins 1 (CCL11), 2 (CCL24) and 3 (CCL26) work in synchronicity with IL-5 to promote eosinophil activation and recruitment (Rosenberg et al., 2013).

1.5.1.5 Dendritic Cells (DC)

Dendritic cells (DCs) are professional APCs that provide the link between the innate and adaptive immune response. DCs are found in most tissues throughout the body and capture, process and present antigens to lymphocytes in secondary lymphoid organs. Murine DCs can be myeloid or lymphoid derived and are identified by expression of CD103 and CD24 (Misharin et al., 2013). DCs induce naïve CD4 T cell activation and differentiation into effector CD4 T cells via three signals. Signal 1 occurs through the antigen specific stimulation of T-cell receptor (TCR) via MHC class II on the DCs. Signal 2 comprises of an interaction between costimulatory molecules such as CD80 and CD86 on the DCs with ligands on T cells CD28, CD40L and CTLA4 (Chen and Flies, 2013). Whilst signal 3 is directed by cytokines secreted from DCs such as IL-2 (Kapsenberg, 2003, Na et al., 2016).

1.5.1.6 Mast cells (MC)

Mast cells (MCs) are immune cells associated with a type 2 immune response and are involved with the defence against bacteria and parasites, such as helminths. However, uncontrolled activation of MCs contributes to several allergic disorders, such as asthma (Otsuka and Kabashima, 2015). MCs cytoplasm is highly granular containing vast amounts of inflammatory mediators such as histamine, cytokines, growth factors and proteases, which are released upon activation and degranulation. MCs are long-lived cells and known to survive for months or years in the tissue, and are abundant in tissues close to the external milieu such as lung, gut and skin (Amin, 2012). The cytokine IL-9 is important for MC maturation and is secreted by CD4 T cells, ILC2s and MCs. They can be identified by expression of CD117, and are activated by an antibody binding to a cell surface receptor on the surface of the MC, such as Immunoglobulin (Ig)E binding to FcεRI (Schwartz et al., 2014).

1.5.1.7 Basophils

Basophils are the rarest granulocyte immune cell (<1% peripheral blood leukocytes) and are associated with a type 2 immune response. Basophils migrate to tissues in response to parasitic infections, however, they also release allergy-related chemical mediators such as histamine upon activation. Basophils drive pro-inflammatory responses by recruiting effector cells such as ILC2s, Th2 cells, eosinophils and macrophages to the inflammatory site (Schwartz et al., 2016). Basophils can be identified by their surface expression of CD49b and CD200R3 and share similar properties with MCs including expression of FcεRI, a high-affinity IgE surface receptor (Dvorak et al., 1982, Schwartz et al., 2014).

1.5.2 Lymphoid cells

1.5.2.1 T lymphocytes

T lymphocytes are derived from HSCs in the BM and migrate to the thymus to complete maturation. The common lymphoid progenitor cells entering the thymus do not express CD4 or CD8 co-receptors and are termed double negative (DN) lymphocytes. Following activation, the DN cells express recombination-activating gene 1 (RAG1). The TCRβ chain is rearranged and paired with the pre-Tα resulting in expression of TCR. The DN lymphocytes then express CD8 followed by CD4 co-receptors and are termed double positive (DP) thymocytes (Godfrey and Zlotnik, 1993). The TCRα chain on the DP thymocyte is rearranged to generate αβ TCR. These DP thymocytes develop into naïve T cells depending on their ability to bind with MHC-I or MHC-II molecules associated with self-peptides (positive selection). Based on interaction with MHC-I or MHC-II, the DP thymocytes differentiate into single-positive (SP) CD8 or CD4 T cells, respectively, by silencing the transcription of the other co-receptor. T cells expressing TCR with negligible affinity for MHC undergo apoptosis, whilst those with very high affinity against self-peptides are destroyed through a process of negative selection. Therefore, T cells with TCR of intermediate affinity are positively selected (Germain, 2002, Luckheeram et al., 2012). CD4 T cells are central in orchestrating adaptive immune responses, whilst CD8 T cells are important for immune defence against intracellular pathogens such as viruses, bacteria and tumours.

1.5.2.1.1 CD4 T (helper) cells

CD4 T helper cells are essential in orchestrating an adaptive immune response. Pioneering research by Mosmann et al. (1986) led to the identification of two distinct murine CD4 T helper (Th) cells, termed Th1 and Th2 cells. Th1 cells were identified to be important in host defence against intracellular viral and bacterial pathogens and are classified by the production of IFN- γ and IL-2. Th1 cell development is dependent on IL-12 which enhances STAT4 and the master regulator T-box transcription factor TBX21 (T-bet) expression (**Figure 1.2**). Whilst Th2 cells direct an immune response against invading parasites. Th2 cell development is dependent on the transcription factor GATA3 and IL-4 cytokine and they secrete IL-4, IL-5 and IL-13 (**Figure 1.2**). In the 2000s, a new CD4 T cell subset was discovered as an IL-17 cytokine secreting cell, and was termed Th17 cells (Ivanov et al., 2006). These cells were identified to have an important role in immunity against extracellular pathogens such as bacteria and fungi. Th17 cells differentiate from naïve CD4 T cells (Th0) cells in the presence of IL-6 and Transforming Growth Factor (TGF)- β and secrete IL-17A, IL-17F, IL-21 and IL-22 (Ivanov et al., 2006). Whilst the Th17 master transcription factors are Retinoic acid receptor-related Orphan Receptor (ROR) γ t and ROR α (**Figure 1.2**) (Ivanov et al., 2006, Yang et al., 2008).

Three further CD4 T cell subsets have been identified, Th9, Th22 and Tfh (**Figure 1.2**). Th9 cells are involved in the protection against parasitic worms, but also are involved in allergic inflammation, autoimmune inflammation and anti-tumour immunity (Kaplan, 2013). Th9 cells secrete IL-9, IL-10 and IL-21 and differentiate from naïve T (Th0) cells in the presence of TGF- β and IL-4 and require transcription factors Signal Transducer and Activator of Transcription (STAT)6, PU.1, Interferon Regulatory Factor (IRF)4 and GATA3 for function. Th22 cells are involved in mucosal immunity, prevention of microbial translocation across epithelial surfaces and promote wound healing. They are associated with various infections, autoimmune diseases, tumours, hepatitis, pancreatitis and rheumatoid arthritis (Jia and Wu, 2014). Th22 are identified as IL-22 secreting cells that require the transcription factor aryl hydrocarbon receptor (AHR) for cell differentiation (Trifari et al., 2009, Jia and Wu, 2014). Follicular Th (Tfh) cells provide assistance to B cell function within the germinal centre. Tfh promote B cell affinity

maturation, class switch recombination, and plasma and memory B cell generation (Liu et al., 2013). Whilst Tfh cell differentiation is regulated by transcription factors B Cell Lymphoma (BCL)6, IRF4, c-MAF, Batf and STAT3/5 (Liu et al., 2013).

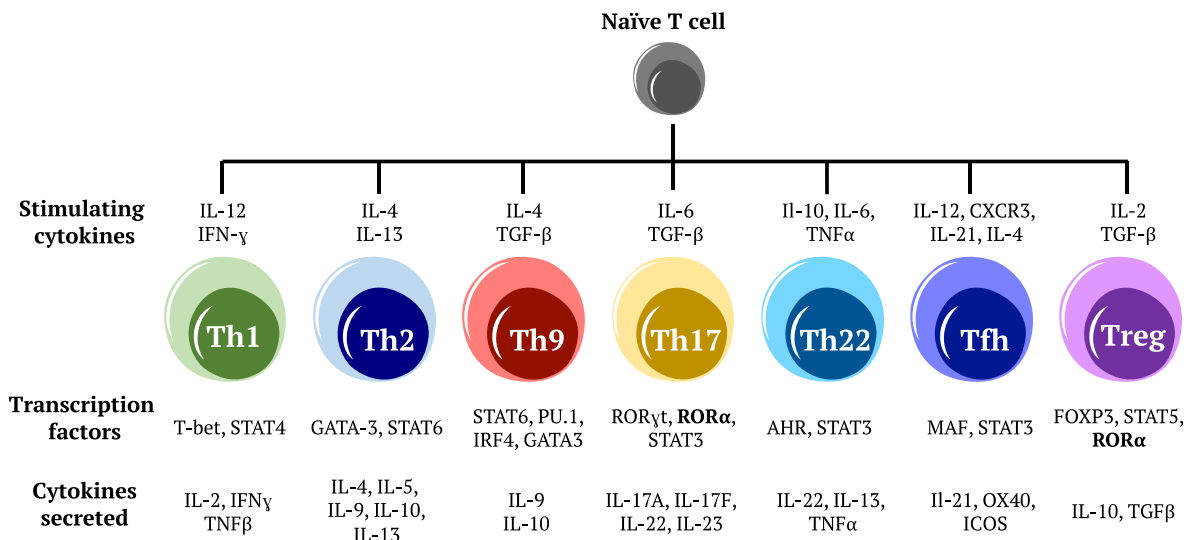


Figure 1.2: T helper cell subsets.

There is an increasing understanding that defining Th cell subsets may be too simplistic and that Th cells are heterogenous cell populations. Early studies on Th cell differentiation relied on *in vitro* experiments, which may not reflect the complex microenvironment *in vivo*. Therefore, lineage specifying transcription factors are frequently co-expressed, with Th cells being able to de-differentiate in the appropriate environment (O'Shea and Paul, 2010). Indeed, GATA3 is critical to Th2 and ILC2 development, and is also expressed by a subset of Tregs (Foxp3⁺) cells (Wohlfert et al., 2011, Halim et al., 2018).

Furthermore, Th cells can be characterised based on T cell memory, effector and tissue residency. Naïve and effector/memory T cells can be identified based on expression of CD44 and CD62L. Naïve T (T_N) cells are defined as CD44⁻CD62L⁺, whilst T central memory (T_{CM}) cells (CD44⁺CD62L⁺) are involved with migration to and within lymph nodes. T_{CM} require further differentiation signals to secrete cytokines. T effector memory (T_{EM}) cells (CD44⁺CD62L⁻) are found in peripheral organs (lung), spleen and blood, and are able to rapidly respond to pathogens (Sckisel et al., 2017). T cells that reside at the site of infection in peripheral organs, are known as T resident memory (T_{RM}) cells. T_{RM}

cells express CD69, a marker for cell activation and antagonizes the SIPR1 receptor, which promotes the exit of T cells from tissue sites. T_{RM} cells CD103 promotes interactions between T_{RM} cell and local epithelial cells, resulting in tissue retention of T cells (Ogongo et al., 2019). With the rapid improvement in modern technologies such as Cre-LoxP genetic manipulation, advances in flow cytometry and single-cell RNA sequencing, this will be important for discoveries in CD4 T cell identification, development and regulation.

1.5.2.1.2 Regulatory T cells (Tregs)

Regulatory T cells (Tregs) are immune cells that act to suppress the immune response and are important for their anti-inflammatory role and maintaining homeostasis. Tregs secrete immunosuppressive cytokines (IL-10, TGF- β and IL-35) and can kill autoreactive T cells and APC through granzyme B/perforin. Tregs compete for IL-2, which is required for T cell clonal expansion, and therefore, Tregs reduce T cell clonal expansion. Tregs also express CTLA-4 and compete for B7 ligands (CD80/86) on APCs resulting in downregulation and reduced cytokine production from DCs. Tregs cells can be identified by the expression of the transcription factor Forkhead box protein P3 (Foxp3). However, there is an increasing understanding of heterogeneity within Tregs with co-expression of other CD4 T cell transcription factors such as T-bet, GATA3 and ROR α (Wohlfert et al., 2011, Yu et al., 2015a, Malhotra et al., 2018, Miragaia et al., 2019). It has been suggested that the Treg cell heterogeneity may have a role in the cross-tissue adaptation from lymphoid tissue (LT) to the non-lymphoid tissue (NLT) environment (Miragaia et al., 2019).

1.5.2.1.3 Th2 cells

Th2 cells are critical for orchestrating the adaptive immune response against large extracellular pathogens such as helminths. Th2 cells secrete cytokines such as IL-4, IL-5 and IL-13 during a type 2 immune response, impact on the local tissue, and activate and recruit other type 2 immune cells. IL-4 promotes B cell antibody class switching to IgE,

IL-5 recruits eosinophils to the inflammatory site, whilst IL-13 promotes mucus production and goblet cell hyperplasia (Walker and McKenzie, 2018).

Th2 cell differentiation involves several mechanisms including transcriptional, metabolic and epigenetic factors. The transcription factor GATA3 is classically termed the “master” regulator of Th2 cells. GATA3 induces Th2 differentiation, cytokine production and promotes inhibition of other T helper cell lineage specific factors (Zhu et al., 2006a). IL-4 is a critical cytokine for Th2 cell differentiation. IL-4 binds to IL-4 receptor (IL-4R) on naïve CD4 T cells and induces Janus Kinase (JAK)1/3 mediated phosphorylation and dimerization of STAT6 (Kaplan et al., 1996). The phosphorylated STAT6 (pSTAT6) translocates to the nucleus and induces expression of GATA3, therefore promoting Th2 cell differentiation. STAT6 also promotes Th2 cell migration to the lung tissue, and the generation of Th2 memory cells (Finkelman et al., 2000, Voehringer et al., 2004). IL-2 promotes clonal expansion of T cells, and also Th2 cell differentiation. STAT5 is a downstream target of IL-2 binding to IL-2R, which induces *Il4* expression, in turn promoting STAT6 and GATA3 expression (Zhu et al., 2003). There are several other transcription factors expressed in Th2 cells, and important for Th2 cell differentiation and function, including ROR α (Haim-Vilmovsky et al., 2020), c-Maf (Kim et al., 1999), STAT3 (Stritesky et al., 2011), IRF4 (Ahyi et al., 2009), Notch/CSL (Zhu, 2015), Ikaros (Quirion et al., 2009) and Nuclear Factor (NF)- κ B (Li-Weber et al., 2004).

Th2 cell differentiation requires protein synthesis which is an energy-intensive process. To facilitate the increase in energy demands, Th2 cells switch from oxidative phosphorylation to aerobic glycolysis (Walker and McKenzie, 2018). This alteration in metabolism, protein synthesis and proliferation are mediated by the kinase mechanistic target of rapamycin (mTOR). Therefore, Th2 cell differentiation is dependent on the mTOR metabolic transition from oxidative phosphorylation to aerobic glycolysis (Walker and McKenzie, 2018). Several microRNAs (miRNA) have been shown to be involved in Th2 cell differentiation. Both miR-24 and miR-27 inhibit Th2 cell differentiation (Pua et al., 2016); whilst miR-19a and miR-155 promote Th2 cell differentiation (Simpson et al., 2014, Okoye et al., 2014). Th2 cell differentiation requires epigenetic reprogramming. CD4 T cell deletion of the histone methyltransferase enhancer of zeste homologue 2 (EZH2), which is required for trimethylation of histone H3 on Lys27, promotes Th1 and Th2 cell differentiation (Tumes et al., 2013). SUV39H1 is a histone methyltransferase

necessary for histone H3 Lys9 (H3K9) trimethylation. Inactivation of SUV39H1 led to the induction of Th1 cell mediated response in a model of type 2 immunity, suggesting that SUV39H1 is essential for the stability of Th2 cells (Allan et al., 2012). As is evident, advances in technology are uncovering more intricate detail on the mechanisms underlying Th2 cell differentiation, activation and function. As work in this area progresses, this will provide further insight into Th2 cell development.

1.5.2.1.4 CD8 (cytotoxic) T cells

CD8 (cytotoxic) T cells are critical cells in the defence against viral, bacterial and protozoal infections, as well as eliminating tumour cells. CD8 T cells are activated in lymphoid tissues by interaction between antigen presented in the MHC-I complex on APCs and TCR on CD8 T cells (Germain, 2002). CD8 T cells are potent, antigen-specific killers and can directly kill infected cells by apoptosis. They secrete cytokines such as TNF- α and IFN- γ , which have anti-tumour and anti-viral microbial effects (Cox et al., 2013).

1.5.2.2 B lymphocytes

B lymphocytes develop in the BM and migrate to secondary lymphoid tissues, such as lymph nodes and the spleen, where they complete maturation and are primed to respond to foreign antigens. B cells can be identified by expression of CD19 and can respond to the antigen directly without the need for prior exposure to APCs. B cells can differentiate into plasma cells, which are antibody secreting cells, or memory B cells, which provide long term immunity. Plasma cells are capable of secreting large quantities of antibodies (IgA, IgD, IgE, IgG and IgM). During helminth infections, a polarised type 2 immune response promotes B cell class switching to IgE and IgG1. During this process, the constant region of the antibody heavy chain is changed, but the variable region of the heavy chain remains the same. Class switching does not affect antigen specificity. Therefore, the antibody retains affinity for the same antigen, but can interact with different effector molecules. IgE activates MCs and basophils, whilst IgG was identified

to provide protective immunity against *Heligmosomoides polygyrus* (McCoy et al., 2008, Harris and Gause, 2011).

1.5.2.3 Innate lymphoid cells (ILC)

Innate lymphoid cells (ILC) are tissue-resident, cytokine secreting lymphocytes, that do not express antigen receptors and are critical in innate immunity. ILCs are divided into 3 subsets (ILC1, ILC2 and ILC3) based on their developmental pathway, phenotype and the cytokines they secrete (**Figure 1.3**). These subsets mirror their Th cell counterparts (Th1, Th2 and Th17, respectively). ILC1s provide protection against intracellular viral and bacterial pathogens. ILC1s are stimulated by IL-12, IL-15 and IL-18, express T-bet and Eomesodermin (EOMES) and secrete IFN- γ and TNF α (Walker et al., 2013). ILC2s are described in greater detail in **Section 1.5.2.3.1**. ILC3s are critical for maintaining gut epithelial integrity and tissue repair. ILC3s are stimulated by IL-1 β , IL-18 and IL-23, express ROR γ t and secrete IL-22 and IL17 (Montaldo et al., 2015).

1.5.2.3.1 Innate lymphoid cells 2 (ILC2)

ILC2s are innate immune cells that are important in anti-helminth immunity, metabolic homeostasis and tissue repair. ILC2s were first identified as a population of IL-25 regulated, IL-4, IL-5, IL-13 producing, non-B and non-T cell, c-kit⁺, Fc ϵ R1⁻ cells during helminth infection (Fallon et al., 2006). Since their discovery, they have been termed innate helper 2 cells (Price et al., 2010), natural helper cells (Koyasu et al., 2010, Halim et al., 2012) and nuocytes (Wong et al., 2012). However, the current accepted nomenclature is ILC2 (Spits et al., 2013).

ILC2s lack the lineage markers seen on T cells, B cells, myeloid cells and erythroid cells. However, ILC2s express Inducible T Cell Costimulator Ligand (ICOS-L), Stem cells antigen (Sca)1, Il-7 α , CD25, Killer cell Lectin like Receptor (KLR)G1 and receptors for the cytokines IL-25 (IL-17BR), IL-33 (T1/ST2) and thymic stromal lymphopietin (TSLP; TSLPR). ILC2s are cytokine secreting cells that secrete IL-4, IL-5, IL-9 and IL-13 as well as IL-6, IL-10, Granulocyte-Macrophage-Colony Stimulating Factor (GM-

CSF) and amphiregulin (Saenz et al., 2010, Walker et al., 2013, Eberl et al., 2015). ILC2s are stimulated by IL-25, IL-33, TSLP. They are also stimulated by the enteric nervous system through the secretion of neuropeptide neuromedin U (Klose et al., 2017). The transcription factors GATA-3 and ROR α are crucial for ILC2 development and function (Hoyler et al., 2012, Mjosberg et al., 2012, Wong et al., 2012, Halim et al., 2012) (**Figure 1.3**).

ILC2s have been categorised into two distinct subsets, natural ILC2 (nILC2) and inflammatory ILC2 (iILC2), based on their expression of IL-17RB (IL-25R) and IL-33R (ST2), respectively (Huang et al., 2015, Huang and Paul, 2016). Helminth infections induce KLRG1⁺IL25⁺ iILC2s and these iILC2s have been shown to migrate from the intestinal lamina propria to peripheral sites such as the lung (Huang et al., 2015).

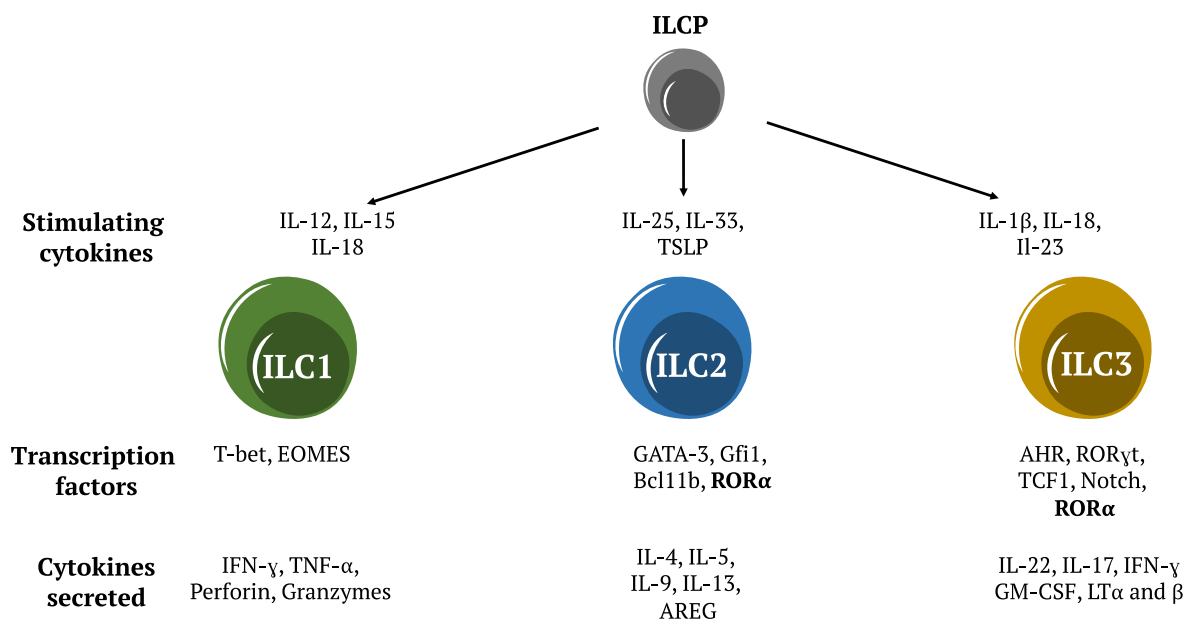


Figure 1.3: Overview of ILCs subsets.

1.5.2.4 Natural killer (NK) cells

Natural killer (NK) cells are large granular innate lymphocytes that represent 5-20% of peripheral blood mononuclear cells (Langers et al., 2012). NK cells are located in lymphoid and non-lymphoid tissues such as bone marrow, lymph nodes, gut, skin, liver,

tonsils, and lungs (Carrega and Ferlazzo, 2012). They have the ability to recognise and destroy a number of abnormal cells and stressed cells, such as tumour cells, virus-infected cells, cells bound by an antibody and allogeneic cells (Langers et al., 2012). Human NK cells can be identified by their expression of CD16 and CD56, whilst murine NK cells can be identified by the expression of NK1.1 (Abel et al., 2018).

1.6 Helminths

Helminths are parasites that have evolved to coexist within multiple host species over millions of years. There are over 100 different parasitic worms known to infect humans and it is estimated that approximately 1.5 billion people are infected with intestinal hookworm, whipworm (*Trichuris trichiura*) and the roundworm (*Ascaris lumbricoides*) (WHO, 2020). Human hookworms (*Necator americanus* and *Ancylostoma duodenale*) infect approximately 700 million people worldwide and are often referred to as a neglected tropical disease, as infections are largely eradicated from the westernised human population. However, helminth infections remain largely present in rural areas of developing countries such as sub-Saharan Africa, the Americas, China and East Asia, and are particularly prevalent in children (Bouchery et al., 2017, WHO, 2020). Helminth infections can be fatal, although often infected individuals show signs of malnutrition, anaemia, diarrhoea, cognitive dysfunction, vitamin deficiencies and growth retardation (Sharpe et al., 2018). In 2010, it was estimated that helminth infections resulted in 4.98 million years of life lived with disability and 5.18 million disability adjusted life years (Pullan et al., 2014). In addition, helminths also cause a major veterinary and agricultural problem throughout the world (Charlier et al., 2014). Therefore, helminth infections are a severe burden globally to both humans and agriculturally.

Currently, there are no vaccines against helminth infections. However, several drugs (albendazole, mebendazole, piperazine, ivermectin, nicolosamide, praziquantel and ievamisole) are used to control helminth infections. These drugs have low cure rates using single-dose administration, and often a common problem with helminth treatment is individuals are repeatedly exposed to infective eggs and larvae, which results in rapid reinfection. As has been apparent in westernised countries, improvements in basic hygiene and access to clean drinking water are key in reducing the prevalence of helminth

infections. There is also anthelmintic drug resistance reported in livestock (Rose et al., 2015), raising the concern that anthelmintic drug resistance may occur in human parasites.

It is evidently clear that helminths have a considerable impact in terms of health and economically globally. However, a full understanding of mechanisms that helminths use to infect and co-exist with the host remains elusive. Therefore, understanding the complex relationship between helminths and the host immune system is important for the generation of new and effective treatment of helminth infections. Additionally, understanding this immune response may also provide therapeutic benefit for autoimmune disorders such as allergies and asthma, as there are similarities in the host immune response to helminth infection, and the pathogenic response observed in these conditions.

1.7 The type 2 immune response

The type 2 immune response is central to tissue homeostasis, anti-helminth immunity and allergic inflammation. The complex lifecycle of helminths involves migration inside and outside of the host, with the primary sites of infections within the host being the skin, lungs and gut, as these sites are the first encountered upon exposure. As helminths are significantly larger in size than other microbes (viruses, bacteria, fungi and protozoa) they can cause direct physical damage to tissues by migration and feeding, as well as damage caused by the dissemination of eggs and release of immunomodulators. The epithelial cell barrier represents the first line of defence, but also is crucial in the detection and initiation of a type 2 immune response. Upon exposure to helminths, allergens or damage, epithelial cells secrete alarmins such as IL-25, IL-33 and TSLP. This initiates a cascade of cellular responses of both the innate and adaptive immune system (**Figure 1.4**).

ILC2s respond to epithelial-derived alarmins and secrete type 2 cytokines (IL-4, IL-5, IL-9 and IL-13). Both ILC2s and DCs promote the activation of adaptive immunity and Th2 cell differentiation which also secrete type 2 cytokines. These cytokines cause a plethora of cellular responses such as recruitment and activation of M2 macrophages, basophils, mast cells and eosinophils (**Figure 1.4**) (Allen and Maizels, 2011, Gause et al., 2013). M2 macrophages are involved in the tissue repair process. IL-4 induces B cell antibody

class switching to IgG1 and IgE and Th2 cell differentiation. Whilst IL-5 is a key cytokine in eosinophil activation and recruitment, resulting in eosinophilic airway inflammation. IL-9 promotes MC activation, resulting in degranulation and release of inflammatory mediators such as histamine. IL-13 induces goblet cell hyperplasia, mucus hypersecretion and smooth muscle hyperreactivity, all of which are required for the weep and sweep expulsion of helminths (Gurram and Zhu, 2019). ILC2s are important cells at mediating the expulsion of *N. brasiliensis* following primary infection (Fallon et al., 2006, Moro et al., 2010, Neill et al., 2010), whilst CD4 T cells (Th2 cell) in the lungs are important at mediating protection following secondary *N. brasiliensis* infection (Harvie et al., 2010, Thawer et al., 2014, Bouchery et al., 2015). ILC2s and CD4 T cells induce both eosinophils and macrophages which have been shown to provide a protective role against secondary *N. brasiliensis* infection (Anthony et al., 2006, Voehringer et al., 2006, Knott et al., 2007, Giacomini et al., 2008, Bouchery et al., 2015).

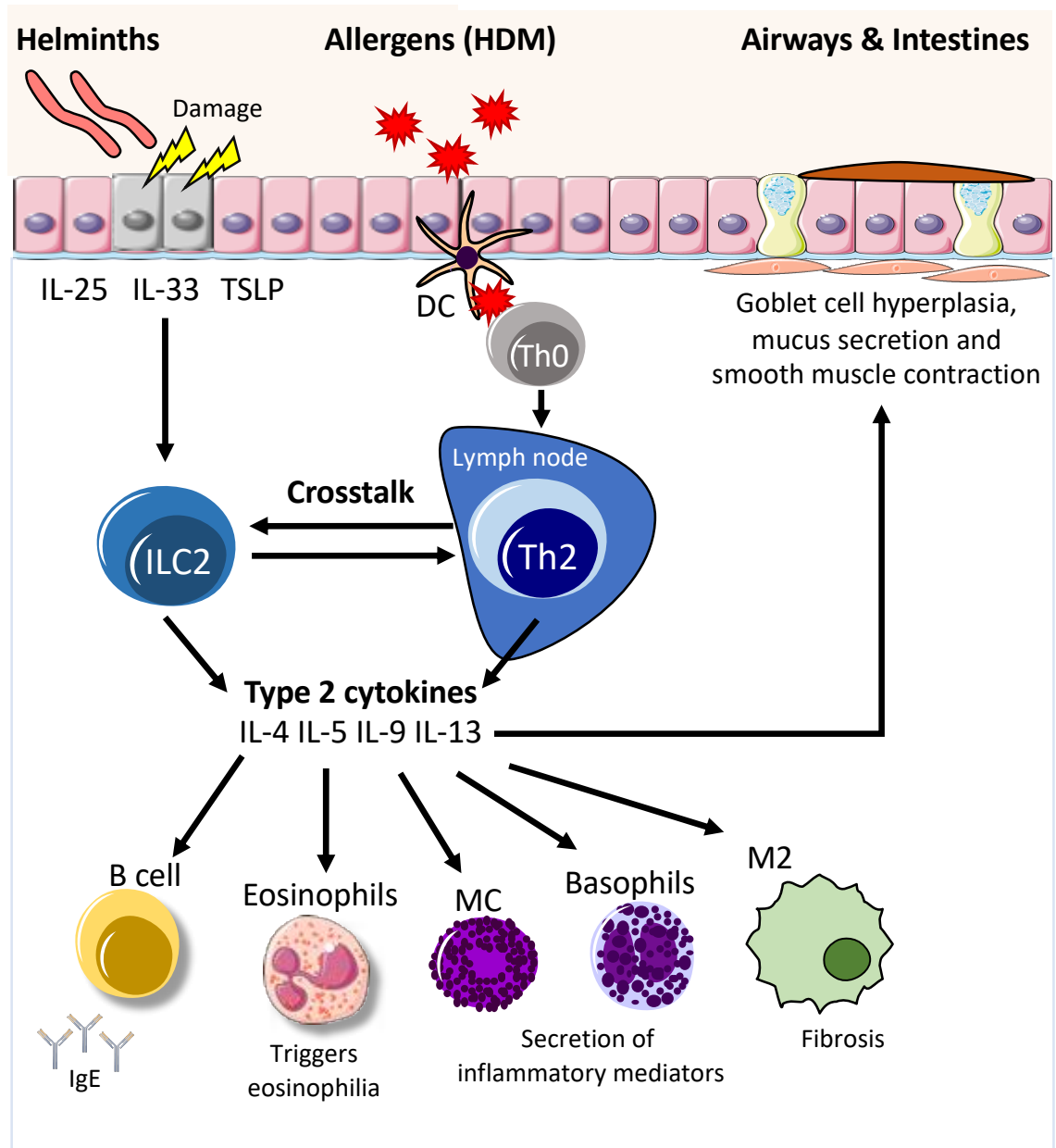


Figure 1.4. Overview of the type 2 immune response.

1.8 Retinoic acid receptor-related orphan receptor alpha (ROR α)

1.8.1 Nuclear receptors

Nuclear receptors (NRs) are a highly conserved transcription factors that provide multicellular organisms with a mechanism to directly control gene expression in response to developmental, environmental and physiological cues. NRs have been classified into a superfamily consisting of 48 members in humans, and 49 members in mice (Zhang et al., 2004). Approximately half of identified NRs do not have a well-defined natural ligand and are termed orphan nuclear receptors (Giguere, 1999). Given their involvement in many biological processes such as cellular proliferation, differentiation, development and homeostasis, NRs have been implicated in several diseases such as cancer, diabetes, obesity and autoimmune disorders. Therefore, NRs provide an attractive target for potential therapeutic benefit.

NRs share a common structure consisting of four major units (**Figure 1.5**). The N-terminal region is highly variable in both sequence and contains the ligand-independent activation function 1 (AF-1) domain. The DNA-binding domain (DBD) resides approximately in the centre of the polypeptide and contains two zinc finger motifs which allow the nuclear receptor to bind to the DNA response elements (Huang et al., 2010). The DBD and ligand binding domain (LBD) are joined via a variable hinge region. The hinge region often contains a DNA minor groove binding residue. The LBD is positioned at the C-terminal and consists of approximately 200-300 residues (Huang et al., 2010). The LBD is often the main focus for drug discovery, as this region is where ligands and coactivators/corepressors interact and affect NR function. Finally, situated within the LBD domain is a ligand-dependent activation function 2 (AF-2) domain. This functions to recruit transcriptional activators in a ligand dependent manner (Zhang et al., 2015). The transcriptional activity of NRs is regulated by the binding of endogenous small lipophilic compounds to the LBD (Zhang et al., 2004, Huang et al., 2010).



Figure 1.5: Schematic of a nuclear receptor.

1.8.2 ROR α background and structure

Retinoic acid receptor-related Orphan Receptors (RORs) consist of a subfamily that comprises ROR α (NR1F1), ROR β (NR1F2) and ROR γ (NR1F3) (Solt and Burris, 2012, Cook et al., 2015). ROR α is as a transcription factor that provides a bridge between hormonal, nutritional and pathophysiological signalling and gene regulation. ROR α was first identified as a steroid hormone nuclear receptor in 1994 (Giguere et al., 1994). There are four ROR α isoforms identified in humans (*RORA* 1-4) mapped to the human chromosome 15q22.2, which consists of 21 exons. Whilst in mice, there are two isoforms identified (*Rora* 1 and 4) mapped to chromosome 9, consisting of 19 exons (Giguere et al., 1995) (**Figure 1.6**). The different ROR α isoforms are generated by alternative promoter usage and exon splicing. Therefore, each isoform has a distinct N-terminal region, which influences the DNA binding specificity. Whilst all ROR α isoforms have a highly-conserved LBD, suggesting each isoform binds the same ligand (Giguere et al., 1994).

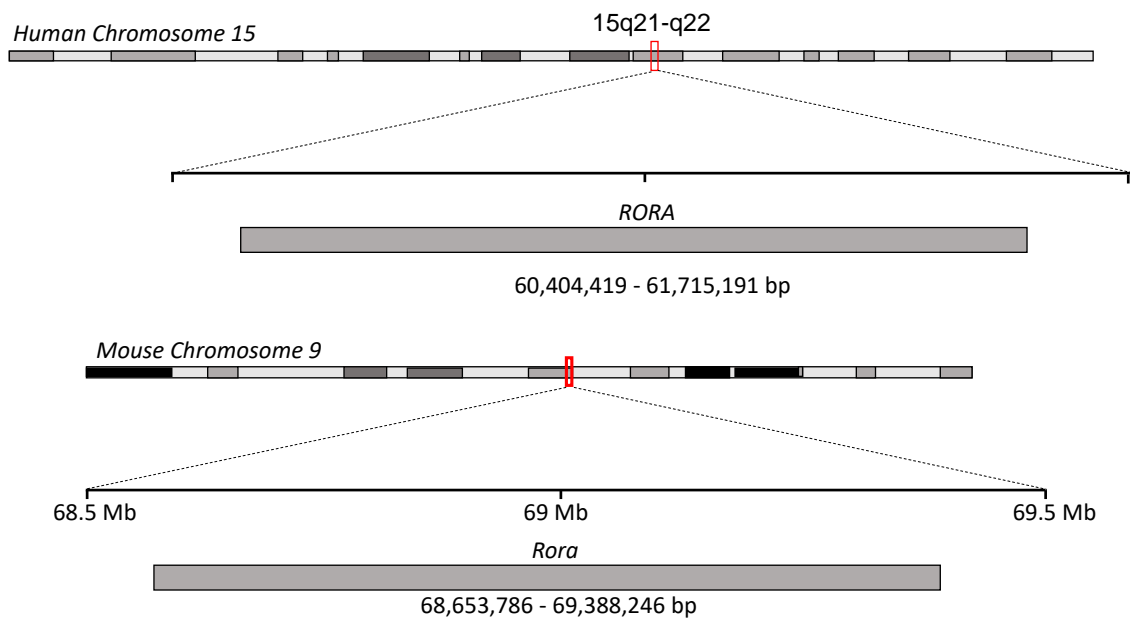


Figure 1.6: *RORA* gene on human chromosome 15 and *Rora* gene on mouse chromosome 9.

1.8.3 Functions of ROR α

ROR α plays an important role in many physiological processes including circadian rhythm, metabolism, cerebellar development, cellular development, cancer and inflammation (**Figure 1.7**). The focus of this thesis investigates the role of ROR α on cellular development and inflammation in the context of a type 2 immune response.

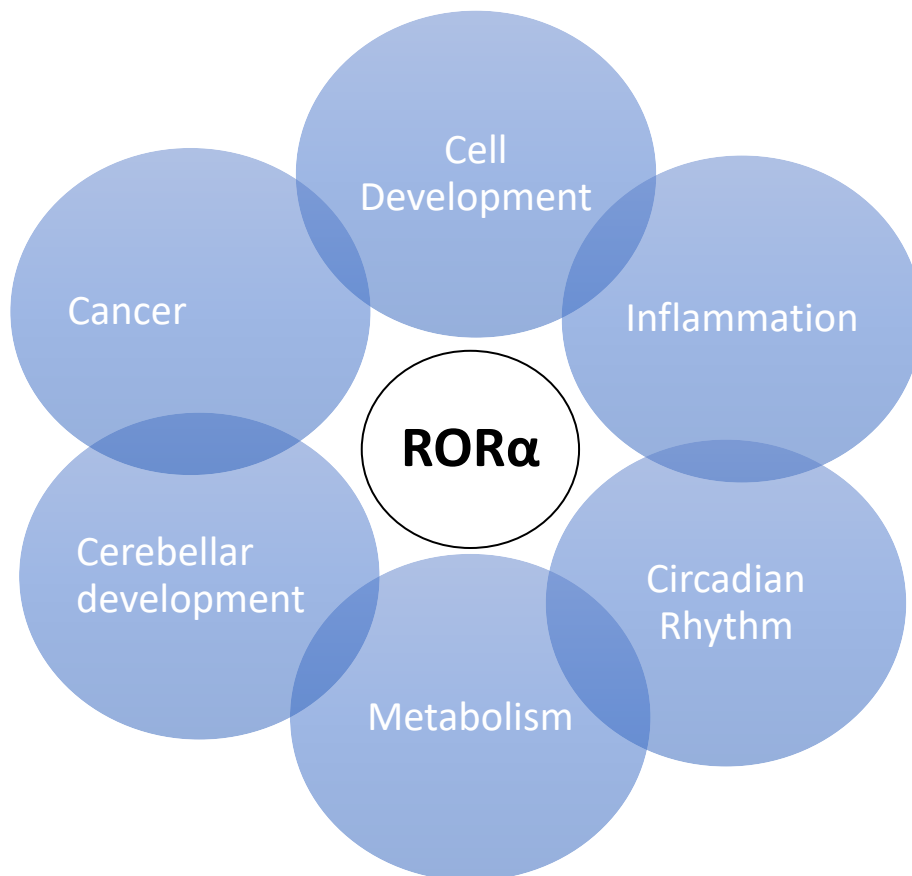


Figure 1.7: Summary of functions of ROR α .

1.8.4 ROR α mechanism of action

ROR α is a transcription factor that regulates gene transcription. In the human brain, ROR α regulates the transcription of over 2,500 genes (Sarachana and Hu, 2013). ROR α binds to specific DNA ROR response elements (ROREs) in the target genes. These ROREs are composed of a A/T-rich sequence (TAAA/TNTAGGTCA). This binding is

controlled by the P-box, a loop located between the final two cysteines within the first zinc finger in the DBD (Giguere et al., 1995, Jetten, 2009). Once ROR α is bound to RORE it recruits coactivators NCOA1 (SRC1), NCOA2 (TOF2 or HROP1), PGC-1 α , p300 and CBP or corepressors NCOR1, NCOR2, RIP140 and neuronal interacting factor X (NIX1) to form the basic transcriptional machinery. This leads to transcriptional regulation of target genes (Jetten, 2009) (**Figure 1.8**). ROR α is constitutively active, therefore, in the absence of a ligand ROR α is still in an active conformational state and binding of a ligand to the ROR α LBD may either repress or enhance activity (Solt and Burris, 2012).

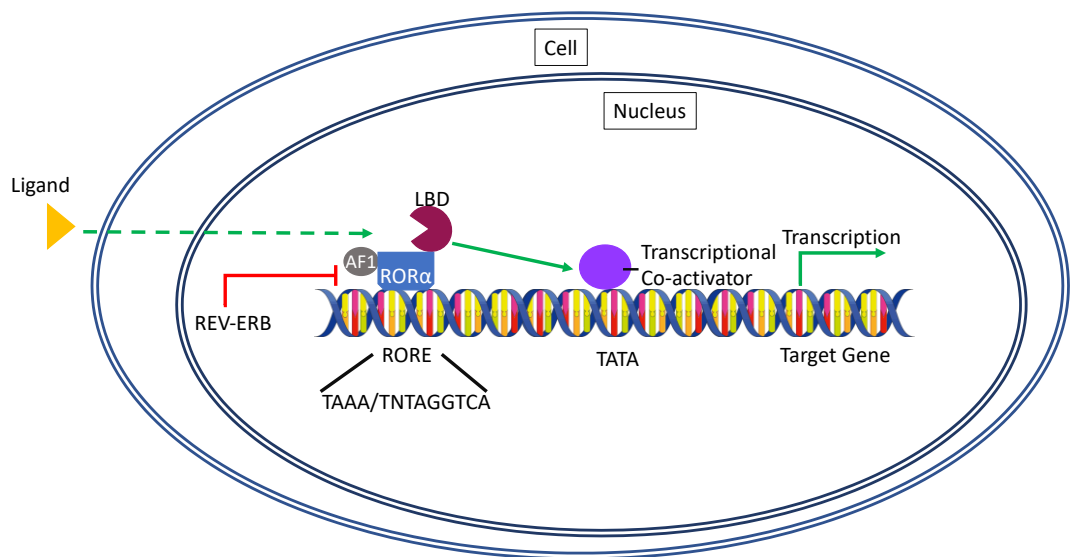


Figure 1.8: ROR α mechanism of action.

1.8.5 *Rora* natural mutant mouse - *Staggerer* (*Rora*^{sg/sg}) mice

The natural mutant mouse, termed staggerer was first observed in the Jackson Laboratory in 1955. The mouse was generated by a cross between a female BALB/cHm x C3H/HeJ and an obese male (Lep^{ob}) of mixed background. The mutation was then backcrossed onto C57BL/6J mouse. These early studies showed that these mice had a staggerer gait, mild tremor, hypotonia and small size and shorter lifespan compared to WT littermates (**Figure 1.9**). Further investigation revealed that the staggerer mice cerebellar cortex was severely underdeveloped (Sidman et al., 1962). The mutation in the staggerer mice was genetically

mapped to the *Rora* gene on chromosome 9 and mice homozygous for the *staggerer* mutation were termed *Rora^{sg/sg}* mice. Heterozygous mice (*Rora^{sg/+}*) are phenotypically comparable to WT mice, therefore the mutation in the *Rora* gene is recessive (Lau et al., 2011). The mutant *Rora* allele was shown to have a spontaneous 122 base pair (bp) deletion in the LBD, resulting in a shift in the reading frame at amino acid 273, causing a truncation 27 residues later. This causes a 6.5kb genomic deletion in these mice and results in a ubiquitous absence of a functional ROR α (**Figure 1.10**) (Hamilton et al., 1996). Therefore, in *Rora^{sg/sg}* mice, the ROR α protein can bind to DNA but due to a truncated LBD, ligands cannot bind resulting in a non-functional protein and no transcription of target genes (Steinmayr et al., 1998, Dussault et al., 1998) (**Figure 1.11**).



Aged 4 weeks

Figure 1.9: Representative photograph of male *Rora^{+/+}* and *Rora^{sg/sg}* mice littermates at 4 weeks of age.

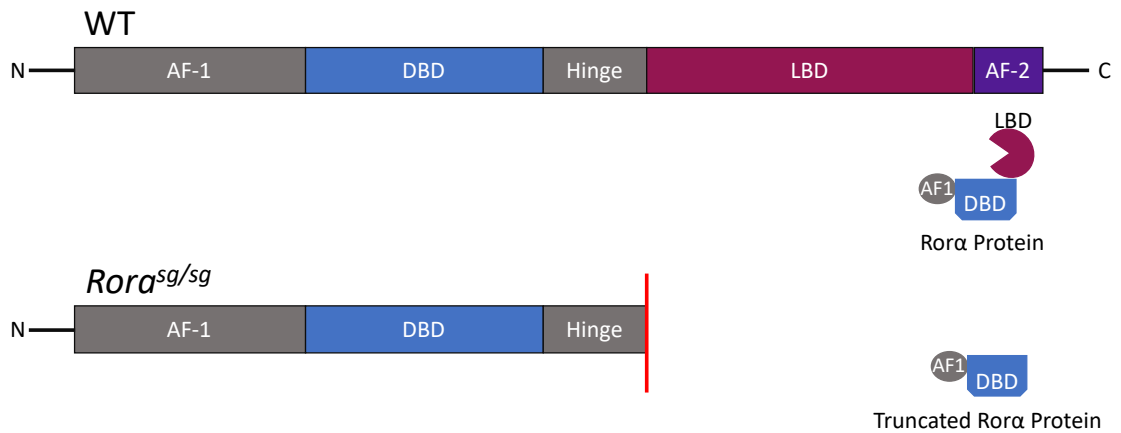


Figure 1.10: Schematic of WT nuclear receptor and the truncated *Rora^{sg/sg}* nuclear receptor.

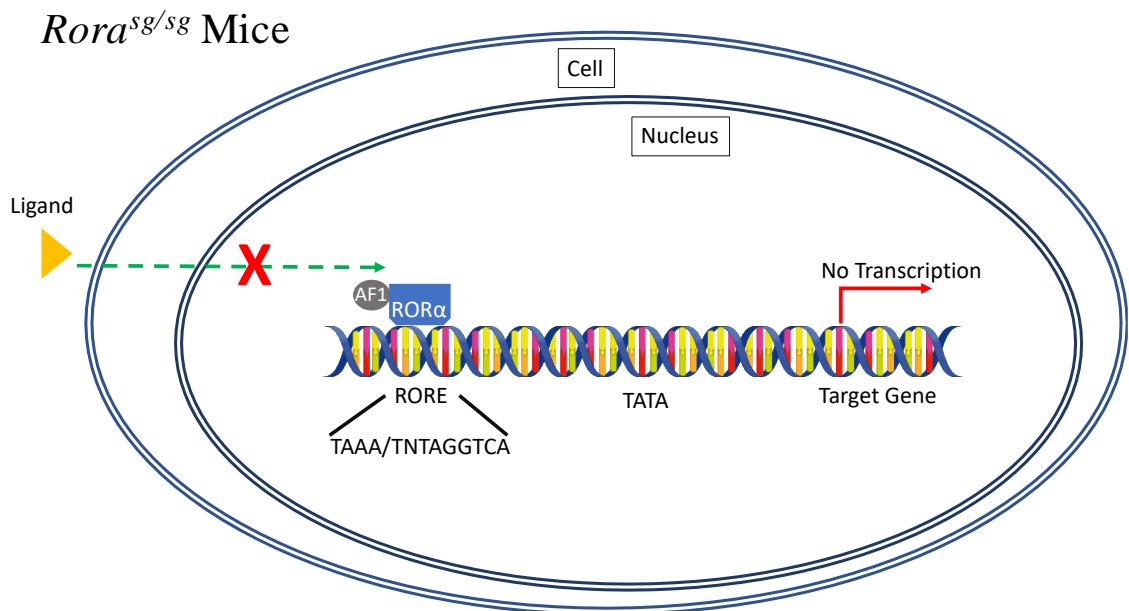


Figure 1.11: Diagram of RORα mechanism in *Rora^{sg/sg}* mice.

1.8.6 RORα expression

RORα is expressed in a variety of tissues such as the lung, liver, skin, skeletal muscle, adipose tissue, kidney, thymus, testes, endothelial cells, mammary arteries and cerebellum (Hamilton et al., 1996, Steinmayr et al., 1998, Delerive et al., 2001, Besnard et al., 2002, Solt and Burris, 2012, Slominski et al., 2014, Zhang et al., 2015). The focus of this thesis is the role of RORα in immune cells during a type 2 immune response. Indeed, *Rora* is expressed in lymphocytes, with high levels in murine CD4⁺ and CD8⁺ T

cells (Dzhagalov et al., 2004). *Rora* is also expressed in Th17 cells (Yang et al., 2008), ILC2s (Wong et al., 2012, Halim et al., 2012), Tregs (Malhotra et al., 2018) and Th2 cells (Van Dyken et al., 2016, Miragaia et al., 2019, Haim-Vilmovsky et al., 2020). Whilst single-cell RNA-sequencing (scRNA-seq) of immune and stromal cells in human airways and lung parenchyma (Vieira Braga et al., 2019) revealed *RORA* was highly expressed in T and NK population in the human lung cells (**Figure 1.12**).

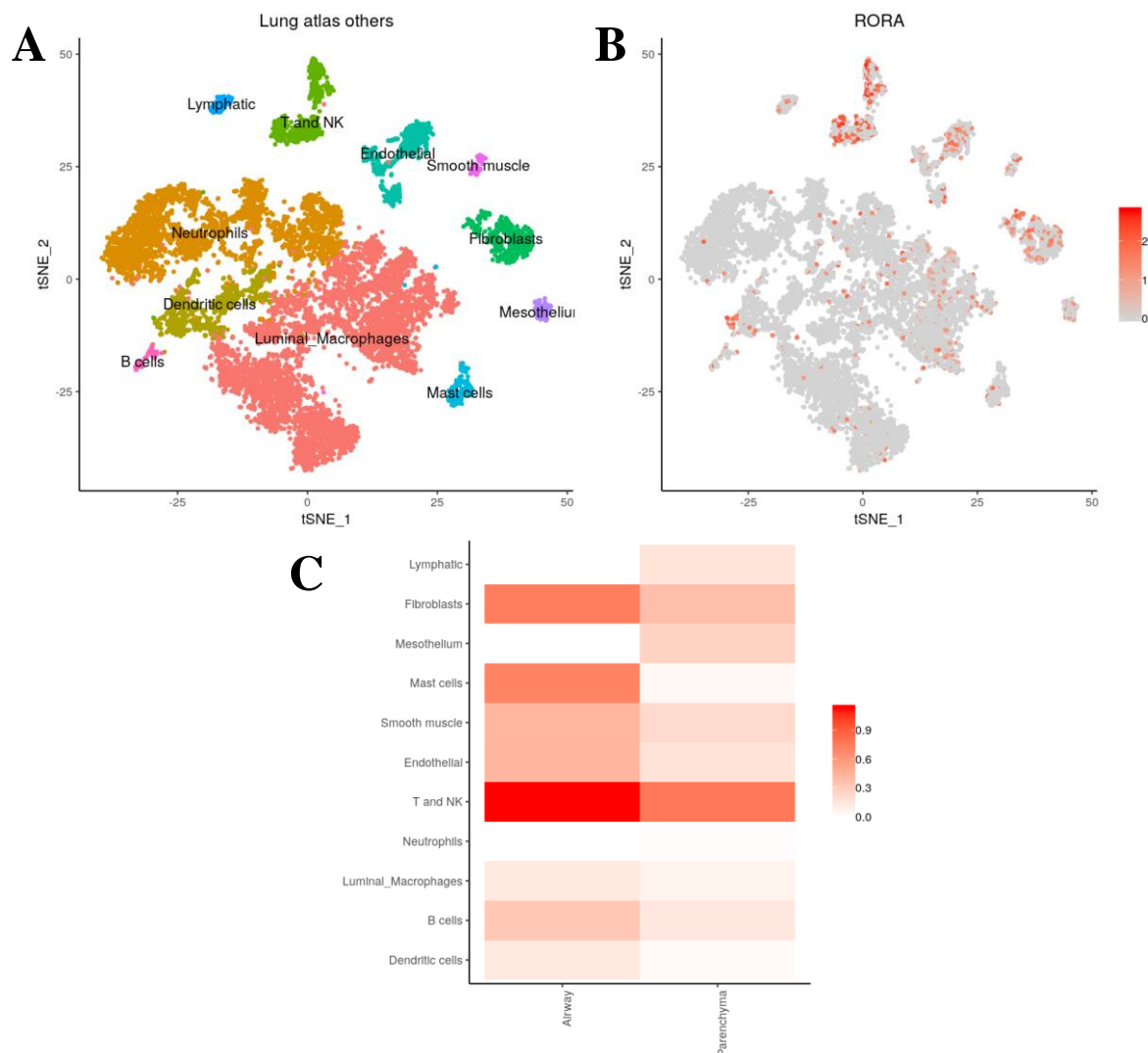


Figure 1.12: Expression of *RORA* in immune cells of human airways and parenchyma. **A**, tSNE analysis of immune cells measured by scRNA-seq. **B**, tSNE analysis of *RORA* expressing immune cells. **C**, Heatmap showing expression of *RORA* across different clusters. (Vieira Braga et al., 2019).

Single-cell CD4 T cells were isolated from the blood and biopsies of healthy controls and scRNA-seq analysis reported *RORA* expression across all CD4 T cell subsets including Th2 cells, with the exception of Th17 cells in the blood (Vieira Braga et al., 2019) (**Figure**

1.13). This contradicts previously published data which reported $ROR\alpha$ has a role in Th17 cell development (Yang et al., 2008). However, this was explained as Th17 cells would not be routinely found in the blood of healthy controls (Vieira Braga et al., 2019).

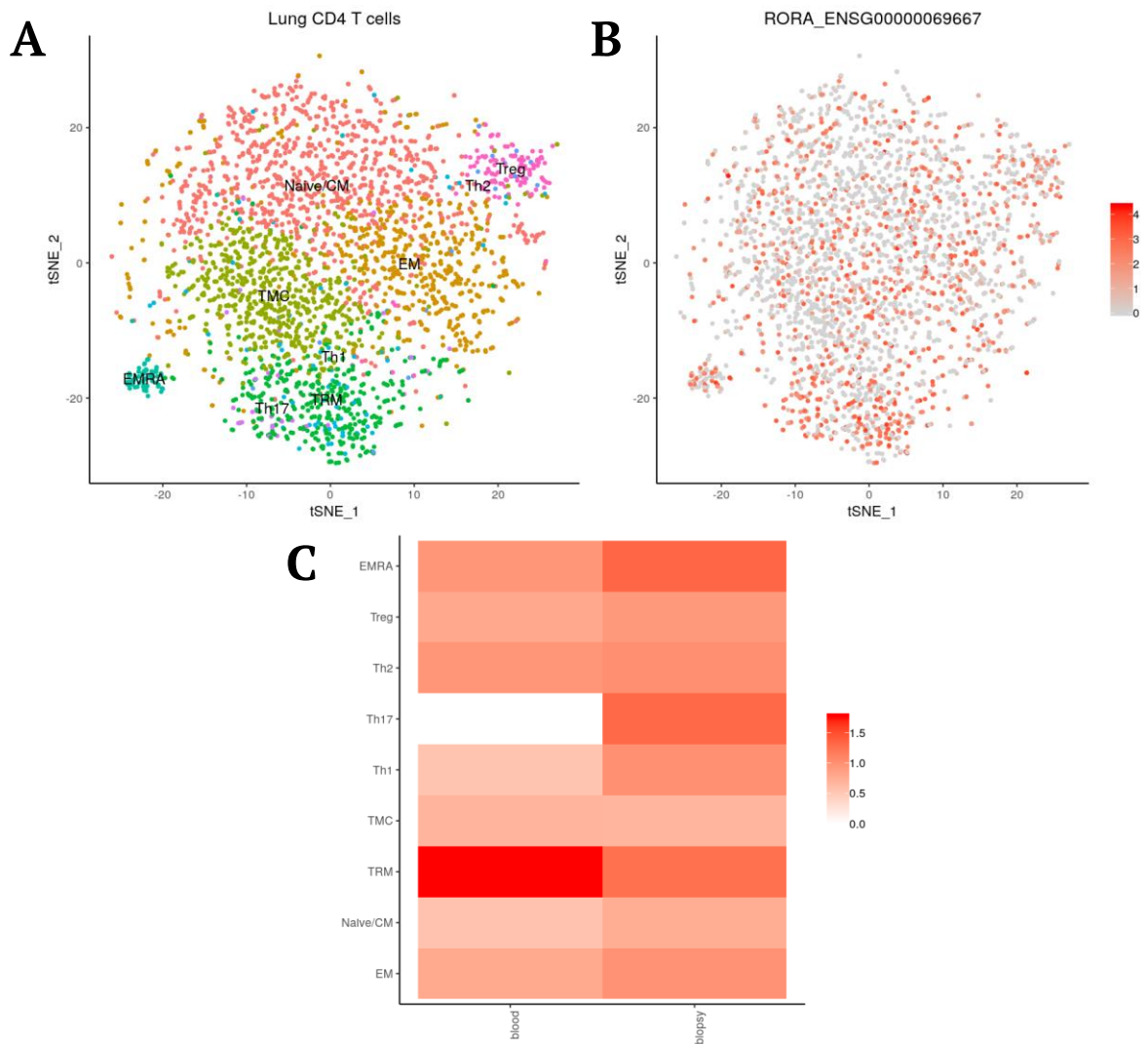


Figure 1.13: Expression of *RORA* in lung CD4 T cells subsets in blood and lung biopsy. **A**, tSNE analysis of lung CD4 T cells measured by single-cell RNA-seq. **B**, tSNE analysis of lung *RORA* expressing CD4 T cells. **C**, Heatmap showing expression of *RORA* across different clusters. (Vieira Braga et al., 2019).

1.8.7 Sex difference in *RORA/Rora* expression

There is evidence to suggest that *RORα* may be differentially regulated within males and females. It was reported that sex hormones regulated the expression of *RORA* in a neuronal cell line (SH-SY5Y) (Sarachana et al., 2011). In this study, the female hormone estradiol upregulated *RORA* expression, whilst the male hormone androgen dihydrotestosterone downregulated *RORA* expression (Sarachana et al., 2011). It was also reported that *RORα* regulates *CYP19A1*, a gene encoding aromatase, an enzyme that converts testosterone to estradiol, which suggests that *RORα* has a positive and negative feedback regulation by female and male hormones, respectively (Sarachana et al., 2011). There was also a study in humans that reported a nominally higher level of *RORα* protein in the frontal cortex of females compared to males (Hu et al., 2015). However, these differences were not statistically significant and may be due to the genetic heterogeneity of human donors and limited sample size. In mice, it has been reported that female mice have higher *Rora* expression compared to male mice in the frontal cortex. Additionally, two *RORα* transcriptional targets, *Cyp19a1* and *Nlgn1*, were higher in the frontal cortex of female mice compared to male mice (Hu et al., 2015). However, there was no significant sex difference in *RORA/Rora* expression in human and mouse cerebellum (Hu et al., 2015). There are conflicting studies reporting on a sex bias in *Rora* expression in murine lung ILC2s. Cephus et al. (2017) reported *Rora* expression was lower in male murine lung ILC2 compared to lung ILC2 from female mice. However, Romera-Hernandez et al. (2019) reported no significant difference in the expression of *Rora* in male and female lung ILC2s. Therefore, a sex difference in *RORA/Rora* expression remains controversial and may be cellular, tissue and context dependent.

1.8.8 *RORα* endogenous ligands

Historically, *RORα* has been termed an orphan receptor due to a lack of defined endogenous ligands, however, several putative ligands of *RORα* have been identified. Kallen et al. (2002) reported the crystal structure of *RORα* ligand binding domain (LBD) and revealed that cholesterol was bound to the LBD. It was also reported that *RORα* transcriptional activity could be modulated by changes in intracellular cholesterol (Kallen

et al., 2002). Further research showed that cholesterol sulfate had a higher binding affinity for ROR α LBD compared to cholesterol, resulting in increased transcriptional activity of ROR α (**Figure 1.14**) (Kallen et al., 2002, Bitsch et al., 2003, Kallen et al., 2004).

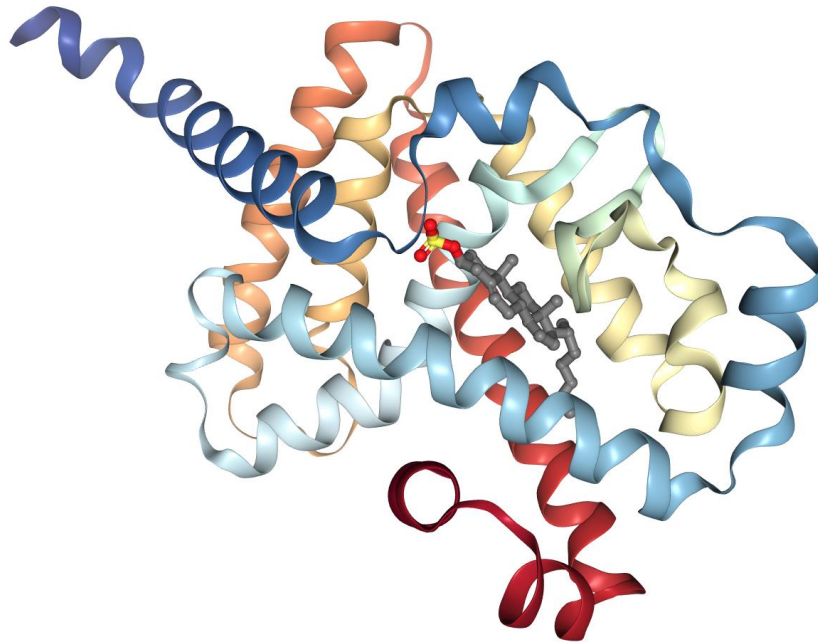


Figure 1.14: Crystal structure of human ROR α ligand binding domain in complex with cholesterol sulfate at 2.2 Å resolution. Image adapted from Kallen et al. (2004).

Wang et al. (2010b) reported that 7-oxygenated sterols function as inverse agonists with high affinity for ROR α and ROR γ . In this study, it was shown that 7 α -hydroxycholesterol (7 α -OHC) modulated expression of the known ROR α target genes *glucose-6-phosphatase* (*G6pase*) and *phosphoenolpyruvate carboxykinase* (*Pepck*) (Chopra et al., 2008, Wang et al., 2010b, Matsuoka et al., 2015). Wang et al. (2010a) reported that the oxysterol, 24S-hydroxycholesterol (24S-OHC) also functions as a high affinity inverse agonist of ROR α , suppressing the expression of several ROR α target genes such as *BMAL1* and *REV-ERB α* (Wang et al., 2010a). Another study also reported that that endogenous D3 hydroxy-derivatives acts as inverse agonist of ROR α/γ inhibiting IL-17 promoter activity in cells overexpressing ROR α/γ (Slominski et al., 2017). Recently, maresin 1 (MaR1) was also reported as an endogenous ligand for ROR α and increased both ROR α /*Rora* mRNA and protein. It was also reported that MaR1 has a higher binding affinity to ROR α compared to cholesterol sulfate (Han et al., 2019). Therefore, there is increasing evidence for putative ROR α endogenous ligands which has led to the suggestion that ROR α is ‘deorphanised’.

1.8.9 ROR α and inflammation

ROR α has been implicated to play a role in the immune system as early as the 1980s, with initial studies assessing the impact of ROR α on inflammatory signalling cascades. Many studies on ROR α and inflammation have focused on its role in regulation of immune signalling pathways and its involvement in immune cell development. Indeed, it was shown that *Rora*^{sg/sg} mice have a reduced size and cellularity of the thymus and spleen compared to heterozygous littermates, suggesting that ROR α has a role in thymopoiesis and lymphocyte development (Trenkner and Hoffmann, 1986, Dzhagalov et al., 2004). It was also reported that *Rora* acts as a negative regulator of the inflammatory response by directly impacting inflammatory signalling cascades. With over-expression of ROR α in smooth muscle inhibiting TNF- α -induced expression of the pro-inflammatory cytokines IL-6 and IL-8, and upregulation of I κ B α . The upregulation of I κ B α inhibits NF- κ B, a transcription factor that promotes inflammation, suggesting that ROR α is a negative regulator of the inflammatory response (Delerive et al., 2001). Furthermore, it was reported that *Rora*^{sg/sg} mice had a higher degree of lung inflammation compared to WT mice following intra-nasal administration of LPS, which was associated with increased levels of the pro-inflammatory cytokines IL-1 β and IL-6 (Stapleton et al., 2005). Therefore, suggesting that ROR α functions as a negative regulator of an LPS-induced inflammatory response (Stapleton et al., 2005).

ROR α has also been linked with allergic and autoimmune diseases, with mice deficient in ROR α and ROR γ protected from experimental autoimmune encephalomyelitis (EAE), a model of the human autoimmune condition multiple sclerosis (MS) (Yang et al., 2008). Whilst it was reported that ROR α was identified as a gene associated with human MS (Eftekharian et al., 2016). ROR α has also been implicated in the allergic skin condition, atopic dermatitis (AD). It was shown that *RORA* expression was elevated in skin from patients with AD (Salimi et al., 2013). However, *RORA* expression is downregulated in dogs with AD (Majewska et al., 2016). ROR α is also associated with asthma in humans (**Section 1.8.11**) (Moffatt et al., 2010, Ramasamy et al., 2012, Persson et al., 2015, Eftekharian et al., 2016), yet the role of ROR α in lung pathology is not fully defined.

1.8.10 ROR α and type 2 immunity

ROR α has been implicated in the generation and maintenance of a type 2 immune response. Early studies reported that *Rora*^{sg/sg} mice are less susceptible to ovalbumin (OVA)-induced airway inflammation, characterised by a reduced lung infiltration of inflammatory cells such as lymphocytes, eosinophils and neutrophils (Jaradat et al., 2006). In addition, the induction of Th2 cytokines (IL-4, IL-5 and IL-13) in the bronchoalveolar lavage (BAL) were lower in OVA-challenged *Rora*^{sg/sg} mice compared to WT mice (Jaradat et al., 2006). Therefore, suggesting ROR α plays a role in the development of Th2-driven allergic lung inflammation. Indeed, ROR α is critical for the development of ILC2s, an innate immune cell with an integral role in type 2 immunity (Wong et al., 2012, Halim et al., 2012). Whilst *Rora*^{sg/sg} mice challenged with papain, a mouse model of eosinophilic airway inflammation, had fewer eosinophils in the lung, BAL and mediastinal lymph nodes (mLN) compared to papain challenged WT mice (Halim et al., 2014). The cytokine IL-33, initiates type 2 immunity through the receptor ST2, leading to activation of Th2 cells and ILC2s, was shown to induce *Rora* expression in these cell types (Haim-Vilmovsky et al., 2020). It was also shown that *Rora* is expressed in Th cells, and that expression is associated with activated Th cells, which promotes lung inflammation in response to *N. brasiliensis* infection (Haim-Vilmovsky et al., 2020).

1.8.11 ROR α and asthma

Asthma is a common chronic heterogenous inflammatory disease of the airways, that affects over 300 million people worldwide (Athari, 2019). It is characterised by a dysregulation of innate and adaptive type 2 immunity, which results in inflamed mucosa and smooth muscle contractions, causing wheezing and shortness of breath (Caminati et al., 2018). Asthma is a complex allergic disorder which results from a combination of both genetic and environmental factors such as air pollutants, respiratory viruses, tobacco smoke endotoxin and allergens in the air and diet (Mukherjee and Zhang, 2011).

ROR α has been implicated in the pathogenesis of asthma. A genome-wide association study (GWAS) identified a single nucleotide polymorphism (SNP) within ROR α (rs11071559) that had an association with asthma (Moffatt et al., 2010, Ramasamy et al., 2012). Another GWAS study identified 7 *RORA* SNPs that were associated with physician diagnosed childhood asthma (Acevedo et al., 2013). Whilst *RORA* expression was significantly upregulated in patients with therapy-resistant asthma (Persson et al., 2015). It was also reported that ROR α have epistasis with Neuropeptide S receptor 1 (NPSR1), an asthma susceptible gene (Acevedo et al., 2013). A recent study analysing single-cell transcriptomes of the immune cells in human airways, showed *RORA* was highly expressed in T cells of the airways in both the healthy control and asthma patients (**Figure 1.15**) (Vieira Braga et al., 2019). Furthermore, it was reported that *RORA* is differentially expressed during lung development in both humans and mice (Melen et al., 2011), which suggests that ROR α may have a role in T cell biology and asthma.

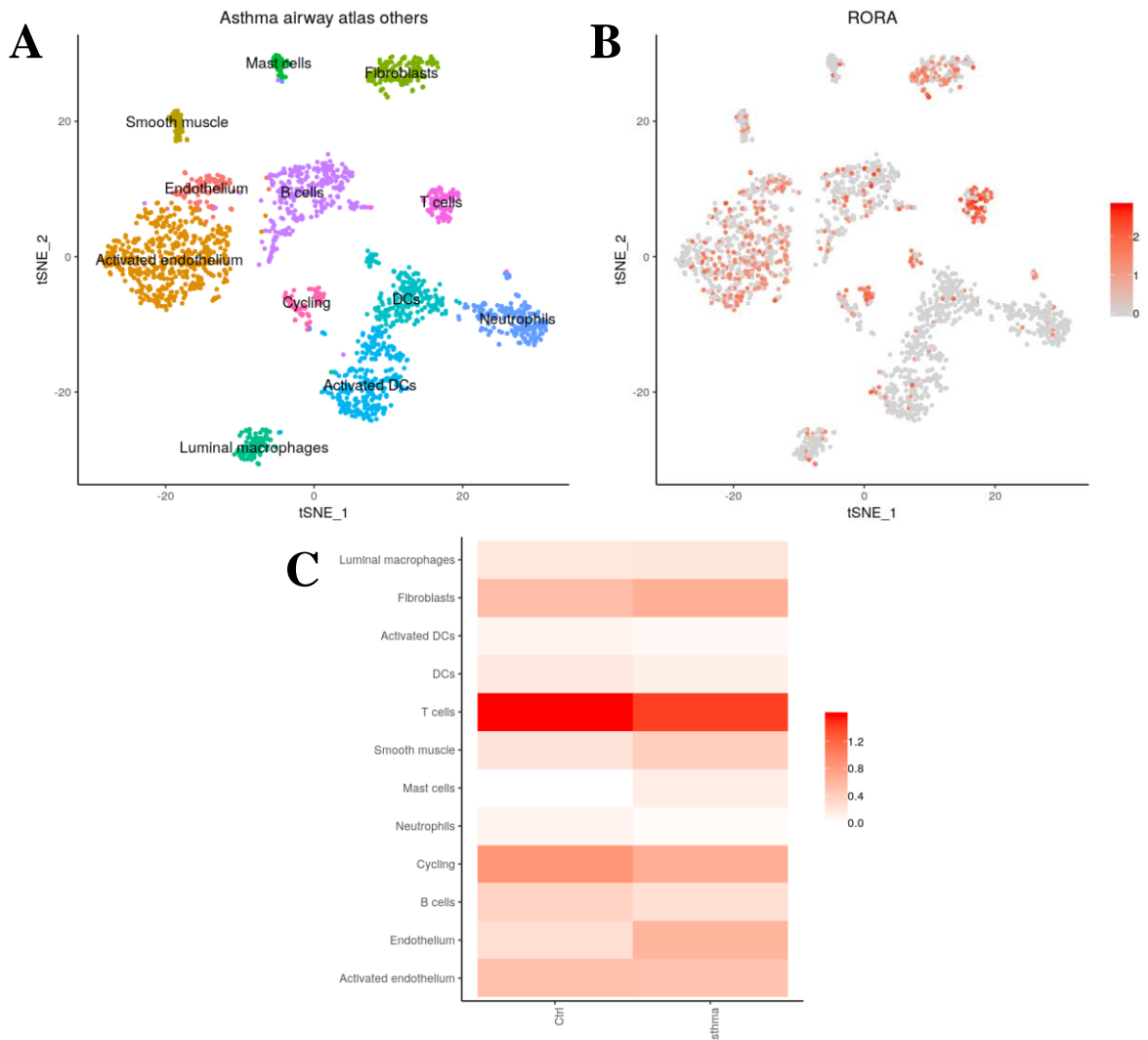


Figure 1.15: Expression of *RORA* in immune cells of human airways in healthy control and asthma patients. **A**, tSNE analysis of immune cells measured by single-cell RNA-seq of combined healthy controls and patients with asthma. **B**, tSNE analysis of *RORA* expressing immune cells of combined healthy controls and patients with asthma. **C**, Heatmap displaying expression of *RORA* across different clusters between healthy control and asthma patients. (Vieira Braga et al., 2019).

1.8.12 *RORα* and cancer

RORα is known to have protective or pathogenic roles in cancer development dependent on the site of the tumour. The *RORA* gene is situated in the middle of a common fragile site (FRA15A - 15q22.2), which is a highly unstable large genomic region of DNA susceptible to breakage and rearrangements (Zhu et al., 2006b). It was shown that *RORα* expression is down-regulated during tumour development and progression, whilst restoring *RORα* inhibited cell proliferation and tumour growth (Kottorou et al., 2012,

Xiong et al., 2012, Fu et al., 2014). ROR α was also identified as a target gene for the tumour suppressor protein p53, a transcription factor which is associated with a loss of function mutation in over 50% human cancers (Ozaki and Nakagawara, 2011). Whilst ROR α expression was also induced by DNA damaging agents such as ionizing radiation and doxorubicin, in a p53-dependent manner (Kim et al., 2011).

ROR α was shown to increase the expression of aromatase, an enzyme that produces oestrogen from androgen, a key regulator of the proliferation and differentiation of breast cancer cells. Therefore, ROR α was shown to stimulate the proliferation of breast cancer cell lines (T47D and MCF7) (Odawara et al., 2009). Whilst a GWAS study reported *RORA* SNPs (rs1482057, rs12914272 and rs4774388) are associated with breast cancer in women (Truong et al., 2014). In gastric cancer, ROR α expression correlated with differentiation, tumour size and lymph node metastasis (Su et al., 2019). With ROR α suppressing cell proliferation, epithelial to mesenchymal transition and invasion in gastric cancer cells through inhibition of Wnt/ β -catenin pathway (Su et al., 2019). In colorectal cancer, there was a correlation of reduction of ROR α phosphorylation in colorectal cancer compared to their normal counterparts (Lee et al., 2010). Thus, as outlined, ROR α has an involvement in numerous human cancers and therefore make it an attractive target for cancer therapy.

1.8.13 ROR α and the circadian rhythm

The mammalian circadian clock plays a crucial role in the rhythmic timing of many physiological and behavioural processes. ROR α has been identified to have a role in regulation of circadian rhythm. The circadian clock is divided into two components, the central clock located in the suprachiasmatic nucleus (SCN) of the hypothalamus and the peripheral clock located in various tissues and cells throughout the body. The molecular clock machinery consists of several transcription/translational feedback loops. This mechanism is controlled by BMAL (Brain and muscle ARNT-like1) and CLOCK (Circadian Locomotor Output Cycles Kaput), which heterodimerise and promote the transcription of clock genes *Period* (*Per1,2,3*) and *Cryptochrome* (*Cry1,2*) through an E box enhancer. PER and CRY proteins inhibit BMAL1 and CLOCK transcription,

therefore restoring the circadian rhythm (**Figure 1.16**) (Sato et al., 2004, Akashi and Takumi, 2005, Guillaumond et al., 2005, Cook et al., 2015).

A second molecular clock feedback loop consists of ROR α and REV-ERB. Both ROR α and REV-ERB are activated by BMAL1/CLOCK, which compete for Rev-ErbA/ROR response elements (RRE) within the regulatory sequence of core clock genes such as *Bmal1* to regulate its transcription (**Figure 1.15**) (Sato et al., 2004, Cook et al., 2015). ROR α also has roles in intestinal epithelium immune function by controlling the diurnal regulation of several PRR, including Nod2 and various TLRs (Mukherji et al., 2013). Furthermore, ROR α also controls diurnal expression of interleukin-1 receptor-associated kinase 1 (IRAK1), Toll-interleukin 1 receptor domain containing adaptor protein (TIRAP) and nuclear factor, interleukin 3 regulated (NFIL3) (Mukherji et al., 2013, Cook et al., 2015).

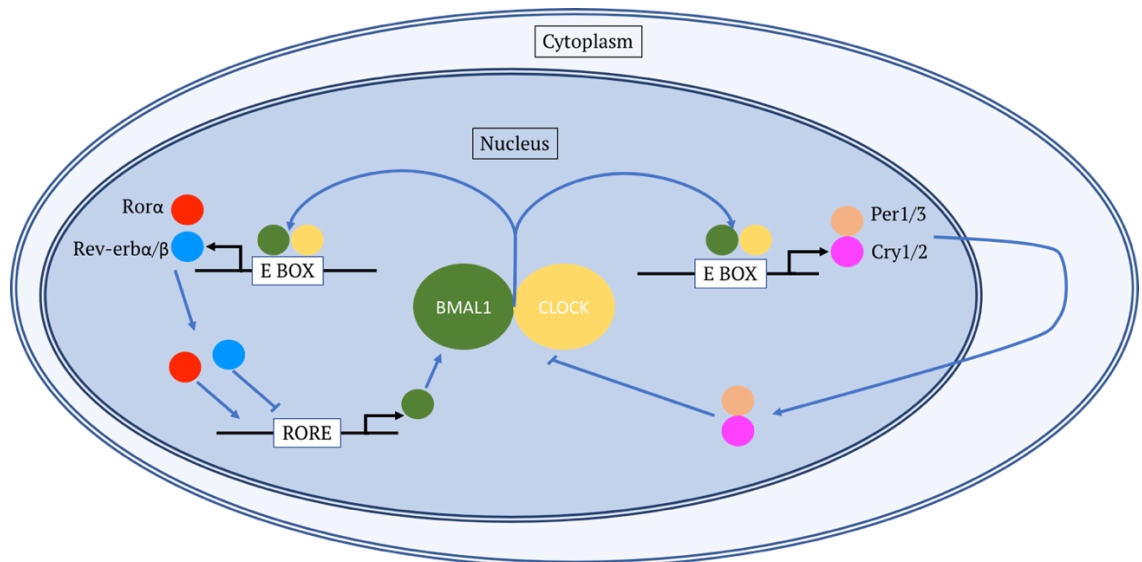


Figure. 1.16: ROR α role in the circadian rhythm. Diagram adapted from Weger et al. (2017).

1.8.14 ROR α in metabolism

Metabolism is a process that controls energy homeostasis and involves several coordinated systems including the circadian clock, gut microbiota, and the endocrine, immune and nervous systems. ROR α has been implicated in the control of metabolism and regulation of lipid and glucose metabolism (Cook et al., 2015). Indeed, *Rora* is expressed in tissues (liver, adipose tissue and skeletal muscle) and cells (ILC2s and macrophages) involved in metabolism and metabolic dysregulation. *Rora*^{sg/sg} mice are resistant to age- and diet-induced obesity, hepatosteatosis and insulin resistance (Lau et al., 2008, Lau et al., 2011, Lau et al., 2015). This is associated with reduced expression of genes associated with metabolism in *Rora*^{sg/sg} mice, including apolipoprotein A-1 (*apoA-1*) and apolipoprotein C-III (*apoC-III*) (Vu-Dac et al., 1997, Mamontova et al., 1998). Further analysis showed that there is an increased *RORA/Rora* expression in adipose tissue of obese humans and mice (Liu et al., 2017, Hams et al., 2020). We have recently reported that *Rora*^{fl/fl}*LysMCre* mice, which do not express *Rora* in myeloid cells, have a reduced weight gain when placed on high fat diet (HFD), compared to control (*Rora*^{fl/fl}) mice (Hams et al., 2020). Whilst *Rora*^{fl/fl}*Il7raCre* mice, a commonly used mouse to model ILC2 deficiency, had an increased weight gain in response to HFD compared to *Rora*^{fl/fl} mice (Hams et al., 2020). We have also shown that the cellular metabolism of macrophages is altered in the absence of *Rora*, with *Rora*-deficient macrophages increasing oxidative phosphorylation (Hams et al., 2021). Whilst conditional deletion of *Rora* in the liver using *Rora*^{fl/fl}*AlbCre* mice had exacerbated weight gain and insulin resistance in a model of diet-induced obesity, which was associated with enhanced transcriptional activity of proliferator-activated receptor- γ (PPAR γ) resulting in uncontrolled lipogenesis (Kim et al., 2017). This increase in PPAR γ in *Rora*^{fl/fl}*AlbCre* mice resulted in impaired negative self-regulation thus protecting against diet-induced hepatosteatosis (Kim et al., 2017).

ROR α was also shown to have a role in glucose metabolism. *Rora*^{sg/sg} mice have a decreased fasting blood glucose level, mildly improved glucose tolerance and increased insulin sensitivity in skeletal muscle, compared to WT mice (Lau et al., 2011). This was attributed to an increased expression of AKT2, which controls glucose uptake in skeletal muscle, in *Rora*^{sg/sg} mice (Lau et al., 2011). Further studies have also identified that

ROR α regulates both adipocyte glyceroneogenesis and hepatocyte gluconeogenesis (Kadiri et al., 2015).

1.8.15 ROR α in cerebellum development

Early studies identified that *Rora*^{sg/sg} mice have severe cerebellar ataxia due to cerebellar neurodegeneration and therefore ROR α has a role in cerebellum development (Sidman et al., 1962, Steinmayr et al., 1998, Dussault et al., 1998). It has since been shown that *Rora* is highly expressed in the brain and is crucial for maturation and maintenance of cerebellar Purkinje cells. ROR α regulates the expression of *Sonic hedgehog* (*Shh*) gene, which is required for the proliferation and survival of cerebellar granule precursors cells, through its activation of the Gli transcription factors. *Rora*^{sg/sg} mice produce less *Shh*, resulting in degeneration of cerebellar granule cells (Gold et al., 2003, Cook et al., 2015). Furthermore, it was shown that deletion of *Rora* from Purkinje cells between postnatal days 10-21 revealed that ROR α is required for the maintenance of Purkinje cells (Chen et al., 2013). *Rora*^{sg/+} mice develop a delayed loss of Purkinje cells after 6 months of age and at 12 months of age have a 35% loss of their Purkinje cells (Zanjani et al., 1992, Doulazmi et al., 2006). Interestingly, this age-related loss of Purkinje cells was more pronounced in male mice compared to female mice and was suggested due to a decrease in circulating sex steroids which have been shown to be neuroprotective (Janmaat et al., 2011).

1.8.16 ROR α and neuropsychiatric disorders

ROR α has reported roles in neuropsychiatric disorders such as autism, post-traumatic stress disorder (PTSD), bipolar disorder, schizophrenia and depression. ROR α is expressed in numerous psychiatrically-relevant regions of the brain such as the cerebral cortex, thalamus and the hypothalamus and known to be involved in cellular development of the Purkinje cells in the cerebellum (**Section 1.8.15**) (Ino, 2004, Chen et al., 2013). A GWAS study identified a ROR α SNP (rs4774388) was associated with the pathogenesis of autism spectrum disorder (ASD) (Sayad et al., 2017). Indeed, *RORA* expression was

reduced in the brains of autistic subjects and ROR α was hypermethylated in lymphoblastoid cell lines from autistic individuals, resulting in a decreased ROR α activity (Hu et al., 2015, Nguyen et al., 2010). It has been reported that disruption of *Rora/RORA* expression may have a greater impact on males, since males may experience greater dysregulation of genes relevant to autism in certain regions of the brain (Hu et al., 2015). ROR α was also associated with bipolar disorder as a GWAS study reported a significant association between bipolar disorder and the ROR α SNPs (rs4774388 and rs116939084) (Lai et al., 2015). Another study identified a direct molecular link between ROR α and miR137, a schizophrenia candidate gene enriched in the brain. It was shown that miR-137 targets the 3'UTR of ROR α in a site-specific manner to regulate expression (Devanna and Vernes, 2014). Another GWAS study identified *RORA* gene as a significant risk locus for PTSD (Logue et al., 2013). It was reported that lower expression of *RORA* was associated with beneficial treatment with therapeutic antidepressant drugs, and is therefore a potential transcriptional marker of antidepressant response (Hennings et al., 2015). Whilst it was also reported that there was an association with a ROR α SNP (rs17303244) and fear disorder (Miller et al., 2013). Thus, there is increasing evidence that ROR α has a role in many neuropsychiatric disorders, and may be a target for therapeutic benefit.

1.8.17 ROR α in immune cells

1.8.17.1 ROR α and macrophages

ROR α has roles in macrophage function and polarisation. Early studies showed that peritoneal macrophages isolated from *Rora*^{sg/sg} mice were hyperexcitable, with increased expression of *Il1 α* , *Il1 β* and *Tnf- α* in response to LPS stimulation compared to WT mice (Kopmels et al., 1992). It was shown that ROR α regulates suppressors of cytokine signalling 3 (SOCS3), a negative mediator of macrophage function and inflammation (Sun et al., 2015). We have shown a role for ROR α -expressing macrophages in the adipose tissue in altering the metabolic state of mice on a high-fat diet (HFD) (Hams et al., 2020). The primary cell populations expressing *Rora*-YFP in adipose tissue were inflammatory adipose tissue macrophages (ATM), with increased frequency of ATM in obese animals. When fed a HFD *Rora*^{fl/fl}*LysMCre* mice, which have a myeloid-cell specific deletion of *Rora*, developed increased weight gain with glucose sensitivity

compared to control animals. We further showed that deletion of *Rora* in myeloid cells is sufficient to impact on genes associated with thermogenesis, suggesting *Rora*-expressing macrophages not only impact on inflammation and obesity, but also regulate metabolic gene expression within the adipose tissue. This study highlights the importance of *Rora*-expressing macrophages in the context of the inflammation and metabolic alterations that underlie obesity (Hams et al., 2020). Recently, we reported that the cellular metabolism of macrophages is altered in the absence of *Rora*, with *Rora*-deficient macrophages increasing oxidative phosphorylation (Hams et al., 2021). ROR α has been shown to be involved in macrophage polarisation. Knockout of ROR α in liver specific macrophages, Kupffer cells (KC), or treatment with a ROR α inverse agonist (SR3335), resulted in increased pro-inflammatory M1 macrophage polarisation. Whilst KCs isolated treated with ROR α agonists SR1078, cholesterol sulfate and JC1-40, resulted in increased M2 polarisation (Han et al., 2017). MaR1 was identified as an endogenous ligand of ROR α and reportedly increased M2 polarity of liver macrophages (Han et al., 2019). Therefore, suggesting that ROR α promotes M2 macrophage polarisation.

1.8.17.2 ROR α and ILC2s cells

ILC2s are innate immune cells that are primarily tissue-resident, cytokine secreting immune cells, which are important in type 2 immunity (**Section 1.5.2.3.1**). ROR α has been shown to be a critical transcription factor in the development and expansion of ILC2s (Wong et al., 2012, Halim et al., 2012) (**Figure 1.17**). *Rora*^{sg/sg} mice have reduced ILC2s in lymph nodes, lung and fat-associated lymphoid clusters and have severely impaired expansion of ILC2s following IL-25 injection, intranasal papain administration, topical MC903 application and *N. brasiliensis* infection (Wong et al., 2012, Halim et al., 2012, Salimi et al., 2013). Indeed, *RORA* was expressed in *in vitro* expanded human ILC2s (Maggi et al., 2017). Whilst *Rora*^{sg/sg} BM chimera mice had reduced ILC2s (Lo et al., 2019). In support of this, treatment of WT mice with a ROR α inverse agonist (SR3335), reduced ILC2s in response to rhinovirus infection (Rajput et al., 2017). In addition, in a model of burned mice with *Enterococcus faecalis* infection, animals treated with SR3335 had reduced ILC2s (Ito et al., 2017). These studies provide further evidence for the critical role for ROR α in ILC2 development.

1.8.17.3 ROR α and ILC3 cells

ILC3s primarily reside in the intestinal mucosal tissue and are important for maintenance of gastrointestinal mucosal homeostasis (Zeng et al., 2019) (**Section 1.5.2.3**). ROR α has been shown to preserve ILC3 lineage identity and function during chronic intestinal infection (Lo et al., 2016) (**Figure 1.17**). It was shown that *Rora*^{sg/sg} BM chimera mice were protected from intestinal fibrosis in the *Salmonella*-driven model of Crohn's disease, due to reduced ILC3 production of IL-17A (Lo et al., 2016). Furthermore, it was shown that ROR α plays a role in preserving ILC3 fate under inflammatory conditions and that, in its absence, these cells have increased expression of *Tbet* and *Ifny* and have a phenotype characteristic of ILC1s (Lo et al., 2019). Therefore, in addition to its known role in ILC2 development, ROR α is reportedly important for ILC3 preservation and function.

1.8.17.4 ROR α and Th17 Cells

Th17 cells are known to participate in host defence against pathogens (**Section 1.5.2.1.1**). However, dysregulation of Th17 cells can lead to autoimmune diseases such as multiple sclerosis, rheumatoid arthritis and inflammatory bowel disease (Jetten, 2011). ROR γ t was shown to be critical for Th17 cell development (Ivanov et al., 2006). However, ROR γ t deficient mice did not have complete ablation of Th17 cells. This led to the discovery that ROR α is also required for Th17 cell development (Yang et al., 2008) (**Figure 1.17**). In this study, it was shown that ROR α is expressed in Th17 cells, and is induced by TGF β and IL-6 in a STAT3 dependent manner (Yang et al., 2008). Whilst overexpression of *Rora* in CD4 T cells drives Th17 differentiation. Furthermore, a deficiency in *Rora* reduced *Il17* and *Il23R* expression, key cytokine and cytokine receptor required for Th17 cell development. It was also shown that co-expression of ROR γ t with ROR α resulted in increased Th17 differentiation. Furthermore, mice lacking ROR α and ROR γ t displayed impaired Th17 cell generation, and these mice had increased protection from EAE, a Th17 mediated disease model associated with CNS inflammation (Yang et al., 2008). In support of these conclusions, similar effects were observed using knock-down of ROR γ t and ROR α expression in human T cells by small interfering RNA (siRNA). This revealed

that there is considerable overlap between ROR α and ROR γ t regulation of key Th17 genes such as IL-17A, *IL-17F*, *IL-23R*, CCL20 and CCR6 (Castro et al., 2017).

1.8.17.5 ROR α and Tregs cells

Tregs are important in suppressing inflammation and maintenance of homeostasis (Section 1.5.2.1.2). ROR α has recently been shown to have a role in Treg function (Figure 1.17). Indeed, *Rora* is expressed in Tregs in the skin, colon and mesenteric lymph nodes (MLN) (Schiering et al., 2014, Malhotra et al., 2018). It was shown that ROR α expression in skin Tregs restrains allergic skin inflammation (Malhotra et al., 2018). Conditional deletion of *Rora* in murine Treg cells (*Rora^{fl/fl}Foxp3^{exfp}Cre*) did not alter the number of skin resident Treg cells, but lead to exaggerated type 2 allergic skin inflammation. Whilst in response to topical application of MC903, a mouse model for atopic dermatitis, or epicutaneous application of OVA, *Rora^{fl/fl}Foxp3^{exfp}Cre* mice had exaggerated allergic skin inflammation (Malhotra et al., 2018). Therefore, suggesting that ROR α is important for Treg function.

1.8.17.6 ROR α and Th2 Cells

Th2 cells are critical in coordinating an adaptive type 2 immune response (Section 1.5.2.1.3). There is increasing evidence that ROR α may have a role in Th2 cells. Indeed, *RORA/Rora* is expressed in Th2 cells (Van Dyken et al., 2016, Maggi et al., 2017, Miragaia et al., 2019, Haim-Vilmovsky et al., 2020). Whilst mice challenged with papain and OVA, a model for type 2 inflammation, have increased *Rora* expression in lung Th2 cells (Liu et al., 2015). Interestingly, it is reported that the transcriptional and epigenetic status of lung Th2 and ILC2 cells shares a high degree of similarity, including expression of transcription factors *Rora*, *Gata3*, *Stat6* and *Bcl11b* (Van Dyken et al., 2016). Further analysis revealed that transcriptional and chromatin landscapes of lung Th2 cells from *N. brasiliensis* infected mice are closer related to lung ILC2s, compared to naïve CD4 T cells and Th2 cells from the lymph nodes (Shih et al., 2016). These data suggest that gene expression in Th2 cells and ILC2s may share the same evolutionarily origins.

Single-cell transcriptomics of the immune cells in human airways revealed that *RORA* was highly expressed T cells in both healthy controls and asthma patients (**Figure 1.15**) (Vieira Braga et al., 2019). A number of mouse studies using type 2 immune inducers have demonstrated *Rora* expression in Th2 cells. RNA-seq analysis of CD4 T cells from spleens of *N. brasiliensis* infected WT mice showed that *Rora* increased over the timecourse of infection. Studies using *Rora* reporter mice exposed to ragweed pollen (RWP), a common allergen which causes lung inflammation, revealed there was an increase in lung CD4 T cells expressing *Rora* (Haim-Vilmovsky et al., 2020). Notably, these ROR α expressing CD4 T cells had an activated phenotype characterised by CD44⁺SELL⁻ expression. Whilst further analysis revealed that following *N. brasiliensis* and *S. mansoni* infection, 83% and 71% of cells that expressed IL-4, IL-13 or IL-10 also expressed *Rora* (Haim-Vilmovsky et al., 2020). Therefore, *Rora* transcripts present in Th2 cells are more correlated with activated, cytokine secreting cells (Haim-Vilmovsky et al., 2020). In addition, scRT-PCR analysis of activated Th2 cells following *N. brasiliensis* infection, revealed a significant overlap of *Rora*, *Gata3* and *Foxp3* genes (Haim-Vilmovsky et al., 2020). It was also reported that there was increased *Rora* expression in murine memory T cells, and increased expression followed lymph tissue to non-lymphoid tissue migration (Miragaia et al., 2019). Therefore, there is accumulating evidence that ROR α has a role in the generation, activation and function of Th2 cells. However, complete understanding of the role of ROR α in Th2 cell biology remains elusive, and this will form the primary focus of this thesis.

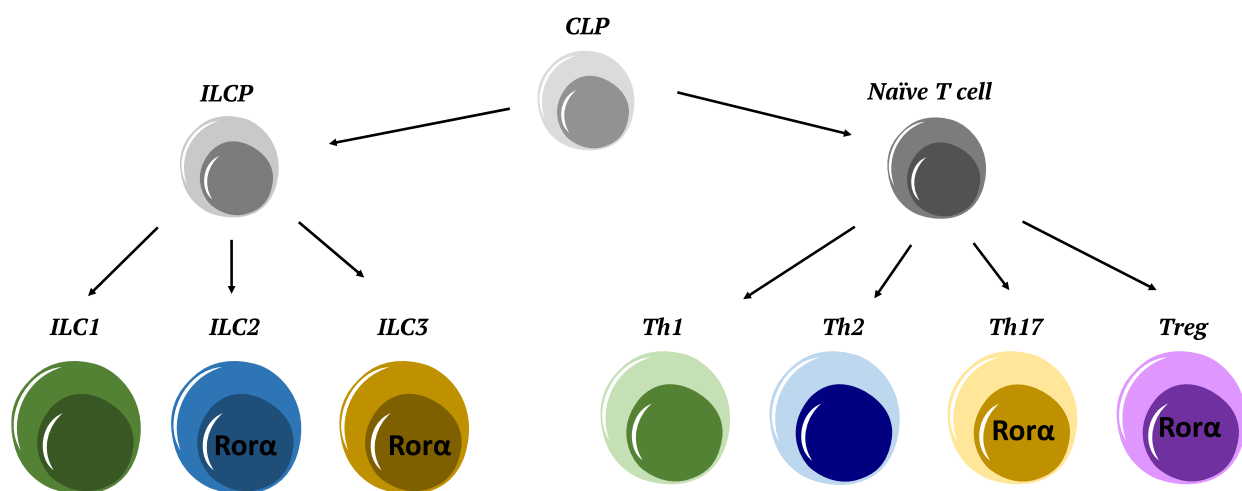


Figure 1.17: Overview of ROR α role in lymphoid cells.

1.9 Thesis objectives

I have outlined above the functional roles ROR α in cerebellar development, circadian rhythm and inflammation. In inflammatory disease ROR α has been shown to be required for the development of immune cells such as ILC2s and Th17 cells. The identification that ROR α was critical for the development of ILC2 cells was discovered using the type 2 inducing helminth *N. brasiliensis*. It was shown that in the absence of a functional ROR α (*Rora*^{sg/sg} mice), ILC2s failed to develop, and *N. brasiliensis* clearance is impaired (Wong et al., 2012, Halim et al., 2012). In this thesis, I will investigate the role of ROR α during a type 2 immune response using novel mouse models with a focus on the lungs to address functions beyond the known role of ROR α in ILC2 development.

The first objective in this thesis is to explore if *Rora* has a role in the regulation of distinct immune cells in the context of the type 2 inducing stimulus *N. brasiliensis* using *Rora*^{sg/sg} mutant mice and *Rora*^{sg/sg} BM chimera mice. Secondly, to identify *Rora* expressing cells in distinct immune cell populations I generated a *Rora* reporter mouse and explored *Rora* expressing cells in uninfected mice and following *N. brasiliensis* infection. The third objective in this thesis was to generate mice in which *Rora* was conditionally deleted in CD4- and Il7ra-expressing cells, using the Cre-Lox recombination technology, to further determine the role of *Rora* in CD4 and Il7ra expressing cells following *N. brasiliensis* infection. The final objective in this thesis was to explore the role of *Rora* during a non-helminth model of type 2 pulmonary inflammation by using the HDM model of allergic asthma-like lung inflammation.

Overall objectives:

- Analyse the role of *Rora* in inflammatory responses to *N. brasiliensis* using ubiquitous mutant *Rora* mice (*Rora*^{sg/sg}) and *Rora*^{sg/sg} BM chimera mice.
- Develop *Rora* reporter mouse to explore the expression of *Rora* in distinct immune cells.

- Develop conditional deleter mouse models using Cre-Lox recombination technology to explore the role of *Rora* has in CD4- and Il7ra-expressing cells.
- Analyse the role of *Rora* in inflammatory responses to HDM using ubiquitous mutant *Rora* mice (*Rora*^{sg/sg}), *Rora* reporter mice and *Rora* CD4 and Il7ra conditional deleter mice.

Chapter 2

Materials and Methods

Chapter 2 Materials and Methods

2.1 Mice

All mice used for experimental work in this thesis were on a C57BL/6J strain background. All mice were bred and housed in a Specific Pathogen-Free (SPF) facility in individually ventilated cages (IVC) under positive pressure. The temperature and humidity of the facility was maintained in the range of 20-24°C and 45-65%, respectively, in accordance with the EU legislation (2010/63/EU). The facility maintains a continuous cycle of 12:12 light cycle, with 7am-7pm of light and 7pm-7am of dark. Mice were fed an irradiated diet (Harlan, UK) and both food and water were supplied *ad libitum*. Mice were sex- and age-matched, with most mice being used at 8-12 weeks of age, and littermate control mice were used whenever possible. All animal experiments were performed in compliance with the Health Products and Regulatory Authority (HPRA) under individual authorisation number AE19136/I414 and approved by Trinity College Dublin's BioResources ethical review board under Project Licences AE19136/P071 and AE19136/P074.

2.1.1 B6.C3(Cg)-*Rorasg/J* Mice

B6.C3(Cg)-Rorasg/J mice, hereon referred to as *Rora^{sg/sg}* mice, have a natural mutation in the *Rora* gene resulting in a 6.5kb genomic deletion of an exon in the *Rora* gene encoding part of the ligand binding domain (Hamilton et al., 1996). *Rora^{sg/sg}* mice show a staggering gait, mild tremor, hypotonia, small size and shorter lifespan compared to WT littermates (Sidman et al., 1962) (**Figure 1.9**). *Rora^{sg/sg}* mice were originally purchased from the Jackson Laboratory (JAX strain number: 002651). Mice were subsequently bred and maintained in house under Project Licence AE19136/P071. Due to the decreased lifespan and phenotype of *Rora^{sg/sg}* mice, breeding harems were maintained as heterozygote pairs (Het). The obvious stunting in homozygous (Hom) progeny meant visual identification was possible, with subsequent confirmation by genotyping. Primers used in the polymerase chain reaction (PCR) to identify *Rora^{sg/sg}* mice as Het, Hom or

WT for the mutation are shown in **Table 2.1**. A representative agarose gel of PCR reaction products for *Rora*^{sg/sg} mice is visualised in **Figure 2.1**.

Primer	Primer Sequence	DNA Band (bp)
1233	TCTCCCTTCTCAGTCCTGACA	WT 318
1234	TATATTCCACCACACGGCAA	
1235	GATTGAAAGCTGACTCGTTCC	Mutant 450
1236	CGTTTGGCAAACCTCCACC	

Table 2.1: Primer sequence and predicted size of PCR product used in the genotyping of *Rora*^{sg/sg} mice.

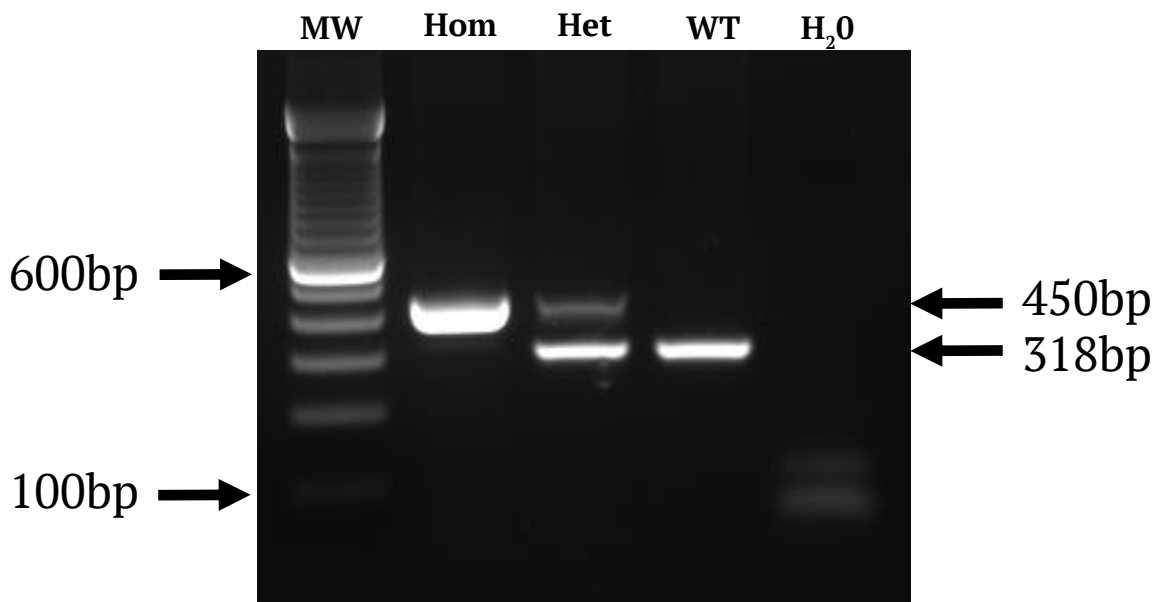


Figure 2.1: Agarose gel with PCR products for genotyping *Rora*^{sg/sg} mice.

2.1.2 *RoraCre* mice

RoraCre mice were kindly donated by Dr. Wirtz from Erlangen, Germany, with permission from Prof. O’Leary from The Salk Institute for Biological Studies, La Jolla, California, USA. These mice were originally generated by the O’Leary laboratory, by insertion of the IRES-Cre cDNA fragment into the 3’ noncoding region of the *Rora* gene (Wu et al., 2010, Chou et al., 2013). Cre expression in *RoraCre* mice was shown to be similar to endogenous *Rora* expression (Nakagawa and O’Leary, 2003). The primers for

genotyping of the *RoraCre* mice are listed in **Table 2.2**. These primers distinguish between WT, Het and Hom mice. The mutant PCR product is larger than that of WT mice due to the insertion of the Cre gene. Representative agarose gels of products from *RoraCre* PCR reactions are visualised in **Figure 2.2**.

Primer	Primer Sequence	DNA Band (bp)
<i>RoraCre</i> Forward	ATACCCAGACATTGTGCGAC	WT 250
<i>RoraCre</i> Reverse	TGTCTGTGCAGTGTTGTTGG	
Neo Forward	AGAGGCCACTTGTGTAGCGC	Mutant 370
<i>RoraCre</i> Reverse	TGTCTGTGCAGTGTTGTTGG	

Table 2.2: Primer sequence and predicted size of PCR product used in the genotyping of *RoraCre* mice.

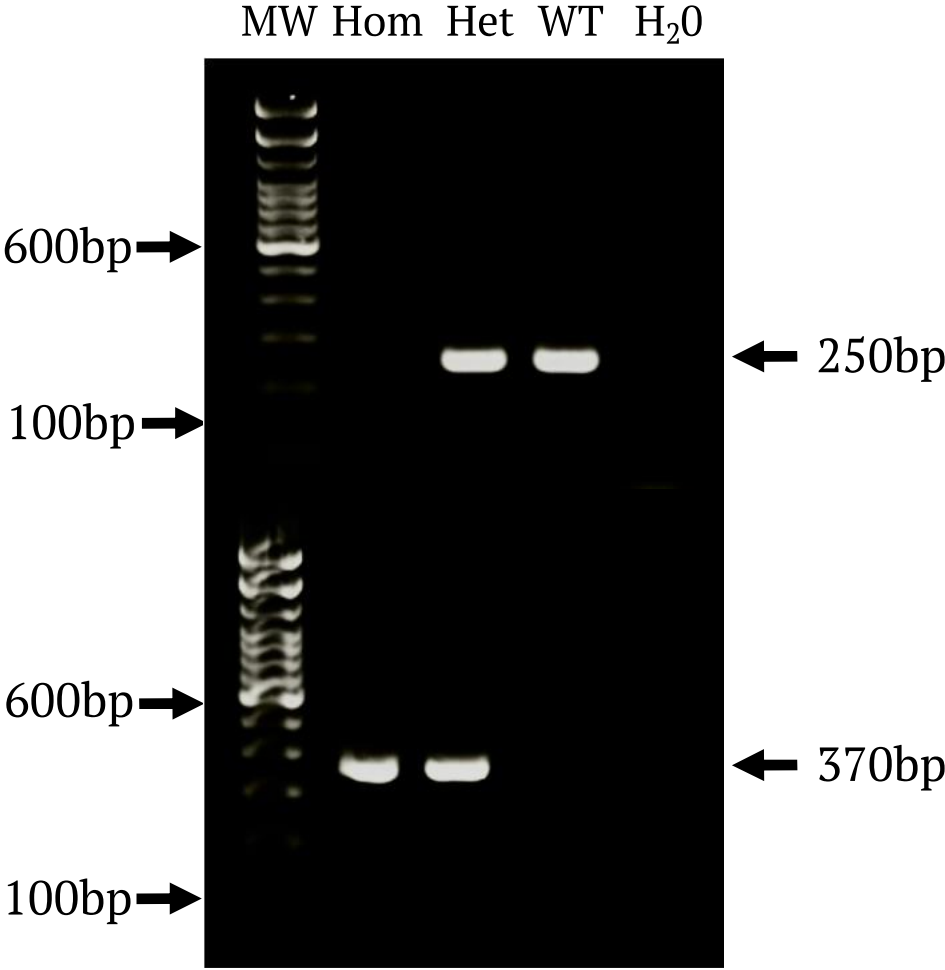


Figure 2.2: Agarose gel with PCR product for genotyping *RoraCre* mice.

2.1.3 B6.129X1-Gt(ROSA)26Sor^{tm(EYFP)Cos}/J Mice

B6.129X1-Gt(ROSA)26Sor^{tm(EYFP)Cos}/J mice were purchased from the Jackson Laboratory (JAX strain number: 006148) and are referred to as *RosaYFP*. These mice have a LoxP-flanked STOP sequence followed by the Enhanced Yellow Fluorescent Protein gene (EYFP) inserted into the Gt(ROSA)26Sor locus. Therefore, when these mice are crossed with mice expressing the Cre recombinase, the LoxP flanked STOP sequence is excised and the EYFP is expressed (Srinivas et al., 2001). These reporter mice were used to monitor the Cre expression in immune cells. The primers for *RosaYFP* mice are listed in **Table 2.3**. These primers distinguish between WT, Het and Hom mice. The mutant mice contain the inserted LoxP sites and therefore have a larger product size (384 bp) compared to the product size from WT mice (142 bp). A representative agarose gel of products from PCR reaction for *RosaYFP* mice is visualised in **Figure 2.3**.

Primer	Primer Sequence	DNA Band (bp)
21306	CTGGCTTCTGAGGACCG	WT 142
24500	CAGGACAACGCCACACA	
24951	AGGGCGAGGAGCTGTTCA	Mutant 384
24952	TGAAGTCGATGCCCTTCAG	

Table 2.3: Primer sequence and predicted size of PCR product used in the genotyping of *RosaYFP* mice.

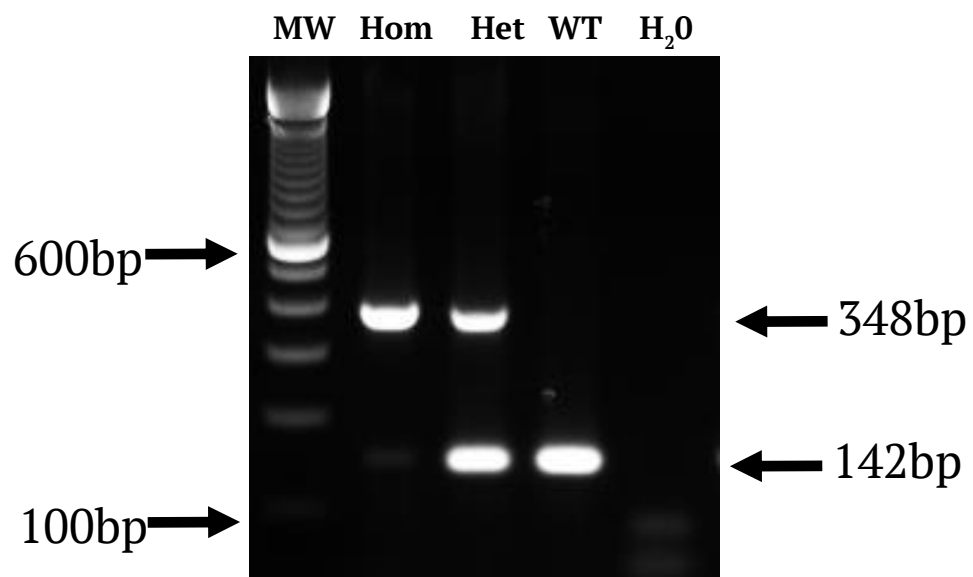


Figure 2.3: Agarose gel with PCR product for genotyping *RosaYFP* mice.

2.1.4 *Rora*^{fl/fl} Mice

Rora^{fl/fl} mice were generated by Lexicon Pharmaceuticals (NY, USA). A target vector containing Locus of X-over of P1 (LoxP) sites was inserted into exon 6 of the *Rora* gene on chromosome 9. The target vector also contains a pLF neomycin (pLFneo) selection cassette, used during transgenic mouse development (**Figure 2.4**). Therefore, cells with the targeted insertion will be resistant to neomycin, allowing for positive selection. As the pLFneo gene is inserted in between the LoxP sites, this gene will be excised in the presence of Cre recombinase.

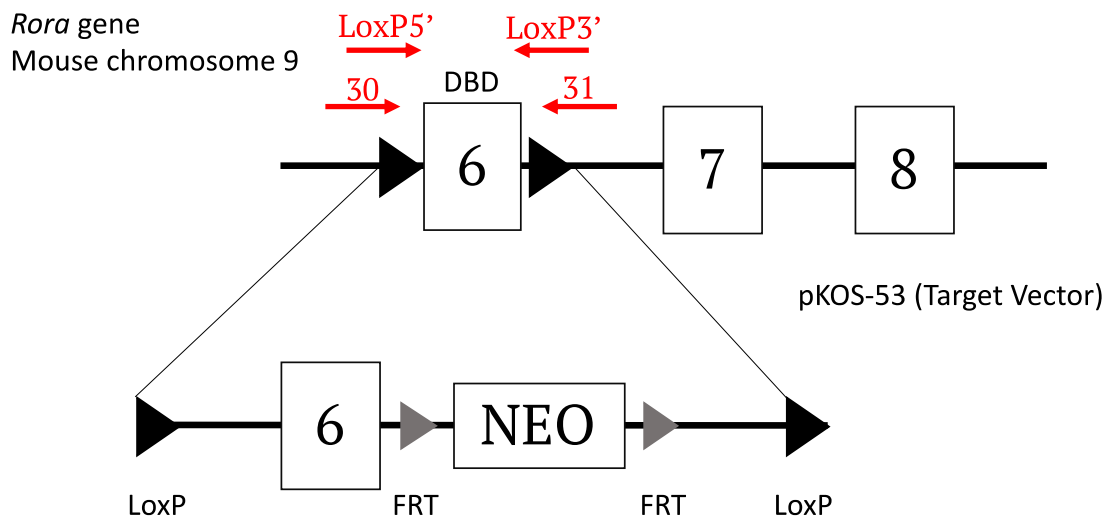


Figure 2.4: Targeting strategy in *Rora*^{fl/fl} mice.

To identify *Rora*^{fl/fl} mice, the genotyping is split into two separate reactions. The first reaction distinguished between WT and *Rora*^{fl/fl} by detecting the presence of the LoxP sites. The primers for this reaction are listed in **Table 2.4** (LoxP5' and LoxP3'). LoxP5' primer is complementary to a sequence located outside the floxed region, whilst LoxP3' is located to a sequence inside the floxed region. Therefore, given that there are two genomic regions (LoxP sites) inserted into the *Rora*^{fl/fl} mice, the PCR product for these mice will be larger, 394 bp, compared to the product from WT mice at 323 bp.

The second PCR reaction detects if the floxed gene sequence in *Rora* has been excised by Cre recombination. This occurs if the *Rora*^{fl/fl} mice are interbred with mice strains expressing Cre recombinase. The 30 and 31 primers (**Table 2.4**), are complementary to

sequences found in the *Rora* gene of both WT and *Rora^{fl/fl}* mice. These complementary sequences are found before and after the floxed region. Therefore, if Cre recombination occurs and excises the *Rora* genomic region, the sequence between the primers 30 and 31 will be shorter, thus have a smaller PCR product (408 bp) compared to the larger genomic sequence of the WT (596 bp). *Rora^{fl/fl}* targeting sequence is in **Appendix I**. Representative agarose gels of the products from both PCR reactions are visualised in **Figure 2.5**.

Primer	Primer Sequence	DNA Band (bp)
Lox P5'	TCTGAATCCACCATACTTCC	WT 323
Lox P3'	AGGTCTGCCACGTTATCTG	LoxP inserted 394
30	CAAGTCTCTGAATCCACCATAC	WT 596
31	CAACTGGCACAAAGGAAGGAC	Cre-Excision 408

Table 2.4: Primer sequence and predicted size of PCR product used in the genotyping of *Rora^{fl/fl}* mice.

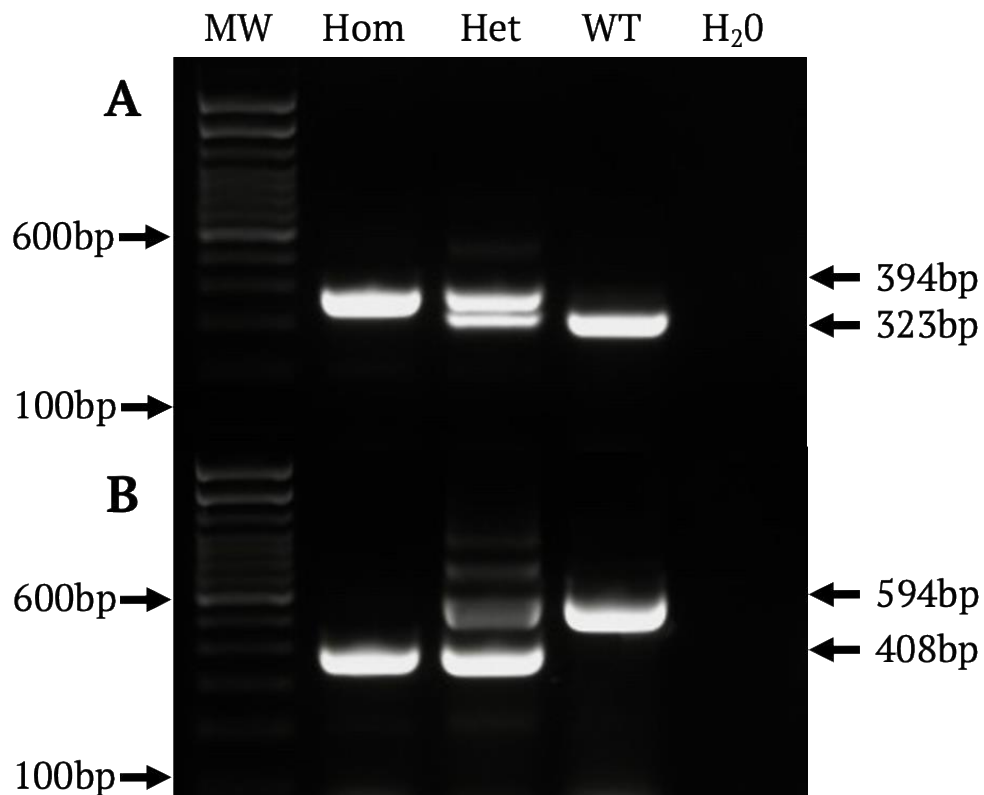


Figure 2.5: Agarose gel with PCR products for genotyping *Rora^{fl/fl}* mice. A, Detection of LoxP insertion in *Rora* sequence (Primers LoxP5 and LoxP3). B, Cre-mediated excision of *Rora* floxed sequence (Primers 30 and 31).

2.1.5 *Tg(Cd4-cre)1Cwi/BfluJ* Mice

Tg(Cd4-cre)1Cwi/BfluJ Mice, hereon in termed *CD4Cre* mice, were purchased from the Jackson Laboratory (JAX strain number: 017336). These mice contain CD4 enhancer, promoter, silencer sequence driving the expression of a Cre recombinase and is observed in CD4-expressing T cells (Sawada et al., 1994, Lee et al., 2001). Primers used in the PCR to identify *CD4Cre* mice as +ve or WT for the mutation are shown in **Table 2.5**. These primers do not distinguish between Het and Hom mice. The presence of the Cre recombinase is detected by a +ve PCR band, whilst WT mice have no PCR product. A representative agarose gel of products from *CD4Cre* PCR reactions is visualised in **Figure 2.6**.

Primer	Primer Sequence	DNA Band (bp)
531	CGATGCAACGAGTGATGAGG	Cre +VE = 250
819	GCATTGCTGTCACTTGGTCGT	WT = No product

Table 2.5: Primer sequence and predicted size of PCR product used in the genotyping of *CD4Cre* mice.

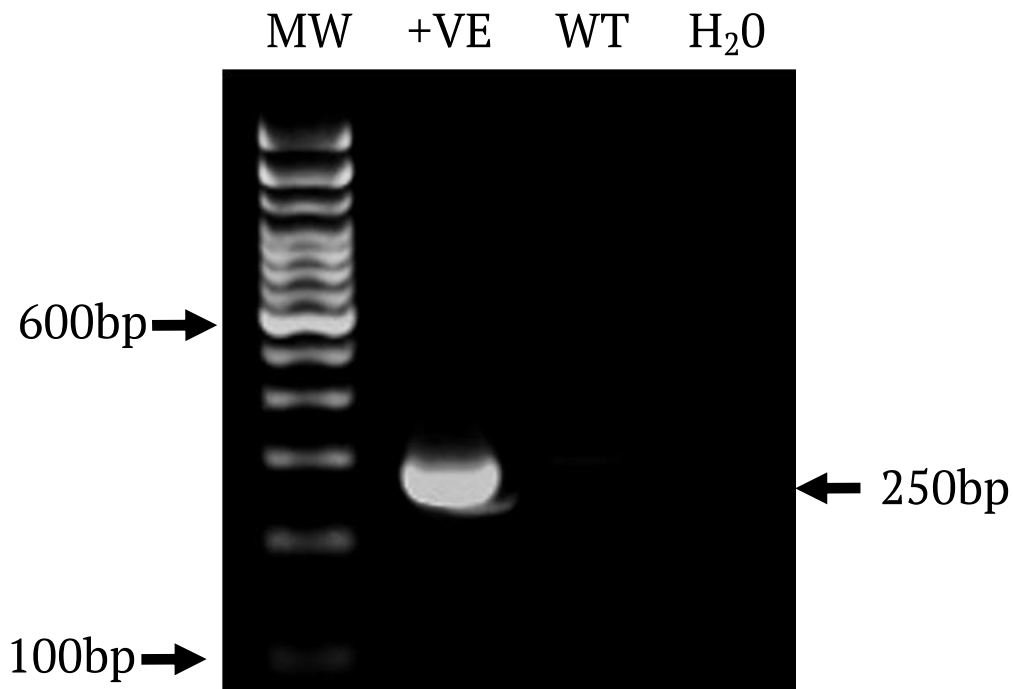


Figure 2.6: Agarose gel with PCR product for genotyping *CD4Cre* mice.

2.1.6 *Il7raCre* Mice

Il7raCre mice were kindly provided by Dr Andrew McKenzie (MRC-LMB, Cambridge, UK) with permission from Prof. Hans-Reimer Rodewald (Heidelberg, Germany). These mice have Cre recombinase in *Il7ra* expressing cells (Schlenner et al., 2010). The presence of the Cre recombinase produces a larger DNA band (600 bp) due to the inserted genomic region compared to the WT band (400 bp). Primers used in the PCR to identify *Il7raCre* mice as Hom, Het or WT for the mutation are shown in **Table 2.6**. A representative agarose gel of products from *Il7raCre* PCR reactions is visualised in **Figure 2.7**.

Primer	Primer Sequence	DNA Band (bp)
4909	CCTGAAAAC TTTGCCCCCTCCATA	Cre 600
4910	CCATAGAATAGTGCAGCCTTGCCTC	WT 400
4911	AGCGAAAGCTCTACCCAGAGC	

Table 2.6: Primer sequence and predicted size of PCR product used in the genotyping of *Il7raCre* mice.

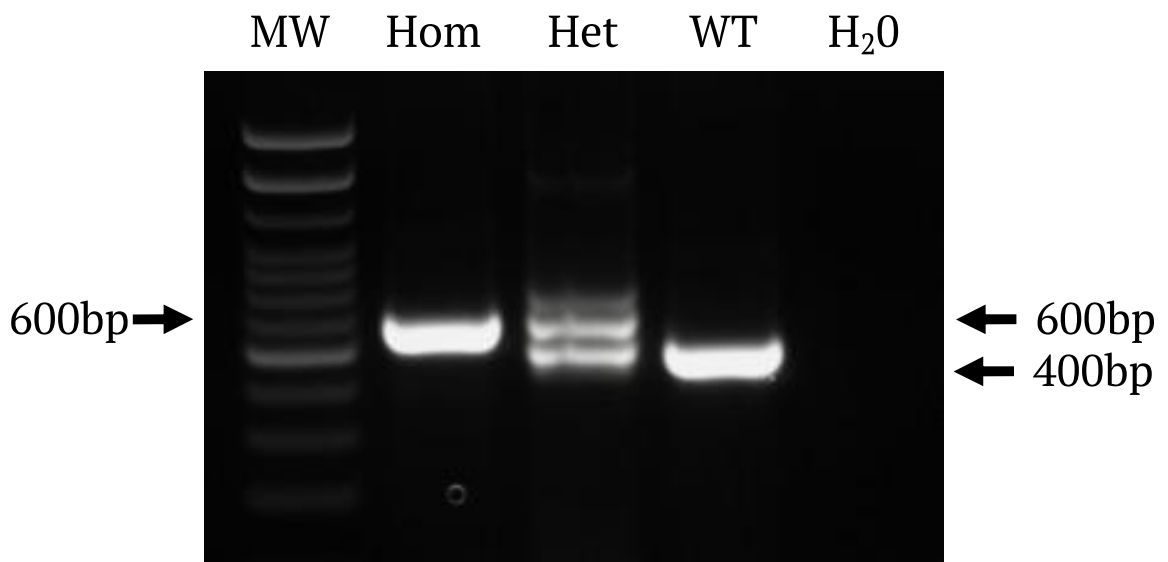


Figure 2.7: Agarose gel with PCR product for genotyping *Il7raCre* mice.

2.1.7 *B6.SJL-Ptprc^aPeprc^b/BoyJ* Mice

B6.SJL-Ptprc^aPeprc^b/BoyJ mice were purchased from the Jackson Laboratory (JAX strain number: 002014) and are referred to as CD45.1 mice. CD45 (protein tyrosine phosphatase, receptor type C) is encoded by *Ptprc* gene and is a surface marker on all haematopoietic cells, except erythrocytes and platelets (Jafri et al., 2017). CD45.1 mice express a differential pan leukocyte marker *Ptprc^a* compared to C57BL/6 mice which express *Pprc^b* allele (CD45.2) (Shen et al., 1985). CD45.1 mice were kept as Hom breeding harems, and therefore did not require identification by genotyping. Instead, these mice could be identified by flow cytometry. Therefore, CD45.1 murine cells express CD45.1 and not CD45.2 when assessed by flow cytometry (**Figure 2.8**).

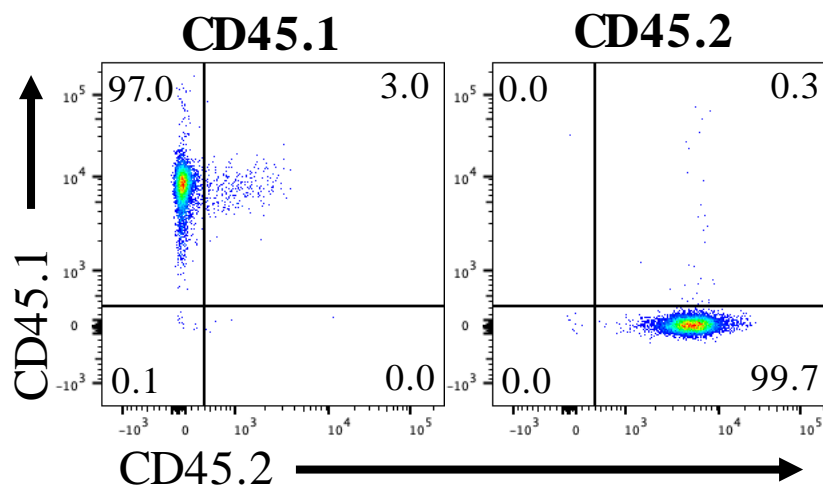


Figure 2.8: Representative flow cytometry plots of CD45.1 and CD45.2 murine spleen cells. Cells gated as lymphocytes, single cells, live, CD45.1 and CD45.2. The number on flow plot represents percentage of parent gate.

2.2 Cre-LoxP system

The Cre-LoxP recombination system is a site-specific recombination technology which has played an important role in the understanding of many biological processes over the past 30 years. This technology enables generation of specific gene deletions, insertions, translocations and inversions (Sauer, 1998). Cre recombinase is a 38-kDa protein encoded by bacteriophage P1. This enzyme causes site specific recombination between two LoxP

sites, a 34-bp region with two 13 bp inverted regions flanking an 8 bp core motif (**Figure 2.9**) (Metzger and Feil, 1999). Cre efficiently excises DNA flanked by LoxP recognition sites in cultured mammalian cells and in mice (Metzger and Feil, 1999) (**Figure 2.10**).

5' ATAACTTCGTATAATGTATGCTATACGAAGTTAT 3'

Figure 2.9: The 34-bp LoxP sequence containing an 8-bp core (underlined) flanked by two 13-bp inverted regions where recombination occurs.

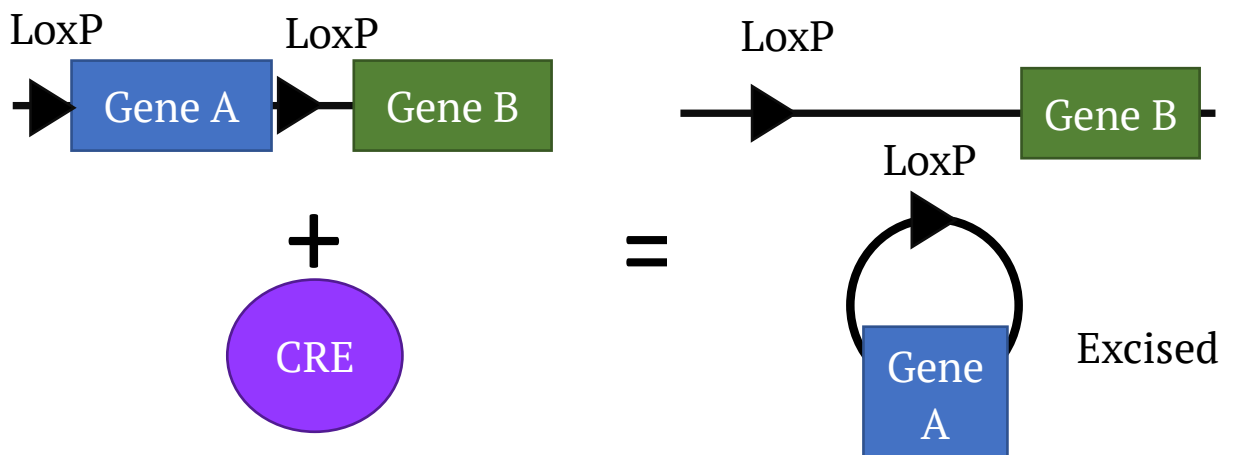


Figure 2.10: Diagram of Cre-LoxP recombination for specific targeted deletion of Gene A.

2.3 Generation of the *Rora* reporter mouse

2.3.1 *Rora* reporter Mice

Rora reporter mice were generated as previously described in Malhotra et al. (2018). To generate *Rora*^{Cre/Cre}*Rosa*^{YFP/YFP} (*Rora* reporter) mice, *Rora*^{Cre/+} mice (**Section 2.1.2**) were crossed with *Rosa*^{YFP/+} mice (**Section 2.1.3**) to generate *Rora*^{Cre/+}*Rosa*^{YFP/+} mice. The *Rora*^{Cre/+}*Rosa*^{YFP/+} mice were backcrossed with *Rora*^{Cre/+}*Rosa*^{YFP/+} to generate *Rora*^{Cre/Cre}*Rosa*^{YFP/YFP} mice (**Figure 2.11**). These mice were used to assess *Rora* expressing immune cell populations by flow cytometry.

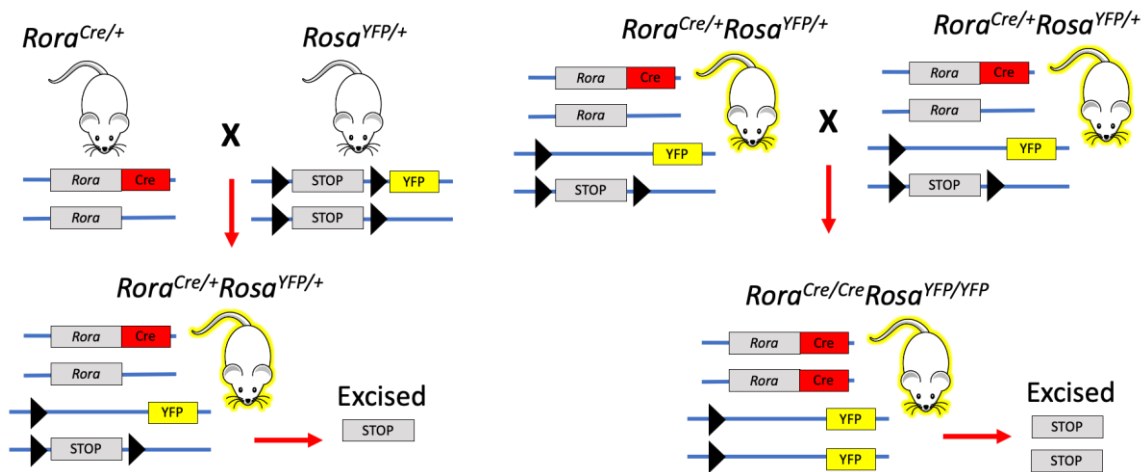


Figure 2.11: Generation of *Rora* reporter mice.

2.4 Generation of conditional *Rora* knock-out mice

The Cre-LoxP technology was first used to generate a mouse model in 1993. The mouse model generated a conditional inactivation of a target gene in a selected cell population (Gu et al., 1993). In germ-line knockout mice, the target gene is inactive in all cells. However, in conditional knockout mice, the gene inactivation is determined by the nature of Cre and its expression pattern. This technology was utilised in this thesis to generate *Rora*^{fl/fl}*CD4Cre* (Halim et al., 2018) and *Rora*^{fl/fl}*Il7raCre* (Oliphant et al., 2014) mice.

2.4.1 *Rora*^{fl/fl}*CD4Cre* Mice

Rora^{fl/fl}*CD4Cre* mice were generated to excise *Rora* from CD4 expressing cells (Halim et al., 2018). To generate *Rora*^{fl/fl}*CD4Cre* mice, homozygous *Rora*^{fl/fl} mice (Section 2.1.4) were crossed with *CD4Cre* mice (Section 2.1.5) to generate *Rora*^{fl/+}*CD4Cre* mice. The progenies were interbred with a homozygous *Rora*^{fl/fl} mouse generating *Rora*^{fl/fl}*CD4Cre*, which are the genotype of the experimental mice used within this thesis (Figure 2.12). Cre-mediated excision of *Rora* is detected by PCR (Figure 2.5). The *Rora*^{fl/fl}*CD4Cre* mice were comparable to WT mice in both size and phenotype and did not develop the ataxia and hypotonia observed in *Rora*^{sg/sg} mice.

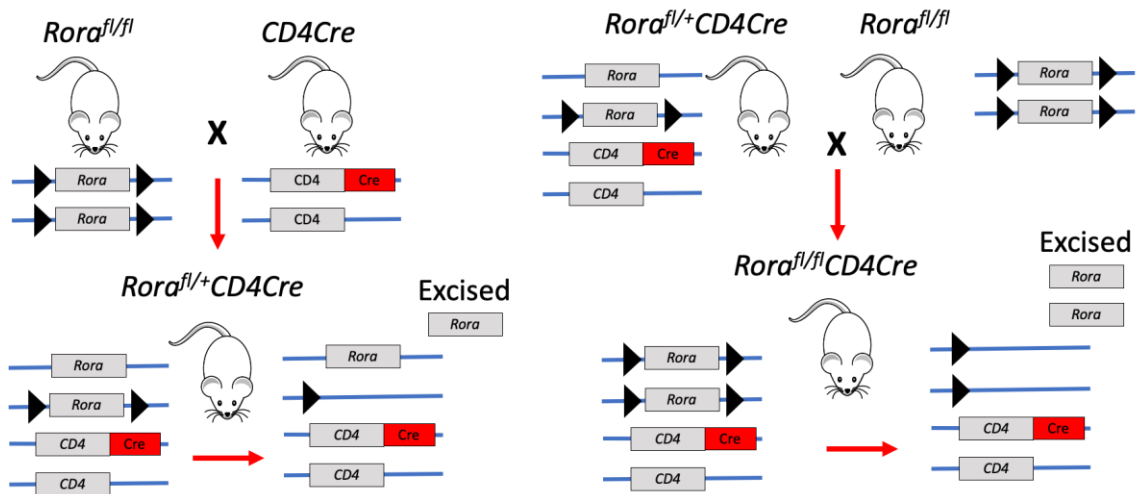


Figure 2.12: Generation of $Rora^{fl/fl}CD4Cre$ mice.

2.4.2 $Rora^{fl/fl}Il7raCre$ Mice

$Rora^{fl/fl}Il7raCre$ mice were generated to excise $Rora$ from $Il7ra$ expressing cells (Oliphant et al., 2014). To generate $Rora^{fl/fl}Il7raCre$ mice, $Rora^{fl/fl}$ mice (Section 2.1.4) were crossed with $Il7raCre$ mice (Section 2.1.6). Approximately, 50% of the progeny would be $Rora^{fl/+}Il7raCre$. These mice would then be backcrossed with $Rora^{fl/fl}$ mice to generate $Rora^{fl/fl}Il7raCre$ mice (Figure 2.13). These mice have $Rora$ excised in $Il7ra$ expressing cells (ILCs, T and B cells). Cre-mediated excision of $Rora$ is detected by PCR (Figure 2.5). The $Rora^{fl/fl}Il7raCre$ mice were also comparable to WT mice in size and phenotype.

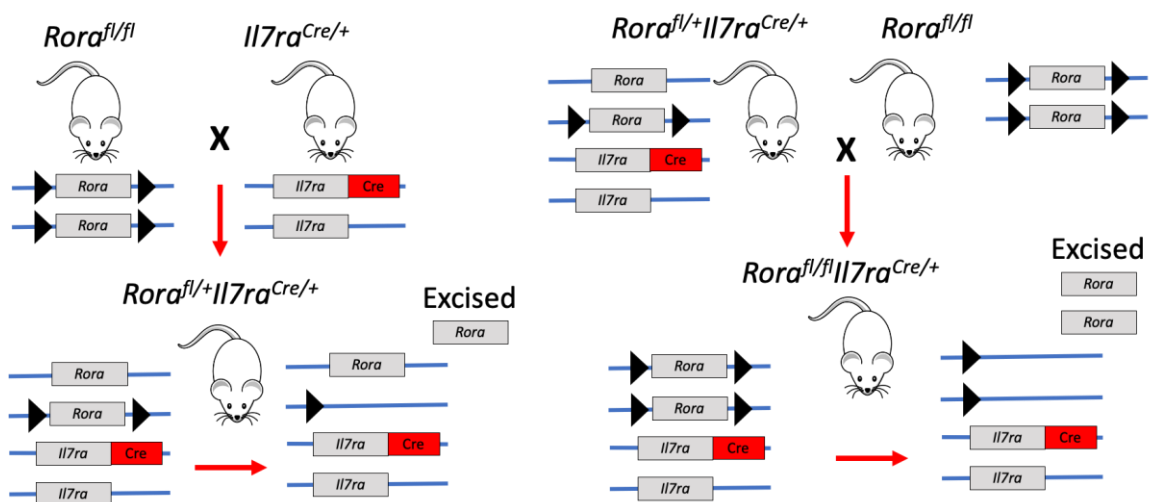


Figure 2.13: Generation of $Rora^{fl/fl}Il7raCre$ mice.

2.5 Isolation of bone marrow (BM) cells

Mice were euthanized by cervical dislocation. The hind legs were aseptically dissected, ensuring not to damage the bones, and stored in sterile RPMI-1640 on ice. The skin and muscle were removed, and the ends of the bones were surgically cut with a scalpel. The bone marrow cavity was washed with RPMI-1640 media, using a 27G needle and a 5 ml syringe. The bone marrow cells were filtered through a 70 μm cell strainer and then centrifuged at 1500 RPM for 5 mins at 4°C. The supernatant was discarded, and red blood cells lysed using 2 ml BD Lysis Buffer. Cells were resuspended in PBS at a density appropriate for reconstitution and generation of BM chimera mice (**Section 2.6**).

2.6 BM Chimera Generation

The use of BM chimera mice allows for the analysis of the function of genes that are expressed in cells of hematopoietic versus non-hematopoietic origin (Duran-Struuck and Dysko, 2009). The use of tagged congenic mice, CD45.1⁺ or CD45.2⁺ cells, allows analysis of successful reconstitution of the bone-marrow in the recipient mice. BM chimeras were generated based on laboratory methods used in Aviello et al. (2014). Recipient mice are sub-lethally irradiated using an X-Ray irradiator (XStrahl CIX3), by receiving a 5 Gray (Gy) dose followed by a 4 Gy separated by a 3-hour rest period. Recipient mice are then reconstituted with donor mice bone marrow cells (1×10^7) injected intravenously through the tail vein. The mice are monitored and scored daily to ensure animal welfare is not impacted. In brief, scoring included assessing body condition and behaviour (score 0, none; score 1, mild; score 2, moderate; score 3, severe). The haematopoietic compartment was left for 6 weeks to repopulate and blood samples were taken to assess immune reconstitution efficiency. After 2 weeks post-blood collection (8 weeks post reconstitution) mice have recovered haematologically (Raabe et al., 2011) and were used for experiments (**Figure 2.14**).

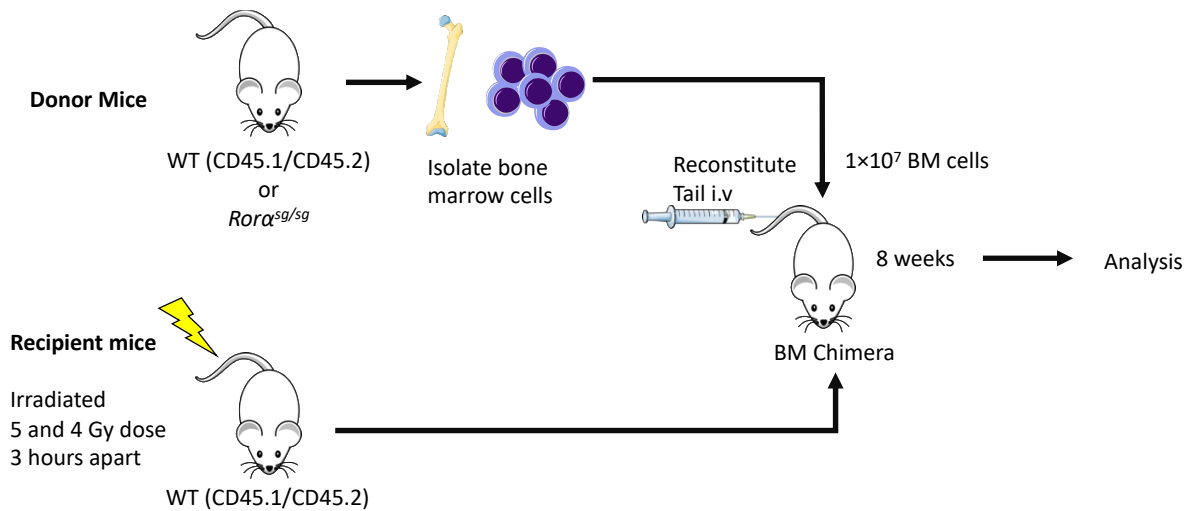


Figure 2.14: Diagram showing generation of bone marrow chimera mice.

As a side effect of generating BM chimera mice, irradiation affects rapidly dividing cells which can be observed in the hair follicles that turn grey over time (Potten, 1970). This can be visually seen in aged bone marrow chimera mice compared to age matched WT mice that have not been irradiated (**Figure 2.15**).

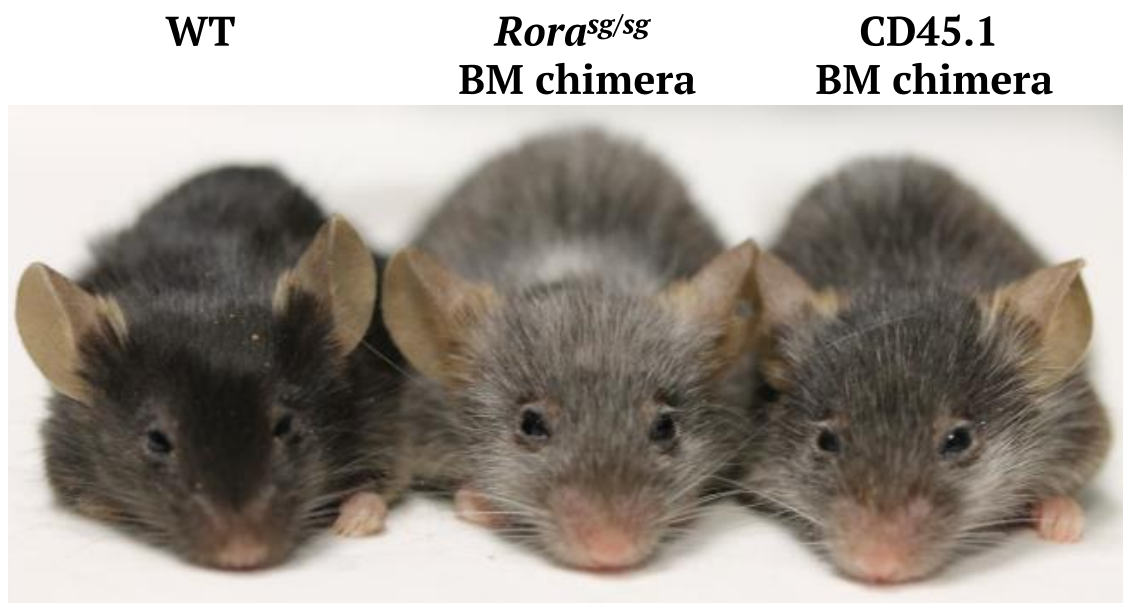


Figure 2.15: Representative photo of age-matched WT and *Rora*^{sg/sg} BM and CD45.1 BM chimera mice.

To confirm the efficiency of BM reconstitution, I generated a 4-way BM chimera model (**Figure 2.16**). Recipient CD45.1 and CD45.2 mice were irradiated and reconstituted with either CD45.1 or CD45.2 BM cells. At 8 weeks post irradiation and reconstitution, mice

were sacrificed and analysed by flow cytometry to assess reconstitution efficiency of CD45.1 and CD45.2 cells.

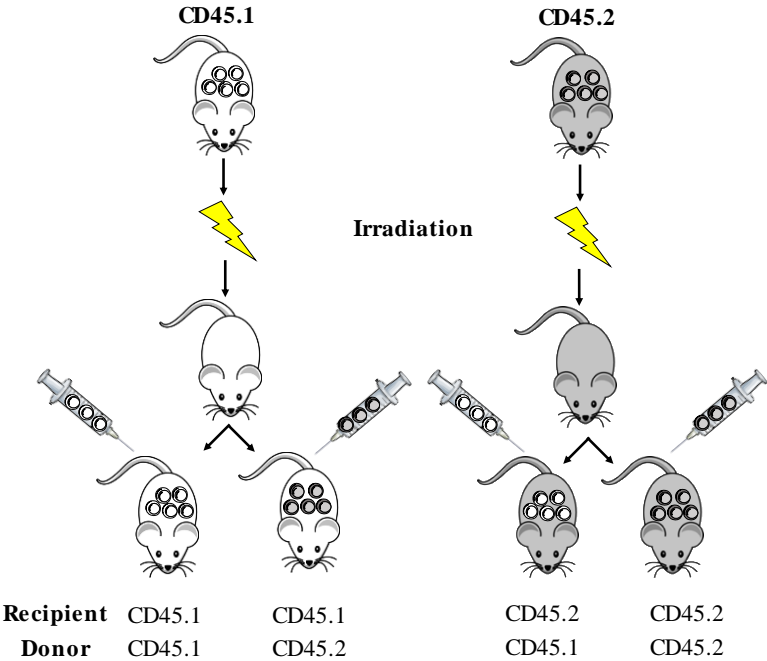
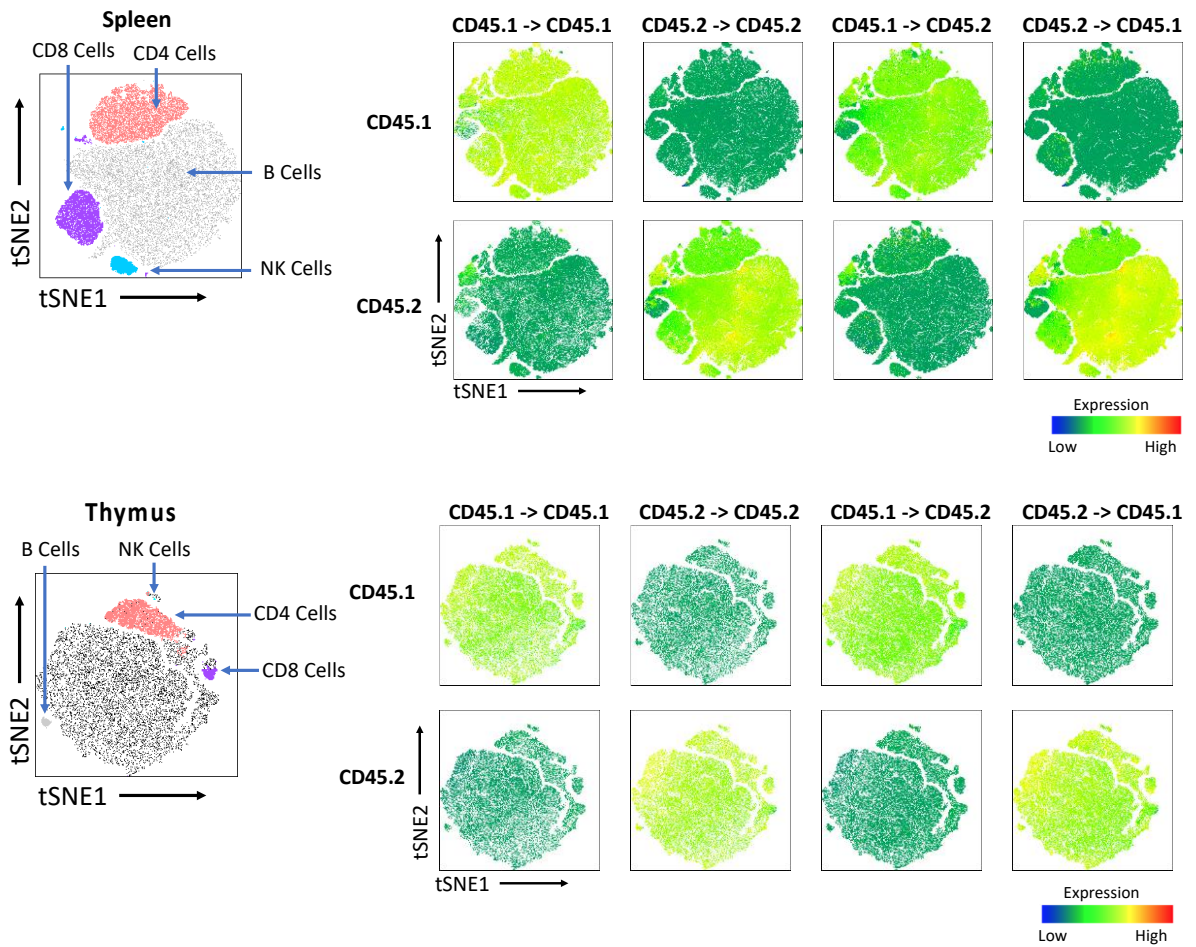


Figure 2.16: Outline of 4-way bone marrow chimera generation to confirm reconstitution efficiency. CD45.1 and CD45.2 recipient mice were irradiated with 9 Gy dose. Recipient mice were reconstituted with 1×10^7 bone marrow cells from either WT CD45.1 or CD45.2.

The reconstitution efficiency was >95% in murine spleen and thymus cells (**Figure 2.17**). Therefore, confirming that this is a viable technique to assess the function of cells from hematopoietic versus non-hematopoietic origin.

A



B

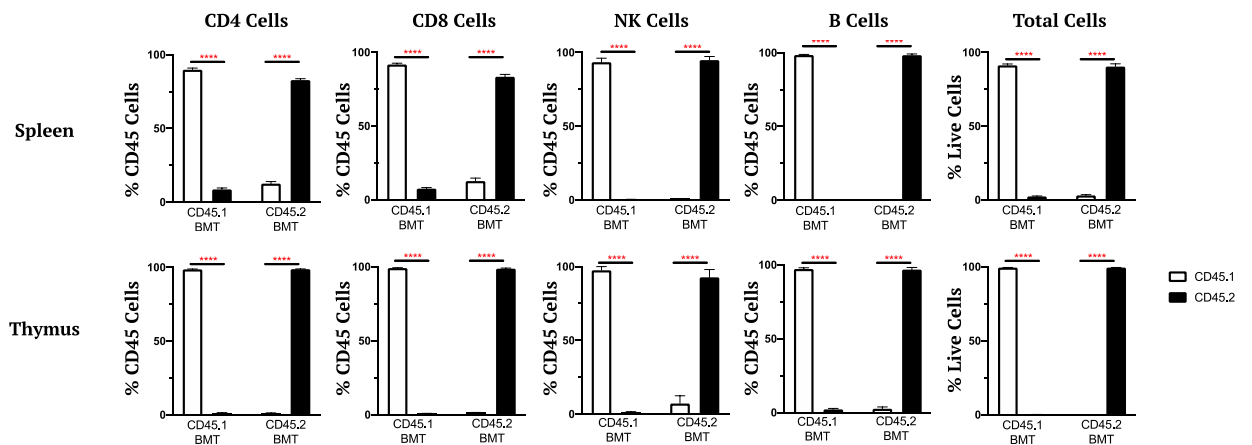


Figure 2.17: 4-way BM chimera mice reconstitution efficiency. CD45.1 and CD45.2 recipient mice were irradiated and reconstituted with BM cells from either CD45.1 or CD45.2. **A**, tSNE analysis. CD45.1 and CD45.2 marker expression in spleen, thymus. Cells populations were gated as cells, single cells, live cells. CD4 cells were CD3⁺CD4⁺, CD8 cells were CD3⁺CD8⁺, B cells were CD3⁻CD19⁺ and NK cells were CD19⁻CD3⁻NK1.1⁺. tSNE plots are concatenates of all the samples for group. **B**, Quantification of 4-way BM chimera reconstitution efficiency of spleen and thymus. CD45.1 BMT = CD45.1

bone marrow transferred into a CD45.2 recipient mice. CD45.2 BMT = CD45.1 bone marrow transferred into a CD45.1 recipient mice. mice per group. Data is representative of means \pm SEM. Differences indicated as two-tailed p values, as assessed by unpaired Student t test. **** $p < 0.0001$. $n = 5$.

2.7 Genotyping and identification of mouse strains

2.7.1 Mice Ear Lysis

The ears of the mice were punched when weaning to allow for identification and also to provide samples for genotyping. The 0.2 cm diameter ear punches were lysed by adding 100 μ l of Direct PCR (Ear) lysis reagent (Viagen, CA) and Proteinase K (20mg/ml) from *Tritirachium album* (Sigma, UK). Proteinase K is a serine protease that cleaves the peptide bonds next to the carboxyl group of hydrophobic amino acid residues, thus breaking down protein in samples allowing for isolation of genomic DNA. The samples were incubated for 3 hours at 55°C with vortexing hourly. Proteinase K was inactivated by heating at 85°C for 45 minutes and genomic DNA samples were used for PCR analysis (**Section 2.7.2**) or stored at -20°C.

2.7.2 Polymerase Chain Reaction (PCR)

Polymerase Chain Reaction (PCR) is used to amplify a single copy of a DNA segment. All PCR reactions were performed using the DNA Engine® Thermal Cycler (Bio-Rad) and PCR protocols used in this thesis are in **Appendix II**. A hot-start step of 94-96°C is required to heat activate the DNA polymerase. Followed by a series of cycles of denaturation (94-98°C for 20-30 seconds) which breaks the hydrogen bonds between DNA strands forming two single-stranded DNA molecules; annealing (50-60°C for 20-40 seconds) of the primers to the single-stranded DNA; and elongation (72-80°C for 15 sec – 7 min) in which DNA Taq polymerase synthesizes a new DNA strand complementary to the DNA template by adding free dNTPs. The cycle of denaturation, annealing and elongation is repeated for 25-40 cycles until a final elongation step, after this point the PCR product is stable at 4°C.

2.7.3 Agarose gel electrophoresis

The amplified PCR products were separated based on size by agarose gel electrophoresis. PCR products were run on a 1.5% agarose gel. A 1.5% agarose gel was prepared by mixing 1.5 g of agarose (Sigma, UK) in 100ml of Tris-borate ethylenediaminetetraacetic acid (TBE). The solution was heated to dissolve the agarose gel, once slightly cooled 1.5µl of 20 mg/ml ethidium bromide (EtBr) (Sigma, UK) was added. The EtBr binds to the amplified DNA which can then be visualised under UV light. The solution was poured into a UV transparent gel casting tray with a comb of appropriate number of wells. After approximately 30 minutes the solution cooled and solidified, and the gel was placed into a gel rig (Bio-Rad). 10 µl of sample was loaded into each well and a lane containing 6 µl of DNA ladder (size: 100-1500 bp, Invitrogen, UK) was added to allow for the size of the PCR products to be determined. The gel was run for 40 minutes at 100 volts and 400 amps using a PowerPac Universal Power supply (Bio-Rad). The DNA bands were visualised using the Fusion FX (Vilber Lourmat, Germany).

2.8 *In vivo* models

2.8.1 *Nippostrongylus brasiliensis* (Nb) lifecycle

Nippostrongylus brasiliensis belongs to the phylum Nematoda and the superfamily Trichostrongyloidea, with the rat as its natural host. The development of *N. brasiliensis* within the host resembles that infection with the hookworms *Necator americanus* and *Ancylostoma duodenale* in man. *N. brasiliensis* is a potent activator of both systemic and mucosal type 2 immune responses and has been extensively used to study host protective immunity, and *in vivo* regulation of type 2 immune responses.

The life cycle of *N. brasiliensis* consists of 5 distinct larval stages (L1-5) with both an external free living (L1-3) and host living (L3-5) stages. The L1 *N. brasiliensis* hatch from eggs after 24 hours at 26°C. Over the next 48 hours, the *N. brasiliensis* undergo two rounds of moulting to reach L3 stage. The L3 larvae are the infective stage and can penetrate the skin and migrate through the vasculature to reach the lungs (day 1 and 2

post-infection), the larvae are coughed up and swallowed, and reach the intestine within 3 to 4 days from the time of infection (**Figure 2.18**). Once in the intestine, *N. brasiliensis* complete their development into adults (day 5). Males measure $3.0\text{--}4.5 \times 0.08\text{--}0.10$ mm, while females measure $4\text{--}6 \times 0.09\text{--}0.13$ mm. By day 6 the L5 have reached the small intestine, where they mate and produce fertile eggs that are passed out from the host in the faeces. Eggs are ellipsoidal with thin shells and measure $50\text{--}70 \times 27\text{--}40$ μm . The host defences cause expulsion of the worms from the gut, and resolution of the infection is complete within 2 weeks in immune competent mice (Camberis et al., 2003).

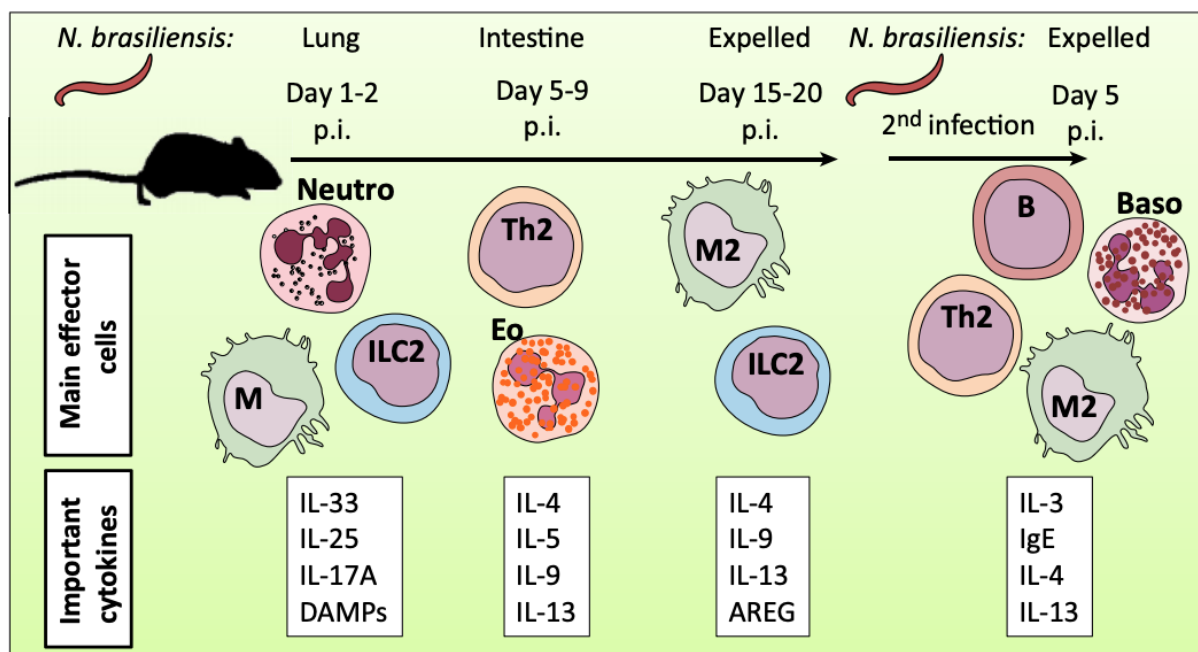


Figure 2.18: The prototypical type 2 immune response against *N. brasiliensis*. (Schwartz et al., 2018)

2.8.2 Lifecycle of *N. brasiliensis* in the rat

Wistar rats were used as a vehicle to generate large numbers of *N. brasiliensis* larvae, which were then used to infect mice for experiments. Rats are the natural host for *N. brasiliensis* and can tolerate a higher infection burden than mice, which enabled collection of a larger number of eggs in the faeces. The lifecycle of *N. brasiliensis* in the rat is outlined in **Figure 2.19**. Female Wistar rats of 150-200 g were injected subcutaneously with 5000 L3 *N. brasiliensis*, using a 23G needle. At day 5 post infection, the rats were placed on a metal grid and on days 6, 7, 8 and 9 faecal pellets were collected.

The faeces were then mashed into a smooth paste and mixed in an equal amount of activated charcoal (Honeywell, USA) (**Figure 2.20**). The charcoal is prepared by continuously washing with reverse osmosis water to remove small fine charcoal particles. The charcoal provides a culture environment suitable for larval development that mimics conditions in the nature.

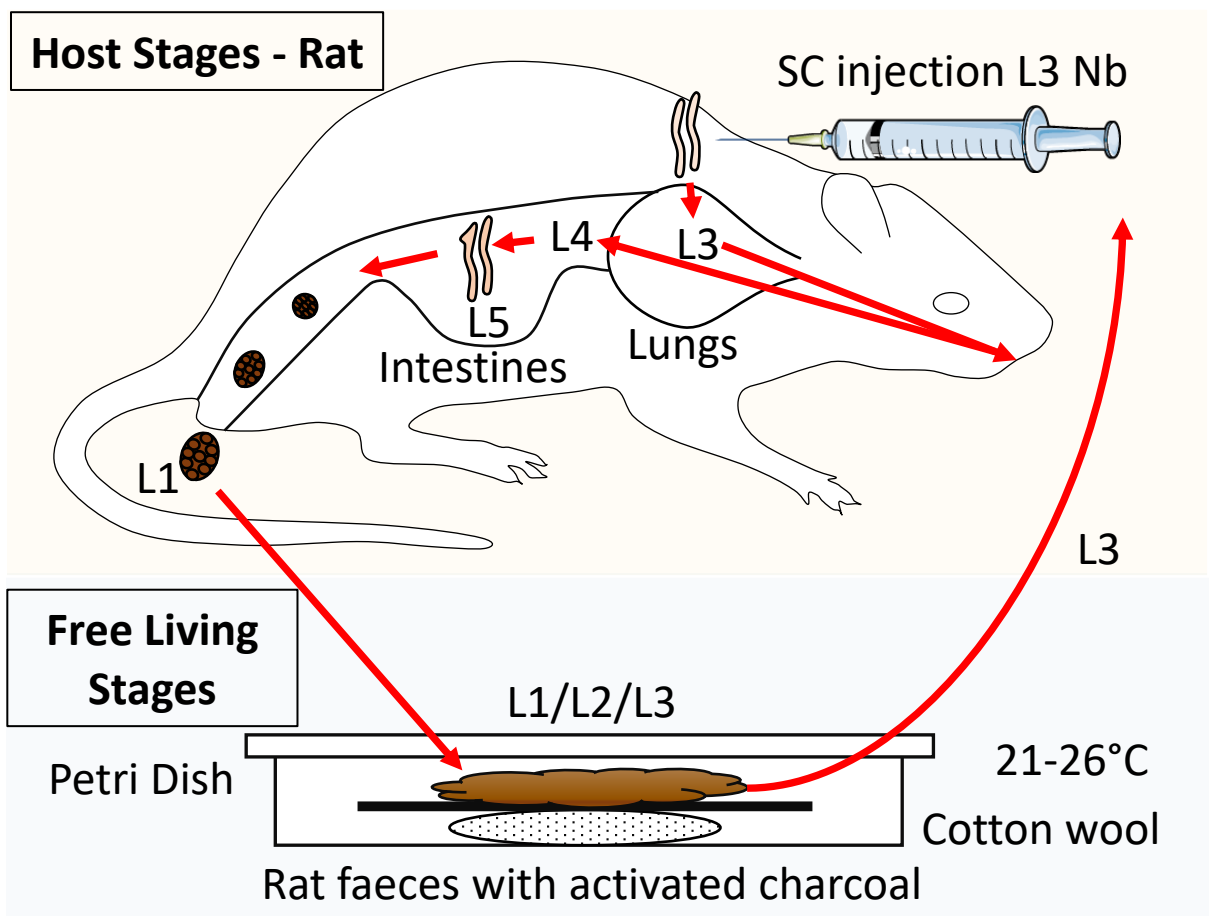


Figure 2.19: Diagram of the *N. brasiliensis* life cycle in the rat.

Petri-dishes are prepared containing a circular cut Whatman filter paper, 70 mm in diameter grade 54 (GE Healthcare Lifescience, UK) on dampened cotton wool. A small amount of faeces and activated charcoal is spread in the middle of the paper (**Figure 2.20**). The petri-dishes are incubated at 21-26°C in damp, sealed, moistened plastic containers, with routine observation to ensure filter paper remains damp. In optimal conditions, the first stage rhabditiform larvae (L1) hatch from eggs after 24 hours. They then develop through two moults to reach the filariform infective stage L3 and migrate to the edge of the tissue paper and ready for harvesting (**Figure 2.20**). The larvae were harvested up to 4 weeks of age as the fitness of the larvae decreases with increasing age.

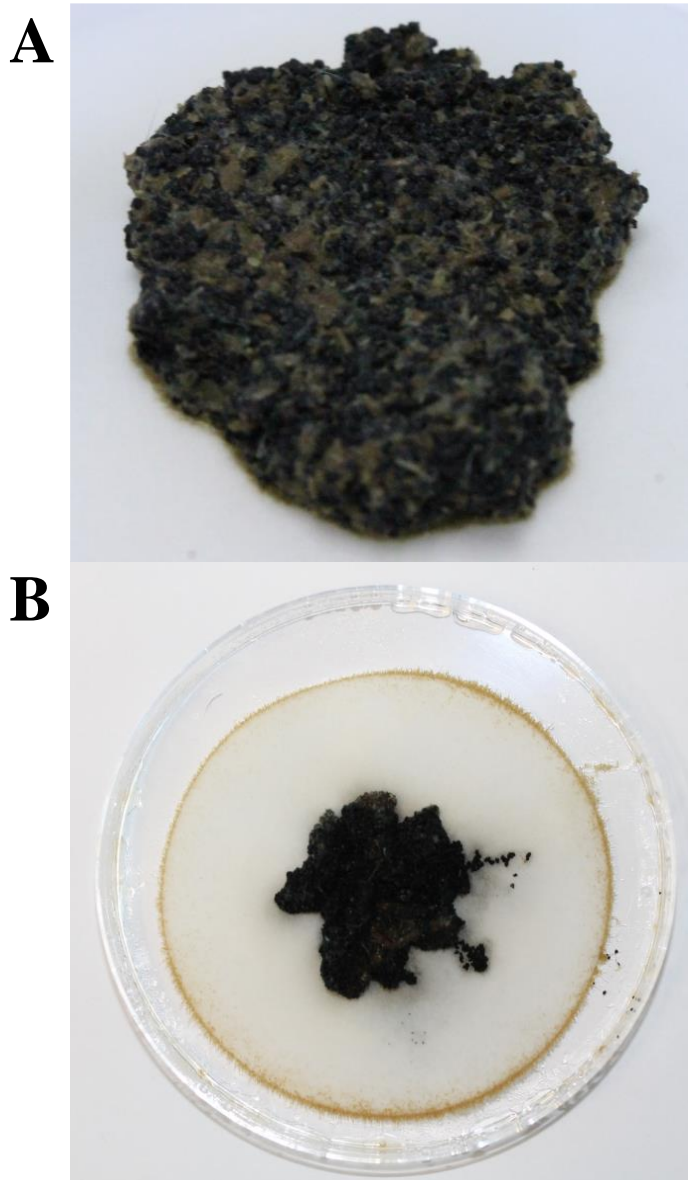


Figure 2.20: Processing *N. brasiliensis* eggs. **A**, Mixture of rat faeces containing *N. brasiliensis* eggs with activated charcoal. **B**, Petri dish (Diameter = 90 mm) containing L3 *N. brasiliensis* that have hatched, moulted to larval stage 3 and migrated from the mixture of faeces and activated charcoal to the extremities of the filter paper.

2.8.3 *N. brasiliensis* larvae recovery and counting

Careful preparation of viable L3 *N. brasiliensis* was essential for consistent infection studies in mice. To harvest *N. brasiliensis*, a petri-dish was filled with tap water and placed under the dissection microscope with the bottom light on. Sections of filter paper with encysted larvae were cut and placed around the edge of the light with the larvae closest to the centre. The heat from the light attracts the larvae to the centre of the petri-

dish (**Figure 2.21**). When the larvae have aggregated in the centre, these are collected and removed from the dish for counting.

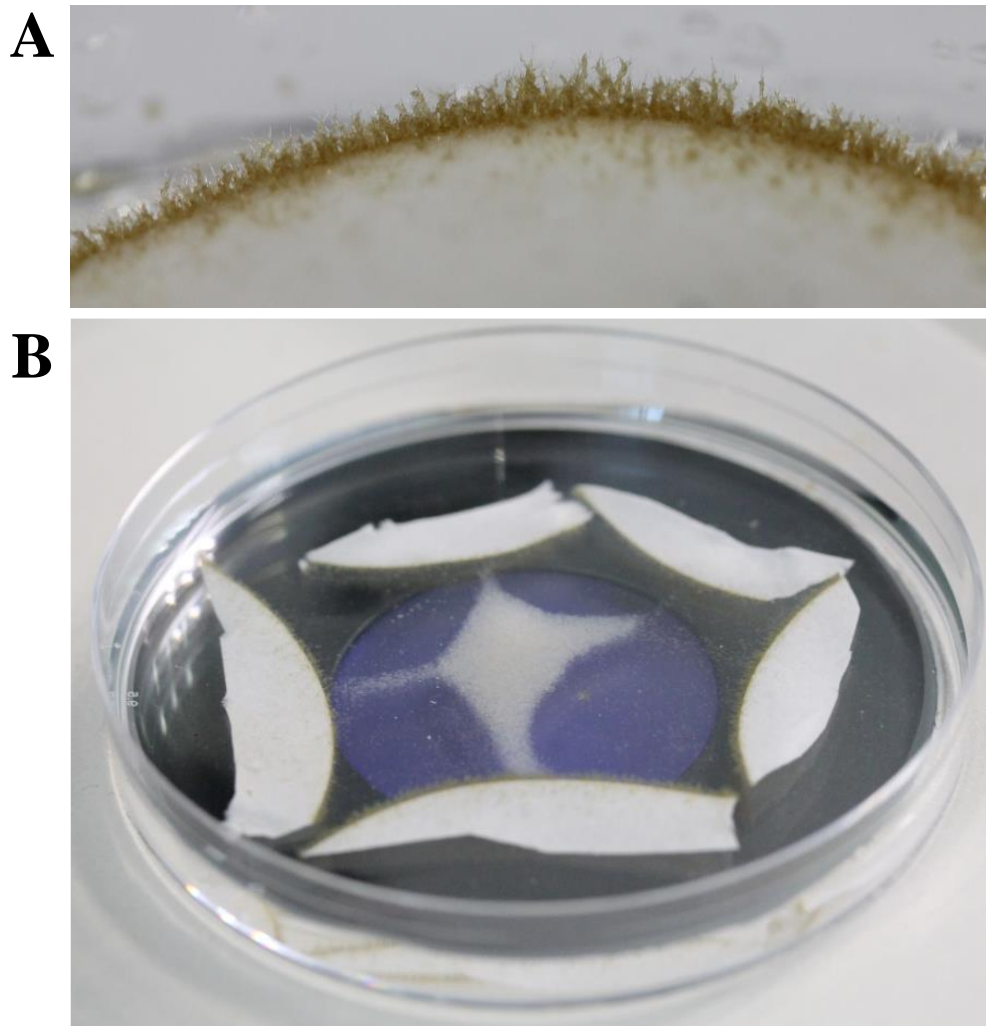


Figure 2.21: Harvesting L3 *N. brasiliensis*. **A**, L3 *N. brasiliensis* migrate to the edge of filter paper after one-week incubation at 27°C. **B**, Migration and aggregation of L3 *N. brasiliensis* in warm water towards the centre of a petri-dish (Diameter 90 mm).

2.8.4 *N. brasiliensis* infection of mice

Experimental mice were injected subcutaneously with 500 L3 *N. brasiliensis* in 100 µl of H₂O using a 23G needle. For primary *N. brasiliensis* infections, mice were infected and then sacrificed at various timepoints for analysis. For secondary *N. brasiliensis* infections, mice were infected followed by a second *N. brasiliensis* infection at day 21 and then

sacrificed at various timepoints. The lifecycle of *N. brasiliensis* in the mice is graphically shown in **Figure 2.22**.

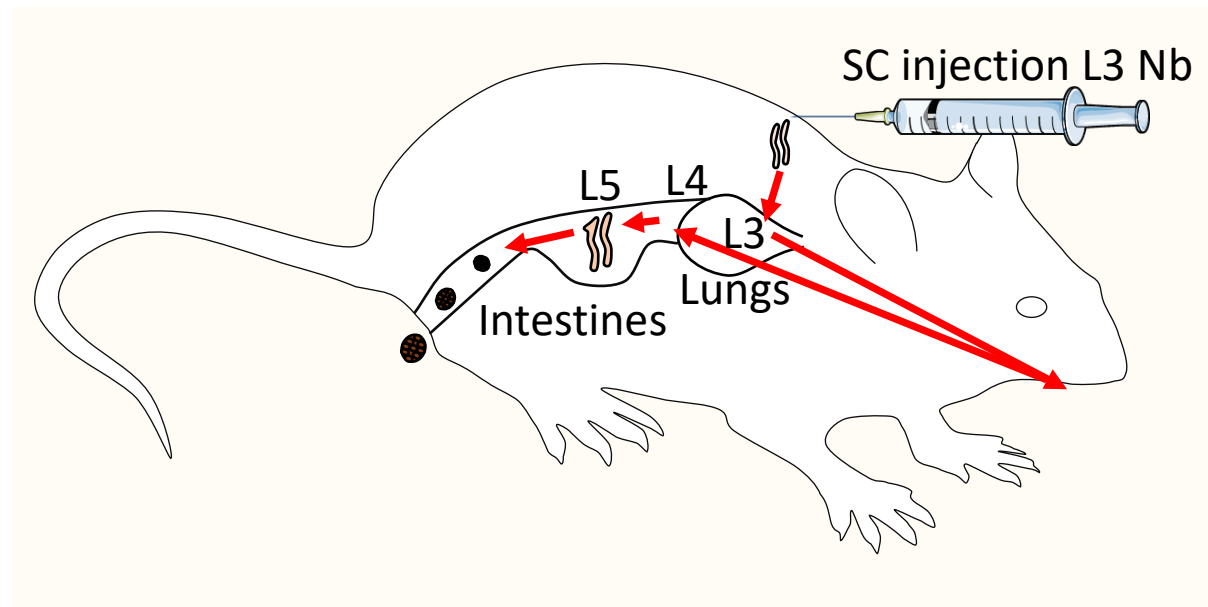


Figure 2.22: *N. brasiliensis* lifecycle in mice.

WT mice were primary infected with 500 L3 *N. brasiliensis* and worms were counted at different time points. The number of worms in the small intestine peaked at day 5 post-infection and were substantially reduced by day 7 (**Figure 2.23**). These results are consistent with previously reported data (Harvie et al., 2010, Halim et al., 2014, Nono et al., 2017, Schwartz et al., 2017), validating the model of *N. brasiliensis* infection.

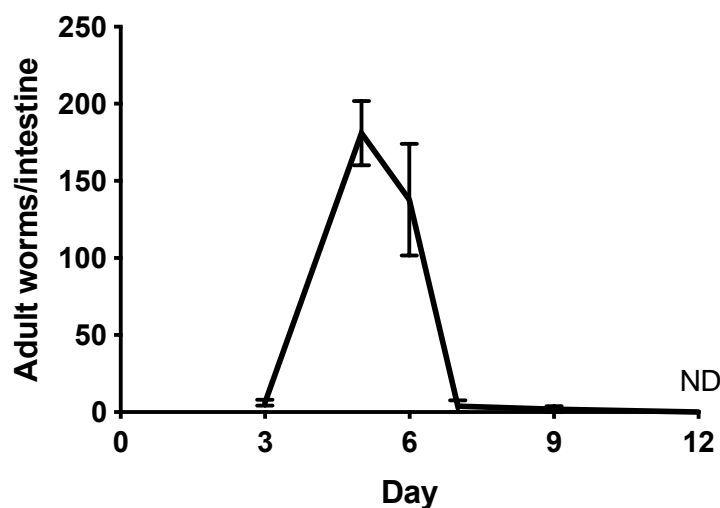


Figure 2.23: Time course of *N. brasiliensis* count in the small intestine of WT mice. WT mice were infected with 500 L3 *N. brasiliensis* subcutaneously. Small intestines were harvested at days 3, 5, 6, 7, 9 and 12 post-infection. Data is representative of two independent experiments. Data is representative of mean \pm SEM. n = 4-10.

The initial site of inflammation in this model of *N. brasiliensis* infection is the lungs. The migration of the larvae causes significant pulmonary, epithelium and vasculature damage and initiates a type 2 immune response in the lungs (Reece et al., 2008, Craig and Scott, 2014). **Figure 2.24** shows representative images over time of WT mice lungs following *N. brasiliensis* infection. At day 3, the *N. brasiliensis* have caused severe haemorrhage and damage in the lungs, which is gradually repaired over time.

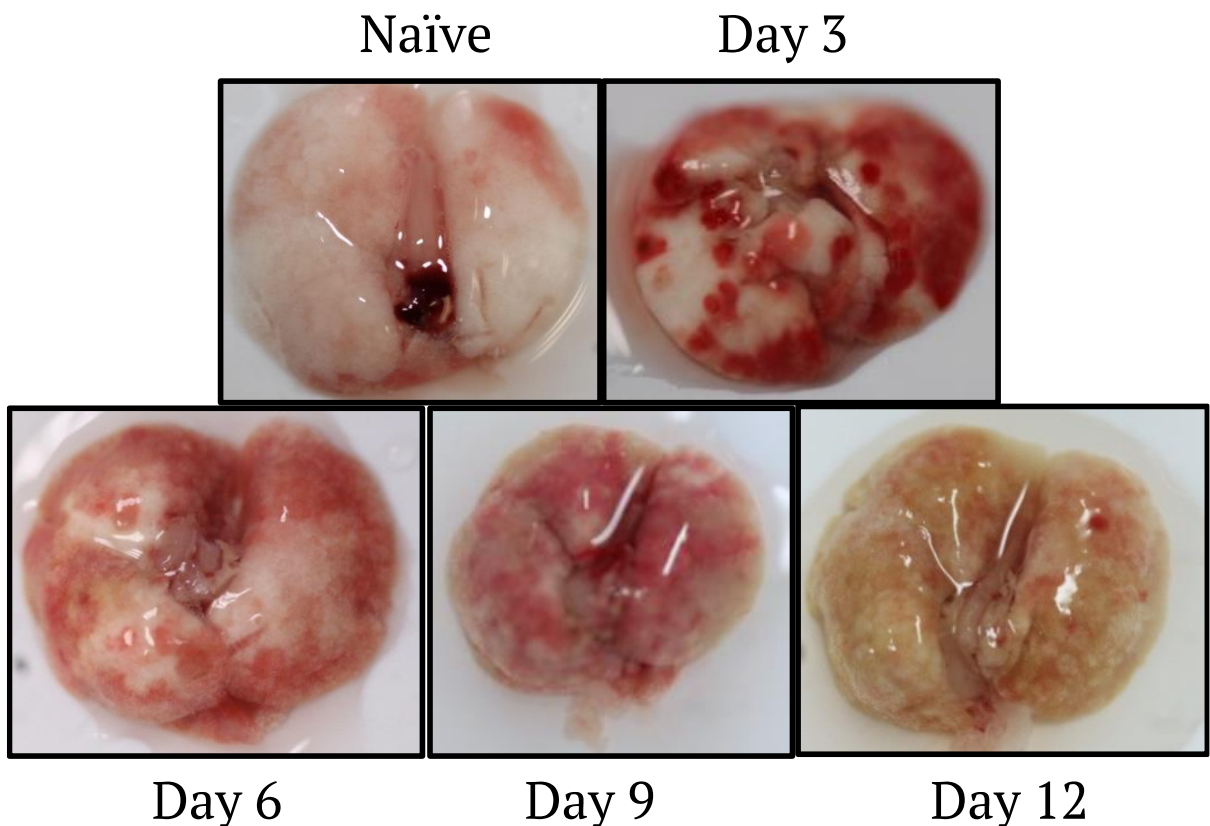


Figure 2.24: Representative photos of WT mice lungs following *N. brasiliensis* infection.

WT lungs cells were assessed by flow cytometry following *N. brasiliensis* infection. **Figure 2.25** shows typical WT data for lung immune cells following primary *N. brasiliensis* infection. From this data, it is clear that the innate response, in this case orchestrated largely by neutrophils, is replaced by a prolonged type 2 response that persists long after the worm has passed through the lung, this is because these cells are required to facilitate tissue repair of the damaged lungs and provide immunological memory (Chen et al., 2012, Bouchery et al., 2015).

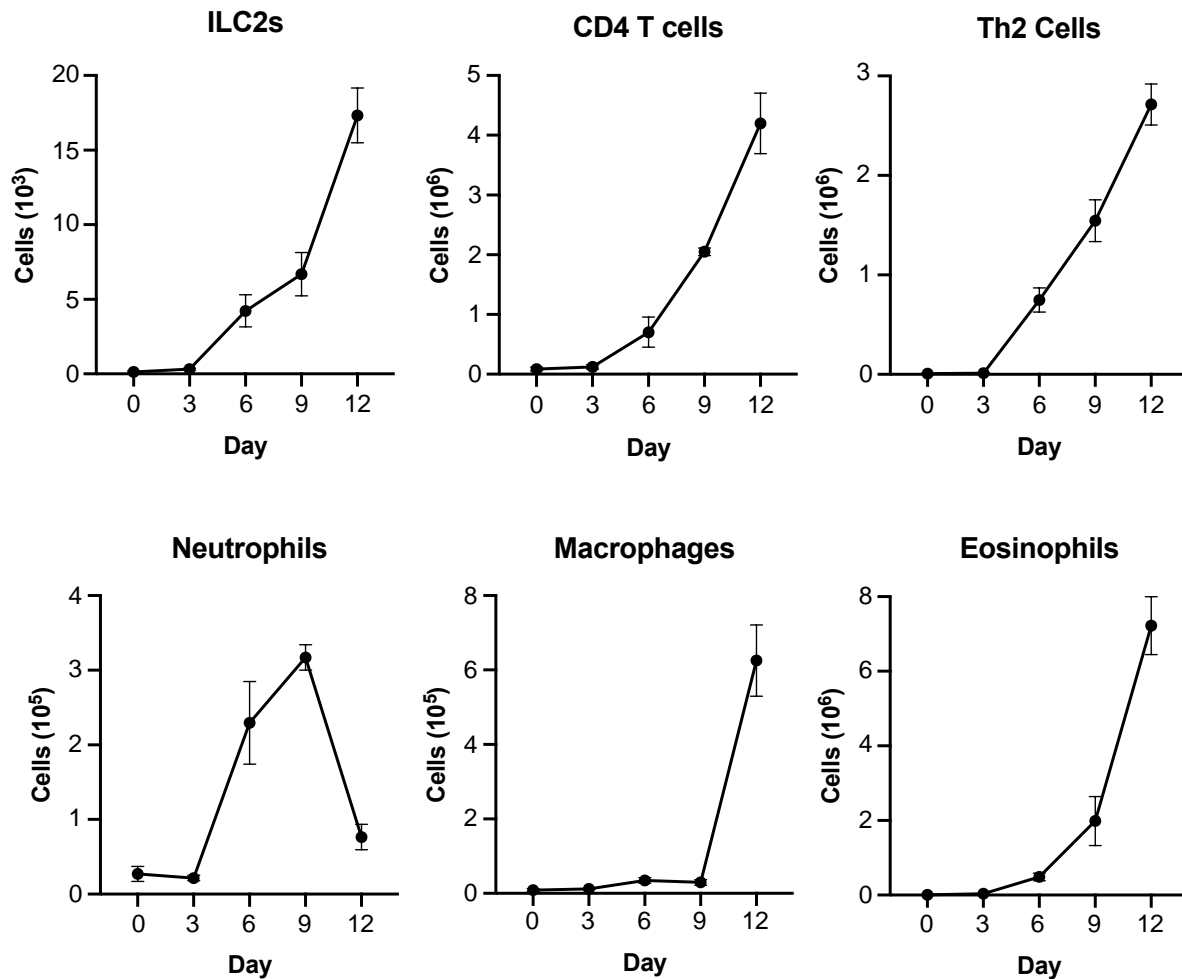


Figure 2.25: Lung immune cells following *N. brasiliensis* infection. Lungs were harvested from WT mice following primary *N. brasiliensis* infection and immune cells assessed by flow cytometry. Cells gated as single cell, live, CD45⁺. ILC2s as Lin⁻, Thy1.2⁺, KLRG1⁺ and GATA3⁺. CD4 T cells as CD4⁺. Th2 cells as CD4⁺ and Gata3⁺. Neutrophils as CD11b⁺ and Ly6G⁺. Eosinophils as SiglecF⁺, CD11b⁺, F4/80⁺ and CD11c⁻. Macrophages as SiglecF⁺, CD11b⁺, F4/80⁺ and CD11c⁺. n = 2-5.

2.8.5 Adult (L5) *N. brasiliensis* counting in murine small intestine

Adult *N. brasiliensis* (L5) (Figure 2.26) were counted in the small intestine. The expulsion of *N. brasiliensis* provides an assessment of a functional a type 2 immune response. The entire small intestine was dissected and transferred to a petri-dish and cut open longitudinally and incubated at 37°C for 4 hours to allow the adult worms to migrate out of the small intestine. The total number of adult worms were counted per small intestine using a dissection microscope.



Figure 2.26: L5 *N. brasiliensis*. Scale bar: 50 μm .

2.8.6 *N. brasiliensis* egg counts in the faeces

Faecal pellets were collected for *N. brasiliensis* egg count to assess fecundity. The elliptical eggs are passed in the faeces as a 16 to 20 cell-stage embryo and are 54 to 62 by 31 to 34 μm in size (**Figure 2.27**). Approximately 5 faecal pellets were collected and weighed. The faecal pellets were dissociated by adding 1 ml of water and shaking. The faeces were left for 1 hour before 3 ml of saturated NaCl was added (176g NaCl in 500ml H₂O). The saturated NaCl provides buoyancy and allows the eggs to float to facilitate the counting. The eggs were counted from dissociated faeces using a 2-chamber McMaster counting slide, with adjustments made for dilution and faeces weight to determine eggs per gram of faeces.



Figure 2.27: *N. brasiliensis* egg. Scale bar: 10 μm .

2.8.7 House dust mite (HDM)

House dust mite (HDM) is a common indoor allergen and up to 85% asthmatics patients respond to this allergen (Gold et al., 2014). HDM is used in mouse model to induce allergic airway inflammation, which is similar to the human disease asthma (Fallon and Schwartz, 2019). HDM extracts (*Dermatophagoides pteronyssinus*) were purchased from Stallergenes Greer (Derp1 146.45 mcg/vial, Protein 2.26 mg/vial and Endotoxin 812.5 EU/vial). To induce allergic airway inflammation, the HDM protocol from Plantinga et al. (2013) was used. Mice were sensitized with 1 µg HDM in 20 µl PBS, via intranasal (i.n.) injection. The mice were then challenged for 5 consecutive days from day 7 to day 11 with 10 µg HDM in 20 µl PBS via i.n. At day 14, mice were sacrificed and analysed. Control mice were sensitized and challenged i.n. with PBS (**Figure 2.28**). Lung histology (**Section 2.23**) demonstrates increased perivascular and peribronchial airway inflammation, and increased mucous production in HDM treated mice compared to PBS treated mice (**Figure 2.29**).

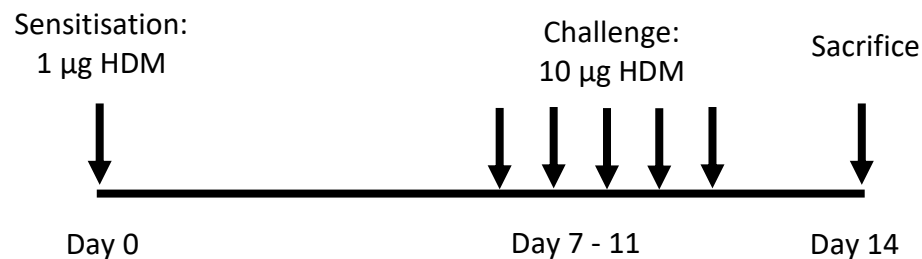


Figure 2.28: Overview of HDM experiment. Mice were sensitised with 1 µg HDM at day 0, then challenged with 10 µg HDM for 5 consecutive days (7-11). Mice were sacrificed at day 14 and analysed.

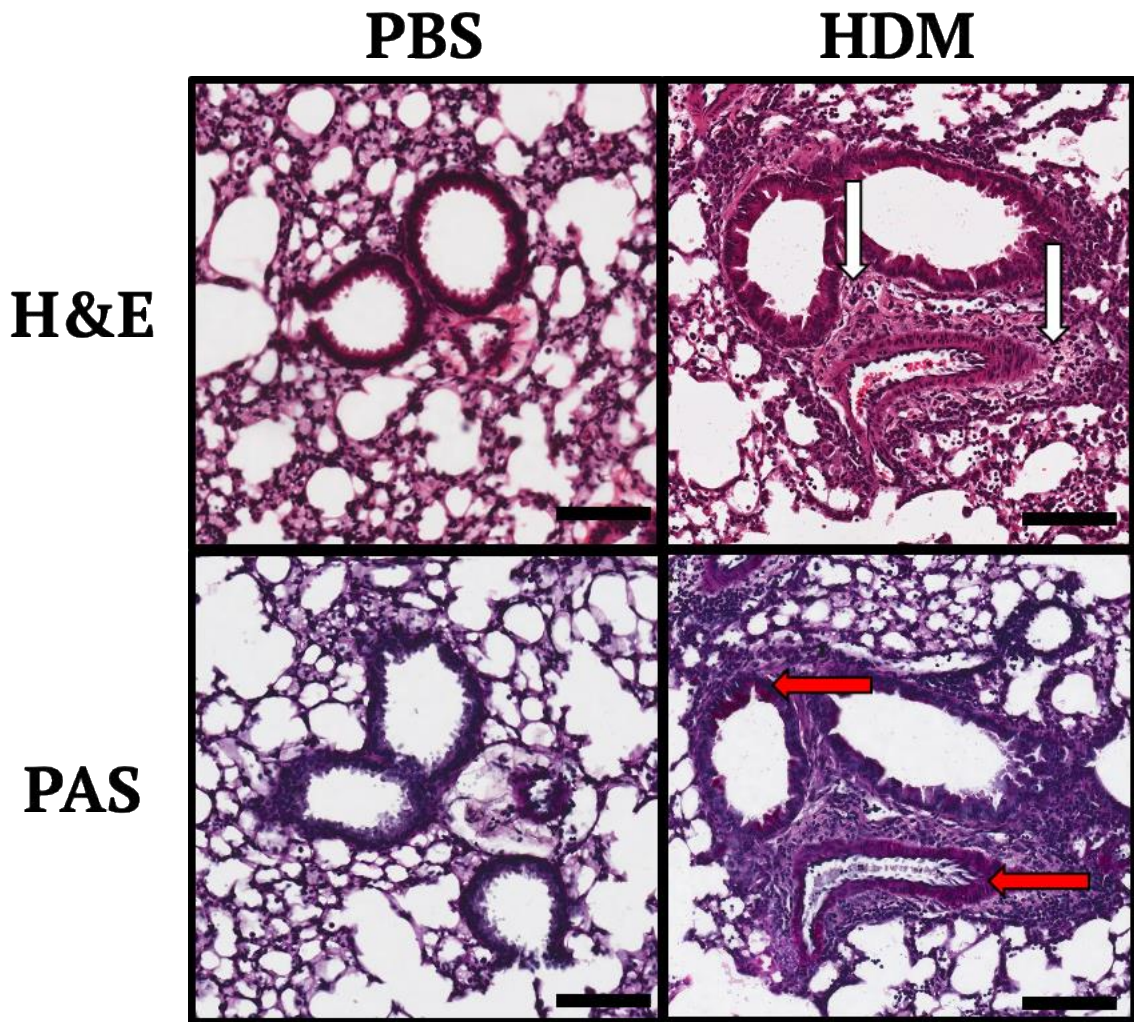


Figure 2.29: Lung histology demonstrates increased cell infiltration and mucous production in HDM treated mice compared to PBS treated mice. Representative histological images of lung sections stained with H&E and PAS. White arrows point to perivascular and peribronchial inflammation. Red arrows point to goblet cell metaplasia. Scale bar = 100 μ m.

2.9 Murine tissue dissection and processing

2.9.1 Lung isolation and generation of a single cell suspension

Murine lungs were dissected from a euthanised mouse, minced and incubated with 1 mg/ml collagenase D from *Clostridium histolyticum* (Roche, Dublin, Ireland) for 30 minutes at 37°C with gentle shaking. Collagenase D degrades collagen and disaggregates tissue aiding the preparation of a single cell suspension. Digested lung samples were mechanically dissociated through a 70 μ m cell strainer (Falcon, Corning) and washed

with RPMI-1640 media. The red blood cells were lysed by incubating with 2 ml of RBC lysis buffer (BD Pharm lyse™) at 37 °C for 5 mins. Cells were then washed with 18 ml of RPMI-1640 media and centrifuged at 1500 RPM for 5 minutes at 4°C. The resultant cells were resuspended in RPMI-1640 media and counted (**Section 2.10**).

2.9.2 Spleen, thymus and mesenteric lymph node (MLN) isolation and single cells suspension

Spleen, thymus or mesenteric lymph node (MLN) were aseptically dissected from a euthanised mouse. The tissues were mechanically dissociated by passing through a 70µm cell strainer (Falcon, Corning). Thymus and MLN cells were then washed in RPMI-1640 media, whilst spleens were washed with RPMI-1640 media and red blood cells were lysed with 2 ml of RBC lysis buffer (BD Pharm lyse™) at 37°C for 5 mins. The cells were washed with 18 ml of RPMI-1640 media and centrifuged at 1500 RPM for 5 minutes at 4°C. The cells were resuspended in RPMI-1640 media and counted (**Section 2.10**).

2.10 Cell counting

Cell density was calculated by haemocytometer counting of the cell suspension using a light microscope and a haemocytometer slide (KOVA International, CA, USA). Cells were diluted 1/20 with media and dead cells visualised using Trypan Blue Solution (Fluka Analytical) allowing these cells to be excluded from the cell count.

Average cell count in four quadrants x trypan blue dilution x 10⁴ = Total cells per ml

2.11 RNA extraction

RNA was extracted from dissected tissue or from collected cells. Tissue, such as lung, was dissected and stored in RNALater (Invitrogen) or snap-frozen in liquid nitrogen. RNA was isolated by phenol-chloroform extraction. To ensure there was no

contamination with RNase, RNase/DNase free plastics and reagents were used, and RNA extraction was performed in a dedicated area, cleaned with 70% ethanol and RNaseZap™ (Sigma, Wicklow, Ireland). Briefly, 50 mg tissue was homogenised (IKA T10 basic Ultra-Turrax; Germany) in 500 µl of TRIzol® Reagent (ThermoFisher, Loughborough, UK). The sample was incubated on ice for 5 minutes to allow for complete dissociation of the nucleoprotein complex. 100 µl of chloroform (Sigma, Wicklow, Ireland) was added and incubated for a further 3 minutes on ice. The sample was centrifuged for 15 minutes at 12,000 g at 4°C. The colourless aqueous phase was transferred to a new tube and 250 µl of isopropanol was added to precipitate the RNA. This was incubated for 10 minutes on ice and then centrifuged at 12,000 g at 4°C. The total RNA precipitate forms a white pellet at the bottom of the tube. The supernatant was discarded and 500 µl of 75% ethanol was added and centrifuged again to wash the pellet. The supernatant was discarded and allowed to air dry for 10 minutes. The RNA was reconstituted in 30 µl RNase free water. RNA concentration was measured based on optical density using the Nanodrop® (ND-1000 Spectrophotometer) using ND1000 version 3.8.1 software. A ratio measurement of absorbance at 260 nm / 280 nm of 2 was considered to represent pure RNA. RNA purity was also analysed by running RNA (1ng) on a 1.5% agarose gel and visualised under UV light (**Figure 2.30**). RNA samples were then converted to cDNA (**Section 2.12**) or stored at -80°C.

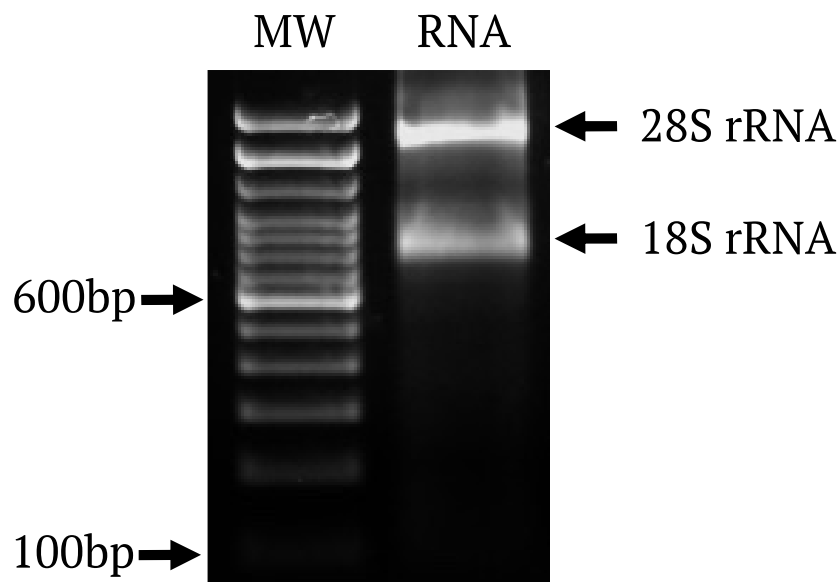


Figure 2.30: RNA purity assessed by agarose gel electrophoresis. RNA (1ng) from WT murine lung was mixed with DNA binding solution (Blue Juice) and ran on a 1.5% agarose gel.

2.12 Complementary DNA (cDNA) synthesis

Complementary DNA (cDNA) synthesis is the process of generating DNA from a single-strand RNA via reverse transcription. Isolated RNA (**Section 2.11**) was reverse transcribed into cDNA using the Quantitect® Reverse Transcription kit (Qiagen, Hilden, Germany) following the manufacturer's instructions. Contaminating genomic DNA remaining from RNA isolation was eliminated by incubating RNA with gDNA Wipeout Buffer for 2 minutes at 42°C. The clean RNA was reverse transcribed to cDNA by incubation at 42°C with a master mix (**Table 2.7**). The Quantiscript Reverse Transcriptase is a multifunctional enzyme that transcribes cDNA from an RNA template. The Quantiscript RT buffer contains dNTPs and stabilises the reaction. Whilst the RT Primer Mix contains a specially optimized mix of oligo-dT and random primers that enable cDNA synthesis from all regions of RNA transcripts. The reverse transcriptase reaction was an incubation of 42°C for 30 minutes followed by an incubation of 95°C for 3 mins to inactivate Quantiscript Reverse Transcriptase. The synthesized cDNA was then proceeded to either quantitative PCR (**Section 2.13**) or stored at -80°C.

Component	Volume (µl)
Template RNA	14
Quantiscript Reverse Transcriptase	1
RT Primer Mix	1
Quantiscript RT Buffer (5X)	4

Table 2.7: cDNA generation master mix.

2.13 Quantitative PCR (qPCR)

Following RNA extraction (**Section 2.11**) and cDNA synthesis (**Section 2.12**), gene expression was detected by quantitative PCR (qPCR). qPCR was performed using an ABI NextStep sequence detection system (Applied Biosystems, UK) with TaqMan Fast reagents (Applied Biosystems, UK). The qPCR master mix is outlined in **Table 2.8** and the gene probes are outlined in **Appendix III**. qPCR was run using a FrameStar 96 well

PCR plate and sealed with film (Applied Biosystems, UK). The qPCR reaction protocol is outlined in **Figure 2.31**.

Component	Volume (μ l)
Template cDNA	2
TaqMan Fast Universal PCR Master Mix (2X)	10
qPCR Probe	1
DEPC H ₂ O	7

Table 2.8: qPCR master mix

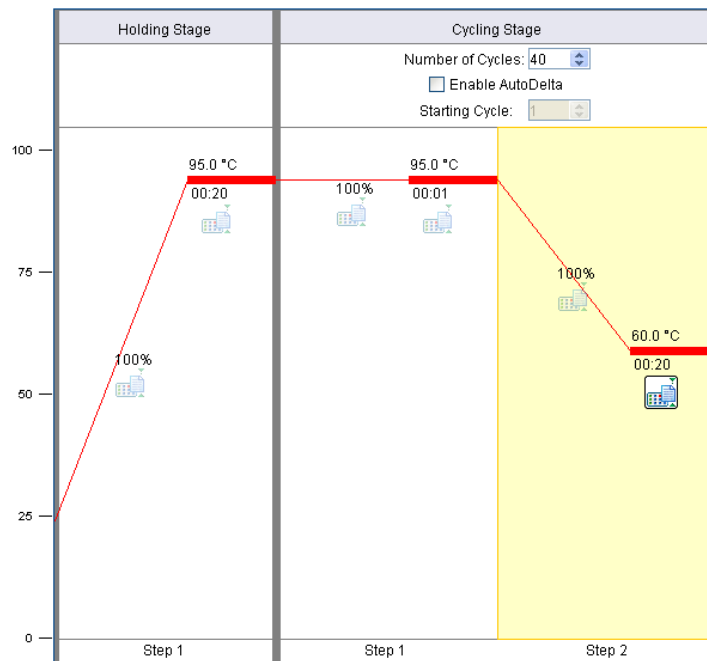


Figure 2.31: Graphical qPCR protocol.

Relative quantification and calculation of the range of confidence was performed with the comparative Delta Delta Cycle Threshold ($\Delta\Delta$ CT) method. Data is presented as relative units indicating a fold-change in mRNA expression that was normalised to housekeeping genes 18S ribosomal RNA.

2.14 Flow-cytometric staining

2.14.1 Surface markers staining

Prior to cell staining, cells were prepared as described in **Section 2.9**. During all cell staining and incubation steps, cells were kept in the dark and at 4°C and all washes were at 1500 RPM at 4°C for 5 minutes. Cell viability was assessed by staining cells with LIVE/DEAD Fixable Aqua Dead Cell Stain Kit (Molecular Probes, Invitrogen, Dublin, Ireland) at 1:1000 dilution in PBS for 30 mins at 4°C. LIVE/DEAD™ Fixable Aqua Dead dye reacts with free amines on cell surface and interior, therefore cells with a compromised cell membrane will absorb the dye and will have a higher fluorescence intensity than live cells with a viable cell membrane. Cells were washed in FACS buffer and incubated with Fc Block (BD Bioscience, Oxford, UK) at 1:100 for 20 mins at 4°C. This prevents non-specific binding of fluorochromes to FC receptors found on monocytes, macrophages, dendritic cells and B cells. Cell surface antibodies labelled with fluorochromes were diluted 1:200 in FACS buffer and incubated for 30 mins at 4°C and were washed in FACS buffer. If no intracellular staining was required, cells were resuspended in FACS buffer and events acquired on the flow cytometer. Flow cytometry antibodies used in this thesis are outlined in **Appendix IV**.

Typical flow gating strategy throughout this thesis is shown in **Figure 2.32**. Cells gated based on forward scatter (FSC) as a measure of relative cellular height and side scatter (SSC) as a measure of relative cellular granularity. Cell doublets were excluded to ensure only single cells were analysed. Doublet discrimination was based on two excluding gates of FSC-A vs FSC-H and SSC-A vs SSC-W. Live cells were gated based on negative staining for LIVE/DEAD™ Fixable Aqua Dead stain.

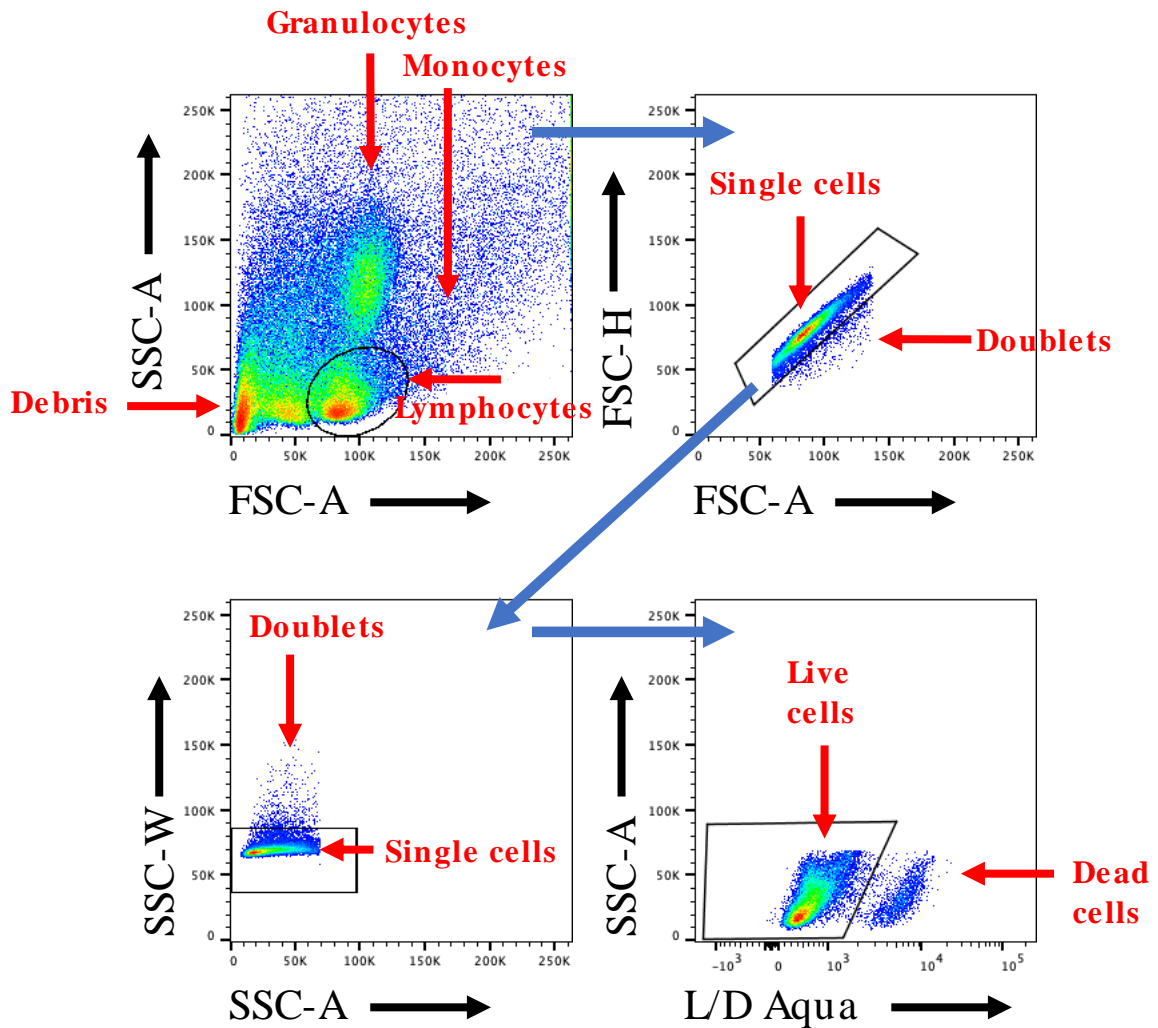


Figure 2.32: Representative flow cytometry gating strategy.

2.14.2 Intracellular (nuclear) staining

Flow cytometry can be used to analyse intracellular (nuclear) antigens such as transcription factors. Therefore, following cell surface marker staining, cells were fixed and permeabilised with Foxp3/Transcription Factor Staining Buffer for 30 mins at 4°C (Invitrogen, Dublin, Ireland). This is a 4X concentration (Buffer B), diluted to 1X using the fix/perm diluent (Buffer A). Cells were washed with Foxp3/Transcription Factor 10X Permeabilisation Buffer (Invitrogen, Dublin, Ireland) diluted to a 1X with PBS. Following fixation/permeabilisation, cells were stained with intracellular fluorochrome labelled antibodies which were diluted in 1:100 in 1X Permeabilisation Buffer for 60

mins at 4°C. Cells were washed and resuspended in FACS buffer and events acquired on the flow cytometer.

Intracellular staining using Foxp3/Transcription Factor fixation permeabilization resulted in considerable loss of *Rora*-YFP expression in *Rora* reporter mice. The optimal intracellular flow cytometry staining protocol for *Rora* reporter mice was a pre-fixation step with 2% PFA for 30 mins, followed by Foxp3 transcription factor fix/perm for 30 mins (Heinen et al., 2014, Ghaedi et al., 2020) (**Figure 2.33**), allowing for detection of *Rora*-YFP expression with intracellular staining of transcription factors (GATA3, Foxp3, Tbet and Rorgt).

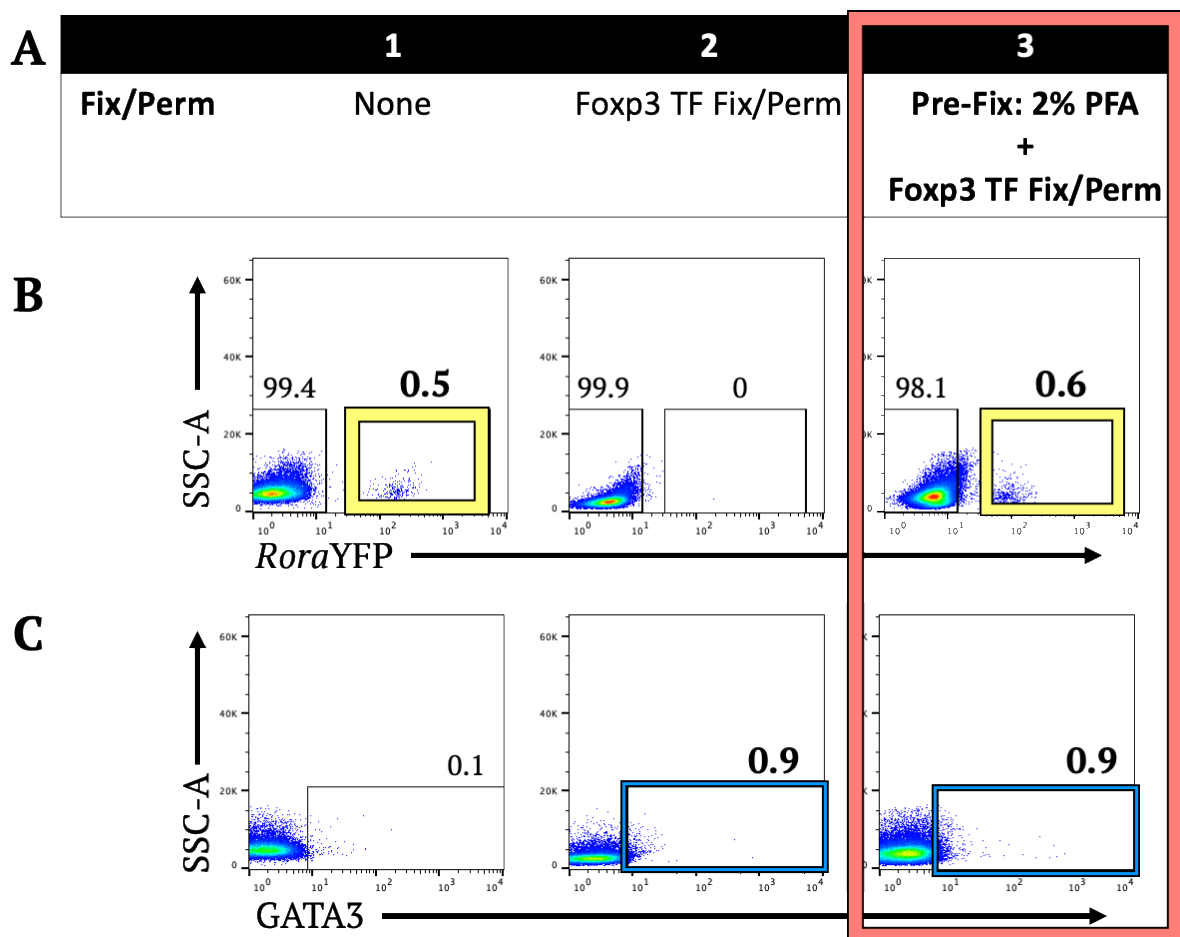


Figure 2.33: Intracellular flow cytometry staining optimisation for *Rora* reporter mice. Splensens were harvested from *Rora* reporter mice. Cell populations were gated as lymphocytes, single cells, Live, CD4⁺, GATA3⁺ and YFP⁺. **A**, Intracellular optimisation conditions. Red box indicates optimum intracellular staining protocol. **B**, *Rora*-YFP expression. Yellow box indicates optimised intracellular staining maintaining YFP expression. **C**, CD4 (Surface expression) and GATA3 (Intracellular expression). Blue box indicates optimised intracellular staining maintaining CD4⁺GATA3⁺ expression.

2.15 Flow-cytometric analysis

Prior to acquiring data, cells were filtered (70 μM) to ensure a single cell suspension. Flow data was acquired on either the CyAn ADP (Beckman Coulter, High Wycombe, UK) or BD LSR Fortessa™. The CyAn ADP has 3 lasers (405, 488 and 635 nm), 9 fluorescent channels and 2 scatter parameters (FSC and SSC). For larger immune marker panels, the BD LSR Fortessa™ was used to acquire data as this cytometer has 4 lasers (405, 488, 561 and 633) and 16 fluorescent channels. The appropriate controls were acquired with samples (unstained, isotype and fluorescent minus one) and gates were drawn using unstained, FMO and isotype controls. Acquired data were analysed using FlowJo™ software version 10.6 (Tree Star, USA). The number on the flow cytometry plots represents the percentage of parent gate, as indicated in figure legends.

Single stained samples and unstained samples were used to compensate for each fluorochrome. Fluorescence minus one (FMO) controls contained all fluorescently labelled antibodies except the antibody being assessed and were used to define non-specific background staining (**Figure 2.34**).

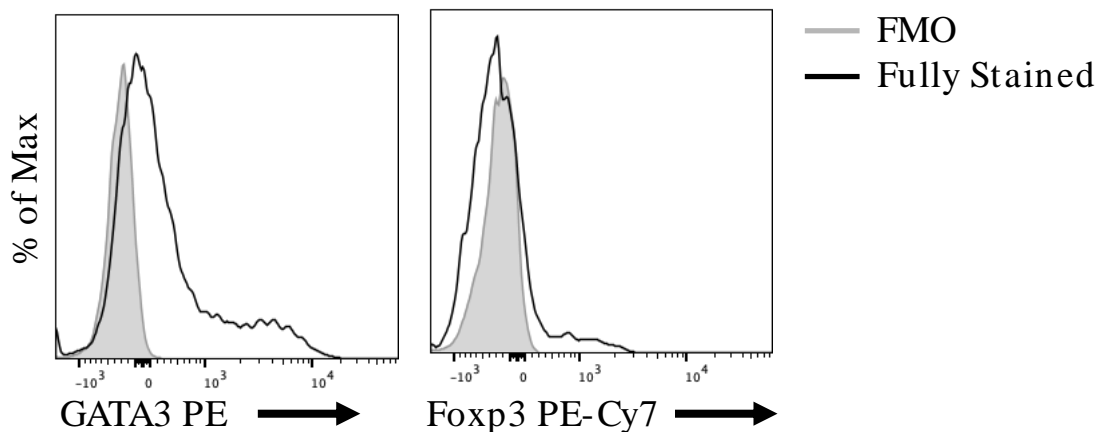


Figure 2.34: Fluorescence minus one (FMO) flow cytometry plots for GATA3 and Foxp3. Cells gated as lymphocytes, single cell, live CD45⁺, CD3⁺, CD4⁺ and either GATA3⁺ or Foxp3⁺. Grey line = FMO. Black line = Fully stained sample.

Isotype controls were used to define non-specific binding of an antibody. Isotype controls are antibodies that lack specificity to the target, developed in the same host species, which have the same Ig subclass, and are conjugated with the same fluorochrome of interest (**Figure 2.35**).

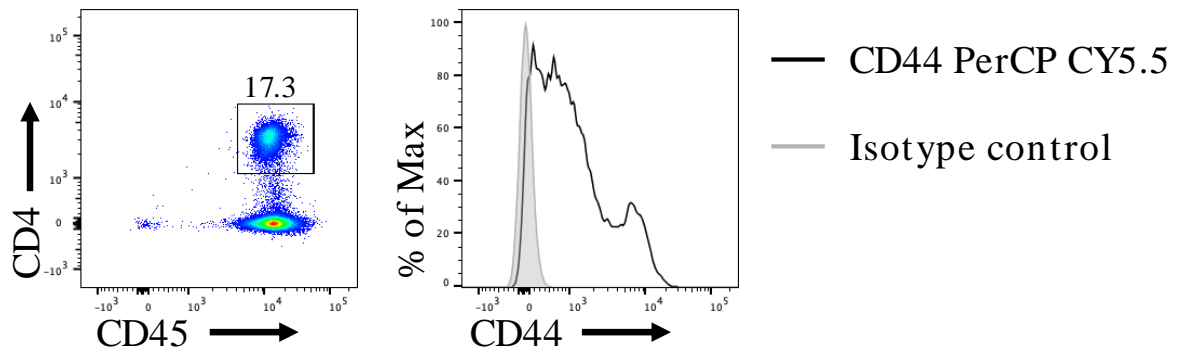


Figure 2.35: Flow cytometry plots for isotype controls. WT spleen was harvested and assessed by flow cytometry. Cells gated as lymphocytes, single cell, live, CD45⁺ and CD4⁺. Grey line = Isotype control (Rat IgG_{2b} PerCP CY5.5). Black line = CD44 (Rat IgG_{2b} PerCP CY5.5).

Flow cytometry data was also analysed using t-Distributed Stochastic Neighbour Embedding (t-SNE), which were generated using FlowJo (**Figure 2.36**) or Cytobank. tSNE is an unsupervised nonlinear dimensionality reduction algorithm that can be used for visualising single cell flow cytometry data in dimension-reduced space. tSNE generates 2 additional parameters tSNE1 and tSNE2, and clusters of cells distributed based on similarities and allowed for visualisation of a third dimension based on colour. tSNE analyses were performed on concatenates of all samples belonging to determine experimental group using 1,000 iterations with the following parameters: Perplexity 30, Theata 0.5, and Learning rate of 200.

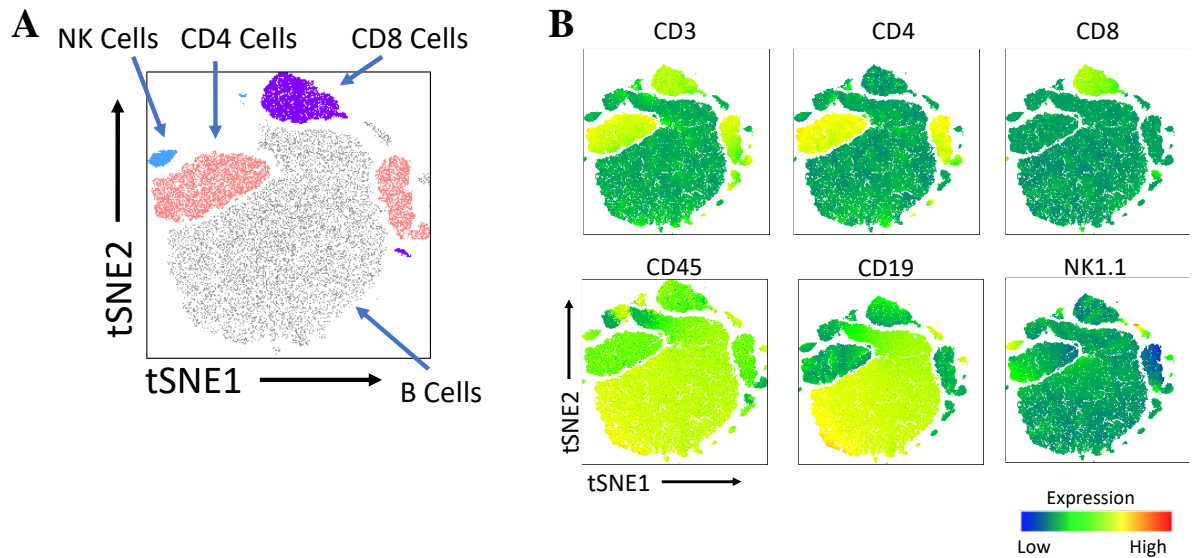


Figure 2.36: Example of tSNE analysis. Splensens were harvested and assessed by flow cytometry. Cells gated as single cell, live, CD45⁺ and tSNE generated **A**, tSNE plot identifying cell populations. CD4 cells (Red) were CD3⁺CD4⁺, CD8 cells (Purple) were CD3⁺CD8⁺, B cells (Black) were CD3⁻CD19⁺ and NK cells (Blue) were CD19⁻CD3⁻NK1.1⁺ **B**, tSNE analysis of marker expression for CD45, CD3, CD4, CD8, CD19 and NK1.1. tSNE plots are concatenates of 5 samples.

2.16 Fluorescence activated cell sorting (FACS)

Fluorescence activated cell sorting (FACS) is a process of isolating cells of interest from a heterogeneous sample, based on light scatter and fluorescent signal. Prior to FACS, relevant tissues were isolated, and a single cell suspension generated as per **Section 2.9**, single cell suspensions were then stained as per **Section 2.14**. All FACS was performed using the BD FACSAria™ Fusion. FACS isolates cells by analysing hydrodynamically focused single cells in a stream, which pass through lasers in a flow cell, and are interrogated based on light and fluorescence signals. The cells of interest are pre-selected using the BD FACSDiva™ software. The stream containing the cells, is then charged at a specific time, based on a calculated time delay. The stream breaks into droplets, then the charged droplets pass an electrostatic deflection system which diverts droplets based on their charge into appropriate collection tubes. The stream is then returned to neutral, once the droplet breaks off. This method proved to be an efficient way of isolating cells of interest with purity of >97% (**Figure 2.37**).

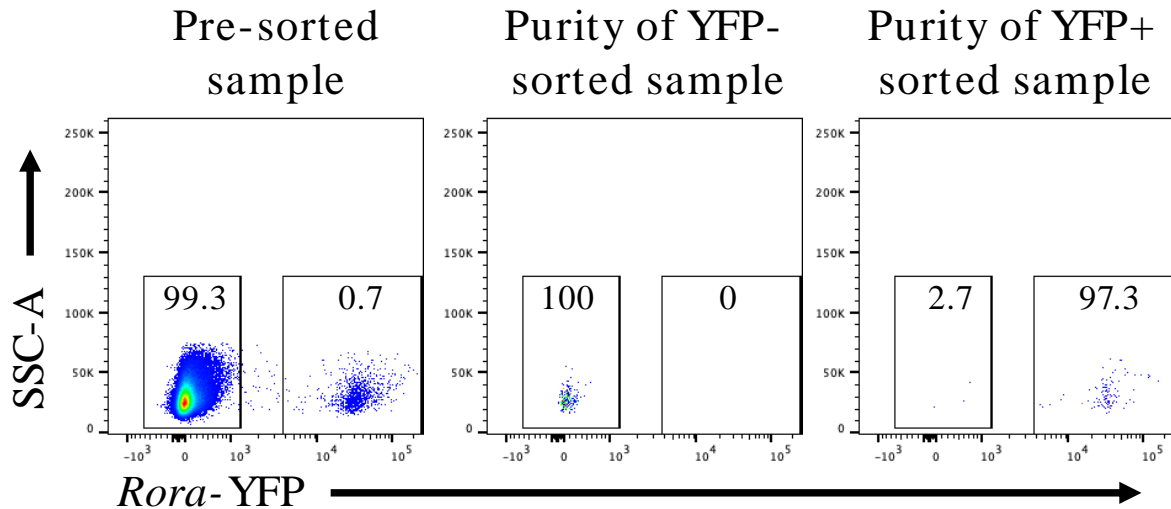


Figure 2.37: Representative FACS plots of showing purity of cell populations. *Rora* reporter mice spleens were isolated and FACS for YFP⁺CD45⁺CD4⁺ and YFP⁻CD45⁺CD4⁺ cells were isolated. Cells pre-gated as lymphocytes, single cell, live, CD45⁺ and CD4⁺.

2.17 CD4⁺ T cell isolation

CD4⁺ T cells were pre-enriched from murine splenocytes prior to FACS by magnetic cell separation (MACS). Cell enrichment increases the final yield of CD4⁺ T cells and reduces the time required for FACS sorting cells, thus increasing the cell viability. CD4⁺ T cells were pre-enriched as per the CD4⁺ T Cell Isolation Kit from MACS (Miltenyi Biotec 130-104-454). As per manufacturer's instructions, cells were resuspended in MACS buffer (1:20 dilution of MACS BAS Stock Solution with autoMACS Rinsing Solution) and incubated with Biotin-Antibody cocktail, for 5 minutes at 4°C. The Biotin-Antibody cocktail contains conjugated antibodies against CD8a, CD11b, CD11c, CD19, CD45R (B220), CD49b (DX5), CD105, Anti-MHC-class II, Ter-119 and TCR γ/δ . The cells are stained with Anti-Biotin MicroBeads and incubated for 10 minutes at 4°C. The magnetically labelled, non-target cells are depleted by retaining them in a MACS column in a magnetic field, using MACS Separator. Whilst the unlabelled CD4⁺ T cells pass through the column and are collected. Flow cytometry confirmed CD4⁺ T cell enrichment. Prior to CD4⁺ T cell enrichment, the CD4⁺ T cells population was 16.3%. Whilst after cell enrichment, the CD4⁺ T cell population was 84.4% (**Figure 2.38**).

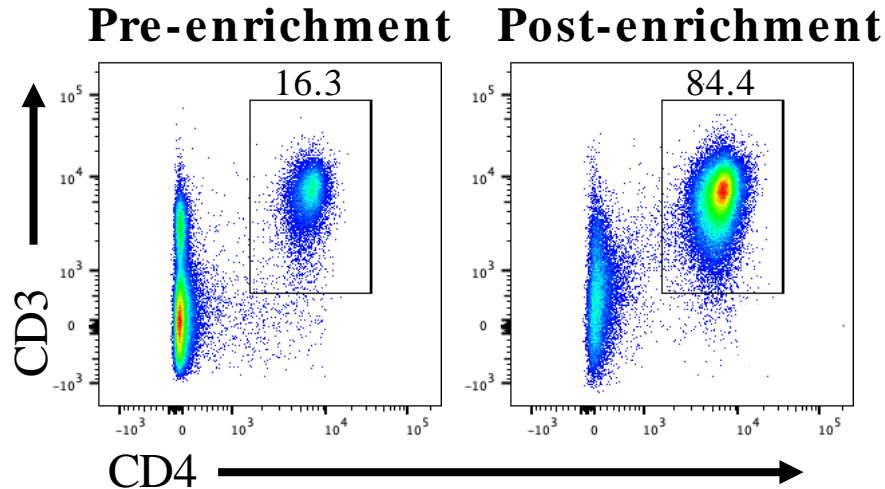


Figure 2.38: Representative flow plots of CD4⁺ T cell isolation by magnetic separation from murine spleen cells. CD4⁺ T cells were gated as lymphocytes, single cells, live, CD3⁺, CD4⁺.

2.18 Naïve CD4 T cell isolation

Naïve CD4⁺ T cells were isolated from murine splenocytes prior to *in vitro* culture by magnetic cell separation (MACS). Naïve CD4 T cells were isolated as per naïve CD4⁺ T Cell Isolation Kit from MACS (Miltenyi Biotec 130-104-453). As per manufacturer's instructions, cells were resuspended in MACS buffer (1:20 dilution of MACS BAS Stock Solution with autoMACS Rinsing Solution) and incubated with Biotin-Antibody cocktail, for 5 minutes at 4°C. The Biotin-Antibody cocktail contains conjugated antibodies against CD8a, CD11b, CD11c, CD19, CD45R (B220), CD49b (DX5), CD105, Anti-MHC-class II, Ter-119 and TCR γ/δ . The cells are stained with Anti-Biotin MicroBeads and CD44 MicroBeads and incubated for 10 minutes at 4°C. The magnetically labelled, non-target cells are depleted by retaining them in a MACS column in a magnetic field, using autoMACS Separator. Whilst the unlabelled naïve CD4 T cells pass through the column and are collected. Prior to CD4⁺ T cell enrichment, the naïve CD4 T cells population was ~18%. Whilst after enrichment, the naïve CD4⁺ T cell population was ~75% (Figure 2.39).

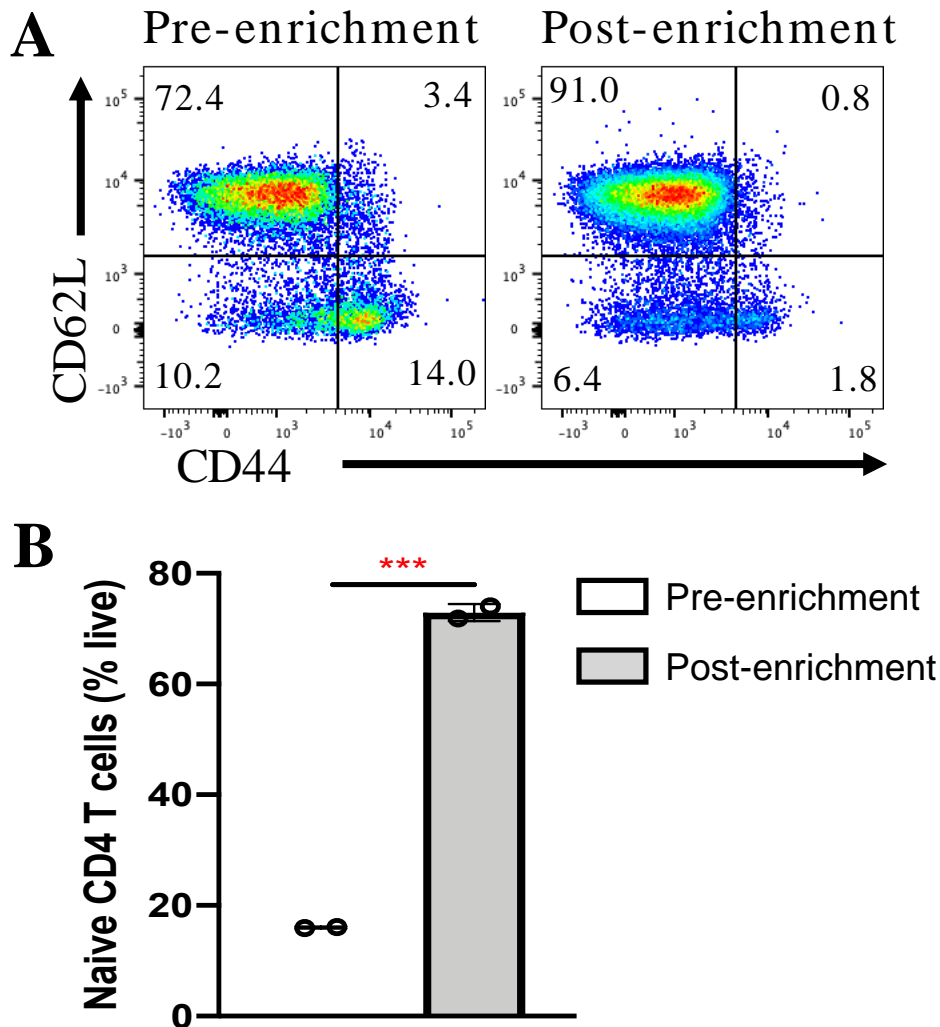


Figure 2.39: Naïve CD4 T cell isolation by AutoMACS. **A**, Representative flow cytometry plots. Cells were gated as lymphocytes, single cells, live, CD45⁺ and CD4⁺. Naïve CD4 T cells were identified as CD44⁻CD62L⁺. **B**, Quantification of naïve CD4 T cells pre- and post-enrichment. Data is representative of mean \pm SEM. Differences indicated as *p* values, as assessed by Student *t* Test ****p*<0.005. *n* = 2.

2.19 *In vitro* CD4 T cell polarisation

Naïve CD4 T cells isolated from spleens as described in **Section 2.18** were polarised into CD4 T cell subsets (Th1, Th2, Th17 and Tregs) based on Schwartz et al. (2017). Naïve CD4 T cells were cultured for 5 days with plate bound anti-CD3 (2 μ g/ml) (clone: 145-2C11 BD bioscience) and soluble CD28 (2 μ g/ml) (clone: 37.51 BD). Cells were also cultured in the presence of polarising cytokines (**Table 2.9**). **Figure 2.40** shows an increase in T cell subpopulation transcription factor and cytokine secreted as assessed by flow cytometry and ELISA, compared to naïve CD4 T cells. Therefore, indicating that

naïve CD4 T cells were polarised towards their respective effector CD4 T cell subsets (Th1, Th2, Th17 and Treg).

Th subset	Cocktail	Concentration
Th0	rmIL-2	20ng/ml
Th1	rmIL-2 rmIL-12	20ng/ml 20ng/ml
Th2	rmIL-2 rmIL-4	20ng/ml 20ng/ml
Th17	rmIL-2 rmIL-6 rhTGF- β	20ng/ml 40ng/ml 5ng/ml
Treg	rmIL-2 rhTGF- β	20ng/ml 5ng/ml

Table 2.9: CD4 T cell polarising cocktails and concentrations

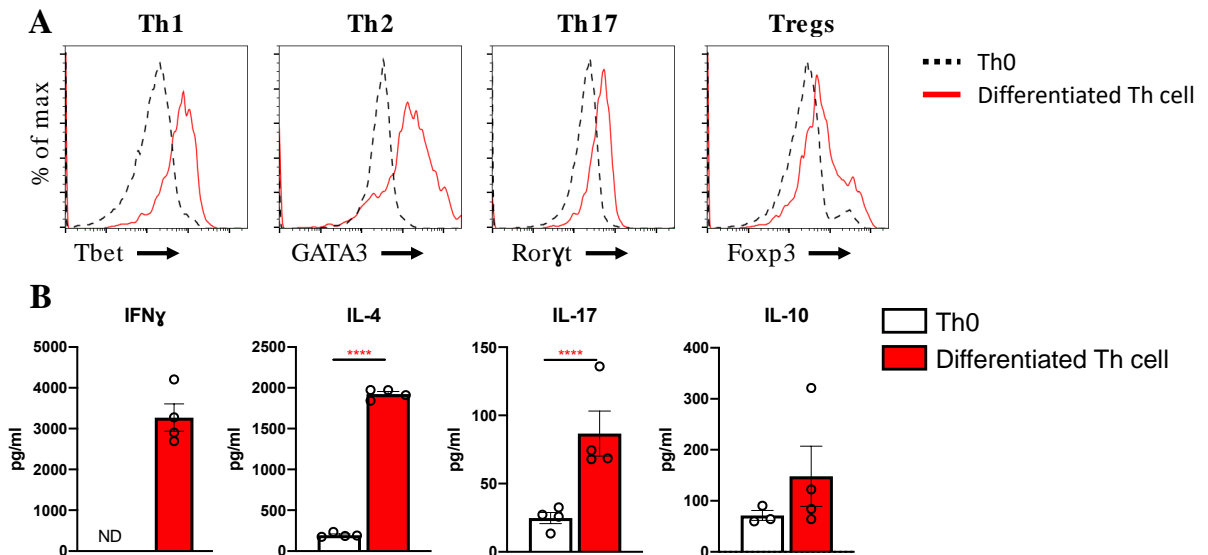


Figure 2.40: *In vitro* CD4 T cell polarisation. Naïve CD4 T cells were isolated from WT mice spleens and cultured in T cell polarisation conditions. **A**, Cells were gated as lymphocytes, single cells, live, CD45⁺ and CD4⁺. Expression of CD4 T cell subpopulation defining transcription factors in differentiated T cells. Th1 (Tbet), Th2 (GATA3), Th17 (Roryt) and Tregs (Foxp3). **B**, Quantification of cytokines secreted by CD4 T cells. Cytokines detected by an ELISA. Th1 (IFN γ), Th2 (IL-4), Th17 (IL-17) and Tregs (IL-10). Data is representative of mean \pm SEM. Differences indicated as *p* values, as assessed by Student *t* Test. *****p*<0.001. ND = Non-detected. n = 3-4.

2.20 Enzyme-linked immunosorbent assay (ELISA)

2.20.1 Cytokine ELISA

Levels of IL-4, IL-5 and IL-13 was quantified in the supernatant from MLN cultures using purified anti-IL-4 (BD Pharmingen), anti-IL-5 (BD Pharmingen) and anti-IL-13 (R&D Systems). Checkerboard titrations of coating and detecting antibodies or antigens were performed to determine optimum concentrations (**Table 2.10**). High binding 96 well plates (Greiner Bio-One, Frickenhausen, Germany) were coated with the respective capture antibody. Plates were incubated overnight at 4°C. The plates were then washed with PBS with 0.05% Tween 20 (PBST) 3 times, and to block any nonspecific binding, plates were coated with blocking buffer (1% BSA in PBS) and incubated for 1 hour at room temperature. The plates were washed again to remove any unbound antibody, samples and standards were added at predetermined dilution in 1% BSA in PBS. The plates were incubated for 2 hours at room temperature, then washed to remove any unbound antigen, and the appropriate detection antibody was added. Following another washing step, streptavidin conjugated to horseradish peroxidase (R&D Systems) was added and incubated for 40 minutes. O-phenylenediamine dihydrochloride (OPD) was used as a chromogenic substrate that utilises the horseradish peroxidase conjugate. OPD tablets were dissolved in 0.05 M phosphate-citrate buffer with H₂O₂. Following washes to remove unbound conjugate, OPD was added to each well. The substrate produces a soluble end product that is orange brown in colour. At maximum colour separation of standards, the reaction is stopped by the addition of sulphuric acid (3M H₂SO₄). The plate absorbance was read at 490 nm using the Versa Max Microplate Reader (Molecular Devices, USA). The cytokine concentrations were calculated against the known standards and a standard curve.

Cytokine	Capture antibody working concentration	Detection antibody working concentration	Top standard concentration
IL-4	2µg/ml	1µg/ml	2000pg/ml
IL-5	2µg/ml	1µg/ml	100ng/ml
IL-13	4µg/ml	200ng/ml	4000pg/ml

Table 2.10: ELISA working standard concentrations.

2.20.2 Total IgE ELISA

Serum IgE was measured using 96 well medium binding plates (Greiner Bio-One, Frickenhausen, Germany). Plates were coated with monoclonal anti-IgE coating antibody (2µg/ml) (BD Pharmingen) overnight at 4°C. Plates were washed with PBST 3 times and 1% BSA was added to the plates for 1 hour to block any non-specific binding to the plate. Diluted serum samples (**Section 2.23**) in 1% BSA in PBS were added and incubated for 2 hours. Bound IgE was detected using monoclonal biotin labelled anti-IgE detection antibody (4µg/ml) (BD Pharmingen) and streptavidin HRP. OPD was again used as a chromogenic substrate. Absorbance was read at 490 nm using the Versa Max Microplate Reader (Molecular Devices, USA). Serum IgE concentrations were calculated using purified IgE as standards (BD Pharmingen).

2.21 Whole blood collection and serum isolation

Whole blood was collected by submandibular bleeding mice, using a 4 mm lancet (Braintree, MA, US). For analysis by flow cytometry, approximately 150 µl of blood was collected into a Vacuette Heparin-coated blood collection tube (VWR, US). For serum isolation, approximately 1 ml of blood is collected into a 1.5 ml Eppendorf. Following blood collection, death was confirmed in the mice by cervical dislocation. The whole blood was left at room temperature and allowed to clot before being placed at 4°C for 1 hour. The whole blood was centrifuged at 2,000 g for 15 mins at 4°C and the serum was collected and stored at -20°C until further analysis.

2.22 Cell culture stimulation

Following *N. brasiliensis* infection, MLN T cells were *in vitro* stimulated using anti-CD3 and anti-CD28 mAb, and type 2 cytokines (IL-4, IL-5 and IL-13) secretion was assessed by ELISA. Activation of TCR complex by anti-CD3 antibody binding to CD3, whilst anti-CD28 binds to CD28 and stimulates T cells without the requirement for CD80 or CD86 from antigen presenting cells. Prior to addition of cells, 96 well plates were incubated with 1 µg/ml anti-CD3 mAb for 2 hours at 37°C. Plates were washed with PBS

and cells were seeded at 2×10^5 per well with the addition of 1 $\mu\text{g/ml}$ anti-CD28 mAb. Culture supernatants were harvested after 72 hours and cytokine production was analysed by ELISA (Section 2.20).

2.23 Histology

2.23.1 Tissue fixation

Murine lungs and small intestines were carefully dissected and immediately fixed in 10% formal saline (100ml of 37% formaldehyde mixed with 8.5g sodium chloride in 900ml distilled water). The samples were kept in 10% formal saline for at least 48 hours at room temperature prior to tissue dehydration. This phase retains the chemical composition, hardens the sample for sectioning and prevents degradation of the tissue.

2.23.2 Tissue dehydration

The tissues were dehydrated to help solidify and facilitate sectioning of the tissue. Tissues were placed in histology cassettes (Sigma) and dehydrated via six increasing concentrations of ethanol baths (70%, 95% and 100% four times for 60 – 120 seconds each time), followed by two xylene baths and two paraffin baths for 1 minute each, and left overnight in liquid paraffin.

2.23.3 Tissue embedding and sectioning

The dehydrated tissue was removed from the cassette and carefully transferred into a mould at the appropriate orientation. Paraffin wax at 58°C was poured into the mould and a labelled cassette was attached using the paraffin embedding station (Leica EG1150H). The sample was left to solidify on the cold plate (Leica EG1150C) at 4°C for approximately 30 minutes. Once the paraffin wax had set, the sample was removed from the mould. Embedded tissue samples were sectioned at 5 μm using a microtome (Leica

RM2235) and floated onto water at 50°C. Sections were then mounted onto a labelled glass slide and left to dry overnight.

2.23.4 Histology staining

Slide sections were stained for Hematoxylin and Eosin (H&E) (**Table 2.11**). Haematoxylin binds to basophilic substances, such as DNA and RNA, and stains the structure violet. Eosin binds acidophilic substances, such as proteins in the cytoplasm and stains the structures pink.

Step	Staining reagent	Time (Min)	Comment
1	Xylene	10	Deparaffinize
2	100% Ethanol	6	Rehydration
3	95% Ethanol	6	Rehydration
4	70% Ethanol	3	Rehydration
5	H ₂ O	1	Rehydration
6	Haematoxylin	8	Nuclei staining
7	H ₂ O	1	Removal of excess haematoxylin
8	Eosin	2	Cytoplasm staining
9	H ₂ O	1	Removal of excess eosin
10	70% Ethanol	1	Dehydration
11	95% Ethanol	2	Dehydration
12	100% Ethanol	2	Dehydration
13	Xylene	20	Removal of ethanol

Table 2.11: H&E staining protocol.

Slides were also stained for Periodic acid–Schiff (PAS) (**Table 2.12**). This stain is used for the detection of glycogen. Periodic acid oxidises the tissue resulting in formation of aldehyde groupings through carbon-to-carbon bond cleavage. These aldehyde groups are detected by the Schiff reagent and stains the structures pink. The slides were imaged using the Aperio ImageScope.

Step	Staining reagent	Time (Min)	Comment
1	Xylene	10	Deparaffinize
2	100% Ethanol	6	Rehydration
3	95% Ethanol	6	Rehydration
4	70% Ethanol	3	Rehydration
5	H ₂ O	1	Rehydration
6	Periodic acid solution	5	Oxidizes the tissue forming aldehyde groups
7	H ₂ O	1	Removal of excess Periodic acid
8	Schiff reagent	15	Detection of aldehyde groups
9	H ₂ O	1	Removal of excess Schiff reagent
10	Haematoxylin	1	Nuclei staining
11	H ₂ O	1	Removal of excess haematoxylin
12	70% Ethanol	1	Dehydration
13	95% Ethanol	2	Dehydration
14	100% Ethanol	2	Dehydration
15	Xylene	20	Removal of ethanol

Table 2.12: PAS staining protocol.

2.23.5 Histology scoring

All histology sections were examined for goblet cell hyperplasia. This was determined by counting the number of positive goblet cells per ten villi from the small intestine based on PAS staining (Schmidt et al., 2012). **Figure 2.41** show representative PAS staining for enumeration of goblet cells in small intestine of uninfected (**Figure 2.41A**) and *N. brasiliensis* infected (**Figure 2.41B**) WT mice.

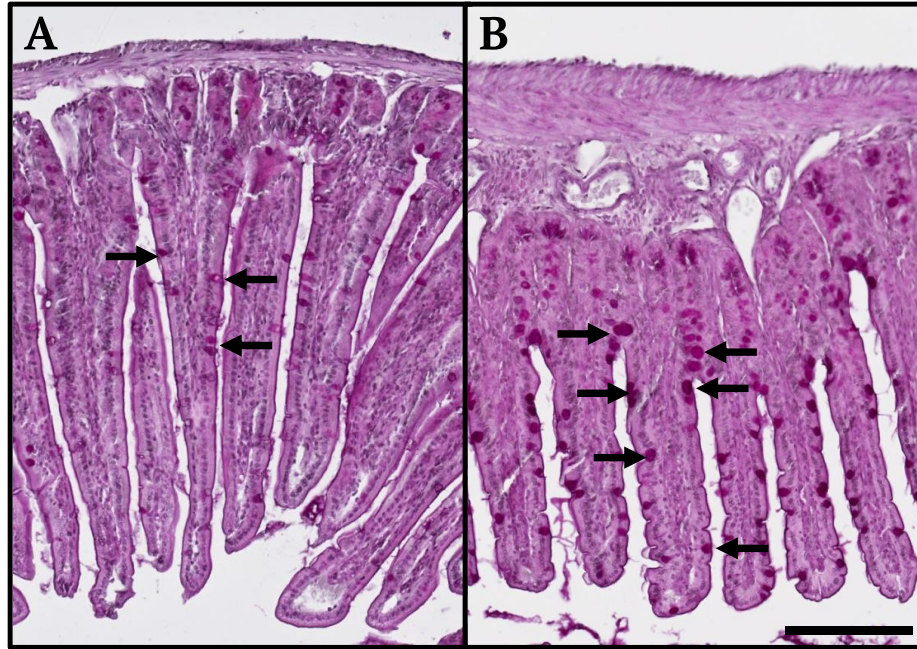


Figure 2.41: Identification PAS⁺ goblet cells in small intestine. Representative histological sections of murine jejunum visualising goblet cell hyperplasia using PAS reagent staining. **A**, Uninfected WT mouse. **B**, *N. brasiliensis* infected WT mouse. Images are visualised at 10x magnification. Black arrows indicate goblet cell. Scale bar = 200 μ m.

2.24 Statistical analysis

All statistical analysis was performed using GraphPad Prism version 8.3 (GraphPad Inc.). Data represented as mean \pm Standard Error of the Mean (SEM). For comparison between two unmatched groups, an unpaired Student t-test were used. For comparison between paired data, a paired Student t-test was used. For comparison between two independent groups that are not normally distributed, a Mann Whitney U test was used. An explanation of statistical results is shown in **Table 2.13**.

<i>P</i> values	Wording	Representation
< 0.0001	Extremely significant	****
0.0001 to 0.001	Extremely significant	***
0.001 to 0.01	Very significant	**
0.01 to 0.05	Significant	*
\geq 0.05	Not significant	ns

Table 2.13: Explanation of GraphPad Prism symbols.

Chapter 3

**Determining the role of *Rora* in
inflammatory responses to *N. brasiliensis*
using ubiquitous mutant *Rora* mice
(*Rora*^{sg/sg}) and *Rora*^{sg/sg} BM chimera mice**

Chapter 3

3.1 Introduction

Retinoic acid-receptor-related orphan receptor alpha (ROR α) is a nuclear transcription factor that is known to have roles in cerebellar development, metabolism, circadian rhythm and immunity (**Chapter 1, Section 1.8**). In the context of immunity, studies on ROR α have primarily focussed on its involvement in immune signalling pathways and cell development. Indeed, it has been shown that ROR α is important in the development of ILC2s (Wong et al., 2012, Halim et al., 2012) (**Chapter 1, Section 1.8.17.2**), Th17 cells (Yang et al., 2008) (**Chapter 1, Section 1.8.17.4**) and Treg function (Malhotra et al., 2018) (**Chapter 1, Section 1.8.17.5**).

There is increasing evidence to suggest that there is a role for ROR α in type 2 immunity (**Chapter 1, Section 1.8.10**), beyond its known role in ILC2 development. In addition to a general role in a functional type 2 response, recent studies have provided accumulating evidence for a role for ROR α in Th2 cells. Indeed, it is apparent that ROR α is expressed in Th2 cells, with increased expression in Th2 cells isolated from mice after challenge with papain or OVA (Liu et al., 2015, Van Dyken et al., 2016, Maggi et al., 2017, Miragaia et al., 2019, Haim-Vilmovsky et al., 2020). It has also been reported that *Rora* expression is associated with activated Th cells in response to *N. brasiliensis* infection, a model of type 2 inflammation (Haim-Vilmovsky et al., 2020). These activated *Rora* expressing CD4 T cells promote lung inflammation in response to *N. brasiliensis* infection (Haim-Vilmovsky et al., 2020). Therefore, while there is increasing evidence of *Rora* expression in a number of cells important in a functional type 2 response, such as ILC2 and Th2 cells, a full understanding of the role of ROR α in type 2 inflammation in the lungs has yet to be defined.

In this chapter, the aim is to investigate the role of ROR α in type 2 immunity by utilising the mouse model of *N. brasiliensis* infection. *N. brasiliensis* infection induces a type 2 immune response (**Chapter 2, Section 2.8.4**), and its lifecycle and morphology are similar to the human hookworms *Necator americanus* and *Ancylostoma duodenale*. Studies investigating the role of ROR α have utilised *Rora*^{sg/sg} mice, which contain a

ubiquitously expressed non-functional, truncated form of the ROR α protein, due to a spontaneous mutation in the *Rora* gene (**Chapter 1, Section 1.8.5**). Therefore, in this chapter, *Rora*^{sg/sg} mice were used to further investigate type 2 immunity in the absence of functional ROR α ubiquitously. To further explore the role of ROR α , I generated *Rora*^{sg/sg} BM chimera mice (**Chapter 2, Section 2.6**) which eliminate any potential confounding factors of *Rora*^{sg/sg} mice, and allowed for empirical analysis of the function of ROR α when expressed in cells of hematopoietic versus non-hematopoietic origin, during a type 2 immune response.

3.2 Chapter Objectives

1. To investigate the role of the transcription factor ROR α in *N. brasiliensis* infection using *Rora*^{sg/sg} mice
2. To investigate the role of the transcription factor ROR α in *N. brasiliensis* infection using *Rora*^{sg/sg} BM chimera mice
3. To investigate the role of the transcription factor ROR α in *in vitro* CD4 T cell polarisation using naïve CD4 T cells isolated from *Rora*^{sg/sg} mice

3.3 Results

3.3.1 Determining the role of the transcription factor ROR α in *N. brasiliensis* infection using *Rora*^{sg/sg} mice

3.3.1.1 *Rora*^{sg/sg} mice have a higher *N. brasiliensis* count in small intestine at day 7 post-infection, compared to WT mice

To determine the role of the transcription factor ROR α in a type 2 immune response, *Rora*^{sg/sg} mice were infected with the helminth *N. brasiliensis*. This infection resembles the lifecycle of the human hookworm and is a potent activator of both systemic and mucosal type 2 immune responses. The lifecycle of *N. brasiliensis* involves migration in the circulatory system to reach the lungs, where the larvae then migrate up the trachea and are swallowed, before reaching the small intestine, where they feed and mate. In WT mice, a type 2 immune response is initiated, which results in worm expulsion and tissue repair. The peak worm count in the small intestine was detected at day 5 post-infection, before complete worm expulsion by day 10 (**Chapter 2, Section 2.8.4**). Using the worm count in the small intestine as a measure of a functioning type 2 immune response, I assessed the impact of a lack of functional ROR α by assessing the worms in the small intestine of *Rora*^{sg/sg} mice compared to WT mice.

There was no significant difference in the number of *N. brasiliensis* in the small intestine of *Rora*^{sg/sg} mice compared to WT mice at day 5 post-infection (**Figure 3.1A**). Therefore, *N. brasiliensis* were not retained abnormally in the lungs of *Rora*^{sg/sg} and WT mice, and were able to migrate to the small intestine. At day 7 post-infection, WT mice had largely expelled *N. brasiliensis* from the small intestine (**Figure 3.1A**). However, in *Rora*^{sg/sg} mice there was a significant ($p>0.01$) higher worm count in the small intestine at day 7 post-infection compared to WT mice (**Figure 3.1A**). In support of these findings, at day 7 post-infection, *Rora*^{sg/sg} mice had a significantly (Mann-Whitney *U*-Test, $p=0.0061$) higher number of eggs in faeces compared to WT mice (**Figure 3.1B**). There were no eggs detected in faeces at day 5 post-infection for either WT or *Rora*^{sg/sg} mice as the *N. brasiliensis* were not fecundate at this time point.

It has previously been reported that *Rora*^{sg/sg} mice have a higher worm count in small intestine at day 6 post-infection (Wong et al., 2012). Here, I present data of a higher worm

count in the small intestine and increased eggs in faeces at day 7 post-infection in *Rora^{sg/sg}* mice compared to WT mice. I have investigated up to day 7 post-infection and it is yet to be determined if *Rora^{sg/sg}* mice completely expel *N. brasiliensis*. However, these results highlight that *Rora^{sg/sg}* mice have a delayed generation of a functional type 2 immune response, characterised by a significantly higher worm count in the small intestine and eggs in faeces at day 7 post-infection.

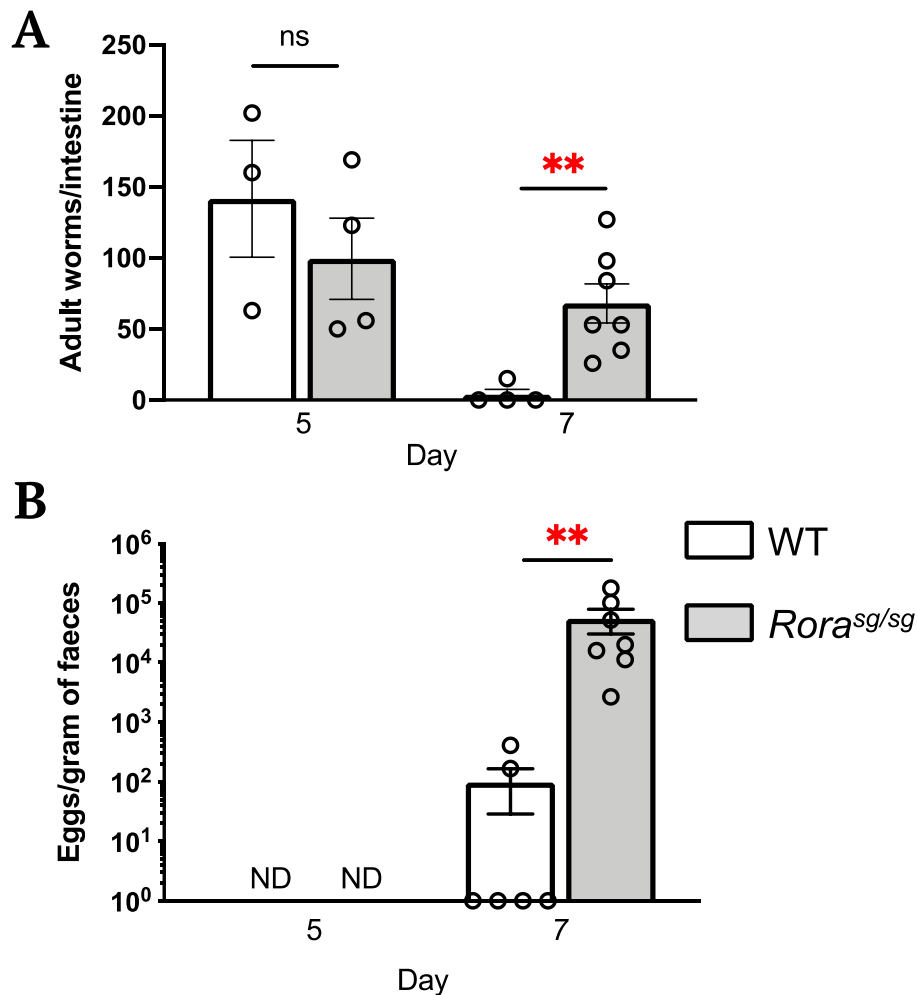


Figure 3.1: *Rora^{sg/sg}* mice have a higher *N. brasiliensis* count in the small intestine and eggs in faeces at day 7 post-infection compared to WT mice. *Rora^{sg/sg}* mice and WT mice were infected with 500 L3 *N. brasiliensis* subcutaneously. **A**, Small intestines were harvested at day 5 and day 7 post-infection. Data is two independent experiments. Data is representative of mean ± SEM. Differences indicated as two-tailed *p* values, as assessed by unpaired Student *t* test. ***p*<0.01. n = 3-7. **B**, Faeces was collected at day 5 and 7 post-infection. Eggs per gram (EPG) of faeces was calculated. Data is two independent experiments. Data is representative of mean ± SEM. Differences indicated as exact *p* value, as by two-tailed Mann-Whitney *U*-test, ***p*=0.0061. ND = non-detected. n = 4-7.

3.3.1.2 *Rora*^{sg/sg} mice have reduced goblet cells in the small intestine compared to WT mice following to *N. brasiliensis* infection

Early studies using *N. brasiliensis* infection noted that goblet cell hyperplasia is associated with parasitic nematode infection, and has a role in worm expulsion (Miller, 1987). Indeed, worm expulsion from the small intestine is reliant on a ‘weep and sweep’ process, in which hyperplasia of mucus secreting goblet cells occurs in the small intestine villi (**Chapter 1, Section 1.7**). Goblet cells secrete mucins that have detrimental effects on nematode vitality and mediate worm rejection (Hasnain et al., 2011). Therefore, given that at day 7 post-infection, *Rora*^{sg/sg} mice have a higher worm count in small intestine compared to WT mice (**Figure 3.1**), I sought to investigate goblet cell hyperplasia in the small intestine following *N. brasiliensis* infection. Goblet cell hyperplasia was determined by enumeration of Periodic Acid Schiff (PAS) positive cells per villus crypt unit (VCU) in the small intestine (Townsend et al., 2000) (**Chapter 2, Section 2.23.5**).

There is a significant ($p < 0.0001$) increase in small intestine goblet cells in WT mice following *N. brasiliensis* infection (**Figure 3.2**). However, there was significantly ($p < 0.0001$) fewer goblet cells in the small intestine of *Rora*^{sg/sg} mice compared to WT mice following *N. brasiliensis* infection (**Figure 3.2**). There was no significant difference in the number of goblet cells in uninfected *Rora*^{sg/sg} mice and WT mice (**Figure 3.2**). Therefore, the reduced goblet cells in *Rora*^{sg/sg} small intestine is specifically observed during a type 2 immune response, rather than a pre-existing disparity between uninfected *Rora*^{sg/sg} and WT mice. The data presented here shows a previously unreported altered small intestine goblet cell hyperplasia in *Rora*^{sg/sg} mice following *N. brasiliensis* infection, which is in accordance with previously published data demonstrating that *Rora*^{sg/sg} mice have reduced goblet cell hyperplasia in small intestine in response to IL-25 administration (Wong et al., 2012).

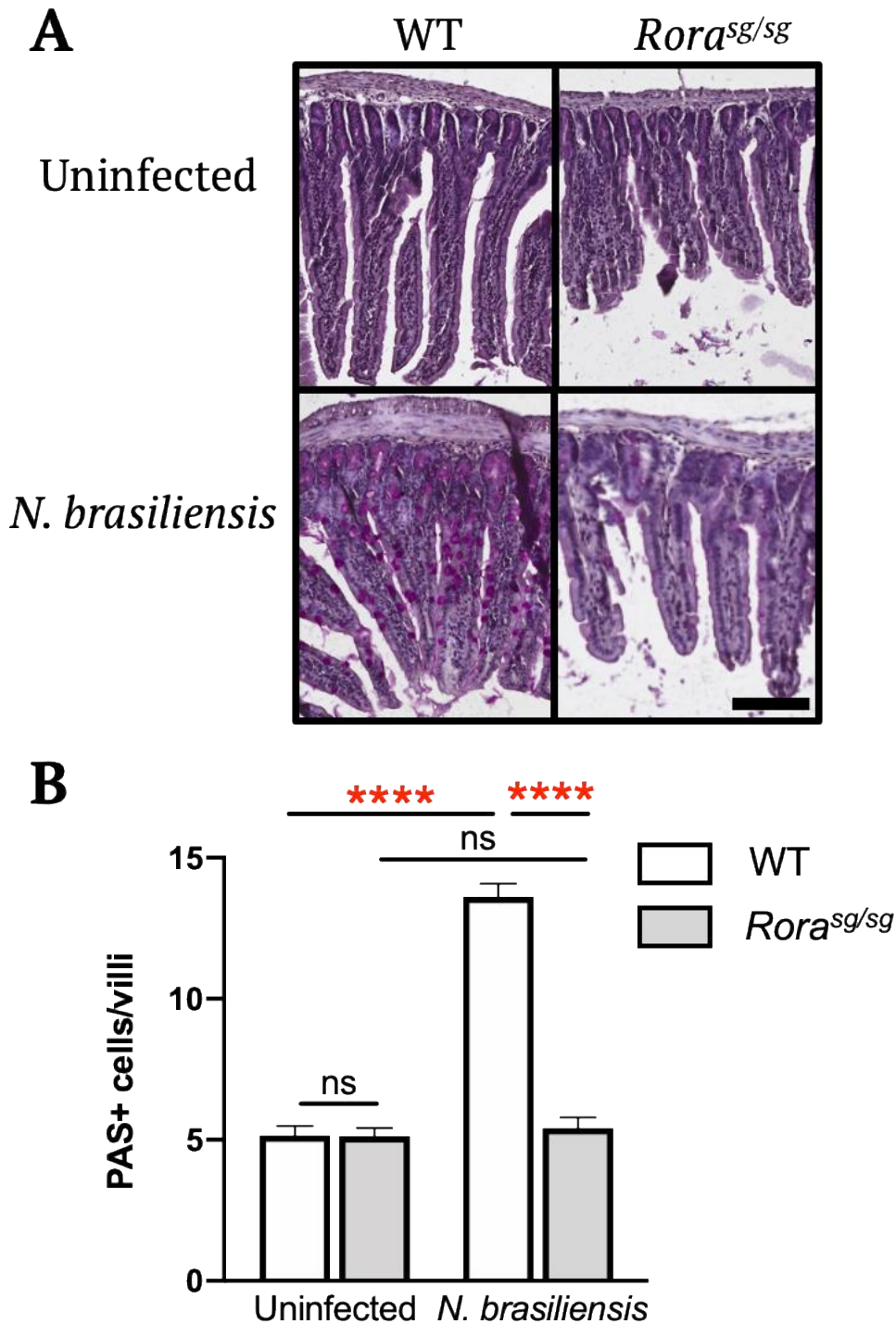


Figure 3.2: *Rora*^{sg/sg} mice have a significantly fewer goblet cells in the small intestine in response to *N. brasiliensis* infection compared to WT mice. *Rora*^{sg/sg} mice and WT mice were infected with 500 L3 *N. brasiliensis* subcutaneously. Small intestine was harvested from uninfected mice and at day 7 post-infection and assessed for goblet cells by PAS histology staining. **A**, Representative histological sections of murine small intestine, visualising goblet cell hyperplasia using PAS reagent staining (Magnification x10). Scale bar = 100µm. **B**, Enumeration of PAS positive goblet cells per villus crypt unit (VCU). Data is representative of mean ± SEM. Differences, indicated as two-tailed *p* values, as assessed by unpaired Student *t* test. *****p*<0.0001. ns = non-significant. n = 4-6.

3.3.1.3 *Rora*^{sg/sg} mice have a reduced frequency of lung ILC2s compared to WT mice in both uninfected condition and following *N. brasiliensis* infection

Having identified that *Rora*^{sg/sg} mice have an altered type 2 immune response, highlighted by a higher worm count and fewer goblet cells in the small intestines following *N. brasiliensis* infection, I sought to further characterise the role of ROR α in a type 2 immune response by assessing the associated immune cells by flow cytometry. The life cycle of *N. brasiliensis* infection involves migration through the hosts lungs causing pulmonary damage and eliciting potent type 2 inflammation, including ILC2 expansion. Indeed, ROR α is important in the development and expansion of ILC2s, and previously identified that *Rora*^{sg/sg} mice are ILC2-deficient (Wong et al., 2012, Halim et al., 2012). However, it has yet to be determined if *Rora*^{sg/sg} mice are deficient of ILC2s in the lung following *N. brasiliensis* infection. Therefore, using flow cytometry, I assessed the frequency of lung ILC2s in *Rora*^{sg/sg} and WT mice in uninfected and *N. brasiliensis* infected mice. The flow cytometry antibody panel for ILC2s is based on the gating strategy used by Omata et al. (2018), where ILC2s were identified as CD45⁺, lineage negative (CD3, CD11b, CD11c, CD19, F4/80, FcER1, Gr1 and γ TCR), KLRG1⁺ and GATA3⁺.

Flow cytometry analysis revealed that WT mice have a significant ($p > 0.001$) increase in lung ILC2s following *N. brasiliensis* infection (**Figure 3.3**). However, *Rora*^{sg/sg} mice have a significantly ($p < 0.01$) reduced frequency of lung ILC2s in both uninfected conditions and following *N. brasiliensis* infection, compared to WT mice (**Figure 3.3**). In addition, there was no increase in frequency lung ILC2s in *Rora*^{sg/sg} mice following *N. brasiliensis* infection. Therefore, indicating that *Rora*^{sg/sg} mice had no expansion of lung ILC2s following infection, as observed in WT mice. It should be noted, the data using *Rora*^{sg/sg} mice is presented as a percentage of cells, as opposed to presenting the total number of cells induced. This is due to the widely reported stunting of *Rora*^{sg/sg} mice compared to WT mice, which also results in significantly smaller organs (**Chapter 2, Section 2.1.1**), therefore presenting data as percentage of cells eliminates any impact of the size difference between groups which may confound the total cell number. These findings highlight that *Rora*^{sg/sg} mice have a reduced frequency of lung ILC2s in both uninfected conditions and following *N. brasiliensis* infection.

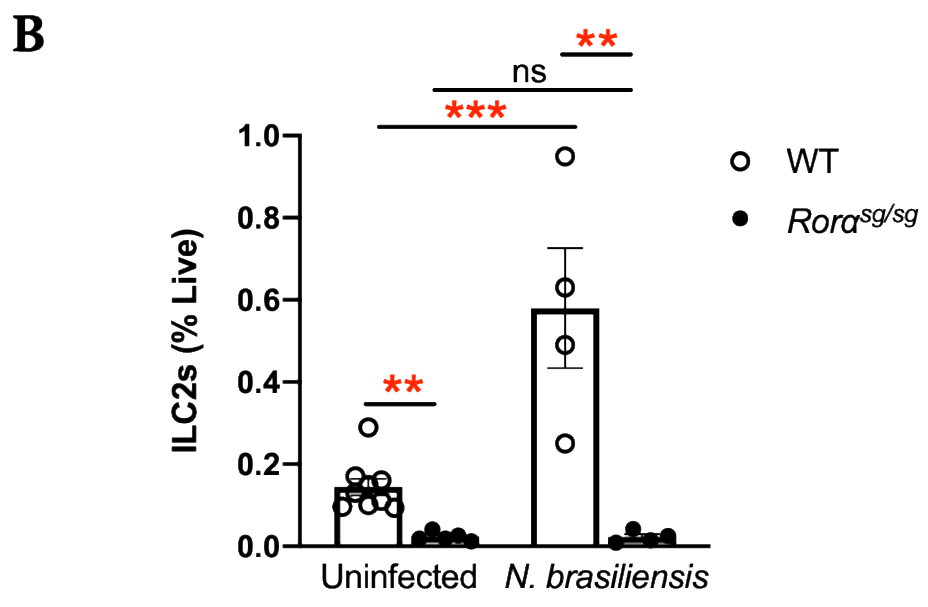
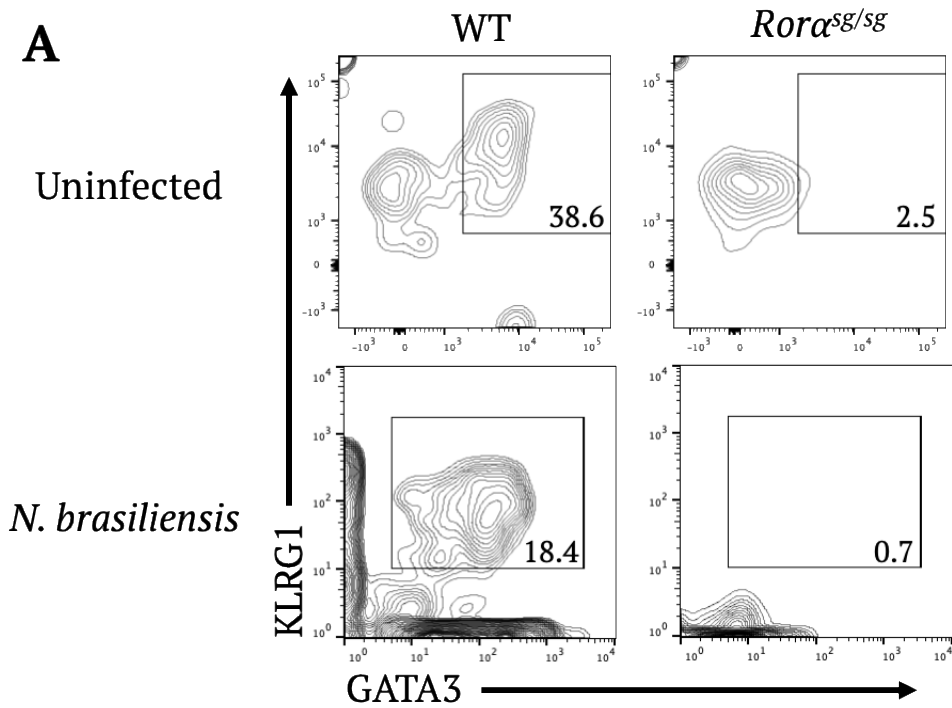


Figure 3.3: *Rora^{sg/sg}* mice have reduced frequency of lung ILC2s in uninfected mice and following *N. brasiliensis* infection compared to WT mice. *Rora^{sg/sg}* mice and WT mice were infected with 500 L3 *N. brasiliensis* subcutaneously. Lungs were harvested from uninfected mice and at day 5 post-infection and assessed by flow cytometry. **A**, Lung ILC2s were identified as lymphocytes, single cells, live cells CD45⁺Lineage⁻ (CD3, CD11b, CD11c, CD19, F4/80, FcER1, Gr1 and γ TCR) KLRG1⁺GATA3⁺. The number on flow cytometry plots represents percentage of CD45⁺Lineage⁻ cells. **B**, Quantification of lung ILC2s. Data representative of three independent experiments. Data is representative of mean \pm SEM. Differences indicated as two-tailed *p* values, as assessed by unpaired Student *t* test. ***p*<0.01, ****p*<0.001. ns = non-significant. n = 4-9.

3.3.1.4 *Rora*^{sg/sg} mice have reduced frequency of lung CD4 T cells compared to WT mice following *N. brasiliensis* infection

Helminth infections also induce the generation and accumulation of lung CD4 T cells (Th2) cells (Voehringer et al., 2004). There is increasing evidence that ROR α has a role in CD4 T cells during a type 2 immune response. Indeed, *Rora* expression in CD4 T cells promotes lung inflammation in response to *N. brasiliensis* infection (Haim-Vilmovsky et al., 2020). Therefore, I investigated the frequency of lung CD4 T cells in *Rora*^{sg/sg} mice following *N. brasiliensis* infection compared to WT mice.

There is a significant increase in frequency of lung CD4 T cells in WT mice at day 5 ($p < 0.05$) and day 7 ($p < 0.005$) post *N. brasiliensis* infection (**Figure 3.4**). However, *Rora*^{sg/sg} mice have a significantly reduced frequency of lung CD4 T cells at both day 5 ($p < 0.01$) and day 7 ($p < 0.05$) post-infection compared to WT mice (**Figure 3.4**). There was no significant difference in the frequency of CD4 T cells in the lungs of uninfected mice (**Figure 3.4**). Therefore, in the absence of a functional ROR α , there is a reduced frequency of lung CD4 T cells following *N. brasiliensis* infection, indicating *Rora* may have a role in CD4 T cell development during a type 2 immune response.

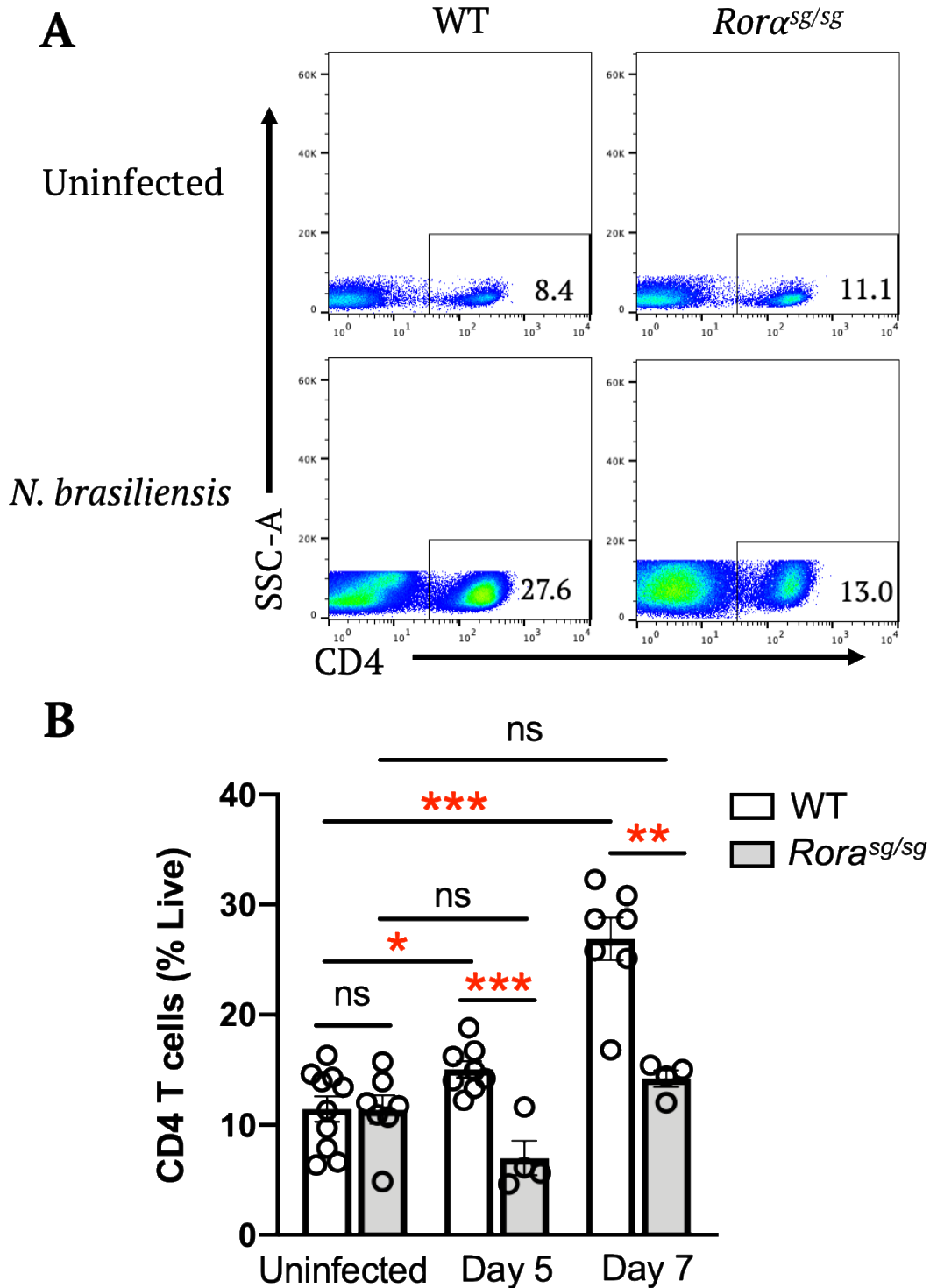


Figure 3.4: *Rora^{sg/sg}* mice have reduced frequency of lung CD4 T cells at day 5 and 7 post *N. brasiliensis* infection compared to WT mice. *Rora^{sg/sg}* mice and WT mice were infected with 500 L3 *N. brasiliensis* subcutaneously and lungs were harvested from uninfected mice and at day 5 and 7 post-infection. **A**, CD4 T cells were identified as lymphocytes, single cells, live cells, CD4⁺. The number on flow cytometry plots represents percentage of live cells. **B**, Quantification of lung CD4 T cells. Data is three independent experiments. Data is representative of mean \pm SEM. Differences indicated as two-tailed *p* values, as assessed by unpaired Student *t* test. **p*<0.05, ***p*<0.01, ****p*<0.005. ns = non-significant. n = 4-10.

3.3.1.5 *Rora*^{sg/sg} mice have a reduced frequency of lung GATA3⁺CD4 T cells compared to WT mice in response to *N. brasiliensis* infection

N. brasiliensis infection induces the conversion of Th1 and Th17 cells into Th2 cells (Panzer et al., 2012). Therefore, having identified that *Rora*^{sg/sg} mice have a reduced lung CD4 T cells following *N. brasiliensis* (**Figure 3.4**), I sought to investigate the frequency of lung GATA3⁺CD4 T cells (Th2) in *Rora*^{sg/sg} mice, compared to WT mice.

There is a significant increase in lung GATA3⁺CD4 T cells in WT mice following *N. brasiliensis* at day 5 ($p < 0.0001$) and day 7 ($p < 0.0001$) post-infection (**Figure 3.5**). However, *Rora*^{sg/sg} mice have a reduced frequency of lung GATA3⁺CD4 T cells compared to WT mice at day 5 ($p < 0.01$) and 7 ($p < 0.01$) post *N. brasiliensis* infection (**Figure 3.5**). There was no increase in the frequency of lung GATA3⁺CD4 T cells following *N. brasiliensis* infection in *Rora*^{sg/sg} mice, as is apparent in WT mice. In addition, there was no significant difference in the lung GATA3⁺CD4 T cells in uninfected WT and *Rora*^{sg/sg} mice, suggesting that the role of *Rora* on GATA3⁺CD4 T cells occurs following *N. brasiliensis* infection. This data indicates that *Rora* may have a role in GATA3⁺CD4 T cell development.

3.3.1.6 *Rora*^{sg/sg} mice have reduced frequency of GATA3⁺CD4 T cell in the mesenteric lymph node (MLN) compared to WT mice following *N. brasiliensis* infection

N. brasiliensis migrate from the lungs to reach the small intestines where sexual propagation occurs. This elicits another localised type 2 immune response in the small intestines. Therefore, having identified that *Rora*^{sg/sg} mice have reduced GATA3⁺CD4 T cells in a lungs, I sought to investigate the frequency of GATA3⁺CD4 T cells in the MLN, and to explore the role of ROR α in GATA3⁺CD4 T cell development across different tissues.

There was a significant ($p > 0.001$) increase in frequency of MLN GATA3⁺CD4 T cells at day 7 post-infection in WT mice. However, *Rora*^{sg/sg} mice have a significantly ($p < 0.005$) reduced frequency of GATA3⁺CD4 T cells in the MLN at day 7 post *N. brasiliensis* infection compared to WT mice (**Figure 3.6**). There was no significant difference in frequency of GATA3⁺CD4 T cells in uninfected *Rora*^{sg/sg} and WT mice. Therefore, in the absence of a functional ROR α , there is reduced GATA3⁺CD4 T cells in the MLN following *N. brasiliensis* infection. These results presented here are consistent with the results generated in the lungs (**Figure 3.5**). Therefore, *Rora* may have a comparable role in GATA3⁺CD4 T cell development across different tissues.

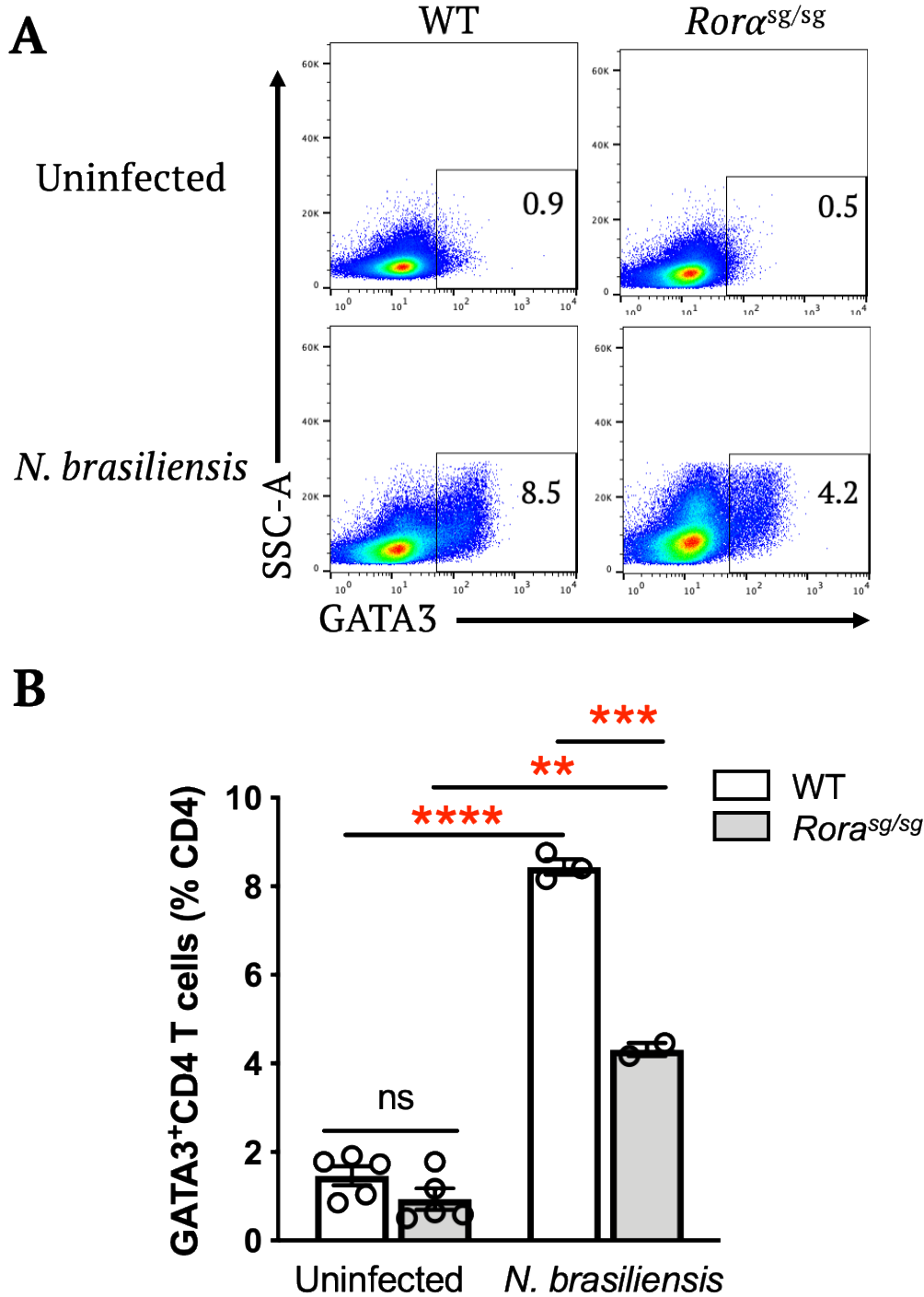


Figure 3.6: *Rora*^{sg/sg} mice have a reduced frequency of MLN GATA3⁺CD4 T cells in response to *N. brasiliensis* compared to WT mice. WT and *Rora*^{sg/sg} mice were infected with 500 L3 *N. brasiliensis* subcutaneously. MLN were harvested from uninfected mice and at day 7 post-infection and assessed by flow cytometry. **A**, Representative flow cytometry plots of gating strategy to identify MLN T cell populations. Cells were identified as lymphocytes, single cells, live cells, CD4⁺ and GATA3⁺. The numbers on flow cytometry flow plot represent percentage of CD4⁺ cells. **B**, Quantification of GATA3⁺CD4 T cells. Data is representative of two independent experiments. Data is representative of mean \pm SEM. Differences indicated as two-tailed *p* values, as assessed by unpaired Student *t* test. ***p*<0.01, ****p*<0.005, *****p*<0.001. ns = non-significant. *n* = 2-5.

3.3.1.7 *Rora*^{sg/sg} mice have a reduced frequency of lung eosinophils in response to *N. brasiliensis* infection compared to WT mice

Having identified that *Rora*^{sg/sg} mice have an altered lung cellular response beyond ILC2 deficiency following *N. brasiliensis* infection, notably a reduced frequency of CD4 T cells and GATA3⁺CD4 T cells, I sought to further characterise the lung immune cells elicited in this model. *N. brasiliensis* infection is also characterised by lung eosinophilia (Voehringer et al., 2004). *Rora*^{sg/sg} mice have been reported to have reduced lung eosinophilia in response to IL-25, as assessed by histological examination, compared to WT mice (Wong et al., 2012). Whilst, *Rora*^{sg/sg} mice challenged with papain and OVA, also had fewer eosinophils in the lung compared to WT mice (Jaradat et al., 2006, Halim et al., 2014). The frequency of lung eosinophils in *Rora*^{sg/sg} mice following *N. brasiliensis* infection is yet to be determined. Therefore, I sought to investigate the frequency of lung eosinophils following *N. brasiliensis* infection in *Rora*^{sg/sg} mice. Eosinophils were identified by flow cytometry based on the gating strategy from Guilliams et al. (2013), CD45⁺CD11b⁺SiglecF⁺F4/80⁺CD11c⁻.

In WT mice there is an increase in lung eosinophils following *N. brasiliensis* infection (**Figure 3.7**). Whilst in *Rora*^{sg/sg} mice there are significantly reduced lung eosinophils at day 5 ($p < 0.05$) and 7 ($p < 0.01$) post-infection (**Figure 3.7**) compared to WT mice. There was no difference in frequency of lung eosinophils in uninfected conditions (**Figure 3.7**). Therefore, these findings indicate that *Rora* may have a role in eosinophil development following *N. brasiliensis* infection.

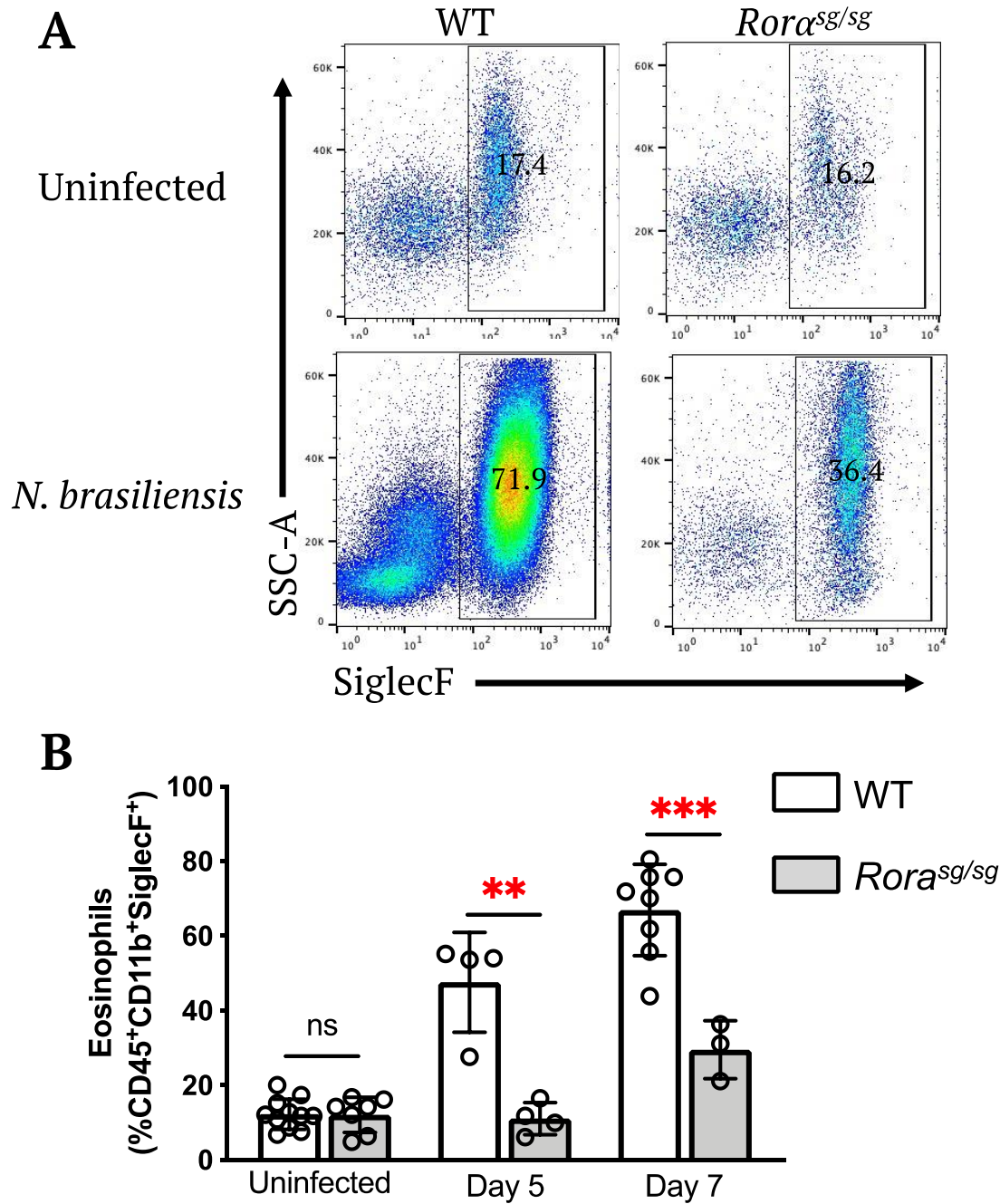


Figure 3.7: *Rora*^{sg/sg} mice have a reduced frequency of lung eosinophils following *N. brasiliensis* infection compared to WT mice. *Rora*^{sg/sg} mice and WT mice were infected with 500 L3 *N. brasiliensis* subcutaneously. Lungs were harvested from uninfected mice and at days 5 and 7 post-infection for flow cytometry analysis. **A**, Representative flow cytometry plots. Eosinophils were identified as single cells, live cells, CD45⁺CD11b⁺F4/80⁺SiglecF⁺CD11c⁻. The number on flow cytometry plot represents the percentage of parent gate (CD11b⁺F4/80⁺) cells. **B**, Quantification of lung eosinophils. Data is representative of two independent experiments. Data is representative of mean \pm SEM. Differences indicated as two-tailed *p* values, as assessed by unpaired Student *t* test. ***p* < 0.01, ****p* < 0.005, ns = non-significant. n = 3-9.

Thus far, I have explored the role of ROR α in during a type 2 immune response by using *Rora*^{sg/sg} mice, which have a ubiquitous mutation in *Rora* gene, rendering the protein non-functional. I have identified that *Rora*^{sg/sg} mice have an altered type 2 immune response following *N. brasiliensis* infection. This is characterised by a higher worm count in the small intestine and eggs in faeces at day 7 post-infection (**Figure 3.1**), and fewer small intestine goblet cells compared in WT mice following *N. brasiliensis* infection (**Figure 3.2**). I then sought to assess the impact of an absence of functional ROR α , on the cellular immune response to *N. brasiliensis* infection. *Rora*^{sg/sg} mice were identified as having reduced lung ILC2s in both uninfected mice and following *N. brasiliensis* infection, compared to WT mice (**Figure 3.3**). Interestingly, it was also observed that *Rora*^{sg/sg} mice had a reduced frequency of lung CD4 T cells following *N. brasiliensis* infection (**Figure 3.4**). Indeed, ROR α is important for Th17 cell differentiation (Yang et al., 2008). However, given *N. brasiliensis* infection induces the conversion of Th1 and Th17 cells into Th2 cells (Panzer et al., 2012), I assessed the frequency of GATA3⁺CD4 T (Th2) cells in *Rora*^{sg/sg} mice following *N. brasiliensis* infection. It was identified that *Rora*^{sg/sg} mice had a reduced frequency of GATA3⁺CD4 T cells in both the lung (**Figure 3.5**) and MLN (**Figure 3.6**). Furthermore, whilst investigating the immune repertoire in the lung, it was also observed that *Rora*^{sg/sg} mice had reduced lung eosinophils compared to WT mice following *N. brasiliensis* infection (**Figure 3.7**). Therefore, in addition to *Rora*^{sg/sg} mice being ILC2 deficient, these mice had a reduced frequency of GATA3⁺CD4 T cells and lung eosinophils following *N. brasiliensis* infection, indicating that *Rora* may have role in lung GATA3⁺CD4 T cells and eosinophil development.

3.3.2 Determining the role of the transcription factor ROR α in response to *N. brasiliensis* infection by generating and utilising *Rora*^{sg/sg} bone marrow (BM) chimera mice

The data presented in this chapter thus far, was generated using *Rora*^{sg/sg} mice. These mice have neurological defects, a stunted phenotype and metabolic disparity. Therefore, to eliminate any confounding effects caused by these abnormalities, I generated *Rora*^{sg/sg} BM chimera mice (**Chapter 2, Section 2.6**). To assess the efficacy of generating BM chimera mice, I generated a 4-way BM chimera mice experiment to assess the reconstitution efficiency of BM cells. Flow cytometry analysis of leukocyte markers

CD45.1 and CD45.2 showed reconstitution efficiency was >95%. Therefore, WT mice were sub-lethally irradiated and reconstituted with either BM cells from WT or *Rora*^{sg/sg} mice. It should be noted that due to the phenotype of *Rora*^{sg/sg} mice, it was not a viable option for *Rora*^{sg/sg} mice to act as recipient mice for WT BM cells. Thus, using *Rora*^{sg/sg} BM and WT BM chimera mice I sought to investigate the role of ROR α in hematopoietic cells during a type 2 immune response following *N. brasiliensis* infection.

3.3.2.1 *Rora*^{sg/sg} BM chimera mice have a delayed *N. brasiliensis* expulsion compared to WT BM chimera mice

Previously I have shown that *Rora*^{sg/sg} mice have an altered type 2 immune response, characterised by a higher worm count in the small intestine and the presence of eggs in faeces at day 7 post *N. brasiliensis* infection (**Figure 3.1**). Due to the phenotype of *Rora*^{sg/sg} mice longer time points were not feasible. However, using *Rora*^{sg/sg} BM chimera mice I was able to assess the type 2 immune response for longer periods. Therefore, I infected WT BM chimera and *Rora*^{sg/sg} BM chimera mice with *N. brasiliensis* and assessed the number of worms in the small intestine, and eggs in faeces at days 5-30 post-infection.

WT BM chimera mice had complete worm expulsion by day 10 post-infection (**Figure 3.8A**). There were no eggs in the faeces of WT BM chimera mice at day 10 post-infection, therefore confirming that worms had been expelled (**Figure 3.8B**). However, *Rora*^{sg/sg} BM chimera mice had a delay in worm expulsion, with some *Rora*^{sg/sg} BM chimera mice still having worms present in the small intestine at day 30 post-infection (**Figure 3.8A**). In support of this observation, *Rora*^{sg/sg} BM chimera mice had more eggs in the faeces from days 7-13 post-infection, further highlighting there were more *N. brasiliensis* worms residing in the small intestines of the *Rora*^{sg/sg} BM chimera mice (**Figure 3.8B**). However, interestingly, there are no eggs in the faeces of *Rora*^{sg/sg} BM chimera mice from day 14 post-infection, even though there were worms present in the small intestine. This may be due to a reduced fecundity of *N. brasiliensis* worms in these mice. There were no eggs detected in faeces of either WT BM and *Rora*^{sg/sg} BM chimera mice from days 3-5, this is due to *N. brasiliensis* not being fecund at these time point. These results support previously published data that *Rora*^{sg/sg} BM chimera mice had impaired worm expulsion

(Wong et al., 2012). However, Wong et al. (2012) reported complete worm clearance by day 11 in *Rora*^{sg/sg} BM chimera mice. The data presented here show worms still present in *Rora*^{sg/sg} BM chimera mice small intestine at day 30 post-infection, indicating that *Rora*^{sg/sg} BM chimera may have an altered adaptive immune response to *N. brasiliensis* infection.

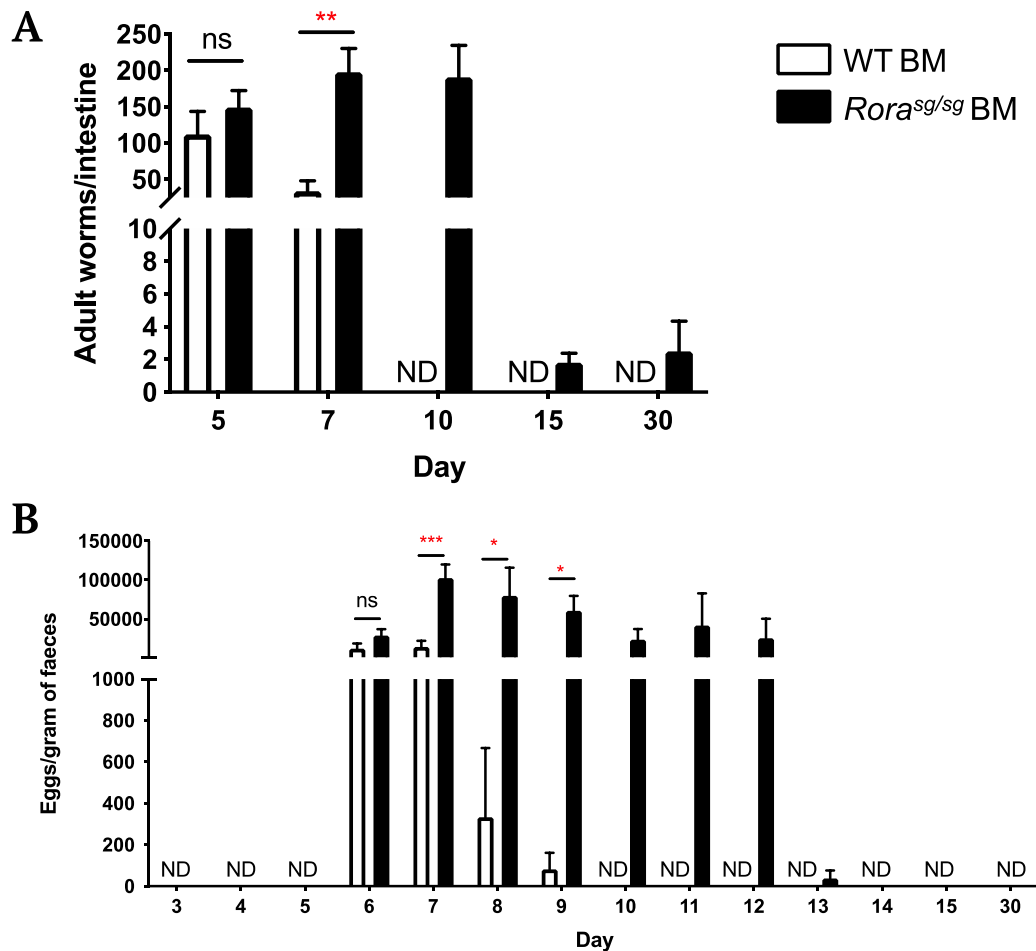


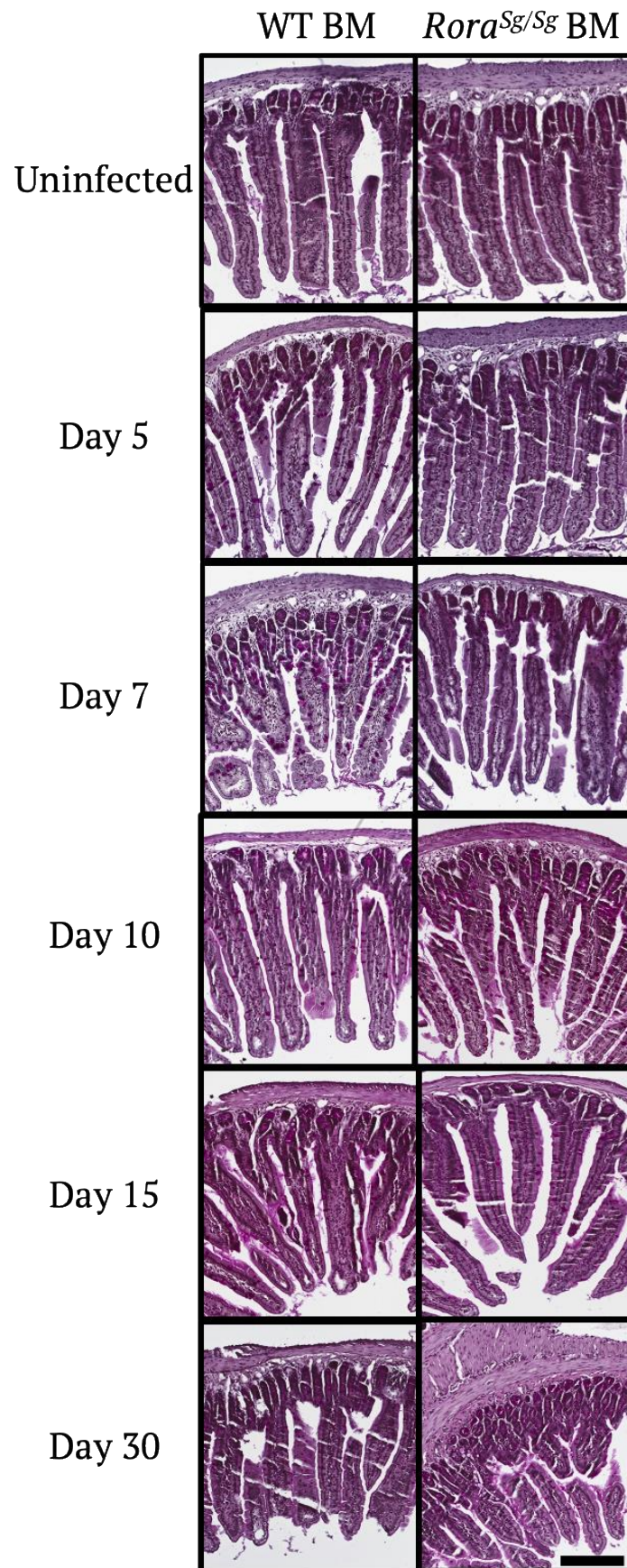
Figure 3.8: *Rora*^{sg/sg} BM chimera mice have a delayed *N. brasiliensis* expulsion compared to WT BM chimera mice. *Rora*^{sg/sg} BM chimera mice and WT BM chimera mice were infected with 500 L3 *N. brasiliensis* subcutaneously. **A**, Small intestines were harvested at day 5, 7, 10, 15 and 30 post-infection. Data is representative of three independent experiments. Data is representative of mean \pm SEM. Differences indicated as two-tailed *p* values, as assessed by unpaired Student *t* test. ***p*<0.01. *n* = 5-15. **B**, Faeces were collected from days 3-30 post-infection. Data is representative of three independent experiments. Data is representative of mean \pm SEM. Differences indicated as two-tailed *p* values, as assessed by Mann-Whitney *U*-test. **p*<0.05, ***p*<0.01, ****p*<0.005. *n* = 5-15.

3.3.2.2 *Rora*^{sg/sg} BM chimera mice have a reduced small intestine goblet cells at days 5 and 7 post *N. brasiliensis* compared to WT BM chimera mice

Having identified that *Rora*^{sg/sg} BM chimera mice have a delay in worm expulsion compared to WT BM chimera mice (**Figure 3.8**), and having previously shown that *Rora*^{sg/sg} mice have a reduced goblet cells compared to WT mice following *N. brasiliensis* infection (**Figure 3.2**), I sought to explore the small intestine goblet cell hyperplasia in *Rora*^{sg/sg} BM and WT BM chimera mice. It has been reported that *Rora*^{sg/sg} BM chimera mice have reduced lung mucus production, which is characteristic of reduced goblet cell hyperplasia, compared to WT BM chimera mice when challenged with i.n. papain (Halim et al., 2014). However, there has been no assessment of goblet cell hyperplasia in the small intestine following *N. brasiliensis* infection in *Rora*^{sg/sg} BM chimera mice.

There is no significant difference in goblet cells per villi in uninfected WT BM and *Rora*^{sg/sg} BM chimera mice (**Figure 3.9**). However, following *N. brasiliensis* infection, *Rora*^{sg/sg} BM chimera mice have significantly reduced goblet cells at day 5 ($p < 0.0001$) and 7 ($p < 0.0001$) compared to WT BM chimera mice (**Figure 3.9**). However, by day 10 post-infection, there was no significant difference in number of goblet cells per villi between WT BM and *Rora*^{sg/sg} BM chimera mice. This may be explained as WT BM chimera mice having expelled the worms by day 10 post-infection and therefore, no requirement for goblet cell hyperplasia. Whilst *Rora*^{sg/sg} BM chimera mice still have worms present in the small intestine, inducing goblet cell hyperplasia and therefore a delayed goblet cell hyperplasia reaching the frequency of WT BM chimera mice at day 10 post-infection. In both WT BM and *Rora*^{sg/sg} BM chimera mice, the number of goblet cells per villi began to decline from day 15 to day 30 post-infection, this coincides with the resolution of and clearance of worms in the small intestine.

A



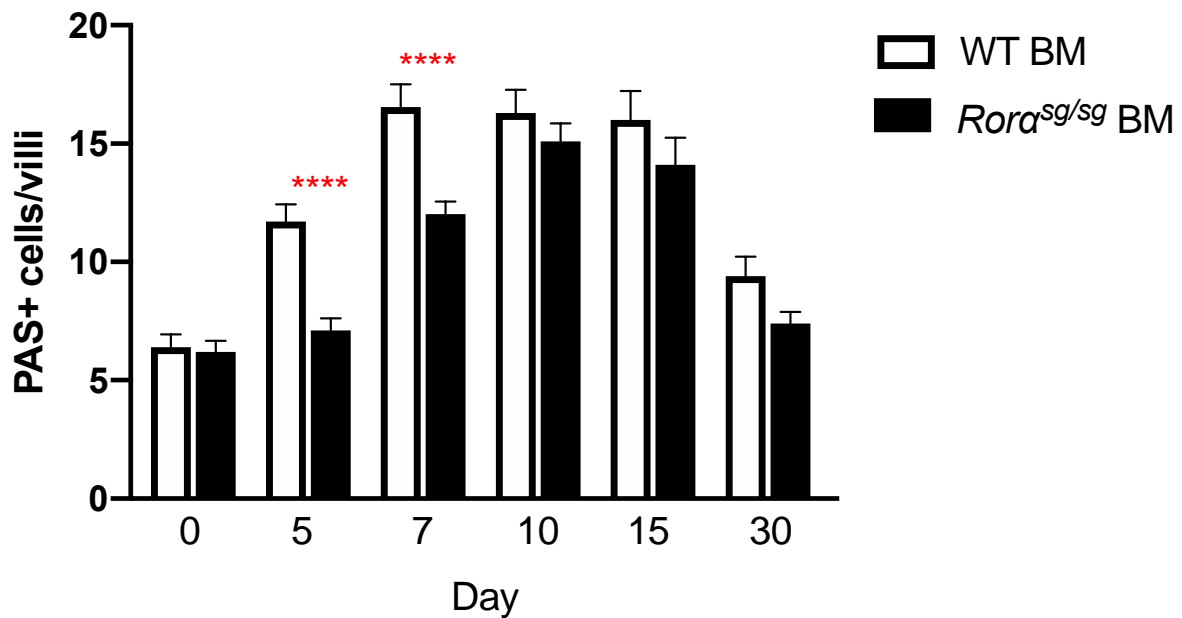
B

Figure 3.9: *Rora*^{sg/sg} BM chimera mice have less goblet cells in small intestine compared to WT BM chimera mice from day 5-7 post *N. brasiliensis* infection. **A**, Representative histological sections of murine small intestine visualising goblet cell hyperplasia using PAS reagent staining (Magnification x10). Scale bar = 100 μ m. **B**, Quantification of PAS⁺ cells per villi. Data is representative of three independent experiments. Data is representative of mean \pm SEM. Differences, indicated as two-tailed *p* values, as assessed by unpaired Student *t* test. *****p*<0.0001. *n* = 5.

3.3.2.3 *Rora*^{sg/sg} BM chimera mice have an altered serum IgE compared to WT BM chimera mice following *N. brasiliensis* infection

N. brasiliensis infection promotes B cell class switching to IgE. The antibody IgE binds to the cell surface receptor Fc ϵ RI on mast cells and basophils resulting in cell degranulation (Martin et al., 2018). Previously it was reported that *Rora*^{sg/sg} BM chimera mice have reduced serum IgE in response to house dust mite (HDM) extract compared to WT BM chimera mice (Gold et al., 2014). Whilst papain challenged *Rora*^{sg/sg} BM chimera mice had substantially reduced levels of serum IgE compared to WT BM chimera mice (Halim et al., 2014). Serum IgE in *Rora*^{sg/sg} BM chimera mice has not yet been investigated following *N. brasiliensis* infection. Therefore, to further appraise the role of

Rora in a type 2 immune response, I sought to measure serum IgE in *Rora*^{sg/sg} BM chimera mice following *N. brasiliensis* infection.

There was no IgE detected in serum of uninfected WT BM chimera and *Rora*^{sg/sg} BM chimera mice, and at day 5 post *N. brasiliensis* infection (**Figure 3.10**). This is expected as B cell secretion of IgE is part of the adaptive immune response and it takes several days to mount an effective response. There was no significant difference in serum IgE between days 7 – 30 post-infection between WT and *Rora*^{sg/sg} BM chimera mice (**Figure 3.10**). However, interestingly, in WT BM chimera mice the peak serum IgE occurred at day 15 post-infection, before declining at day 30. Whilst in *Rora*^{sg/sg} BM chimera mice, serum IgE continually increases with each time point, reaching a peak at day 30 post-infection. This may reflect the presence of worms in the small intestines of *Rora*^{sg/sg} BM chimera mice up to 30 days post-infection, which are still stimulating a type 2 response in these mice. Whilst worms have been expelled in WT BM chimera mice and resolution of the immune response has commenced in these animals. These findings suggest that *Rora*^{sg/sg} BM chimera mice have an altered adaptive immune response to *N. brasiliensis* infection.

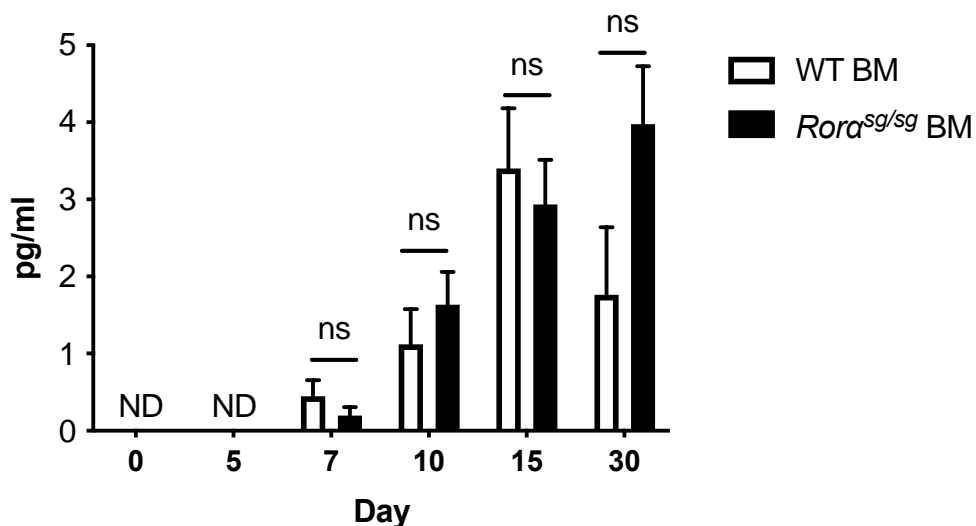


Figure 3.10: *Rora*^{sg/sg} BM chimera mice have altered serum IgE at day 30 post *N. brasiliensis* infection compared to WT BM chimera mice. WT and *Rora*^{sg/sg} BM chimera mice were infected with 500 L3 *N. brasiliensis* subcutaneously. Whole blood was collected at day 0, 5, 7, 10, 15 and 30 post-infection and assessed for serum IgE as detected by an ELISA. Data is representative of three independent experiments. Data is representative of mean \pm SEM. Differences, indicated as two-tailed *p* values, as assessed by unpaired Student *t* test. ns = non-significant. n = 5.

3.3.2.4 *Rora*^{sg/sg} BM chimera mice MLN cells have delayed T cell type 2 cytokine (IL-4, IL-5 and IL-13) secretion following *N. brasiliensis* infection

CD4 T cells secrete cytokines that are critical for orchestrating an adaptive type 2 immune response. Th2 cells secrete IL-4, IL-5 and IL-13 which promote immune cell differentiation, migration and activation of inflammatory cells and goblet cell hyperplasia (**Chapter 1, Section 1.7**). It has been reported that *Rora* expressing CD4 T cells were associated with expression of cytokines *Il4* and *Il13* (Haim-Vilmovsky et al., 2020), indicating that ROR α may have a role in CD4 T cell cytokine secretion. It has also been reported that lung and mediastinal lymph nodes (medLN) cells from *Rora*^{sg/sg} BM chimera mice had reduced ability to secrete type 2 cytokines (IL-4 and IL-5) following intra-nasal papain treatment, compared to WT BM chimera mice (Halim et al., 2014). Therefore, I investigated the role of ROR α in Th2 cytokine secretion from MLN cells isolated from WT BM chimera and *Rora*^{sg/sg} BM chimera mice following *N. brasiliensis* infection. The cells were cultured in the presence of anti-CD3 and CD28, to activate the T cells, and cytokine secretion was determined after 72 hours by ELISA (**Chapter 2, Section 2.22**).

There was an increase in levels of IL-4, IL-5 and IL-13 detected in supernatant of MLN isolated from WT BM chimera following *N. brasiliensis* infection. This reached a peak cytokine secretion in MLN cells isolated from animals at day 7 post *N. brasiliensis* infection, before beginning to decline at day 10 post-infection (**Figure 3.11**). In contrast, *Rora*^{sg/sg} BM chimera MLN cells had a reduced and delayed secretion of cytokines following T cell stimulation. *Rora*^{sg/sg} BM chimera MLN cells cytokine secretion reached peak in MLN cells isolated at day 10 post *N. brasiliensis* infection. Therefore, these findings indicate that ROR α may have a role T cell type 2 cytokine secretion.

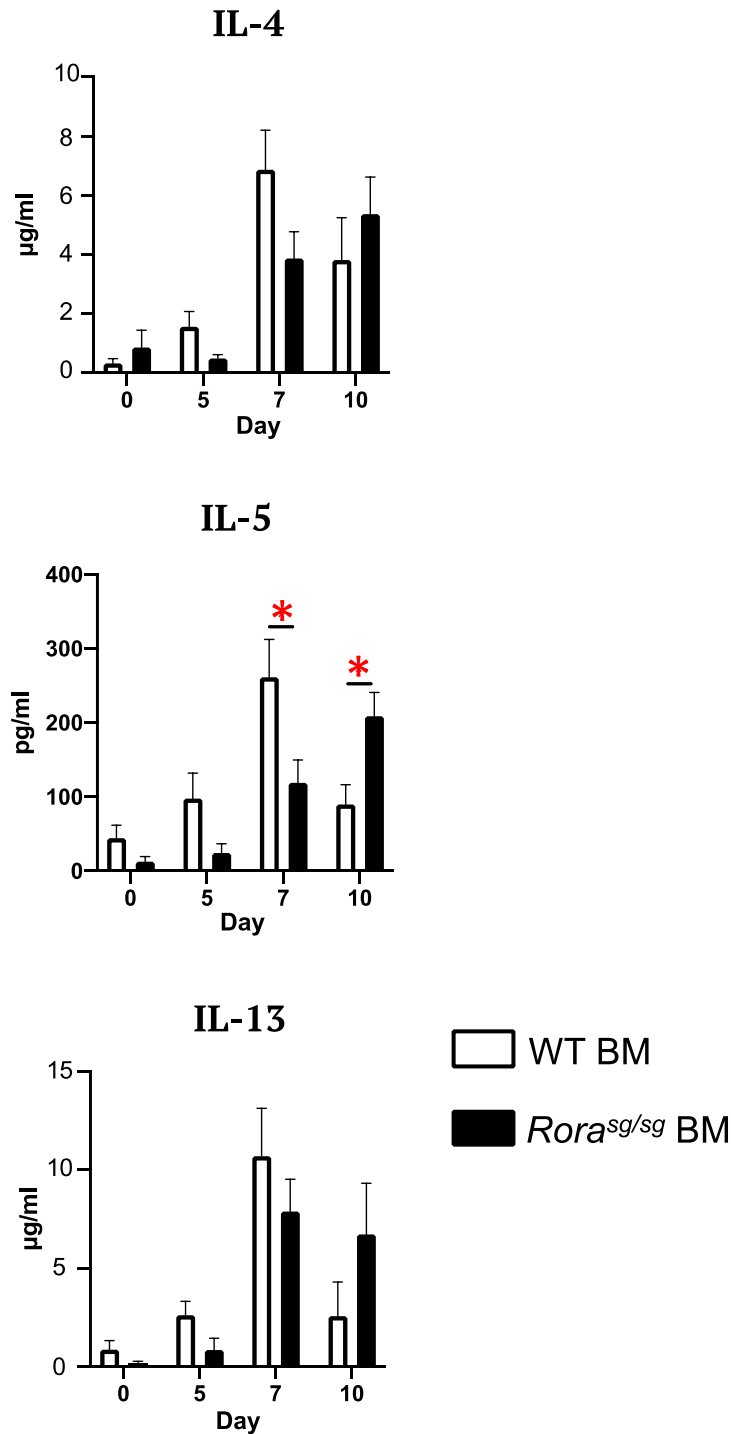


Figure 3.11: *Rora*^{sg/sg} BM mice MLN cells have altered T cell cytokines (IL-4, IL-5 and IL-13) secretion following *N. brasiliensis* infection, compared to WT BM chimera mice T cells. *Rora*^{sg/sg} BM chimera mice and WT BM chimera mice were infected with 500 L3 *N. brasiliensis* subcutaneously. MLN cells were cultured for 72 hours from day 0, 5, 7 and 10 post-infection with anti-CD3 and anti-CD28. Cytokine secretion was measured by an ELISA for IL-4, IL-5 and IL-13. Data is representative of three independent experiments. Data is representative of mean \pm SEM. Differences, indicated as two-tailed *p* values, as assessed by unpaired Student *t* test. **p*<0.05. n = 5.

The results presented in this chapter thus far have explored the role of *Rora* following a primary *N. brasiliensis* infection. In summary, *Rora*^{sg/sg} mice have a higher worm count in the small intestine, reduced frequency of lung ILC2s, CD4 T, GATA3⁺CD4 T cells and eosinophils following primary *N. brasiliensis* infection compared to WT mice. On further investigation, *Rora*^{sg/sg} BM chimera mice have a delayed worm expulsion, altered serum IgE and delayed T cell cytokine secretion compared to WT BM chimera mice. These findings indicate that there may be a role for ROR α beyond ILC2 development during *N. brasiliensis* infection. Therefore, I sought to investigate the role of ROR α in immune cells during a primary and secondary *N. brasiliensis* infection using *Rora*^{sg/sg} BM chimera mice.

3.3.2.5 *Rora*^{sg/sg} BM chimera mice have increase *N. brasiliensis* count in primary and secondary *N. brasiliensis* infection compared to WT BM chimera mice

ILC2s have been shown to play a role in IL-13 mediated expulsion of *N. brasiliensis* from the gut following primary infection (Fallon et al., 2006, Neill et al., 2010). It has also been shown that *Rag2*^{-/-} mice which have a strong innate immune responses, but defective adaptive immune responses, are unable to expel *N. brasiliensis* infection, suggesting that ILC2s work in concert with adaptive immune response (Neill et al., 2010). Therefore, having identified that *Rora*^{sg/sg} BM chimera mice have a delayed worm expulsion to primary *N. brasiliensis* infection (**Figure 3.8**), and *Rora*^{sg/sg} mice had reduced frequency of lung ILC2s (**Figure 3.3**), CD4 T cells (**Figure 3.4**) and GATA3⁺CD4 T cells (**Figure 3.5**), suggesting *Rora*^{sg/sg} BM chimera mice may have an altered adaptive immune response to secondary *N. brasiliensis* infection. Therefore, I assessed the role of ROR α in secondary *N. brasiliensis* infection. To investigate this, *Rora*^{sg/sg} BM and WT BM chimera mice were infected with *N. brasiliensis* (primary infection), followed by a secondary *N. brasiliensis* infection at 21 days later (**Chapter 2, Section 2.8.4**).

Consistent with previous results presented in this chapter (**Figure 3.8**), *Rora*^{sg/sg} BM chimera mice had a significantly ($p > 0.01$) higher worm count at day 7 post primary infection compared to WT BM chimera mice (**Figure 3.12A**). Interestingly, following secondary *N. brasiliensis* infection, there were worms present in *Rora*^{sg/sg} BM chimera

mice, whilst there were no worms present in WT BM chimera mice. In WT mice, following secondary *N. brasiliensis* infection, migrating larvae are killed between days 0 and 5, and only a few worms reach the intestine in WT mice (Thawer et al., 2014, Schwartz et al., 2018). There appears to be more eggs in the faeces of *Rora^{sg/sg}* BM chimera mice following primary and secondary *N. brasiliensis* infection, however, these results did not reach statistical significance (**Figure 3.12A**). These results indicate that *Rora^{sg/sg}* BM chimera mice have an altered adaptive type 2 immune response compared to WT BM chimera mice, and *Rora^{sg/sg}* BM chimera failed to develop resistance to reinfection.

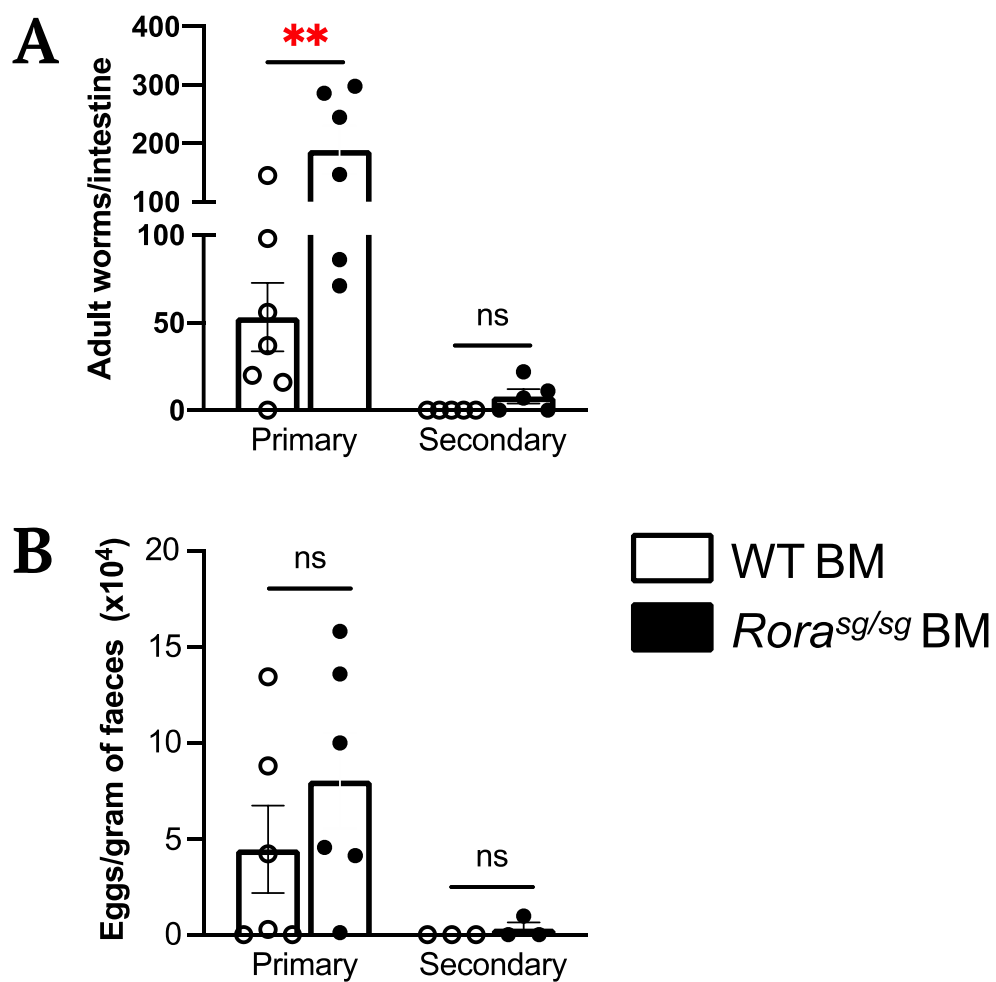


Figure 3.12: *Rora^{sg/sg}* BM chimera mice have a higher worm count following primary and secondary *N. brasiliensis* infection compared to WT BM chimera mice. *Rora^{sg/sg}* BM chimera mice and WT BM chimera mice were infected primary or secondary *N. brasiliensis* infection. **A**, Small intestines were harvested at day 7 post primary and secondary *N. brasiliensis* infection. **B**, Quantification of eggs in faeces. Data is representative of mean ± SEM. Differences indicated as two-tailed *p* values, as assessed by unpaired Student *t* test. ***p* < 0.01, ns = non-significant. n = 5-7.

3.3.2.6 *Rora*^{sg/sg} BM chimera mice have a reduced frequency of lung ILC2s following *N. brasiliensis* infection compared to WT BM chimera mice

ROR α is important for ILC2 development and expansion (Wong et al., 2012, Halim et al., 2012). Whilst having previously confirmed that *Rora*^{sg/sg} mice had reduced lung ILC2s (**Figure 3.3**), the frequency of lung ILC2s in *Rora*^{sg/sg} BM chimera mice following primary and secondary *N. brasiliensis* infection has not yet been determined. Therefore, I assessed the frequency of lung ILC2s in WT BM and *Rora*^{sg/sg} BM chimera mice in uninfected mice and following primary and secondary *N. brasiliensis* infection.

Flow cytometry analysis revealed that *Rora*^{sg/sg} BM chimera have significantly reduced frequency ($p>0.01$ and $p>0.01$, respectively) and total ($p>0.01$ and $p>0.05$, respectively) lung ILC2s compared to WT BM chimera mice following primary and secondary *N. brasiliensis* infection (**Figure 3.13**). In WT BM chimera mice, there is an increase in frequency and total lung ILC2s following *N. brasiliensis* infection. However, there was no difference in total lung ILC2s in *Rora*^{sg/sg} BM chimera mice in uninfected, primary and secondary *N. brasiliensis* infected mice (**Figure 3.13**). Therefore, indicating that there is no expansion of lung ILC2s in *Rora*^{sg/sg} BM chimera mice following primary and secondary *N. brasiliensis* infection. This data indicates that *Rora*^{sg/sg} BM chimera mice are ILC2-deficient and that ILC2 expansion is not induced in these animals.

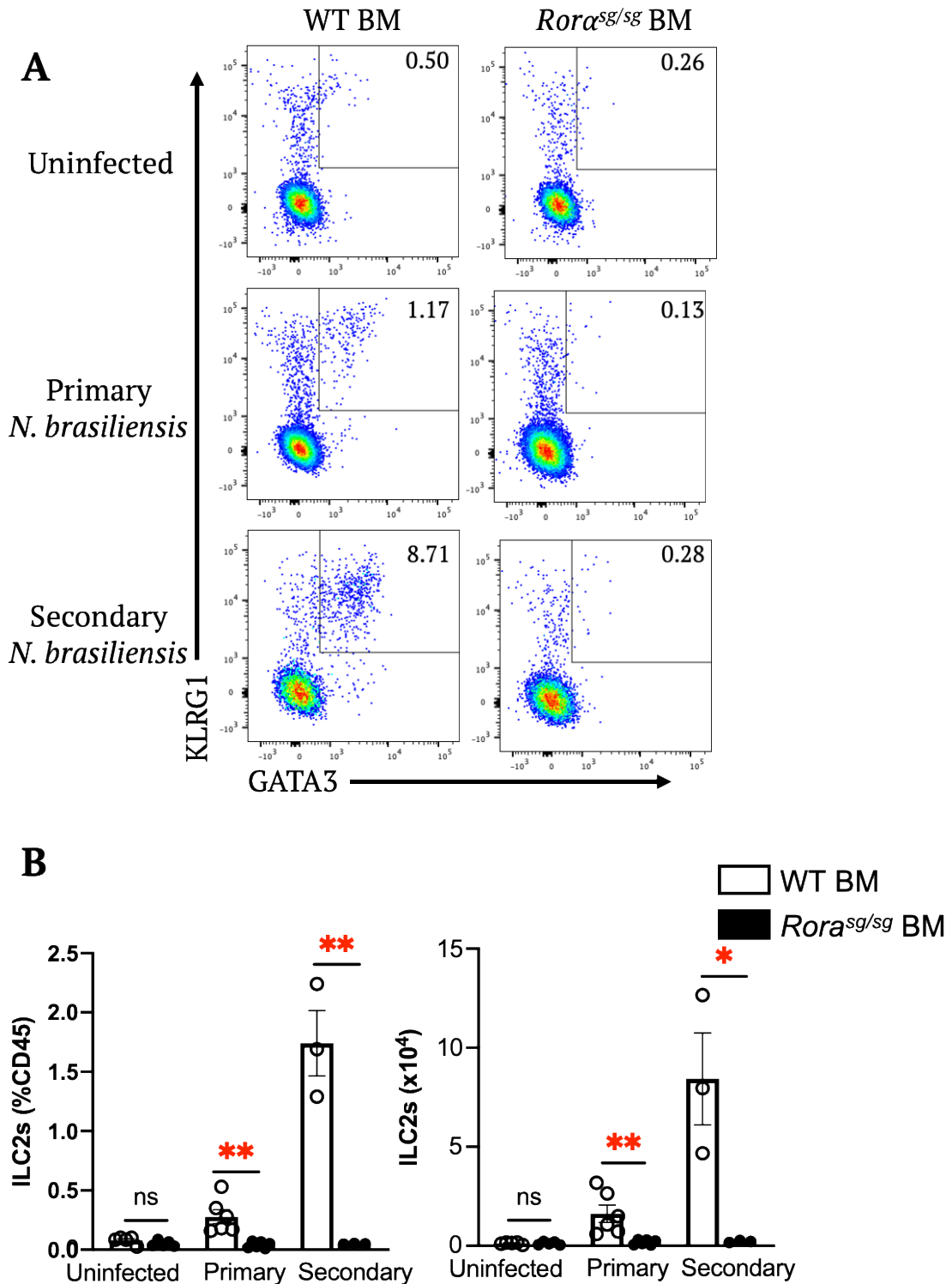


Figure 3.13: *Rora*^{sg/sg} BM mice have reduced lung ILC2s following *N. brasiliensis* infection compared to WT BM mice. *Rora*^{sg/sg} BM mice and WT BM mice were either infected with primary or secondary *N. brasiliensis* infection. Lungs were harvested and assessed by flow cytometry. **A**, Lung ILC2s were identified as lymphocytes, single cells, live cells CD45⁺Lineage⁻(CD3, CD4, NK1.1, SiglecF, F4/80, Ly6G and Gr1) KLRG1⁺GATA3⁺. The number on flow plot represents percentage of KLRG1⁺GATA3⁺. **B**, Quantification of lung ILC2s. Data is two independent experiments. Data is representative of mean \pm SEM. Differences indicated as two-tailed *p* values, as assessed by unpaired Student *t* test. ***p* < 0.01, ns = non-significant. n = 3-6.

3.3.2.7 *Rora*^{sg/sg} BM chimera mice have reduced lung CD4 T cells following *N. brasiliensis* infection compared to WT BM chimera mice

The lung is an important site for priming CD4 T cell mediated protective immunity against *N. brasiliensis* infection (Harvie et al., 2010) and ILC2-mediated immunity against *N. brasiliensis* requires CD4 T cells (Bouchery et al., 2015). Previous results presented in this chapter identified that *Rora*^{sg/sg} mice had reduced lung CD4 T cells following primary *N. brasiliensis* infection (**Figure 3.4**). It was also reported that papain challenged *Rora*^{sg/sg} BM chimera mice have reduced lung CD4 T cells and compared to WT BM chimera mice (Halim et al., 2014). However, the frequency of CD4 T cells in lungs of *Rora*^{sg/sg} BM chimera mice following primary and secondary *N. brasiliensis* infection has yet to be explored. Therefore, I assessed the frequency of lung CD4 T cells by flow cytometry following primary and secondary *N. brasiliensis* infection in WT BM and *Rora*^{sg/sg} BM chimera mice.

Interestingly, there is a reduced frequency of lung CD4 T cells in *Rora*^{sg/sg} BM chimera mice compared to WT BM chimera mice following primary *N. brasiliensis* infection (**Figure 3.14**). There was no significant difference in frequency of lung CD4 T cells in uninfected mice, therefore indicating that *Rora* had no role in development of CD4 T cells in uninfected conditions. This data supports the results generated in the *Rora*^{sg/sg} mice, that *Rora*^{sg/sg} mice had reduced lung CD4 T cells following *N. brasiliensis* infection (**Figure 3.4**). Furthermore, there was no significant difference in the percentage of lung CD4 T between WT BM and *Rora*^{sg/sg} BM chimera mice following secondary *N. brasiliensis* infection. However, interestingly, there was significantly ($p>0.05$) reduced total lung CD4 T cells in *Rora*^{sg/sg} BM chimera mice following secondary *N. brasiliensis* infection compared to WT BM chimera mice. The disparity between frequency and total lung CD4 T cells following secondary *N. brasiliensis* infection is a result of a reduced total lung cells in *Rora*^{sg/sg} BM chimera mice, compared to WT BM chimera mice. Even though the percentage of CD4 T cells is the same between *Rora*^{sg/sg} BM chimera and WT BM chimera mice following secondary *N. brasiliensis* infection, there are significantly ($p>0.01$) fewer absolute lung CD4 T cells in *Rora*^{sg/sg} BM chimera mice. This highlights why it is important to present both total immune cells and cell frequency to get the full understanding of the results. This data indicates that in the absence of a functional *Rora*

in haematopoietic cells, there is reduced lung CD4 T cells following *N. brasiliensis* infection. Thus, *Rora* may have a role in lung CD4 T cell development following *N. brasiliensis* infection. Indeed, lung-resident CD4 T cells play an essential role in mediating host resistance to secondary *N. brasiliensis* infection (Harvie et al., 2010, Harvie et al., 2013, Thawer et al., 2014). Therefore, the reduction of lung CD4 T cells in *Rora*^{sg/sg} BM chimera mice may explain the presence of *N. brasiliensis* in the small intestine following secondary infection (**Figure 3.12**).

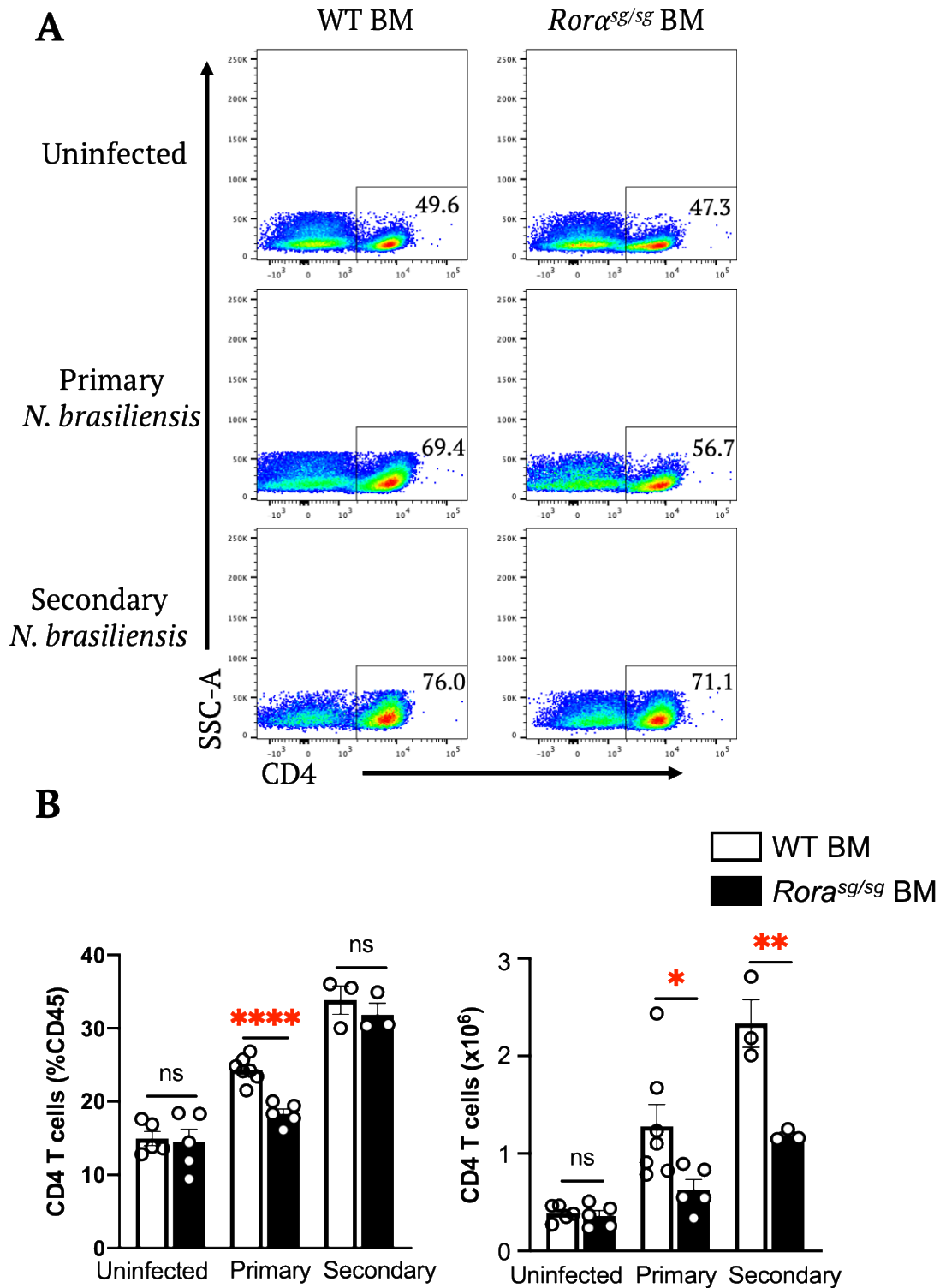
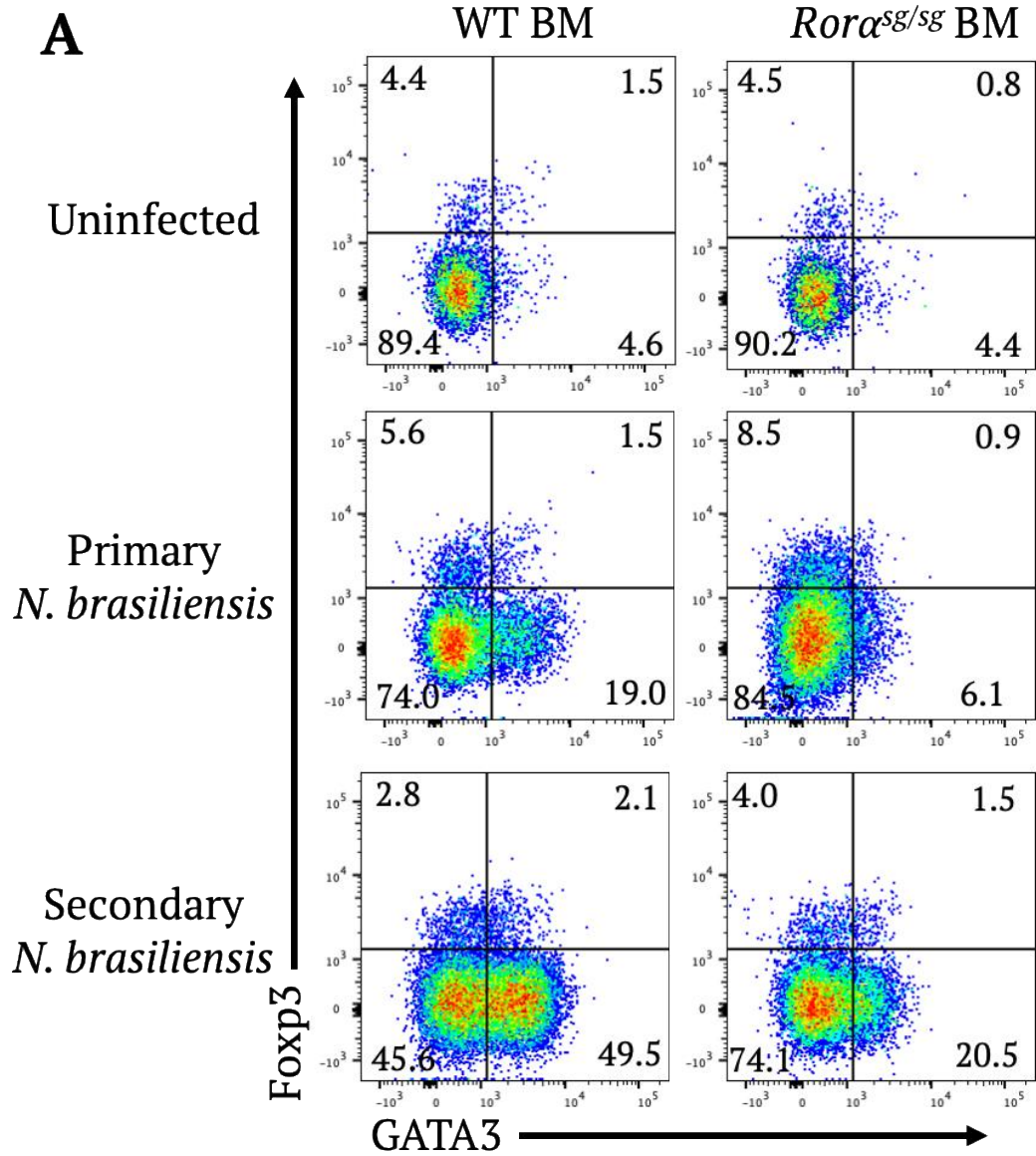


Figure 3.14: *Rora*^{sg/sg} BM mice have reduced lung CD4 T cells following *N. brasiliensis* infection compared to WT BM mice. *Rora*^{sg/sg} BM mice and WT BM mice were infected with primary or secondary *N. brasiliensis* infection. Lungs were harvested and assessed by flow cytometry. **A**, Lung CD4 T cells were identified as lymphocytes, single cells, live cells CD45⁺CD3⁺CD4⁺. The number on flow plot represents percentage of parent gate CD3⁺ cells. **B**, Quantification of lung CD4 T cells. Data is two independent experiments. Data is representative of mean \pm SEM. Differences indicated as two-tailed *p* values, as assessed by unpaired Student *t* test. **p*<0.05, ***p*<0.01, ns = non-significant. n = 3-6.

3.3.2.8 *Rora*^{sg/sg} BM chimera mice have reduced lung GATA3⁺CD4 T cells following *N. brasiliensis* infection

Having previously identified that *Rora*^{sg/sg} BM chimera mice had reduced lung CD4 T cells following *N. brasiliensis* infection (**Figure 3.14**), indicating a role for *Rora* in lung CD4 T cell development during infection, I then sought to further characterise these lung CD4 T cells. Indeed, it is known that ROR α is important for the development of Th17 cells (Yang et al., 2008) and *Rora* has a role in function of skin Treg (Foxp3⁺) cells during allergic inflammation (Malhotra et al., 2018). Whilst it is reported that papain challenged *Rora*^{sg/sg} BM chimera mice have reduced lung GATA3⁺CD4 T cells compared to WT BM chimera mice (Halim et al., 2014). Infection with *N. brasiliensis* induces conversion of Th1 and Th17 into Th2 cells and increases lung GATA3⁺ (Th2), GATA3⁺Foxp3⁺ (GATA3⁺Tregs) and Foxp3⁺ (GATA3⁻Tregs) cells (Panzer et al., 2012, Halim et al., 2018), however, the role of *Rora* in the generation of these cells has yet to be explored. Therefore, I investigated the role of *Rora* in the frequency of lung GATA3⁺, Foxp3⁺ and GATA3⁺Foxp3⁺ CD4 T cells following primary and secondary *N. brasiliensis* infection using *Rora*^{sg/sg} BM chimera mice.

There is a reduced frequency of lung GATA3⁺CD4 T cells in *Rora*^{sg/sg} BM chimera mice compared to WT BM chimera mice following primary and secondary *N. brasiliensis* infection (**Figure 3.15**). This is consistent with the results generated using the *Rora*^{sg/sg} mice (**Figure 3.5**). There was no significant difference in the frequency of lung Foxp3⁺ and GATA3⁺Foxp3⁺ CD4 T cells between WT BM and *Rora*^{sg/sg} BM chimera mice in uninfected mice and following primary and secondary *N. brasiliensis* infection (**Figure 3.15**). These findings indicate that *Rora* had no role in the development of lung Foxp3⁺ and GATA3⁺Foxp3⁺ following *N. brasiliensis* infection. However, these results provide further evidence that *Rora* may have a role in lung GATA3⁺CD4 T development following both primary and secondary *N. brasiliensis* infection.



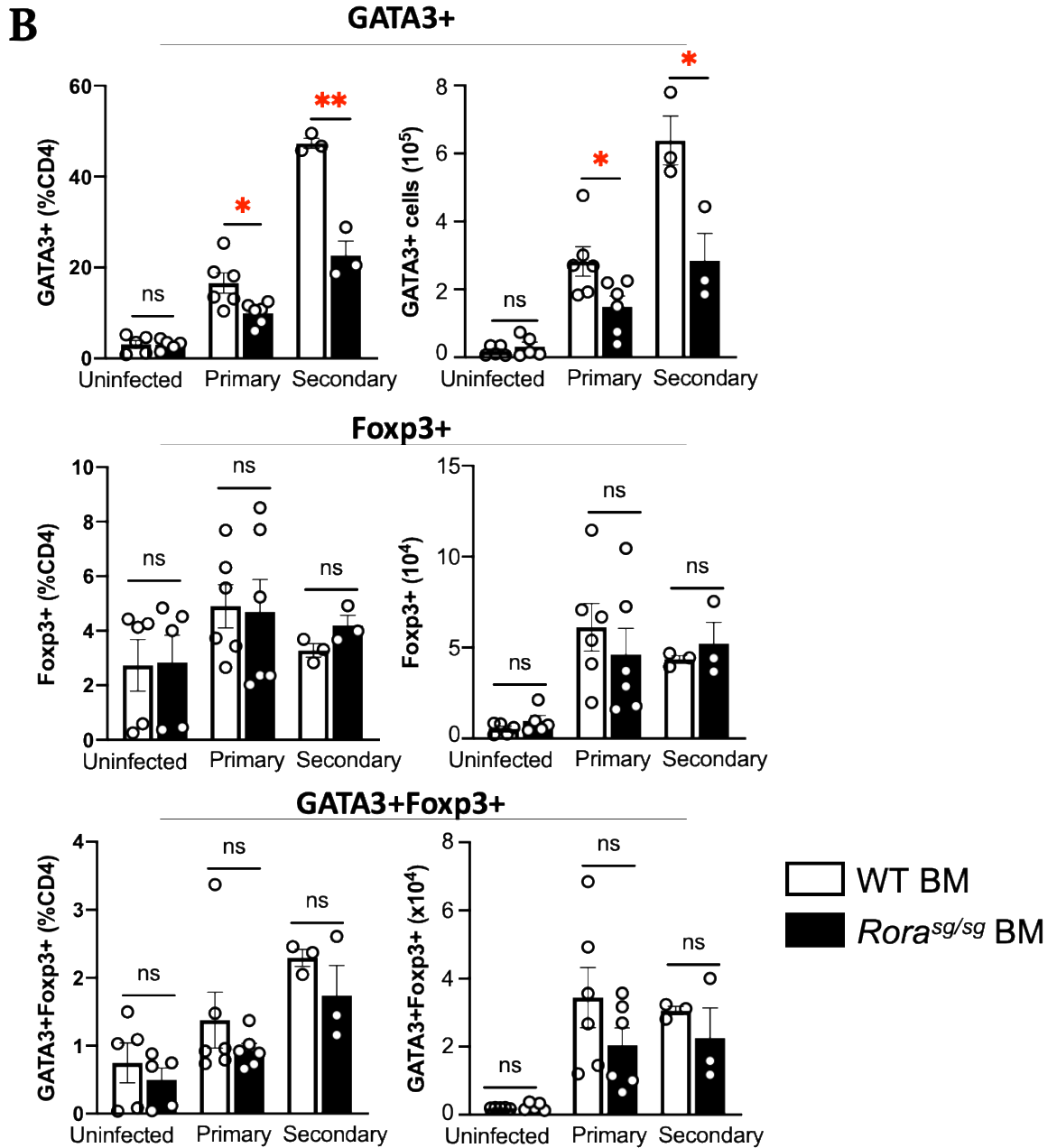


Figure 3.15: *Rora*^{sg/sg} BM chimera mice have significantly reduced lung GATA3⁺CD4 T cells following *N. brasiliensis* infection compared to WT BM chimera mice. *Rora*^{sg/sg} BM and WT BM chimera mice were infected with primary or secondary *N. brasiliensis* infection. Lungs were harvested for flow cytometry analysis. **A**, Lung cells were identified as lymphocytes, single cells, live cells CD45⁺CD3⁺CD4⁺ and either GATA3⁺, Foxp3⁺ or GATA3⁺Foxp3⁺. The number on flow plot represents percentage of parent gate CD4⁺ cells. **B**, Quantification of lung GATA3⁺, Foxp3⁺ and GATA3⁺Foxp3⁺ CD4 T cells. Data is representative of mean \pm SEM. Data is two independent experiments. Differences indicated as two-tailed *p* values, as assessed by unpaired Student *t* test. **p*<0.05, ns = non-significant. n = 3-6.

3.3.2.9 *Rora*^{sg/sg} BM chimera mice have reduced lung eosinophils following *N. brasiliensis* infection

As mentioned previously, *N. brasiliensis* infection is characterised by lung eosinophilia (Voehringer et al., 2004). Results presented in this chapter identified that *Rora*^{sg/sg} mice had reduced lung eosinophils following primary *N. brasiliensis* infection (**Figure 3.7**), indicating that *Rora* may have a role in lung eosinophil development. To further expand on these findings, I investigated the frequency of lung eosinophils in *Rora*^{sg/sg} BM chimera mice following primary and secondary *N. brasiliensis* infection.

There is significantly ($p < 0.05$) reduced frequency of lung eosinophils following primary *N. brasiliensis* infection in *Rora*^{sg/sg} BM chimera mice compared to WT BM chimera mice (**Figure 3.16**). This supports previously published data that reported papain challenged *Rora*^{sg/sg} BM chimera mice had fewer eosinophils in the lung compared to WT BM chimera mice (Halim et al., 2014). There also appears to be fewer lung eosinophils following secondary *N. brasiliensis*, however, these results did not reach statistical significance (**Figure 3.16**). There was no significant difference in frequency of lung eosinophils in uninfected *Rora*^{sg/sg} BM and WT BM chimera mice (**Figure 3.16**). Therefore, indicating *Rora* may have a role in eosinophil development following *N. brasiliensis* infection.

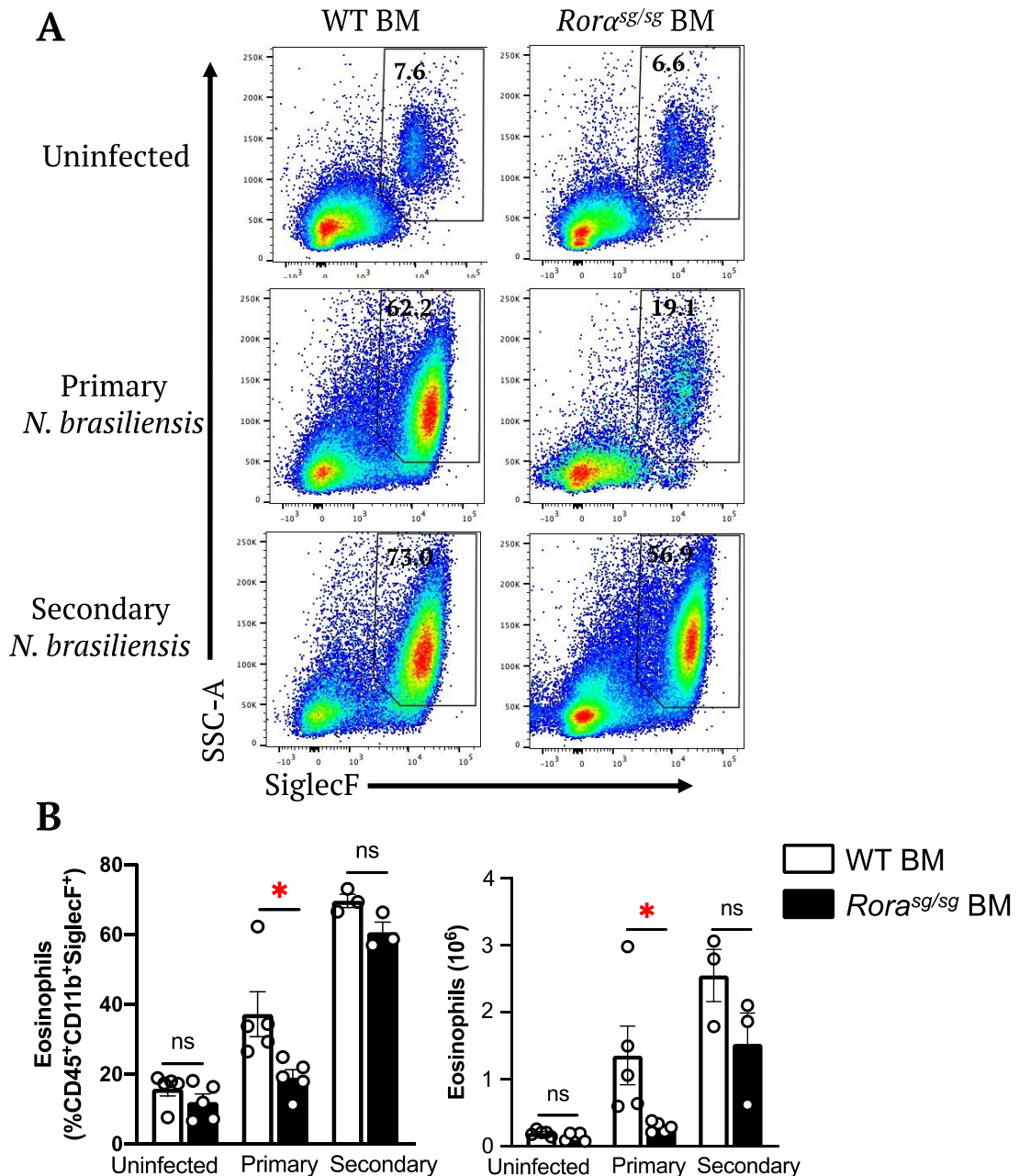


Figure 3.16: *Rora*^{sg/sg} BM mice have a reduced frequency of lung eosinophils following *N. brasiliensis* infection compared to WT BM mice. *Rora*^{sg/sg} BM mice and WT BM mice were either infected with primary or secondary *N. brasiliensis* infection. Lungs were harvested for flow cytometry analysis. **A**, Representative flow cytometry plots. Eosinophils were identified as single cells, live cells, CD45⁺Ly6G⁻CD11b⁺SiglecF⁺. The number on flow cytometry plot represents the percentage of parent gate. **B**, Quantification of lung eosinophils. Data is two independent experiments. Data is representative of mean ± SEM. Differences indicated as two-tailed *p* values, as assessed by unpaired Student *t* test. **p*<0.05. ns = non-significant. n = 3-5.

Lung eosinophils gated in **Figure 3.16** were identified based on the gating strategy adapted from Guillemins et al. (2013). Indeed, eosinophils express the surface marker SiglecF (Rosenberg et al., 2013). However, SiglecF is also expressed on various other

immune cells. Therefore, to confirm eosinophils were identified correctly by the flow cytometry gating strategy, I used the back-gating function in FlowJo to investigate the forward and side scatter profile of gated cells. As eosinophils are granulocytes, they have a high granularity, which is indicated by a high side-scatter (SSC) as assessed by flow cytometry. The results show that the CD45⁺CD11b⁺SiglecF⁺ lung cells have a high SSC-A and an intermediate FSC-A (**Figure 3.17**). This is characteristic of eosinophils which are granulocytes, therefore, indicating that this gating strategy correctly identifies lung eosinophils.

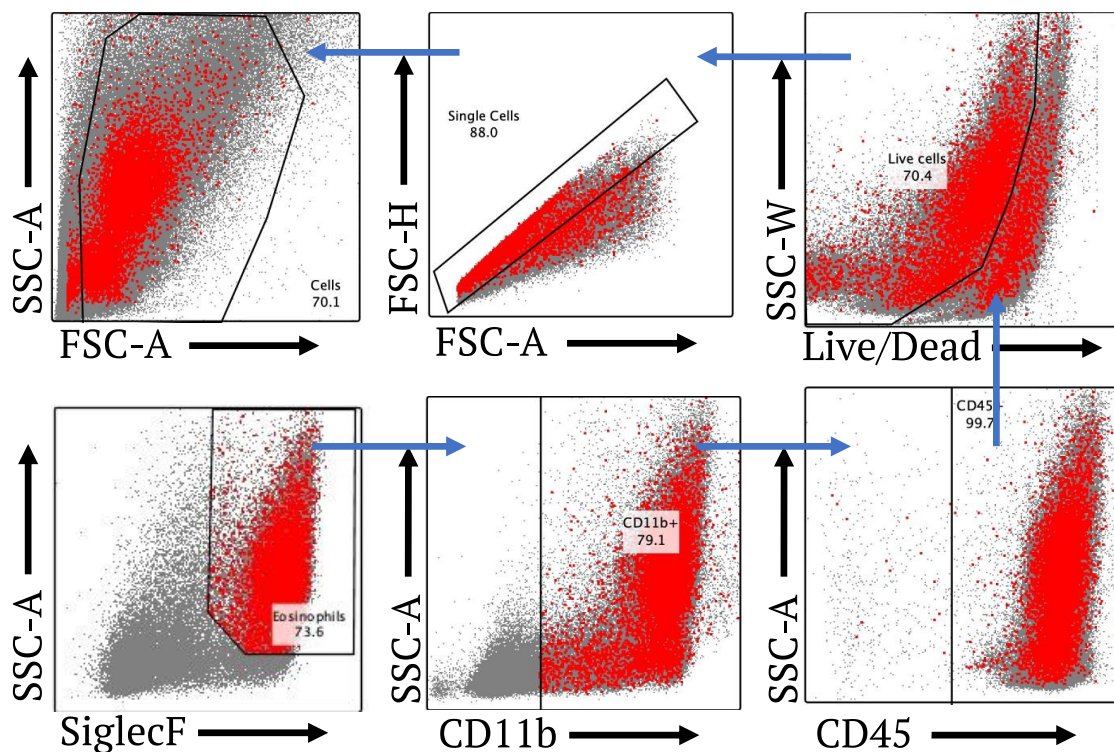


Figure 3.17: The SiglecF⁺CD11b⁺ lung population contains eosinophils. Back-gating of the CD45⁺ CD11b⁺SiglecF⁺ lung population shows gated population located with high SSC-A and intermediate FSC-A gate.

3.3.3 Determining the *in vitro* CD4 T cell polarisation of *Rora*^{sg/sg} naïve CD4 T cells

3.3.3.1 Naïve CD4 T cells isolated from *Rora*^{sg/sg} mice have reduced *in vitro* polarisation towards GATA3⁺ and Rorγt⁺ compared to WT mice naïve CD4 T cells

In this chapter, the role of RORα during a type 2 immune response was investigated using *N. brasiliensis* infection as an *in vivo* mouse model for type 2 immunity. Interestingly, it

was observed that *Rora*^{sg/sg} mice and *Rora*^{sg/sg} BM chimera mice have a reduced frequency of GATA3⁺CD4 T cells compared to WT mice following *N. brasiliensis* infection, suggesting that ROR α is important for GATA3⁺CD4 T cell development. To further investigate the role of ROR α in T cell development, I assessed the capacity of ROR α to impact on *in vitro* CD4 T cell polarisation. To explore this, I generated naïve CD4 T cells from splenocytes isolated from WT and *Rora*^{sg/sg} mice (**Chapter 2, Section 2.18**), and induced polarisation into Th cell subsets (Th1, Th2, Th17 and Tregs). Following the culture of naïve CD4 T cells in the presence of specific cytokines and antibodies (**Chapter 2, Section 2.19**), CD4 T cell polarisation was determined by assessing classical Th cell transcription factors expression by flow cytometry (Th1 – Tbet, Th2 – GATA3, Th17 – Ror γ t, and Tregs – Foxp3).

Interestingly, naïve CD4 T cells isolated from *Rora*^{sg/sg} mice have significantly reduced GATA3⁺ (Th2) ($p < 0.05$) and Ror γ t⁺ (Th17) ($p < 0.005$) polarisation compared to those isolated from WT mice (**Figure 3.18**). As mentioned, ROR α is required in Th17 cell differentiation (Yang et al., 2008), and in accordance with this, naïve CD4 T cells isolated from *Rora*^{sg/sg} mice have a reduced Ror γ t⁺ CD4 T (Th17) cell polarisation. There was no significant difference in Tbet⁺ (Th1) or Foxp3⁺ (Treg) cell polarisation between *Rora*^{sg/sg} and WT CD4 T cells (**Figure 3.18**). It has been reported that while ROR α has a role in Treg function, it does not play a role in the development of Tregs (Malhotra et al., 2018), which may explain why I observed no difference in Treg polarisation between WT and *Rora*^{sg/sg} naïve CD4 T cells. At present, there are no known roles for ROR α in either the development or function of Tbet⁺ (Th1) CD4 T cells, and the data presented support this assumption that a deficiency of ROR α in CD4 T cells had no impact on Tbet⁺ (Th1) CD4 T cell polarisation. Therefore, the *in vitro* data presented here supports the *in vivo* results, that *Rora* is important for GATA3⁺CD4 T (Th2) cell development.

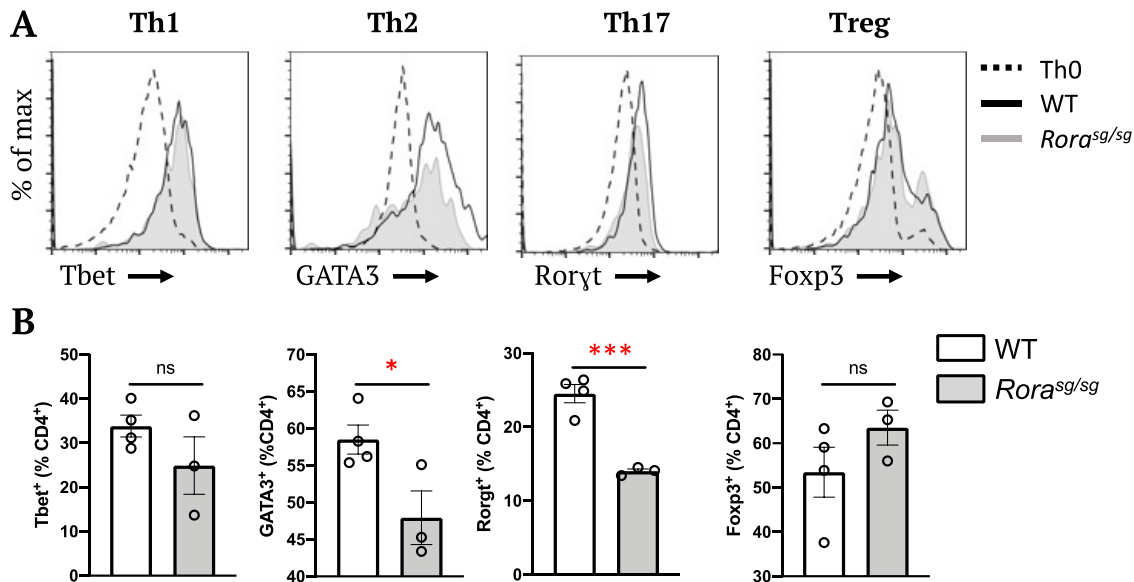


Figure 3.18: Naïve CD4 T cells isolated from *Rora^{sg/sg}* mice have reduced *in vitro* polarisation towards GATA3⁺ and Rorγt⁺ compared to naïve CD4 T cells from WT mice. Naïve CD4 T cells were isolated from *Rora^{sg/sg}* and WT spleens using AutoMACS and cultured in T cell polarisation conditions. **A**, CD4 T cell subpopulation were defined by expression of transcription factors by flow cytometry. Cells were gate as lymphocytes, single cell, live, CD45⁺CD4⁺ and either Tbet⁺ (Th1), GATA3⁺ (Th2), Rorγt⁺ (Th17) or Foxp3⁺ (Tregs). **B**, Frequency of *in vitro* differentiated T cell subpopulations. Data is representative of mean ± SEM. Differences indicated as *p* values, as assessed by Student *t* Test **p*<0.05. ****p*<0.005. ns = non-significant. n = 3-4.

3.4 Discussion

RORα is a transcription factor that is involved in many physiological functions such as circadian rhythm, metabolism and immunity. Studies on RORα in immunity have identified roles in immune signalling pathways and integral involvement in cell development. Indeed, RORα is involved in the development and function of ILC2s (Wong et al., 2012, Halim et al., 2012), Th17 cells (Yang et al., 2008) and Tregs (Malhotra et al., 2018). There is accumulating evidence that RORα has a role in the generation, activation, and function of Th2 cells. Indeed, it has been shown that RORα is expressed in Th2 cells, and mice challenged with papain or OVA have an increased *Rora* expression in lung Th2 cells (Liu et al., 2015, Van Dyken et al., 2016, Maggi et al., 2017, Miragaia et al., 2019, Haim-Vilmovsky et al., 2020). Whilst recently, it was reported that *Rora* expression in Th cells was associated with activated Th cells, and *Rora* expression in CD4 T cells promotes lung inflammation in response to *N. brasiliensis* infection (Haim-Vilmovsky et al., 2020). This data indicates a role for RORα in Th2 cells during

inflammation. However, a complete understanding of the role of ROR α in a type 2 immune response remains elusive.

In this chapter, I investigated the role of ROR α in response to infection with the type 2 inducing helminth, *N. brasiliensis*. To address this, I utilised *Rora*^{sg/sg} mice, which have a ubiquitously expressed non-functioning ROR α protein. The results presented in this chapter show that *Rora*^{sg/sg} mice have a higher *N. brasiliensis* worm count and reduced goblet cells in the small intestine, compared to WT mice, following primary *N. brasiliensis* infection. These results expand on previously published data in which *Rora*^{sg/sg} mice had a higher worm count at day 6 post *N. brasiliensis* infection and reduced small intestine goblet cells in response to IL-25 administration (Wong et al., 2012). These parameters, in particular, the ability of an animal to effectively clear an infection with *N. brasiliensis*, are reliant upon a functional type 2 immune response. As worm clearance was delayed in *Rora*^{sg/sg} mice, this indicates an altered type 2 response in the absence of functional ROR α .

To determine the underlying mechanism resulting in an altered type 2 immune response to *N. brasiliensis* infection, I characterised the immune cell repertoire in the lungs of both WT and *Rora*^{sg/sg} mice following infection but flow cytometry. Indeed, ROR α is critical for ILC2 development (Wong et al., 2012, Halim et al., 2012), and as expected, *Rora*^{sg/sg} mice had a reduced frequency of lung ILC2s in both uninfected and following *N. brasiliensis* infection. Interestingly, it was also observed that *Rora*^{sg/sg} mice had reduced frequency of lung CD4 T cells, GATA3⁺CD4 T cell and eosinophils following primary *N. brasiliensis* infection. Whilst there was no significant difference in the frequency of lung CD4 T cells, GATA3⁺CD4 T cells or eosinophils in uninfected *Rora*^{sg/sg} mice and WT mice. Therefore, indicating that in the absence of a functional ROR α , there was no difference at basal condition and the reduced frequency of immune cells is observed only during type 2 inflammation. Further analysis showed that *Rora*^{sg/sg} mice had a reduced frequency of GATA3⁺CD4 T cells in MLN following *N. brasiliensis* infection, therefore indicating the role of ROR α on GATA3⁺CD4 T cell development does not appear to be tissue specific, but rather affects both lymphoid and non-lymphoid tissue. The findings presented in this chapter indicate that *Rora* may have role in development of GATA3⁺CD4 T cells and eosinophils, in addition to ILC2 development during a type 2 immune response.

The results discussed thus far, investigated the role of ROR α by utilising *Rora*^{sg/sg} mice. Indeed, *Rora*^{sg/sg} mice have a ubiquitous absence of a functional ROR α and have developmental and neurological abnormalities that result in stunted development and smaller size. Therefore, I generated *Rora*^{sg/sg} BM chimera to circumvent the potential confounding effects of the neural abnormalities and investigated the role ROR α in haematopoietic cells. Using *Rora*^{sg/sg} BM chimera mice I was able to explore the role of *Rora* in hematopoietic cells during a type 2 immune response. Firstly, it was identified that *Rora*^{sg/sg} BM chimera mice have a delayed worm expulsion and a delayed goblet cell hyperplasia, similar to that observed in *Rora*^{sg/sg} mice. Interestingly, it was also observed that in several *Rora*^{sg/sg} BM chimera mice there were still worms present at day 30 post-infection, suggesting *Rora*^{sg/sg} BM chimera mice may have an altered adaptive immune response. To further appraise the role of *Rora* during a type 2 immune response, I assessed the serum IgE following *N. brasiliensis* infection. Indeed, *N. brasiliensis* infection promotes B cell class switching to IgE and binds to the cell surface receptor Fc ϵ RI on mast cells and basophils resulting in cell degranulation (Martin et al., 2018). The findings presented here showed that *Rora*^{sg/sg} BM chimera mice had altered reduced and delayed detection of serum IgE. This supports previous publications which report that *Rora*^{sg/sg} BM chimera mice have been shown to have reduced serum IgE in response to HDM compared to WT BM chimera mice (Gold et al., 2014). Whilst papain challenged *Rora*^{sg/sg} BM chimera mice had reduced levels of serum IgE compared to WT BM chimera mice (Halim et al., 2014). Interestingly, the delayed worm expulsion in *Rora*^{sg/sg} BM chimera mice coincides with a delayed detection of serum IgE. The precise role of IgE during *N. brasiliensis* infection remains controversial. It has been reported that the presence of B cells and antibody production are dispensable for expulsion of *N. brasiliensis* from primary and secondary infections (Liu et al., 2010). Whilst it has also been reported that B2 cell IgE enhances helminth clearance in a mast cell-dependent manner, whereas B1 cell IgE blocks B2 cell-mediated helminth clearance (Martin et al., 2018). However, taken together, the results presented here further indicate that *Rora*^{sg/sg} BM chimera mice had an altered type 2 immune response following *N. brasiliensis* infection, compared to WT BM chimera mice.

The adaptive type 2 immune response is orchestrated by CD4 T cells and the cytokines they secrete. Recently, it has been reported that *Rora* expressing CD4 T cells were associated with expression of cytokines type 2 cytokines, IL-4 and IL-13 (Haim-

Vilmovsky et al., 2020), suggesting a role for *Rora* in CD4 T cell cytokine secretion. Results presented in this chapter show that T cell cytokine secretion from *Rora*^{sg/sg} BM chimera mice MLN cells was reduced and had a delayed secretion of type 2 cytokines (IL-4, IL-5 and IL-13) following *N. brasiliensis* infection compared to WT BM chimera mice. These findings indicate that *Rora* may have role in T cell cytokine secretion.

The results discussed thus far explored the role of ROR α during a primary *N. brasiliensis* infection. These findings highlighted a potential role for *Rora* in lung GATA3⁺CD4 T cell development. Indeed, both ILC2s and CD4 T cells are required for a robust *N. brasiliensis* infection, as *Rag2*^{-/-} mice, which do not have T or B cells but have ILC2s, were unable to induce complete worm expulsion (Neill et al., 2010). Whilst the lungs were an important site for CD4 T cells for immune-mediated protection in secondary *N. brasiliensis* infection (Harvie et al., 2010, Thawer et al., 2014, Bouchery et al., 2015). Therefore, having identified ROR α may have a role in lung GATA3⁺CD4 T cell development, I explored the role of *Rora* during a primary and secondary *N. brasiliensis* infection using *Rora*^{sg/sg} BM chimera mice. Immune competent mice develop a rapid and selective development of a profound Th2 immune response to infection by *N. brasiliensis* and that appears able to confer life-long protective immunity against reinfection. Following secondary *N. brasiliensis* infection, migrating larvae are killed between days 0 and 5, and only a few worms reach the intestine in WT mice (Thawer et al., 2014, Schwartz et al., 2018). The results presented in this chapter showed that following a secondary *N. brasiliensis* infection there were worms still present in the small intestine of *Rora*^{sg/sg} BM chimera mice, whilst there were none present in WT BM chimera mice. Therefore, indicating that *Rora*^{sg/sg} BM chimera mice had altered adaptive immune following *N. brasiliensis* infection and failed to develop resistance to reinfection. It should be noted that these results did not reach statistical significance. Therefore, further experiments should look to increase N number, to determine if this observed difference reaches statistical significance. In addition, further assessment should be done to assess an earlier time points post-secondary infection (e.g day 5 post-secondary infection). This would provide further insight into to the role of *Rora* in immune cells during recall infections, and may further highlight any delayed development of recall immunity to secondary *N. brasiliensis* infection in *Rora*^{sg/sg} BM chimera mice. In addition, future experiments should also assess the worm frequency in the lungs. This will give an insight to the worm migration and immune response, particularly as the lungs

are an important site for mediated protective immunity to secondary infection. It should also be noted that having previously identified *Rora*^{sg/sg} BM chimera mice still have *N. brasiliensis* present at day 30 in the small intestine following primary infection. It may be possible that *N. brasiliensis* identified following secondary *N. brasiliensis* are remaining from the primary infection, due to overlap in days assessed. Although, following primary infection, *N. brasiliensis* stopped producing eggs at day 13 post infection, whilst eggs are detected at day 7 post-secondary infection in *Rora*^{sg/sg} BM chimera mice. Thus, indicating that the majority of worms detected in small intestine are from secondary infection, rather than remaining from primary infection. However, future experiments should take this delayed clearance in *Rora*^{sg/sg} BM chimera mice into account and either have an extended period between primary and secondary infection (30+ days) to allow for complete worm expulsion, or include a anthelmintic (Ivermectin) treatment following primary infection

Rora^{sg/sg} BM chimera mice had reduced lung ILC2s following *N. brasiliensis* infection. Whilst interestingly, it was also observed that *Rora*^{sg/sg} BM chimera mice had a reduced frequency of lung CD4 T cells, GATA3⁺CD4 T cells following primary and secondary *N. brasiliensis* infection. This supports previous published results that showed that *Rora*^{sg/sg} BM chimera mice had fewer GATA3⁺CD4 T cells in the lungs compared to WT BM chimera mice in response to papain (Halim et al., 2014). Whilst exploring the role of *Rora* on CD4 T cell phenotype, there was no difference in frequency of lung Foxp3⁺ and GATA3⁺Foxp3⁺ CD4 T cells between *Rora*^{sg/sg} BM and WT BM chimera mice, indicating that *Rora* had no role in development of these cells following *N. brasiliensis* infection. Therefore, taken together, the results presented in this chapter indicate that *Rora* may have a role in lung GATA3⁺CD4 T cell development following *N. brasiliensis* infection.

In support of the *in vivo* results, *in vitro* CD4 T cell polarisation studies presented in this chapter showed that naïve CD4 T cells isolated from *Rora*^{sg/sg} mice had reduced ability to polarise towards both GATA3⁺ (Th2) and Rorγt⁺ (Th17) compared to WT naïve CD4 T cells. Therefore, indicating that RORα has a role in GATA3⁺ (Th2) and Rorγt⁺ (Th17) CD4 T cell development. Indeed, RORα is known to be involved in Th17 cell differentiation (Yang et al., 2008). Therefore, these results support the *in vivo* data and indicate a role for *Rora* in GATA3⁺CD4 T cell development.

Interestingly, in addition to the observed reduced frequency of lung GATA3⁺CD4 T cells, *Rora*^{sg/sg} BM chimera mice also had reduced frequency of lung eosinophils following *N. brasiliensis* infection. This is consistent with the *Rora*^{sg/sg} mice results presented in this chapter and in support of a previous publication which reported *Rora*^{sg/sg} BM chimera mice had fewer eosinophils in the lung compared to WT BM chimera mice following papain challenge (Halim et al., 2014). Indeed, both ILC2s and CD4 T cells secrete IL-5 which drives lung eosinophilia following infection (Yasuda et al., 2012). Therefore, as *Rora*^{sg/sg} mice and *Rora*^{sg/sg} BM chimera mice have reduced lung ILC2s and CD4 T cells, this may possibly result in reduced secretion of IL-5 and therefore, reduced frequency lung eosinophils. It is also reported that mice deficient in eosinophils failed to expel worms by day 7 post-secondary infection, and eosinophils can limit the number of *N. brasiliensis* reaching the lungs on secondary infection (Knott et al., 2007, Voehringer et al., 2006). Whilst eosinophils were shown to contribute to worm killing in air pouches containing *N. brasiliensis* (Giacomin et al., 2008). Therefore, the reduced eosinophils in *Rora*^{sg/sg} and *Rora*^{sg/sg} BM chimera mice, may explain the increased worm count in the small intestine following *N. brasiliensis* infection. Further research is required to investigate the precise role of ROR α in lung eosinophil development, as *Rora*^{sg/sg} mice and *Rora*^{sg/sg} BM chimera mice have a non-functional, truncated form of the ROR α protein in eosinophils, therefore, the reduced role frequency could be due to a role of ROR α on eosinophil development.

As mentioned, CD4 T cells have been shown to coordinate the immune response to *N. brasiliensis* reinfection in the lungs (Harvie et al., 2010) and early studies reported that memory Th2 cells induce M2 macrophages to mediate protection against nematode parasites (Anthony et al., 2006). Since then, ILC2s have been shown to work in concert with CD4 T cells to induce M2 macrophages in the lungs to arrest *N. brasiliensis* development and reducing worm burden following secondary infection (Bouchery et al., 2015). Therefore, another possible explanation for the increased worm count in *Rora*^{sg/sg} BM chimera mice following secondary *N. brasiliensis* infection may be due to a reduced frequency of lung CD4 T and ILC2s which in turn failed to induce M2 macrophage blocking of *N. brasiliensis* development.

It is important to present both percentage and total number of cells, wherever possible, to have a full understanding of the biology. In **Figure 3.14**, there is a reduced total number

of CD4 T cells in *Rora*^{sg/sg} BM chimera mice following secondary *N. brasiliensis* infection, compared to WT BM chimera mice. However, there is no difference in percentage of CD4 T cells between WT and *Rora*^{sg/sg} BM chimera mice. A possible explanation for this disparity between cell frequency and cell counts is due to *Rora*^{sg/sg} BM chimera mice having reduced total number of lung CD45⁺ cells compared to WT BM chimera mice, and consequently a reduced total number of CD4 T cells. Thus, indicating that *Rora* has a role in CD4 T cell development and/or recruitment in the lungs. However, frequency of cells as a percentage (%CD45), is affected by alterations in other immune cell frequencies. For instance, *Rora*^{sg/sg} BM chimera mice have a reduced frequency of eosinophils (**Figure 3.16**) compared to WT BM chimera mice. This will impact on the frequency of CD4 T cells (%CD45), and may increase to compensate the reduced frequency of eosinophils in *Rora*^{sg/sg} BM chimera mice. Therefore, highlighting why it is important to present both frequency and total number of cells to gain a full understanding of the biology. In **Figure 3.15**, *Rora*^{sg/sg} BM chimera mice have reduced percentage (%CD4) and total GATA3⁺CD4 T cells, compared to WT BM chimera mice. These results are limited to the CD4 T cell markers used within the flow cytometry panel (GATA3 and Foxp3), and further conclusions regarding other CD4 T cell subsets (e.g. Th1 and Th17) cannot be drawn from this data. However, taking this into account, results indicate that *Rora* has a role in development of GATA3⁺CD4 T cells.

In summary, ROR α is known to have a role in ILC2 development (Wong et al., 2012, Halim et al., 2012), Th17 cell differentiation (Yang et al., 2008) and Treg cell function (Malhotra et al., 2018). The findings presented in this chapter indicate that ROR α may have a role beyond ILC2 development during a type 2 immune response and may be implicated in GATA3⁺CD4 T cells and eosinophils development. In this chapter, I used *Rora*^{sg/sg} mice, which contain a ubiquitous spontaneous mutation in *Rora* gene, and generated *Rora*^{sg/sg} BM chimera mice. Although a very useful mouse models for exploring the role of ROR α , *Rora* is absent in every cell in *Rora*^{sg/sg} mice and haematopoietic cells in *Rora*^{sg/sg} BM chimera mice, therefore making it is difficult to decipher the exact role of *Rora* in specific immune cells. To address this, I generated a *Rora* reporter mouse which allows for the investigation of single cell *Rora* expressing cells by flow cytometry. Therefore, using the *Rora* reporter mice, I was able to explore the *Rora* expressing cells during type 2 inflammation. This will be explored in Chapter 4 of this thesis.

Chapter 4

**Generation of a *Rora* reporter mouse to
determine the *Rora* expressing immune
cells in type 2 immunity**

Chapter 4

4.1 Introduction

In **Chapter 3** I explored the function of ROR α during the initiation and maintenance of a type 2 immune response, using *N. brasiliensis* infection as a model for type 2 immunity. To investigate the role of ROR α , *Rora*^{sg/sg} mice were used, which have ubiquitous absence of a functional ROR α . *Rora*^{sg/sg} mice were shown to be ILC2-deficient and had an delayed worm expulsion compared to WT mice. Interestingly, *Rora*^{sg/sg} mice also had a reduced frequency of lung CD4 T cells, GATA3⁺CD4 T cells and eosinophils compared to WT mice following *N. brasiliensis* infection. In support of these findings, *Rora*^{sg/sg} BM chimera mice were generated and also had a reduced frequency of lung ILC2s, CD4 T cells, GATA3⁺CD4 T cells and eosinophils compared to WT BM chimera mice following *N. brasiliensis* infection. Therefore, these findings indicate that ROR α may have a role beyond ILC2 development in a type 2 immune response, with a role in GATA3⁺CD4 T cell and eosinophil development. Furthermore, *in vitro* analysis revealed that naïve CD4 T cells isolated from *Rora*^{sg/sg} mice had a reduced GATA3⁺ (Th2) polarisation, compared to WT naïve CD4 T cells. The findings in **Chapter 3** were identified using either *Rora*^{sg/sg} mice or *Rora*^{sg/sg} BM chimeras, where ROR α is non-functional in either all cells, or all cells of a haematopoietic origin, respectively. Therefore, although a role for ROR α was identified in specific immune cells, it is difficult to fully delineate the presence of ROR α in distinct immune cell populations. Therefore, in this chapter I sought to determine *Rora* expression in distinct immune cell populations.

At present, there are no commercially available antibodies for flow cytometry that effectively detect ROR α expression in murine cells. Recently, several publications have reported the generation of a *Rora* reporter mouse which generate a fluorescent protein in cells expressing *Rora* (Malhotra et al., 2018, Walker et al., 2019, Haim-Vilmovsky et al., 2020, Ghaedi et al., 2020). The use of *Rora* reporter mice allows for the detection *Rora* expressing single cells by flow cytometry. Indeed, Malhotra et al. (2018) used a *Rora* reporter mouse to show that ROR α in skin-resident Tregs is important for restraining allergic skin inflammation. Whilst Walker et al. (2019) generated a ‘5x polychromILC’ transcription factor reporter mouse (Id2, Bcl11b, Gata3, ROR γ t and ROR α), and explored

ILC development in the bone marrow. Recently, Ghaedi et al. (2020) used a *Rora* reporter mice to reveal ILC progenitors and effector ILC2 subsets in the lung. Whilst Haim-Vilmovsky et al. (2020) used the *Rora* reporter mouse generated in Walker et al. (2019) and reported ROR α regulates activated Th cells during inflammation. Therefore, in this chapter I sought to generate a *Rora* reporter mouse to investigate *Rora* expressing cells following *N. brasiliensis* infection.

4.2 Chapter Objectives

1. Generation of a *Rora* reporter mouse
2. To investigate the *Rora*-YFP expressing immune cells populations in uninfected conditions
3. To investigate the *Rora*-YFP expressing immune cells following *N. brasiliensis* infection

4.3 Results

4.3.1 Generation of $Rora^{Cre/Cre}Rosa^{YFP/YFP}$ mice

To generate the *Rora* reporter mice (**Chapter 2, Section 2.3**), I crossed a $Rora^{Cre/+}$ mice with $Rosa^{YFP}$, to generate $Rora^{Cre/+}Rosa^{YFP/+}$ mice. The $Rosa^{YFP}$ mice contain a STOP sequence flanked by LoxP sequences, followed by an YFP gene. When crossed with a mouse expressing a Cre recombinase, the STOP sequence is excised and the YFP expression is observed in cells that are expressing *Rora*. Therefore, cells expressing *Rora* are irreversibly labelled by a YFP. The $Rora^{Cre/+}Rosa^{YFP/+}$ mice were then backcrossed with $Rora^{Cre/+}Rosa^{YFP/+}$ to generate $Rora^{Cre/Cre}Rosa^{YFP/YFP}$ mice. The *Rora* reporter mice had a comparable size to WT mice and they did not develop the staggerer phenotype observed in $Rora^{sg/sg}$ mice (**Figure 4.1**). Therefore, indicating that *Rora* gene targeting and generation of the *Rora* reporter mouse had no discernible effect on the *Rora* gene as observed in $Rora^{sg/sg}$ mice.



Figure 4.1: Gross appearance of WT and *Rora* reporter mice. *Rora* reporter mice are comparable in size to WT mice. The photograph is of 8 week-old male WT and *Rora* reporter mouse.

4.3.2 *Rora*^{Cre/Cre}*Rosa*^{YFP/YFP} mice have highest frequency of YFP⁺CD45 cells

To confirm that *Rora* reporter mice expressed YFP, splenocytes were isolated from control (*Rora*^{Cre/+} and *Rora*^{Cre/cre}) and *Rora* reporter (*Rora*^{Cre/+}*Rosa*^{YFP/+}, *Rora*^{Cre/+}*Rosa*^{YFP/YFP}, *Rora*^{Cre/Cre}*Rosa*^{YFP/+} and *Rora*^{Cre/Cre}*Rosa*^{YFP/YFP}) mice and assessed for YFP expressing CD45⁺ cells by flow cytometry.

There was no YFP detected in CD45⁺ cells from control mice (*Rora*^{Cre} and *Rora*^{Cre/Cre}), whilst CD45⁺ cells isolated from *Rora* reporter mice expressed some YFP (*Rora*^{Cre/+}*Rosa*^{YFP/+}, *Rora*^{Cre/+}*Rosa*^{YFP/YFP}, *Rora*^{Cre/Cre}*Rosa*^{YFP/+} and *Rora*^{Cre/Cre}*Rosa*^{YFP/YFP}) (**Figure 4.2A**). There was an increased frequency of YFP expressing CD45⁺ cells from *Rora*^{Cre/Cre}*Rosa*^{YFP/YFP} mice, which have two alleles expressing YFP (**Figure 4.2B**). Therefore, *Rora*^{Cre/Cre}*Rosa*^{YFP/YFP} were used for all further experiments to ensure consistency and hereon in termed *Rora* reporter mice.

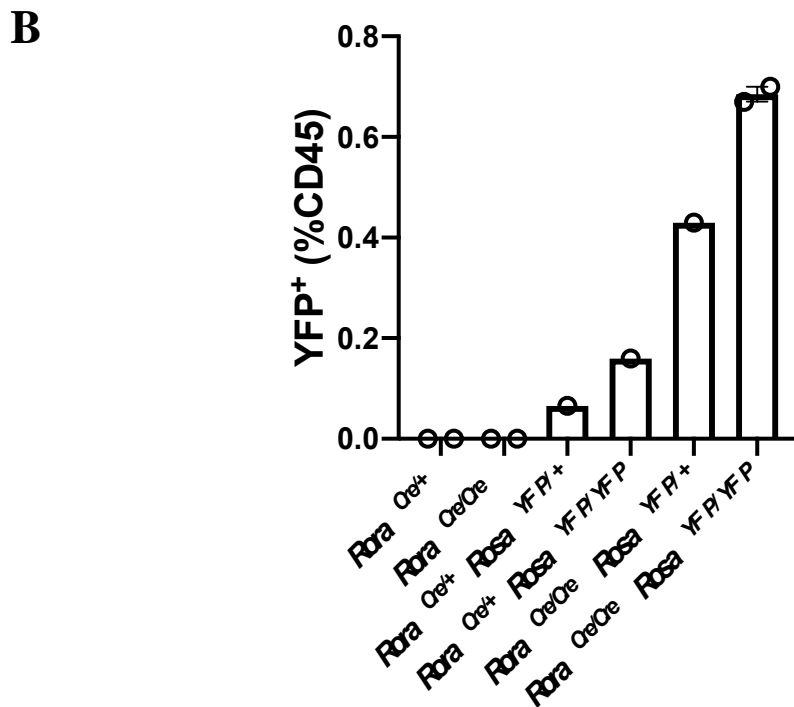
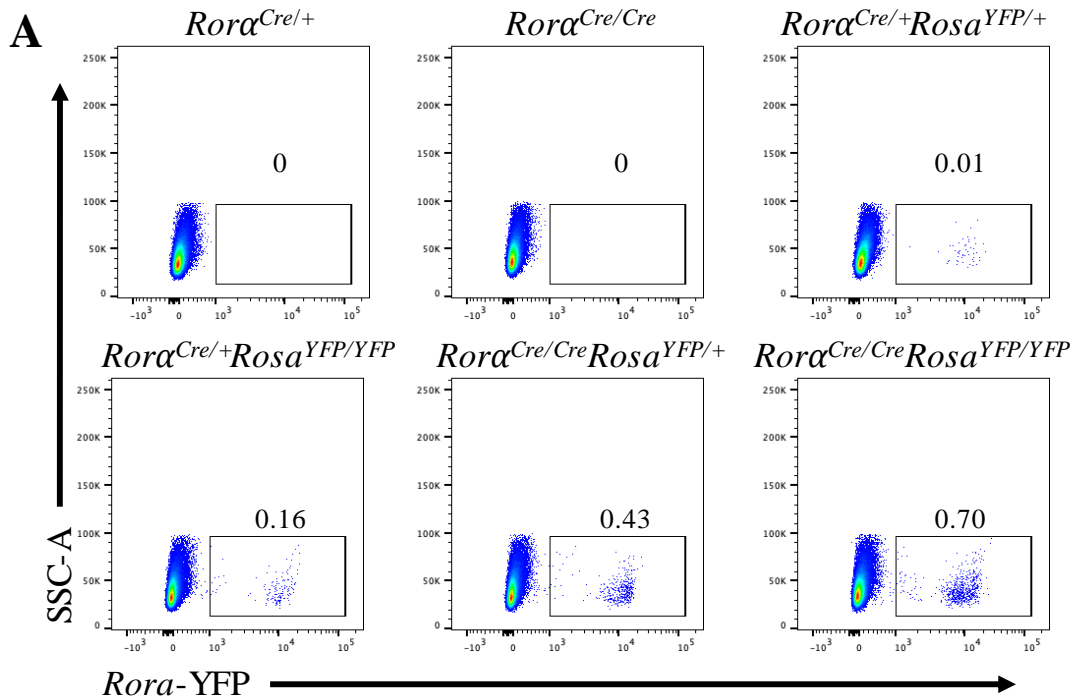


Figure 4.2: *Rora*^{Cre/Cre}*Rosa*^{YFP/YFP} mice have highest frequency of YFP expressing CD45⁺ cells. Splens from *Rora*^{Cre/+}, *Rora*^{Cre/Cre}, *Rora*^{Cre/+Rosa}^{YFP/+}, *Rora*^{Cre/+Rosa}^{YFP/YFP}, *Rora*^{Cre/CreRosa}^{YFP/+} and *Rora*^{Cre/CreRosa}^{YFP/YFP} were harvested and assessed for YFP expression by flow cytometry. **A**, Cells were gated as lymphocytes, single cell, live, CD45⁺. The number on flow cytometry plots reflect percentage of CD45⁺ cells. **B**, Quantification of YFP⁺ expressing CD45 cells. n = 1-2.

4.3.3 YFP⁺ expressing CD45 cells are *Rora* expressing cells

I have confirmed that a proportion of CD45⁺ cells isolated from *Rora* reporter mice express YFP⁺ as assessed by flow cytometry (**Figure 4.2**). To confirm that the YFP expression in these cells is associated with *Rora*, I used qPCR to assess the expression of *Rora* mRNA in the YFP⁺CD45⁺ cells. Splenocytes were prepared from *Rora* reporter mice and stained with a marker for CD45 and an equal number of CD45⁺YFP⁺ and YFP⁻ cells were sorted by FACS (**Figure 4.3A**). The purity of CD45⁺YFP⁺ sorted cells was >96%, whilst the purity of CD45⁺YFP⁻ sorted cells was 100% (**Figure 4.3A**). RNA was isolated from these cells and *Rora* expression was assessed by qPCR and compared to a housekeeping control. There is higher expression of *Rora* mRNA in the YFP expressing CD45⁺ (CD45⁺YFP⁺) cells compared to CD45⁺ cells that do not express YFP (CD45⁺YFP⁻) (**Figure 4.3B**). This confirms that the YFP expressing CD45⁺ cells also express *Rora* mRNA.

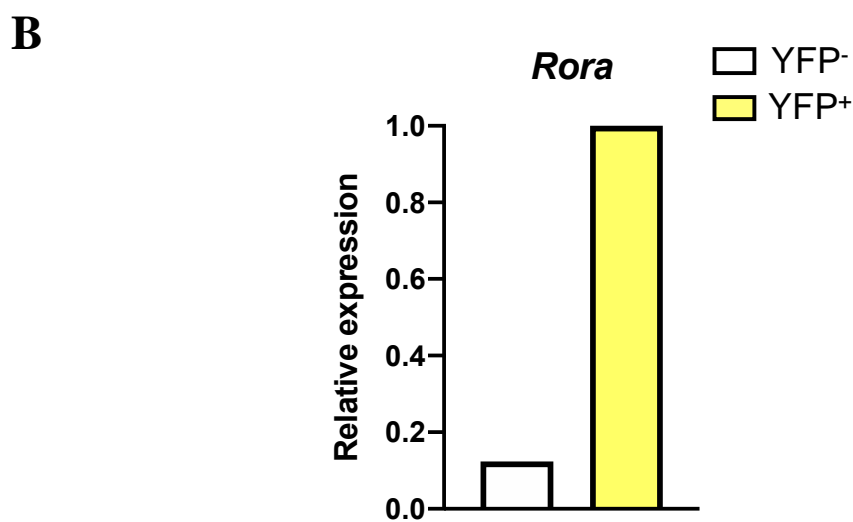
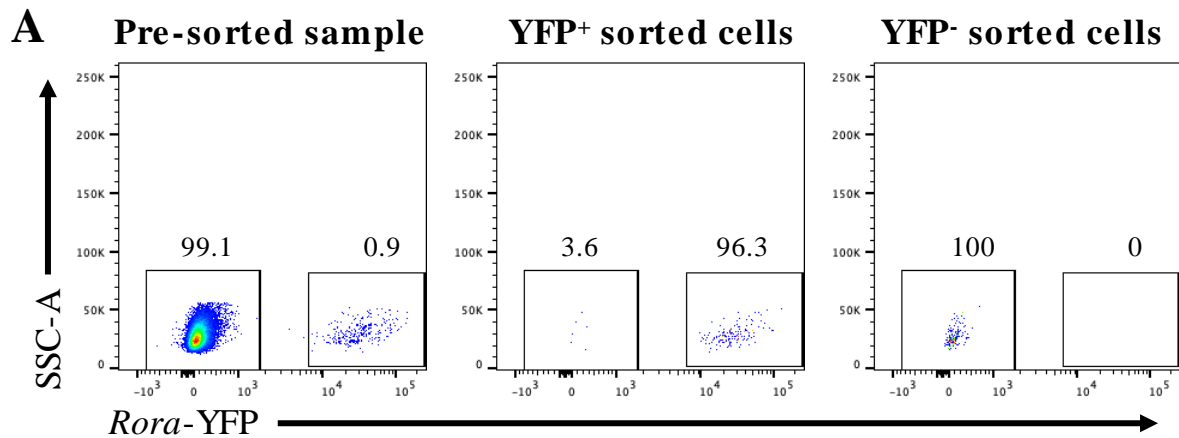


Figure 4.3: YFP⁺ expressing CD45 cells are *Rora* expressing cells. *Rora* reporter mice spleen cells were isolated and stained for CD45 and FACS sorted for cells, single cells, live, CD45⁺, YFP⁺ and YFP⁻ populations. **A**, Flow cytometry plots of pre-sorted sample, and purity of YFP⁺ sample was 96.3% and purity of YFP⁻ sample was 100%. The number on flow cytometry plots reflect percentage of parent gate (CD45⁺). **B**, *Rora* expression in CD45⁺YFP⁺ and CD45⁺YFP⁻ spleen cells. *Rora* RNA expression assessed by qPCR relative to 18S. n = 1.

4.3.4 ILC2s express *Rora*-YFP

Having confirmed CD45⁺YFP⁺ cells from *Rora* reporter mice express *Rora* mRNA, I assessed *Rora*-YFP expression in ILC2s, as an example of a cell type known to express *Rora*, to further validate the specificity of the mouse (Wong et al., 2012, Halim et al., 2012). As confirmed in **Chapter 3**, *Rora*^{sg/sg} mice are ILC2 deficient (Wong et al., 2012, Halim et al., 2012), therefore, I also assessed the frequency of lung ILC2s in *Rora* reporter

mice compared to control mice, to identify if the insertion of the YFP disrupts the function of the *Rora* gene.

Analysis by flow cytometry revealed there was no significant difference in frequency of lung ILC2s from control (*Rora*^{Cre/Cre}) and *Rora* reporter (*Rora*^{Cre/Cre}*Rosa*^{YFP/YFP}) mice. Therefore, *Rora* gene targeting and generation of the *Rora* reporter mouse had no discernible effect on the frequency of lung ILC2s (**Figure 4.4A**). As expected, flow cytometry analysis identified a population of lung ILC2s which expressed *Rora*-YFP (**Figure 4.4B**). Whilst there was no detection of *Rora*-YFP expressing lung ILC2s from control mice (**Figure 4.4B**). Approximately >50% of the lung ILC2s from naïve *Rora* reporter mice were *Rora*-YFP⁺ (**Figure 4.4C**). This is in support of Ghaedi et al. (2020), which also reported that not all lung ILC2s were *Rora*-YFP⁺. This may possibly be due to the identification of ILC2 heterogeneity, and other transcription factors being involved in ILC2 development such as GATA3 and Bcl11b (Hoyler et al., 2012, Mjosberg et al., 2012, Califano et al., 2015, Walker et al., 2015, Yu et al., 2015b, Walker et al., 2019, Ghaedi et al., 2020).

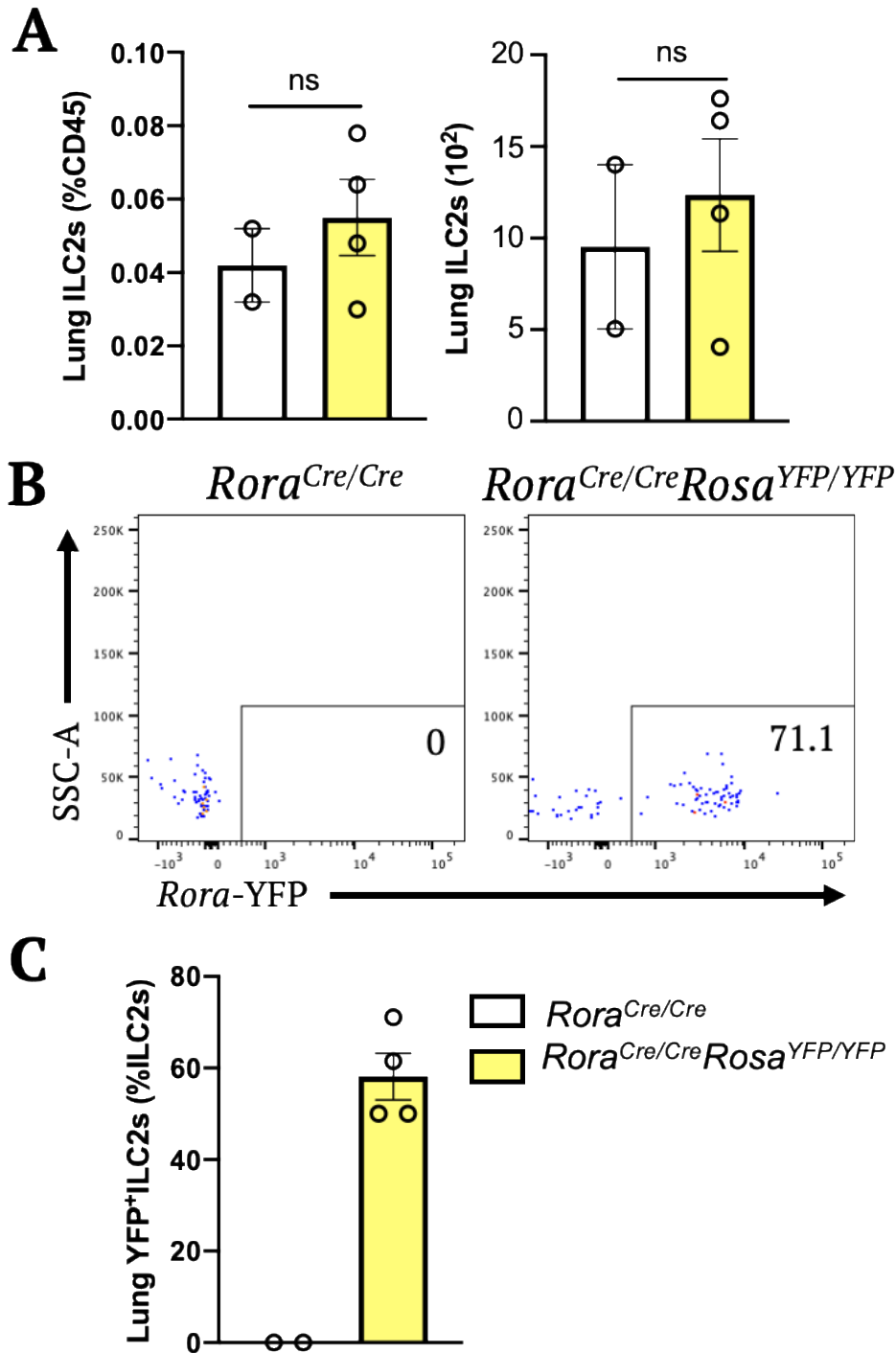


Figure 4.4: Identification of *Rora*-YFP expressing lung ILC2s. *Rora*^{Cre/Cre} and *Rora*^{Cre/Cre} *Rosa*^{YFP/YFP} mice lungs were harvested and assessed by flow cytometry. **A**, Quantification of lung ILC2s gated as lymphocytes, single cells, live, CD45⁺, lineage negative (CD3, CD4, SiglecF, CCR3, Ly6c, CD19), CD127⁺ and KLRG⁺. **B**, Representative flow cytometry plots of lung ILC2 expressing *Rora*-YFP⁺. The numbers on the flow cytometry plot represent percentage of *Rora*-YFP⁺ ILC2 cells. **C**, Quantification of *Rora*-YFP expressing lung ILC2s. **C**, Differences, indicated as two-tailed *p* values, as assessed by unpaired Student *t* test. ns = non-significant. n = 2-4.

Here I have shown the validation of a *Rora* reporter mouse. Analysis revealed YFP⁺CD45 cells had increased expression of *Rora* mRNA compared to YFP⁻CD45 cells. Importantly, the *Rora* reporter mice did not display any characteristics which would indicate that the *Rora* gene in these mice is non-functional, such as a smaller size or ILC2 deficiency, and therefore these *Rora* reporter mice provide an excellent tool with which to identify *Rora* expressing immune cells by flow cytometry both in naïve animals, and following induction of a type 2 response.

4.3.5 tSNE clustering of *Rora*-YFP expressing CD45⁺ cells

The generation of a *Rora* reporter mouse allowed for identification of *Rora*-YFP expressing cells by flow cytometry. I utilised these mice to investigate the presence of *Rora* expressing cells in the lungs of uninfected mice. Therefore, I stained cells isolated from the lung with markers for T cells, B cells, eosinophils, macrophages, monocytes and neutrophils (CD4, CD19, CD127, SiglecF, CD11b, CD11c, Ly6C and Ly6G cells), and performed a tSNE clustering algorithm to explore *Rora* expressing CD45⁺ cells in the lung. A tSNE is an unsupervised nonlinear dimensionality reduction algorithm that can be used for visualising single cell flow cytometry data in dimension-reduced space. Therefore, the clusters of cells are distributed based on similarities and allowed for visualisation of a third dimension.

The tSNE analysis revealed clusters of distinct populations of lung CD45⁺ cells based on *Rora*-YFP, CD4, CD19, CD127, SiglecF, CD11b, CD11c, Ly6C and Ly6G cells (**Figure 4.5**). There was no overlap of clusters from markers of distinct cells such as CD4 and CD19. Therefore, indicating that the tSNE accurately arranged clusters into distinct cell populations. Interestingly, the tSNE clustering analysis identified a proportion of *Rora*-YFP expressing cells which had an overlapping expression with CD4, CD19, CD127 and SiglecF cells (**Figure 4.5**). Therefore, indicating that *Rora* may have a role in cells expressing CD4, CD19, CD127 and SiglecF. Indeed, CD4 is a marker for T cells and ROR α is known to be expressed in T cells (Yang et al., 2008, Van Dyken et al., 2016, Malhotra et al., 2018, Miragaia et al., 2019, Haim-Vilmovsky et al., 2020). CD19 is a marker for B cells and ROR α is reportedly expressed in IgA⁺ memory B cells (Wang et

al., 2012). CD127 (IL7R α) is expressed throughout the lymphoid system, with both ILC2s and CD4 T cells expressing *Il7a*, and it is involved in the maturation of thymocytes and the survival and function of T cells (Fry and Mackall, 2005, Schlenner et al., 2010, Spits et al., 2013, Lev et al., 2019). *RORA* is also known to be expressed in human CD127⁺ILCs (Björklund Å et al., 2016). Whilst SiglecF is a marker commonly found on eosinophils, which is interesting as this supports data generated in **Chapter 3**, showing decreased eosinophilia in the absence of functional ROR α . However, as of yet, there are no sited publications reporting *Rora* expression in eosinophils.

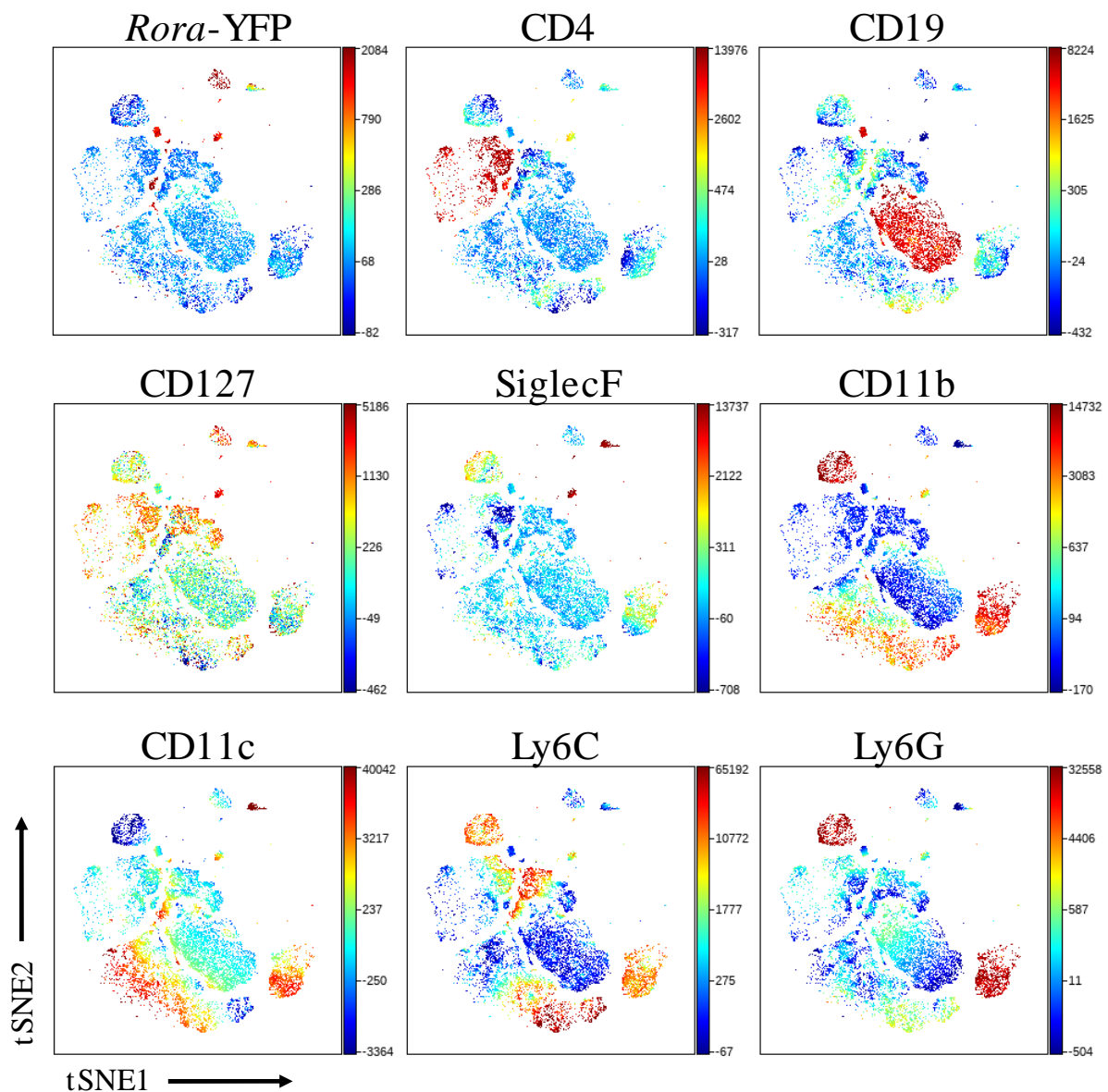


Figure 4.5: Identification of *Rora*-YFP expressing lung CD45⁺ cells. tSNE clustering of live, single, CD45⁺ cells from lungs of *Rora* reporter mouse. Lungs were harvested from *Rora* reporter mice and assessed by flow cytometry. tSNE clustering show expression of *Rora*-YFP, CD4, CD19, CD127, SiglecF, CD11b, CD11c, Ly6C and Ly6G. Blue = lowly expressed. Red = highly expressed.

4.3.6 *Rora*-YFP expressing lung CD4 T cells

The tSNE clustering analysis revealed a population of *Rora*-YFP expressing lung CD4 T cells (**Figure 4.5**). Indeed, CD4 T cells are known to express *Rora* (Yang et al., 2008, Van Dyken et al., 2016, Malhotra et al., 2018, Miragaia et al., 2019, Haim-Vilmovsky et al., 2020). Therefore, to validate the identification of a *Rora* expressing CD4 T cell population in *Rora* reporter mice, I investigated *Rora*-YFP expression in lung CD4 T cells between *Rora* reporter and control (WT and *Rora*^{Cre/Cre}) mice by flow cytometry.

There was no significant difference in frequency of lung CD4 T cells between control mice and *Rora* reporter mice (**Figure 4.6A**). Therefore, generation of the *Rora* reporter mouse had no impact on the frequency of lung CD4 T cells, as observed in **Chapter 3** in *Rora*^{sg/sg} mice. Flow cytometry analysis revealed a population of *Rora* expressing CD4 T cells in the lung of *Rora* reporter mice (**Figure 4.6B**), which was not apparent in control mice (**Figure 4.6C**). Therefore, generation of the *Rora* reporter mice did not impact on frequency of CD4 T cells, and confirmed the presence of a population of *Rora* expressing CD4 T cells in the lungs.

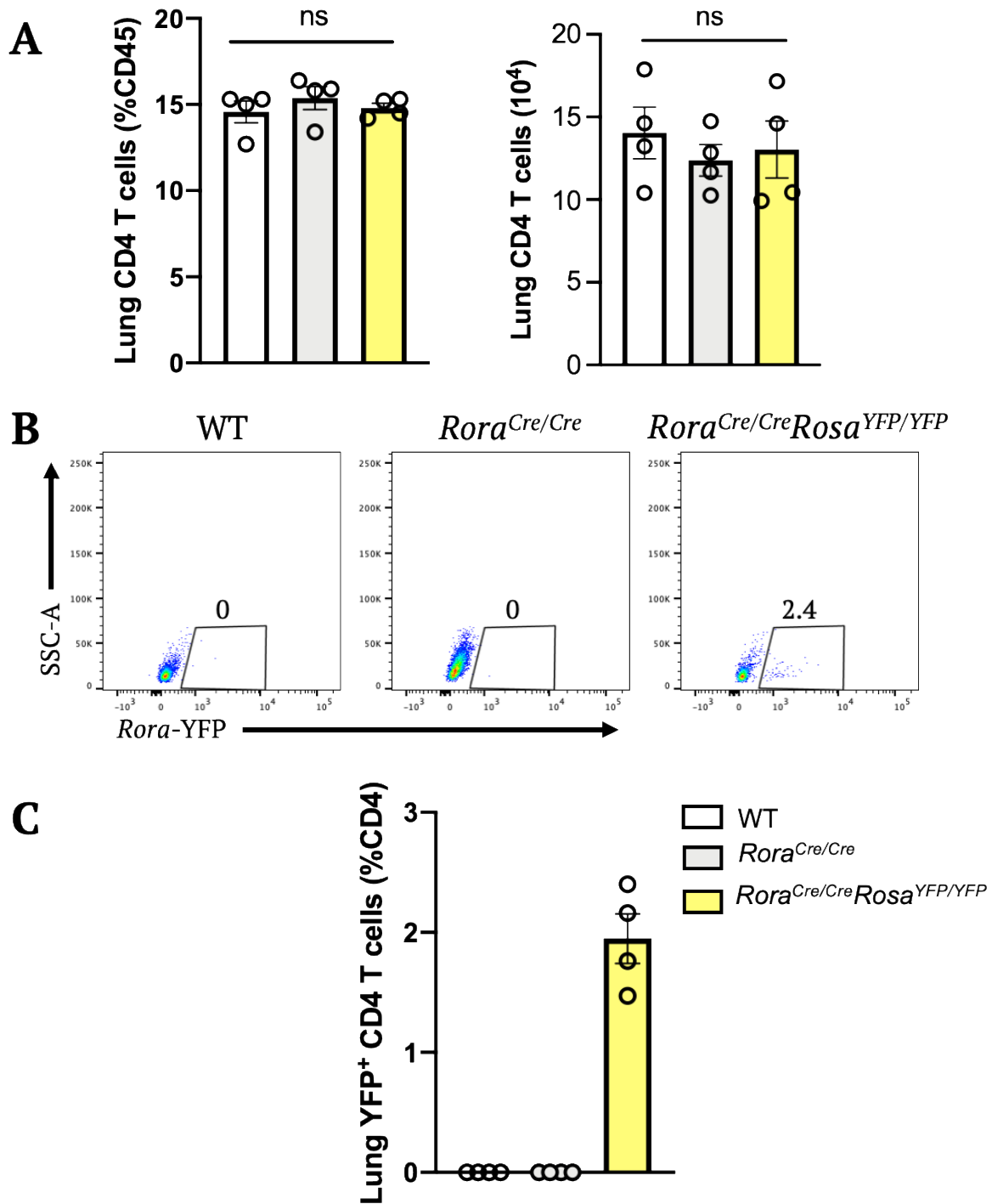


Figure 4.6: Identification of *Rora*-YFP expressing lung CD4 T cells. WT, $Rora^{Cre/Cre}$ and $Rora^{Cre/Cre}Rosa^{YFP/YFP}$ mice lungs were harvested and assessed by flow cytometry. **A**, Quantification of lung CD4 T cells. CD4 T cells were gated as lymphocytes, single cells, live, CD45⁺, CD4⁺. The numbers on the flow cytometry plot represent percentage of *Rora*-YFP⁺ CD4 T cells. **B**, Representative flow cytometry plots of *Rora*-YFP expressing CD4 T cells. Number on flow cytometry plot represents percentage of CD4 T cells. **C**, Quantification of *Rora*-YFP⁺ expressing CD4 T cells. Differences, indicated as two-tailed *p* values, as assessed by unpaired Student *t* test. ns = non-significant. n = 4.

4.3.7 *Rora*-YFP expressing CD4 T cells express *Rora* mRNA

Having shown that CD45⁺YFP⁺ cells express *Rora* mRNA and identifying a population of CD4 T cells that express *Rora*-YFP⁺, I assessed the *Rora* mRNA expression in *Rora*-YFP expressing CD4 T cells, to confirm these are *Rora* expressing CD4 T cells. Splenocytes were isolated from *Rora* reporter mice as a rich source of CD4 T cells, and stained with markers for CD45 and CD4. CD45⁺CD4⁺YFP⁺ cells and CD45⁺CD4⁺YFP⁻ cells were isolated by FACS and assessed for *Rora* mRNA expression by qPCR.

The FACS sort purity of >97% for CD45⁺CD4⁺YFP⁺ and 100% for CD45⁺CD4⁺YFP⁻ (**Figure 4.7A**), confirming RNA was isolated from a pure population of cells. Furthermore, qPCR analysis revealed that CD45⁺CD4⁺YFP⁺ cells expressed *Rora* mRNA. Whilst no *Rora* mRNA was detected from CD45⁺CD4⁺YFP⁻ cells (**Figure 4.7B**), confirming that CD45⁺CD4⁺YFP⁺ cells are indeed *Rora* expressing cells. As CD4 T cells are a heterogenous population with co-expression of transcription factors, I investigated the co-expression of *Rora* in CD4 T cells with CD4 T cell subset transcription factors (*Tbx21* – Th1, *Gata3* – Th2, *Roryt* – Th17, and *Foxp3* – Treg). There was expression of *Gata3*, *Foxp3* and *Tbx21* mRNA detected in both *Rora*-YFP⁺ and *Rora*-YFP⁻ cells (**Figure 4.7C**). Therefore, indicating that CD4 T cells co-express *Rora* with *Gata3*, *Foxp3* and *Tbx21*, suggesting that *Rora* is expressed in Th2, Treg and Th1 cells, respectively. However, there was no significant difference in expression of *Gata3*, *Foxp3* and *Tbx21* in *Rora*-YFP⁺ and *Rora*-YFP⁻ expressing CD4 T cells. Interestingly, following *N. brasiliensis* infection, activated *Rora* expressing cells also expressed *Gata3*, *Foxp3* and *Tbx21*, indicating a role for *Rora* in Th2, Tregs and Th1 cells (Haim-Vilmovsky et al., 2020). Furthermore, it is known that *Rora* and *Roryt* are important for Th17 cell development (Yang et al., 2008). However, there was no *Roryt* mRNA detected in either *Rora*-YFP⁺ and *Rora*-YFP⁻ CD4 T cells. It is possible that as CD4 T cells were isolated from naïve *Rora* reporter mice, the frequency of Th17 cells (*Roryt*) was undetectable, therefore there was an absence of *Roryt* mRNA in either *Rora*-YFP⁺ and *Rora*-YFP⁻ CD4 T cells in the spleen. Therefore, taken together, these findings indicate that *Rora*-YFP expressing CD4 T cell are *Rora* mRNA expressing CD4 T cells, and there is an overlap in *Rora* expressing CD4 T cells with *Gata3*, *Foxp3* and *Tbx21* expressing CD4 T cells.

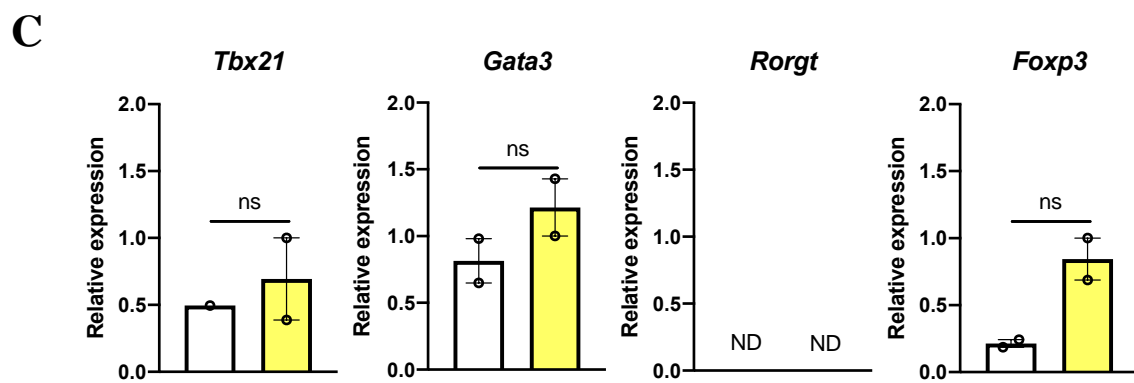
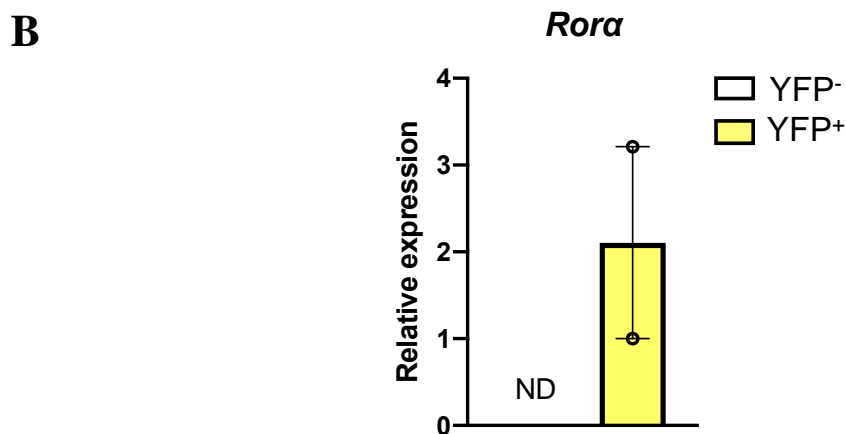
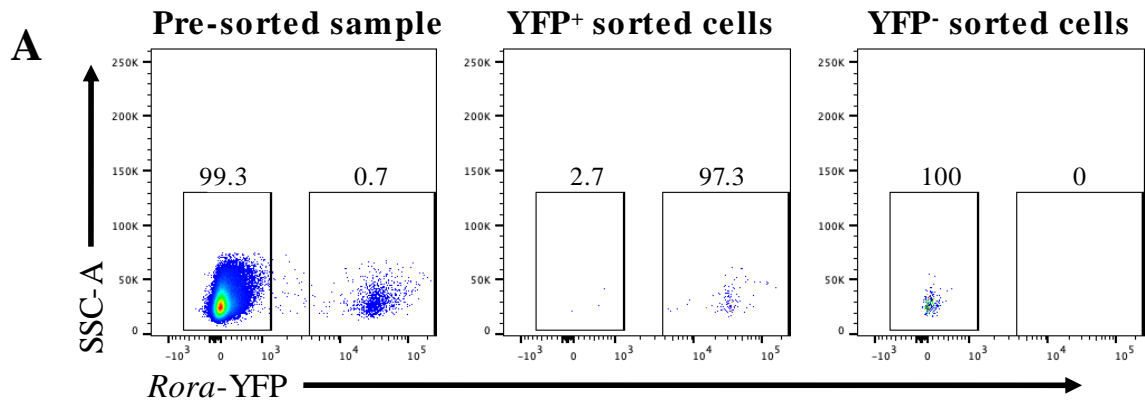


Figure 4.7: Transcription factor expression in *Rora*-YFP⁺ and *Rora*-YFP⁻ CD4 T cells. *Rora* reporter mice spleen cells were isolated and stained for CD45 and FACS sorted based on live, CD45⁺CD4⁺YFP⁺ and CD45⁺CD4⁺YFP⁻. **A**, Representative flow cytometry plots of *Rora* reporter spleen cells stained with CD45 and CD4. The purity of the CD45⁺CD4⁺YFP⁺ sorted population was >97%. Purity of the CD45⁺CD4⁺YFP⁻ sorted population was 100%. **B**, *Rora* gene expression. **C**, *Tbx21*, *Gata3*, *Rorgt* and *Foxp3* gene expression. Gene expression normalised to *18S*. Data is representative of means \pm SEM. Differences, indicated as two-tailed *p* values, as assessed by unpaired Student *t* test. ND = Non-detected. *n* = 2.

4.3.8 *Rora* reporter mice had a comparable type 2 immune response to control mice following *N. brasiliensis* infection

The results presented in this chapter thus far have focused on the identification of *Rora* expressing immune cells in naïve animals. Therefore, I assessed if *Rora* reporter mice had comparable physiological responses following *N. brasiliensis* infection to control mice, which is important to ensure the role of *Rora*-expressing cells can be fully appraised in this model. In **Chapter 3**, it was shown that *Rora*^{sg/sg} mice and *Rora*^{sg/sg} BM chimera mice, have an altered functional type 2 immune response as characterised by a higher worm count at day 7 post *N. brasiliensis* infection. If the generation of a *Rora* reporter mice interfered with the functioning of the *Rora* gene, this may produce a similar functional phenotype as observed in *Rora*^{sg/sg} mice and *Rora*^{sg/sg} BM chimera mice, with a higher worm count day 7 post-infection. Therefore, I infected *Rora* reporter and control (WT and *Rora*^{Cre/Cre}) mice with *N. brasiliensis* and assessed the resulting immune response.

There was no significant difference in the small intestine worm count at day 7 post-infection between *Rora* reporter mice and control mice (**Figure 4.8**). Therefore, indicating the generation of the *Rora* reporter mouse had no significant effect on the function of the *Rora* gene.

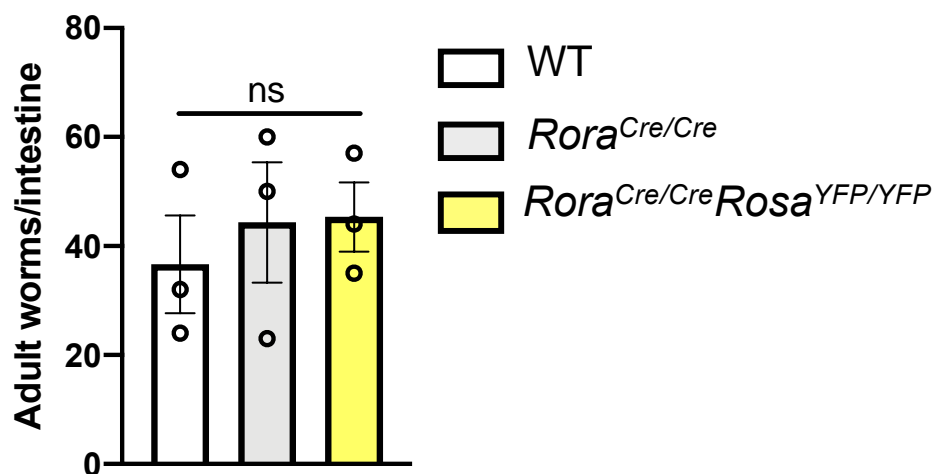


Figure 4.8: No significant difference in *N. brasiliensis* count in small intestine between *Rora* reporter and control mice at day 7 post-infection. WT, *Rora*^{Cre/Cre} and *Rora*^{Cre/Cre} *Rosa*^{YFP/YFP} mice were infected with 500 L3 *N. brasiliensis* subcutaneously. Small intestines were harvested at day 7 post-infection. Data is representative of means \pm SEM. Differences indicated as two-tailed p values, as assessed by unpaired Student *t* test. ns = non-significant. n = 3.

In **Chapter 3** it was also shown that *Rora*^{sg/sg} mice and *Rora*^{sg/sg} BM chimera mice had reduced frequency of lung ILC2s, CD4 T cells and eosinophils following *N. brasiliensis* infection. Therefore, I examined the lung immune cell frequency in both uninfected and *N. brasiliensis* infected *Rora* reporter and control (*Rora*^{Cre/Cre}) mice, to confirm that the generation of *Rora* reporter mice did not impact the function of the *Rora* gene.

There was no significant difference in the frequency of the lung immune cells assessed (ILC2s, CD4 T cells, eosinophils and macrophages) between *Rora* reporter mice and control mice (**Figure 4.9**). Therefore, the generation of the *Rora* reporter mouse had no discernible effect on the frequency of CD4 T cells, ILC2s, eosinophils and macrophages in uninfected mice or following *N. brasiliensis* infection. These findings indicate that the generation of a *Rora* reporter mouse did not alter the physiological responses. Therefore, allowing for the detection of *Rora* expressing cells whilst preserving all regulatory functions. This was important for future studies where I will investigate *Rora* expressing cells during *N. brasiliensis* infection.

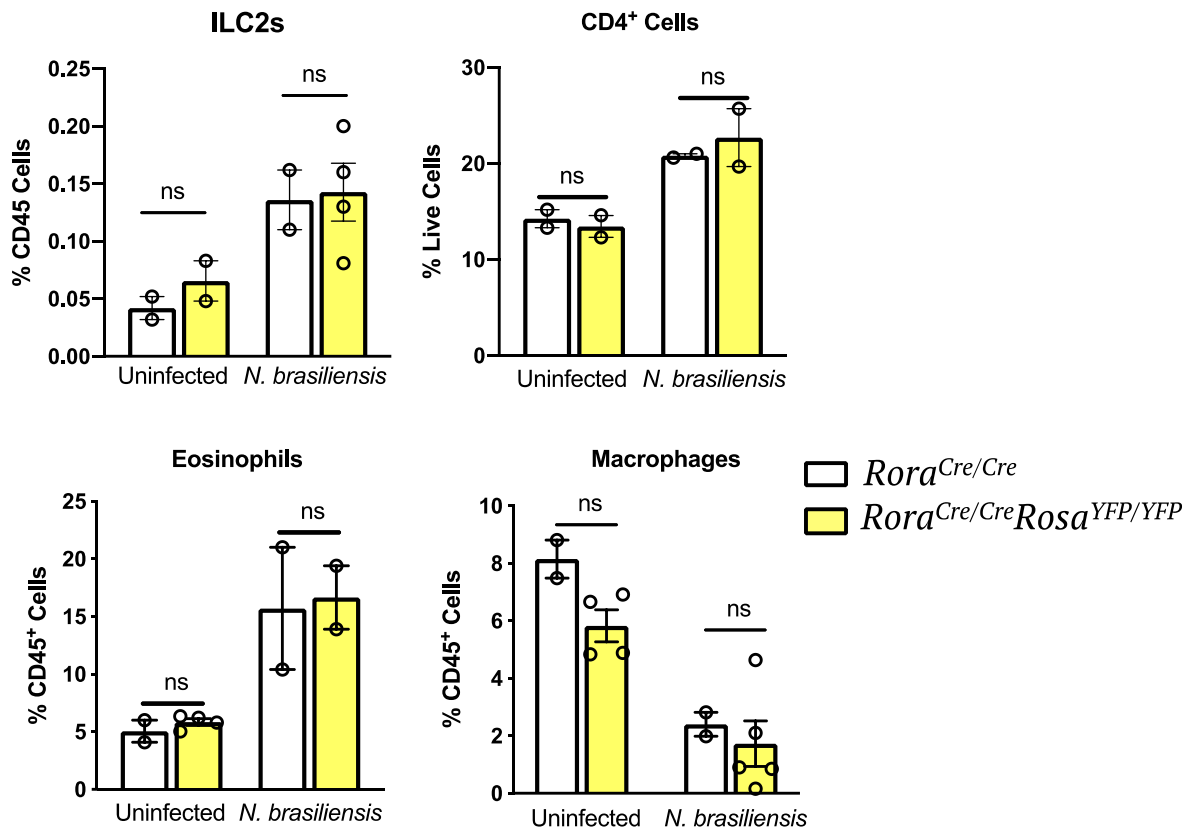


Figure 4.9: No significant difference in frequency of lung immune cells in uninfected and *N. brasiliensis* infected *Rora* reporter and control mice. *Rora*^{Cre/Cre} and *Rora*^{Cre/Cre}*Rosa*^{YFP/YFP} mice were infected with 500 L3 *N. brasiliensis* subcutaneously. Lungs were harvested at day 7 post-infection for flow cytometry analysis. Cell populations were gated as cells, single cells, live, CD45⁺. CD4 T cells as CD4⁺. ILC2s as lineage negative (CD3, CD4, SiglecF, CCR3, Ly6c, CD19), CD127⁺KLRG⁺GATA3⁺. Eosinophils as SiglecF⁺CD11b⁺F4/80⁺CD11c⁻. Macrophages as SiglecF⁺CD11b⁺F4/80⁺CD11c⁺. Differences assessed by unpaired Student *t* test. ns = non-significant. n = 2-5.

4.3.9 Identification of lung *Rora*-YFP expressing CD45⁺ cells following *N. brasiliensis* infection

Having identified that *Rora* reporter mice have a comparable immune response to control mice, I sought to explore the *Rora* expressing lung cells following *N. brasiliensis* infection. I infected *Rora* reporter mice with *N. brasiliensis* and performed an unsupervised tSNE cluster algorithm on lung CD45⁺ cells to visualise *Rora*-YFP expressing cells. Interestingly, tSNE analysis revealed several populations of *Rora*-YFP expressing cells which overlapped with the expression of CD4, CD19, SiglecF and

CD11b clusters. Therefore, indicating that *Rora* may have role in CD4, CD127, CD19, SiglecF and CD11b expressing cells during *N. brasiliensis* infection (**Figure 4.10**).

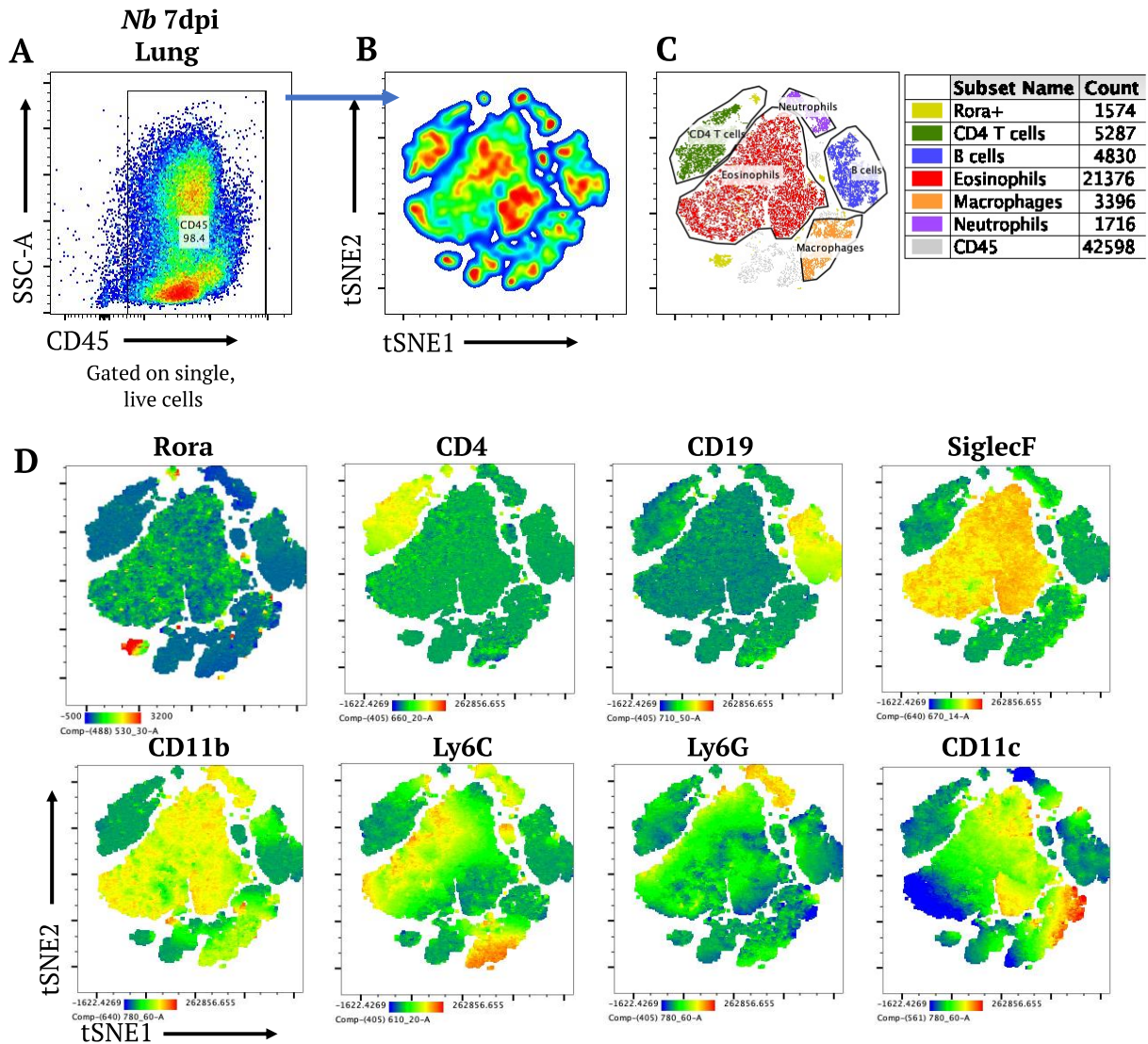


Figure 4.10: Identification of *Rora*-YFP expressing lung CD45⁺ cells following *N. brasiliensis* infection. *Rora* reporter mouse was infected with 500 L3 *N. brasiliensis* subcutaneously. Lungs were harvested at day 7 post-infection and assessed by flow cytometry. **A**, Pre-grouped CD45⁺ cells gated on single, live cells. **B**, tSNE clustering pseudocolour density plot. **C**, Identification of lymphoid and myeloid cells (CD4 T cells, B cells, eosinophils, macrophages and neutrophils) **D**, tSNE clustering show expression of *Rora*-YFP, CD4, CD19, SiglecF, CD11b, CD11c, Ly6C and Ly6G. Blue = lowly expressed. Red = highly expressed.

4.3.10 Increased expression of transcription factors (*Gata3*, *Foxp3* and *Rora*) in CD4 T cells following *N. brasiliensis* infection

Recently, it has been shown that following *N. brasiliensis* infection, there is an overlap of gene expression between *Rora*, *Gata3* and *Foxp3* in CD4 T cells (Haim-Vilmovsky et al., 2020). Indeed, I have shown that *Rora*-YFP expressing CD4 T cells co-express *Gata3* and *Foxp3* in uninfected animals (**Figure 4.7**). Therefore, I explored the expression of *Rora*, *Gata3* and *Foxp3* mRNA in CD4 T cells following *N. brasiliensis* infection. To investigate this, CD4 T cells were isolated from spleens of WT mice using autoMACS CD4 T cell separation, and measured expression of *Rora*, *Gata3* and *Foxp3* mRNA by qPCR.

There was an increase in expression of the transcription factors *Gata3* and *Foxp3* in CD4 T cells following *N. brasiliensis* infection (**Figure 4.11**). Indeed, following *N. brasiliensis* infection there is an increase in lung GATA3⁺ (Th2), GATA3⁺Foxp3⁺ and Foxp3⁺ (Tregs) cells (Halim et al., 2018). Interestingly, there is also an increase in *Rora* mRNA expression in CD4 T cells following infection (**Figure 4.11**). This supports recent RNA-seq data which shows an increase in *Rora* expression in spleen CD4 T cells following *N. brasiliensis* infection (Haim-Vilmovsky et al., 2020). Therefore, taken together, these results indicate that *N. brasiliensis* infection increases the expression of *Rora* mRNA in CD4 T cells, indicating that *Rora* has a role in CD4 T cells during a type 2 immune response.

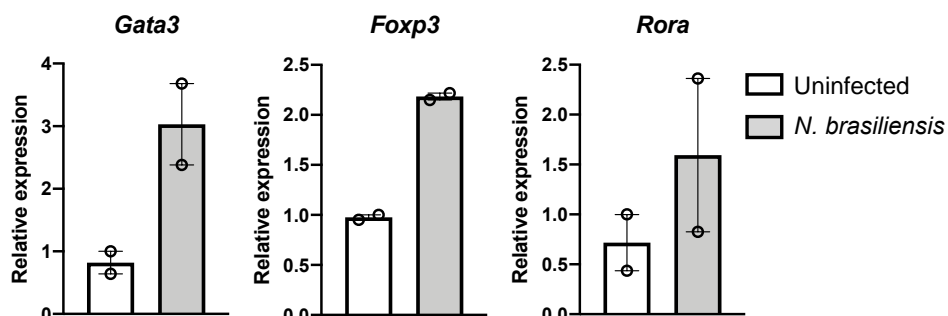


Figure 4.11: Increase in mRNA expression of transcription factors (*Gata3*, *Foxp3* and *Rora*) in CD4 T cells following *N. brasiliensis* infection. WT mice were infected with 500 L3 *N. brasiliensis* subcutaneously and spleens were harvested from uninfected mice and at day 7 post-infection. CD4 T cells were isolated from spleens by AutoMACS. RNA was isolated from the CD4 T cells and gene expression was quantified by qPCR and normalized based on 18S expression. Expression of transcription factors *Gata3*, *Foxp3* and *Rora*. Data is representative of mean \pm SEM. n = 2.

4.3.11 Increase in *Rora*-expressing lung CD4 T cells following *N. brasiliensis* infection.

Lung CD4 T cells play an essential role in mediating host resistance to secondary *N. brasiliensis* infection (Harvie et al., 2010, Harvie et al., 2013, Thawer et al., 2014). Therefore, having identified a population of *Rora*-YFP expressing lung CD4 T cells in uninfected and *N. brasiliensis* infected *Rora* reporter mice by tSNE clustering (**Figure 4.10**), and *N. brasiliensis* infection increases *Rora* mRNA in CD4 T cells, I then assessed the frequency of lung *Rora* expressing CD4 T cells following primary and secondary *N. brasiliensis* infection.

Consistent with results previously reported in this chapter (**Figure 4.6**), there is a population of *Rora* expressing lung CD4 T cells in uninfected mice (**Figure 4.12**). Following primary *N. brasiliensis* infection, there is a significant ($p<0.05$) increase in frequency of lung *Rora* expressing CD4 T cells (**Figure 4.12**). Interestingly, following secondary *N. brasiliensis* infection, there is a further increase in frequency of *Rora* expressing CD4 T cells in the lungs. These results support data generated in **Chapter 3**, showing a decreased frequency of CD4 T cells in the absence of functional ROR α following primary and secondary *N. brasiliensis* infection. Therefore, indicating that *Rora* may have a role in lung CD4 T cells development following *N. brasiliensis* infection. The lungs are an important site for immune-mediated protection in secondary *N. brasiliensis* infection (Harvie et al., 2010, Bouchery et al., 2015). Therefore, it may be possible that there is a population of lung *Rora* expressing CD4 T cells which expands upon secondary infection.

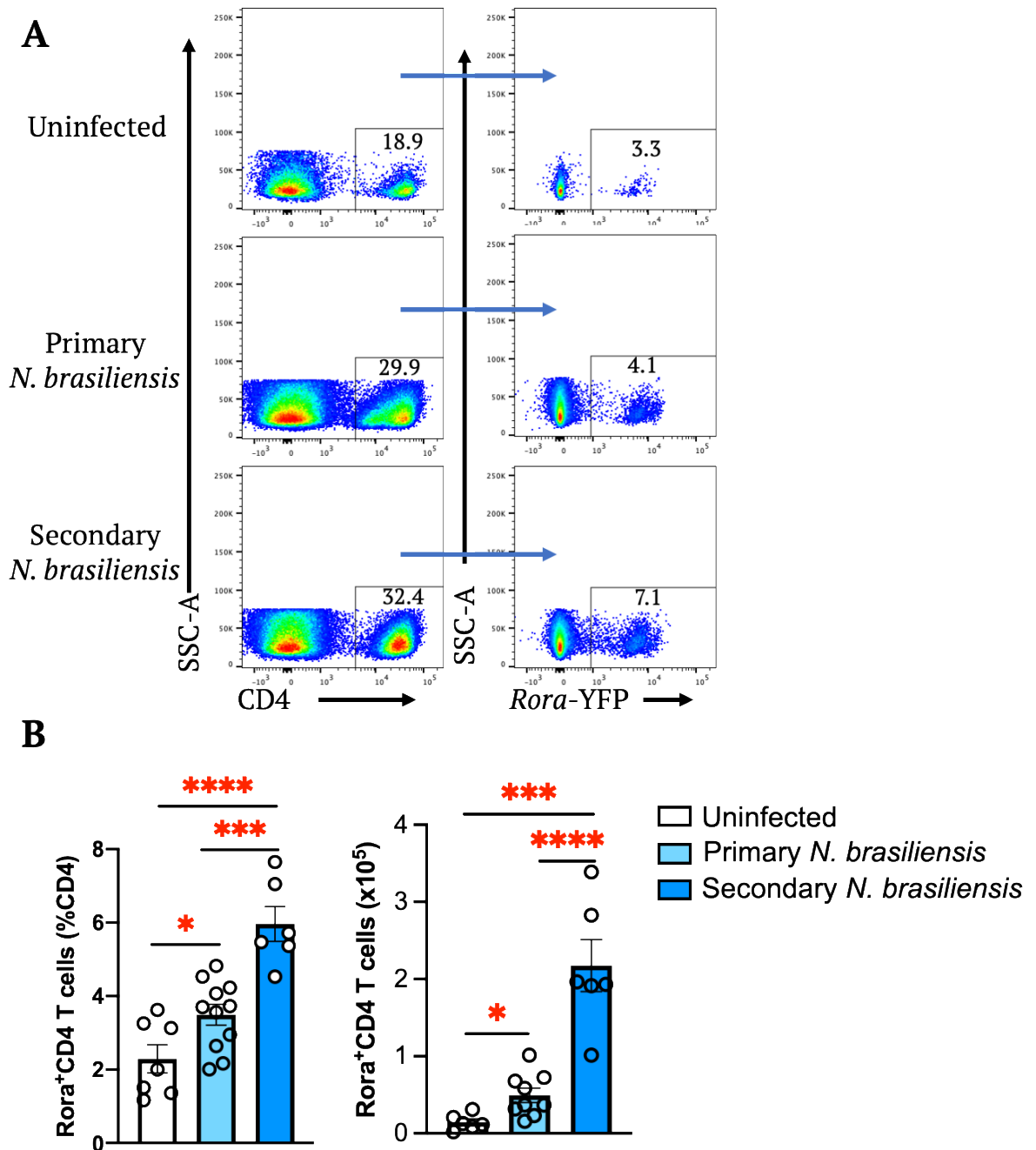


Figure 4.12: Increase in lung *Rora*-YFP expressing CD4 T cells following *N. brasiliensis* infection. *Rora* reporter mice were either uninfected or infected with primary or secondary *N. brasiliensis* infection. Lungs were harvested for flow cytometry analysis. **A**, Cell populations were gated as lymphocytes, single cells, live, CD45⁺, CD4⁺ and *Rora*-YFP⁺. **B**, Quantification of lung *Rora*-YFP expressing CD4 T cells. Data is representative of mean ± SEM. Differences indicated as two-tailed *p* values, as assessed by unpaired Student *t* test. **p*<0.05, ****p*<0.005, *****p*<0.001 n = 6-11.

4.3.12 Increase in frequency of lung *Rora*-expressing GATA3⁺CD4 T cells following *N. brasiliensis* infection.

N. brasiliensis infection increases the frequency of lung GATA3⁺, GATA3⁺Foxp3⁺ and Foxp3⁺ cells in control animals (**Chapter 3, Section 3.3.2.8**) (Halim et al., 2018). I have identified that following *N. brasiliensis* infection there is an increase in the frequency of *Rora* expressing lung CD4 T cells (**Figure 4.12**), and an increase in *Rora*, *Gata3* and *Foxp3* mRNA expression in CD4 T cells following *N. brasiliensis* (**Figure 4.11**). Therefore, I assessed the frequency of CD4 T cell subsets, GATA3⁺ (Th2), Foxp3⁺ (Tregs) and GATA3⁺Foxp3⁺ (GATA3⁺Tregs) that co-expressed *Rora*-YFP following *N. brasiliensis* infection.

There are populations of *Rora* expressing GATA3⁺, Foxp3⁺ and GATA3⁺Foxp3⁺ CD4 T cells present in the lungs of uninfected mice, which increases in frequency following *N. brasiliensis* infection (**Figure 4.13**). Interestingly, the percentage of *Rora* expressing GATA3⁺ CD4 T cells decreased from uninfected to primary infection, before increasing with secondary infection. Whilst the absolute number of lung *Rora* expressing GATA3⁺ CD4 T cells increases following both primary and secondary infection. Conversely, the percentage of *Rora* negative GATA3⁺ CD4 T cells increased from uninfected to primary infection. This indicates that ROR α may have a greater role in GATA3⁺ CD4 T cells in the secondary infection compared to primary infection. Furthermore, there was no difference in the percentage of *Rora* expressing Foxp3⁺ CD4 T cells between uninfected and primary infection, whilst an increase in percentage during secondary infection. There was also an increase in the absolute number of *Rora* expressing Foxp3⁺ CD4 T cells following *N. brasiliensis* infection. This may also indicate a role for *Rora* expressing Foxp3⁺ CD4 T cells during secondary infection. There was no significant difference in the frequency and total *Rora* expressing GATA3⁺Foxp3⁺ CD4 T cells in the lungs between uninfected and *N. brasiliensis* infected mice, indicating that *Rora* may have no role in GATA3⁺Foxp3⁺ CD4 T cells during *N. brasiliensis* infection.

Therefore, taken together, these findings may indicate a role for *Rora* in GATA3⁺ and Foxp3⁺ CD4 T cell development during following *N. brasiliensis* infection, with a possible greater role following reinfection. Indeed, lung-resident CD4 T cells mediate host resistance to secondary *N. brasiliensis* infection (Harvie et al., 2010, Harvie et al.,

2013, Thawer et al., 2014), in **Chapter 3**, in the absence of functional ROR α there was an increase in worm burden following secondary infection and a decreased frequency of lung GATA3⁺ CD4 T cells following *N. brasiliensis* infection, whilst there was no difference in the frequency of Foxp3⁺ CD4 T cells. Therefore, it may be possible that *Rora* expressing GATA3⁺ CD4 T cells are a lung-resident memory Th2 cell important for immunity against *N. brasiliensis* infection.

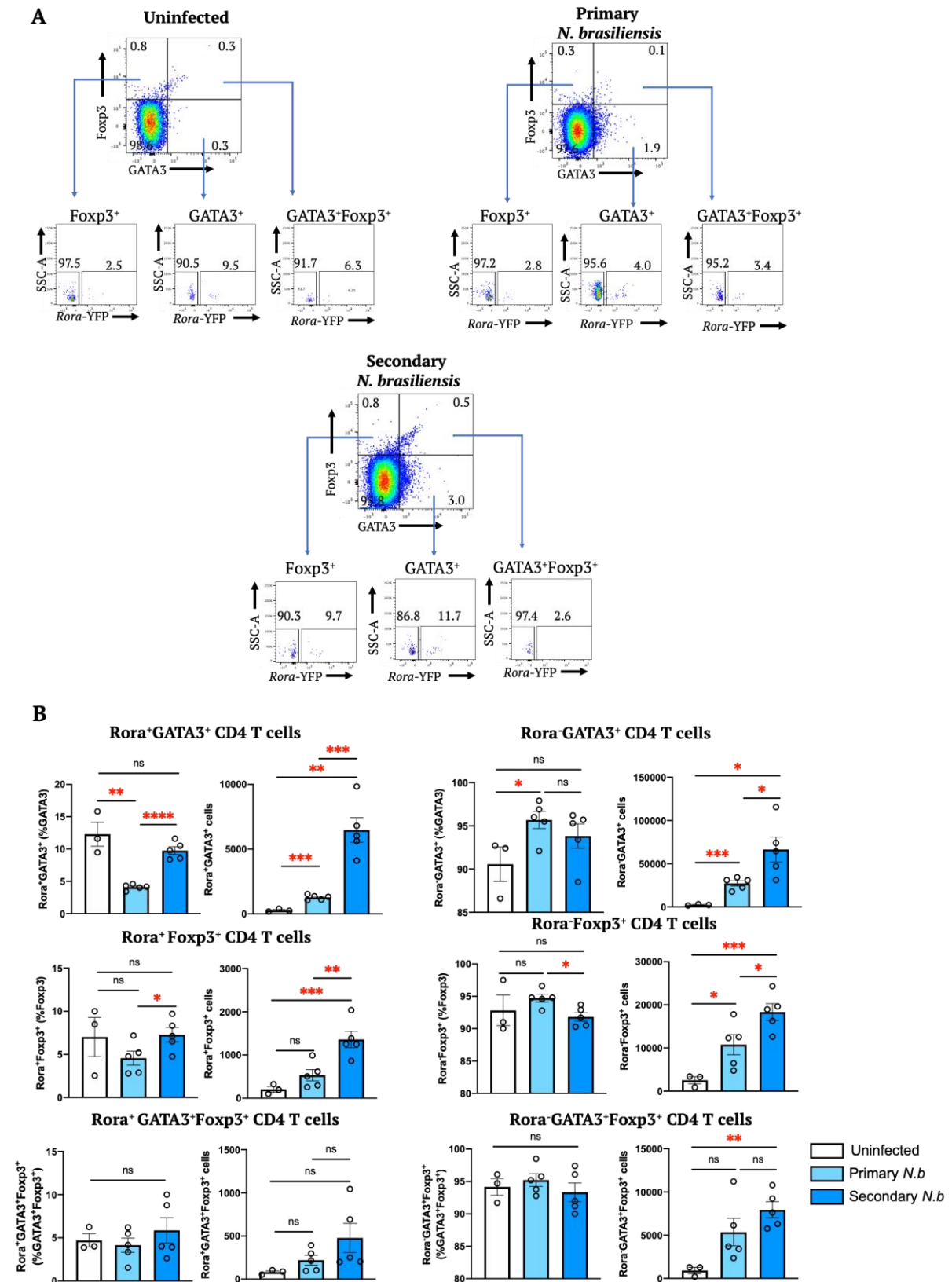


Figure 4.13: Increase in lung *Rora* expressing GATA3⁺CD4 T cells and Foxp3⁺CD4 T cells following *N. brasiliensis* infection. *Rora* reporter mice were either uninfected or infected with primary or secondary *N. brasiliensis* infection. Lungs were harvested for flow cytometry analysis. A, Cell populations were gated as lymphocytes, single cells, live, CD45⁺CD4⁺. T cell subpopulations were gated as GATA3⁺, GATA3⁺Foxp3⁺ and

Foxp3⁺. The number on the flow plots reflects percentage of parent gate. **B**, Quantification of Rora⁺GATA3⁺, Rora⁺GATA3⁺Foxp3⁺, Rora⁺Foxp3⁺ cells, Rora⁻GATA3⁺, Rora⁻GATA3⁺Foxp3⁺ and Rora⁻Foxp3⁺ cells. Data representative of means ± SEM. Differences indicated as two-tailed *p* values, as assessed by unpaired Student *t* test. **p*<0.05, ***p*<0.01, ****p*<0.005, *****p*<0.001. ns = non-significant. n = 3-5.

4.3.13 *Rora* is expressed by activated CD4 T cells

It is reported that RORα regulates activated CD4 T helper cells during inflammation, and there was a correlation between *Rora* expression and CD4 T cell activation in spleen cells (Haim-Vilmovsky et al., 2020). Therefore, having identified that following *N. brasiliensis* infection there is an increase in frequency of *Rora*-expressing lung CD4 T cells (**Figure 4.11**), an increase in *Rora* mRNA expression in CD4 T cells (**Figure 4.12**), and an increase in frequency of *Rora*-expressing lung GATA3⁺CD4 T cells (**Figure 4.13**), I assessed the activation status of *Rora* expressing CD4 T cells in the lungs by determining the expression of activation markers (CD44, CD62L and CD69) by flow cytometry.

Interestingly, unsupervised tSNE clustering analysis of lung CD4 T cells revealed a *Rora*-YFP cluster in both uninfected and *N. brasiliensis*-infected mice which expressed activation markers CD44 and CD69 (**Figure 4.14A**). CD44 is a marker of T cell activation, a property of long-lived memory cells, and implicated in cell migration, activation and differentiation (Guan et al., 2009). CD69 is a biomarker of T cell activation status (Schoenberger, 2012). Whilst the tSNE clustering revealed that *Rora*-YFP cluster did not express CD62L (L-Selectin), a naïve CD4 T cell marker (**Figure 4.14A**). The tSNE clustering analysis revealed that following *N. brasiliensis* infection there are *Rora* expressing CD4 T cells which overlap with activation expression markers (CD44 and CD69). In support, flow cytometry gating on *Rora* expressing CD4 T cells revealed that these cells are activated cells based on CD44 and CD69 expression, and following *N. brasiliensis* there was an increase in *Rora* expressing activated CD4 T cells (**Figure 4.14B**). These results indicate that *Rora* expressing lung CD4 T are activated CD4 T cells.

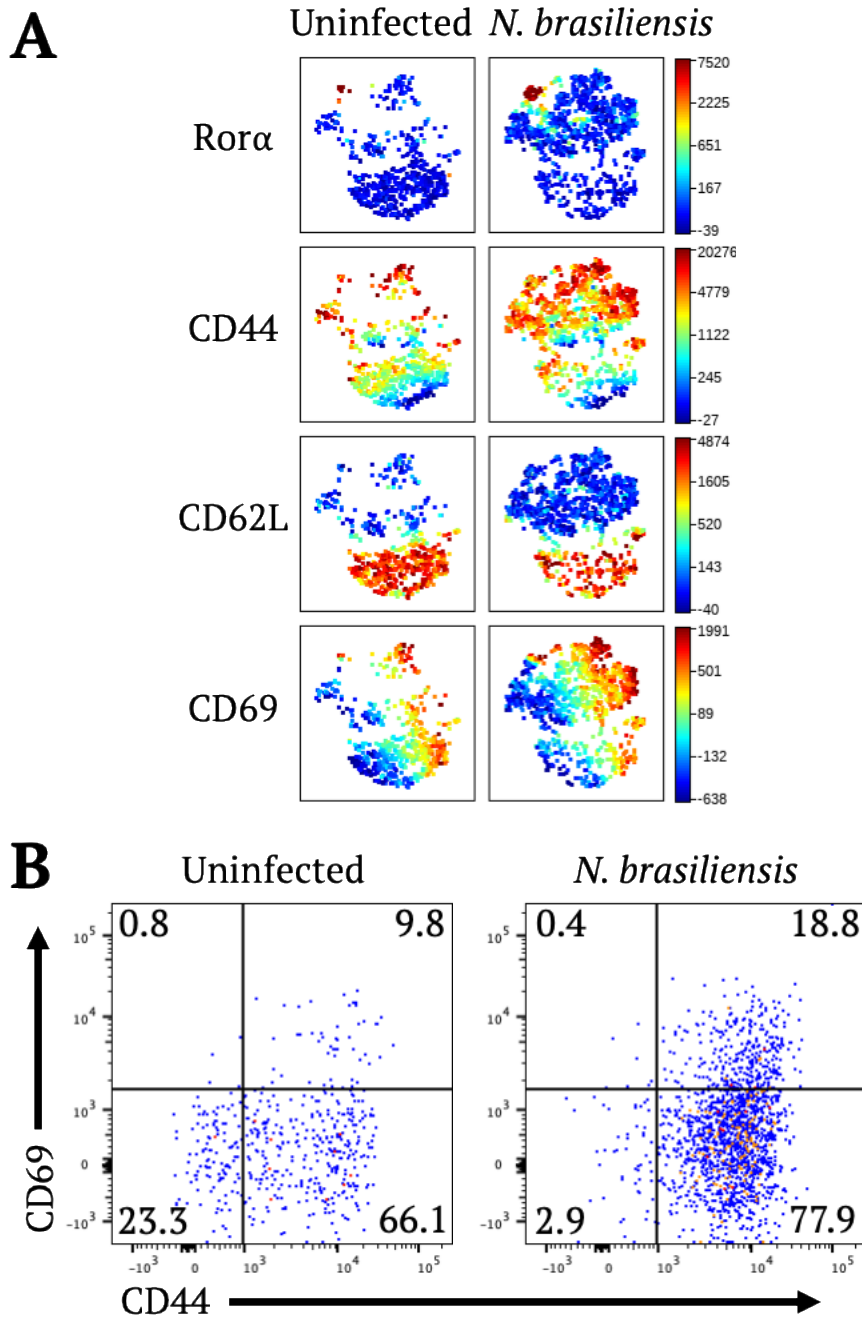


Figure 4.14: *Rora*-YFP expressing CD4 T cells are clustered with activated CD4 T cell markers. *Rora* reporter mouse was infected with 500 L3 *N. brasiliensis* subcutaneously and lungs were harvested 7 days post-infection, and assessed by flow cytometry. **A**, tSNE clustering of CD4⁺ cells from lungs of uninfected and *N. brasiliensis* infected *Rora* reporter mouse. tSNE plots show expression of *Rora*-YFP, CD44, CD62L and CD69. **B**, *Rora* expressing activated CD4 T cells. Cell gated as lymphocytes, single cells, live, CD45⁺CD4⁺*Rora*-YFP⁺. Activation assessed by CD44 and CD69 markers.

4.3.14 *Rora* is associated with lung effector memory CD4 T (T_{EM}) cells

In mice, CD4 T cells can be categorised into memory and naïve phenotypes based on CD62L and CD44 expression. Indeed, CD4 T cells expressing CD44⁻CD62⁺ are considered naïve CD4 T cells (T_N), CD44⁺CD62⁺ are considered central memory (T_{CM}), whilst CD44⁺CD62⁻ are considered effector or effector memory CD4 T cells (T_{EM}) (Sckisel et al., 2017). Following *N. brasiliensis* infection, there is an increase in number of lung T_{EM} CD4 T cells (Thawer et al., 2014). I have identified that *Rora*-YFP expressing lung CD4 T cells clustered to activated CD4 T cells as determined by tSNE analysis of activation markers (**Figure 4.14**), thus suggesting that *Rora* may be important in the activation of CD4 T cells. To fully appraise the role of ROR α in the function of CD4 T cells, I investigated the frequency of lung *Rora* expressing T_N , T_{CM} and T_{EM} CD4 T cells, in uninfected conditions and following *N. brasiliensis* infection.

Flow cytometry analysis showed that *Rora* expressing CD4 T cells were significantly associated with T_{EM} cells in uninfected mice, compared to T_N ($p < 0.005$) and T_{CM} ($p < 0.01$) CD4 T cells (**Figure 4.15**). Following primary *N. brasiliensis* infection there was an increase in *Rora* expressing T_{EM} CD4 T cells, whilst following secondary *N. brasiliensis* infection, there was further increase in *Rora* expressing T_{EM} CD4 T cells. Results are presented as a percentage of lung CD4 T cells, in contrast to presenting results as a percentage of T_N , T_{CM} , T_{EM} , respectively. This takes into account changes in frequency T_N , T_{CM} , T_{EM} following infection, and therefore allows for comparison of *Rora* expressing T_N , T_{CM} , T_{EM} CD4 T cells. These findings support Miragaia et al. (2019) which identified a population of *Rora* expressing memory cells T cells in NLT. There was no difference in the frequency of *Rora* expressing T_N and T_{CM} cells following *N. brasiliensis* infection. Indeed, as mentioned, CD4 T cells are important at mediating immunity against secondary *N. brasiliensis* infection and following host priming during a primary infection there is a population of tissue resident activated effector CD4 T cells (Harvie et al., 2010, Thawer et al., 2014). These findings indicate that *Rora* may have a role in development of T_{EM} CD4 T cells following *N. brasiliensis* infection.

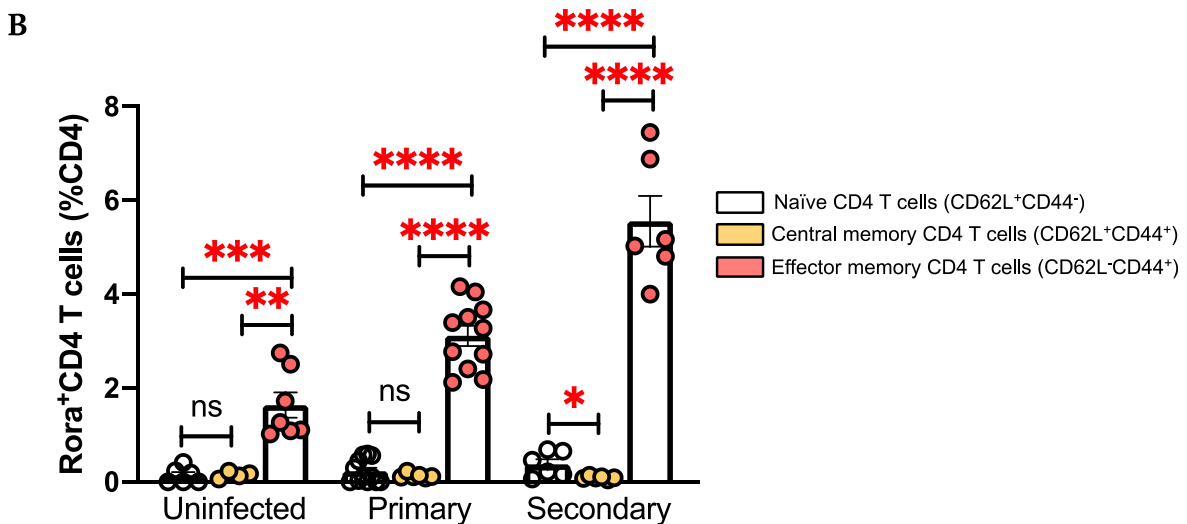
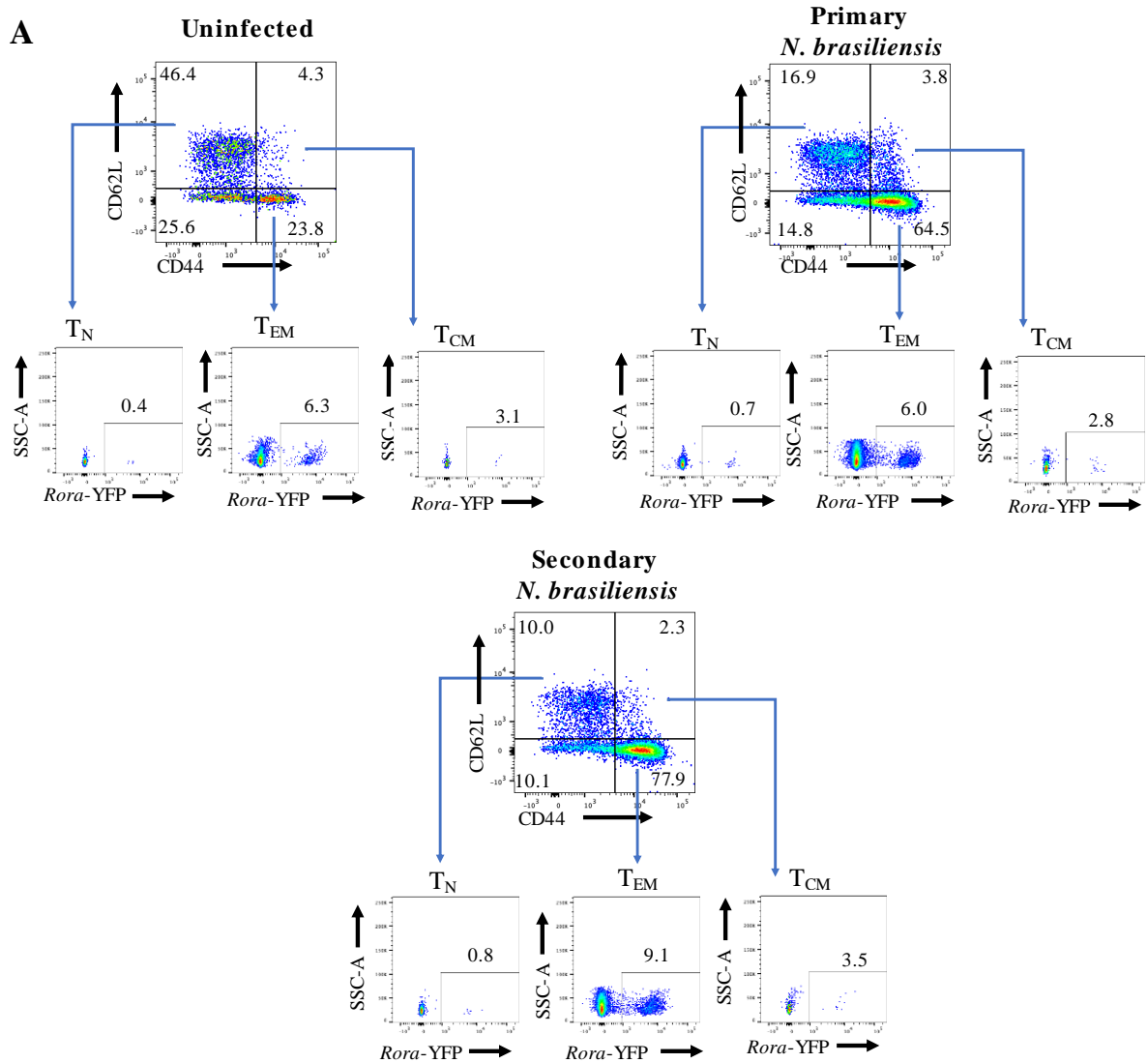


Figure 4.15: *Rora* expression is associated with effector memory CD4 T cells. *Rora* reporter mice were either uninfected or infected with primary or secondary *N. brasiliensis* infection. Lungs were for flow cytometry analysis. **A**, Cell populations were gated as lymphocytes, single cells, live, CD45⁺, CD4⁺. Naïve CD4 T cells (T_N) were identified as CD62L⁺CD44⁻. Central memory CD4 T cells (T_{CM}) were identified as CD62L⁺CD44⁺.

Effector memory CD4 T cells (T_{EM}) were identified as $CD62L^-CD44^+$. **B**, Quantification of lung *Rora*-YFP expressing naïve and activated CD4 T cells. The numbers on flow cytometry plots represents percentage of parent gate. CD44 vs CD62L flow cytometry plot numbers represent percentage of CD4. *Rora*YFP flow cytometry plot numbers represent percentage of T_N , T_{EM} , and T_{CM} , respectively. Data representative of means \pm SEM. Differences indicated as two-tailed *p* values, as assessed by unpaired Student *t* test. **p*<0.05, ***p*<0.01, ****p*<0.005, *****p*<0.001. ns = non-significant. n = 6-12.

4.3.15 Increase in *Rora* expressing CD69⁺ and CD103⁺ CD4 T cells following *N. brasiliensis* infection.

Having identified that *Rora* expressing CD4 T cells were clustered with activated CD4 T cell markers (CD44 and CD69) by an unsupervised tSNE clustering analysis (**Figure 4.14**) and also associated with T_{EM} CD4 T cell phenotype in the lungs (**Figure 4.15**). I sought to further characterise *Rora* expressing CD4 T cells. It has been reported in a different *Rora* reporter mouse strain, that *Rora* expressing cells possessed an activated phenotype, based on expression of CD44, ICOS and CD38, and downregulation of CD62L (Haim-Vilmovsky et al., 2020). Therefore, using the marker CD69 as a marker for cell activation, I assessed the frequency of *Rora* activated (CD69⁺) CD4 T cells. Furthermore, *Rora* is also reportedly expressed in memory cells T cells (Miragaia et al., 2019). Therefore, using CD103, which is as a marker for CD4 memory T cells and residency at the epithelial surfaces of mucosal barriers, such as the lung (Ogongo et al., 2019), I assessed the frequency of *Rora* expressing memory (CD103⁺) lung CD4 T cells in the lung. Using both CD69 and CD103, I assessed the frequency of *Rora* expressing activated and tissue resident lung CD4 T cells following *N. brasiliensis* infection.

Flow cytometry analysis revealed that following primary *N. brasiliensis* infection, there is an increase in *Rora* expressing CD69⁺ and CD103⁺ CD4 T cells (**Figure 4.16**). Whilst following a secondary *N. brasiliensis* infection, there is a further increase in *Rora* expressing CD69⁺ and CD103⁺ CD4 T cells (**Figure 4.16**). Therefore, *RORα* may have a greater role in CD4 T cells during secondary infection. These findings support Haim-Vilmovsky et al. (2020) which reported *Rora* is associated with activated T cells and Miragaia et al. (2019) which reported that *Rora* was associated with memory T cells. Therefore, these findings indicate that *Rora* may have a role in both activation, memory and residency of lung CD4 T cells following *N. brasiliensis* infection.

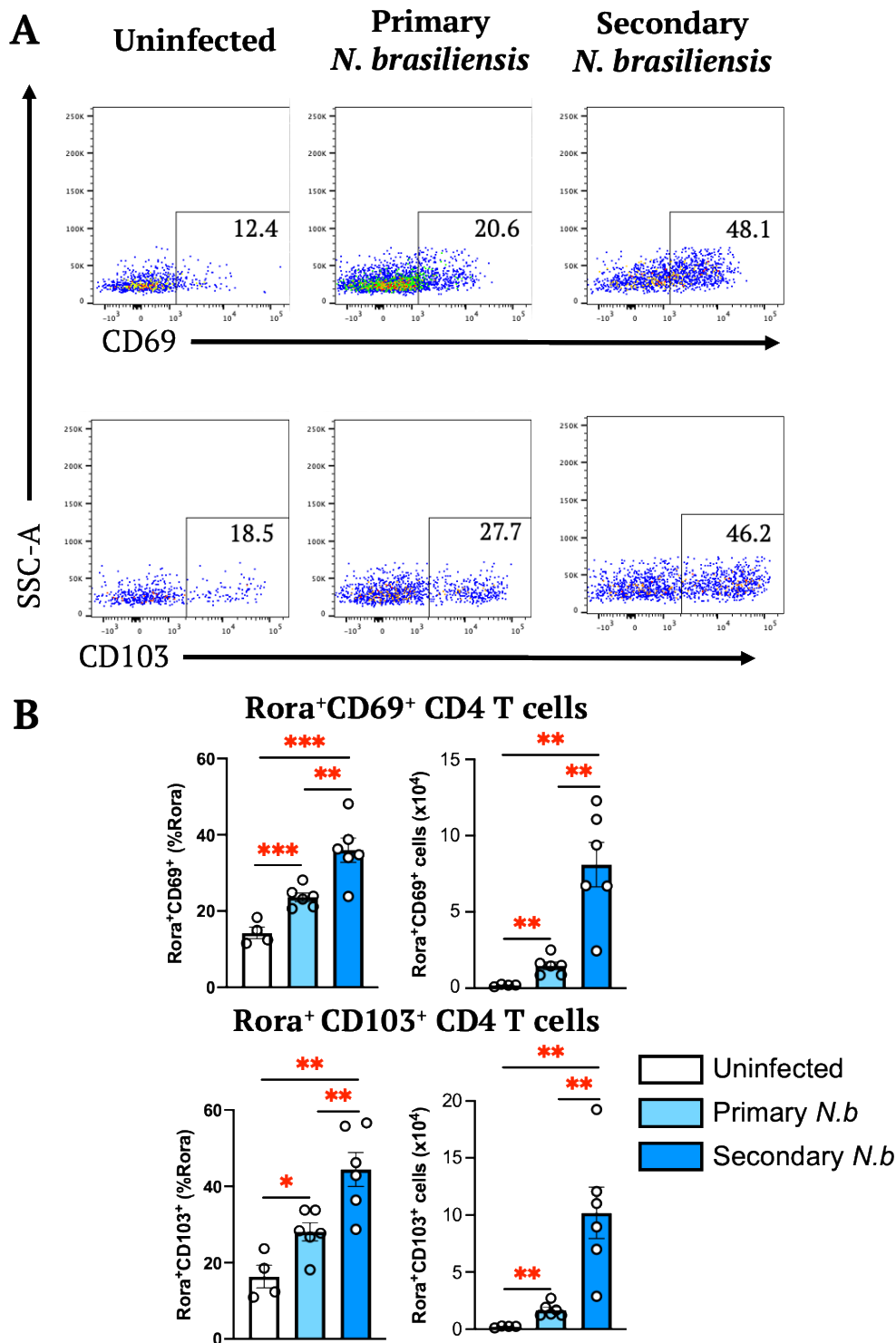


Figure 4.16: Increase in *Rora* expressing CD69⁺ and CD103⁺ CD4 T cells following *N. brasiliensis* infection. *Rora* reporter mice were uninfected or infected with primary or secondary *N. brasiliensis* infection. Lungs were for flow cytometry analysis. **A**, Cell populations were gated as lymphocytes, single cells, live, CD45⁺, CD4⁺, *Rora*-YFP⁺ and either CD69⁺ or CD103⁺. **B**, Quantification of lung *Rora*-YFP expressing CD69⁺ and CD103⁺ CD4 T cells. Data representative of means \pm SEM. Differences indicated as two-

tailed p values, as assessed by unpaired Student t test. * p <0.05, ** p <0.01, *** p <0.005. n = 4-6.

4.3.16 Increase in frequency of *Rora* expressing CD4 T cells in the lung compared to MLN following *N. brasiliensis* infection

Non-lymphoid tissues (NLTs) harbour a pool of adaptive immune cells that differ from their respective draining lymph nodes (Miragaia et al., 2019). Th2 cells differentiate in the lymph nodes following helminth infection, and their residency to tissue results in development of different functional phenotypes (Harris et al., 2002). It has been reported that *Rora* expression increased in T cells following NLT tissue adaptation (Miragaia et al., 2019). Haim-Vilmovsky et al. (2020) also reported differential *Rora* expression in CD4 T cells isolated from lungs, medLN, spleen, and small intestine lamina propria (siLP), with highest frequency in the siLP. Therefore, given *N. brasiliensis* infection elicits a type 2 immune response in the lungs (NLT) and the small intestine, I investigated the frequency of *Rora* expressing CD4 T cells in NLT (lungs) and LT (MLN) following *N. brasiliensis* infection explore any tissue specific differences in frequency of *Rora* expressing CD4 T cells.

Following a primary and secondary *N. brasiliensis* infection there is significantly (p <0.001 and p <0.0001, respectively) increased frequency of *Rora* expressing CD4 T cells in the lungs compared to MLN (**Figure 4.17**). There was no significant difference in frequency of *Rora* expressing CD4 T cells between lungs and MLN in uninfected mice. Following secondary *N. brasiliensis* infection, there was a further increase in *Rora* expressing CD4 T cells in the lungs compared to lungs after primary infection. Whilst there was no difference in frequency of *Rora* expressing CD4 T cells in MLN between uninfected, primary and secondary infection. These results indicate that ROR α may have a tissue specific role in CD4 T cells in the lungs. The enrichment of *Rora* expressing CD4 T cells in peripheral tissues (lungs) may reflect its association with CD4 T cell activation, effector functor (T_{EM}), residency (CD103), or it may also indicate a role in CD4 T cell migration to peripheral tissues. Further studies should explore the frequency of *Rora* expressing CD4 T cells in the lung and medLN.

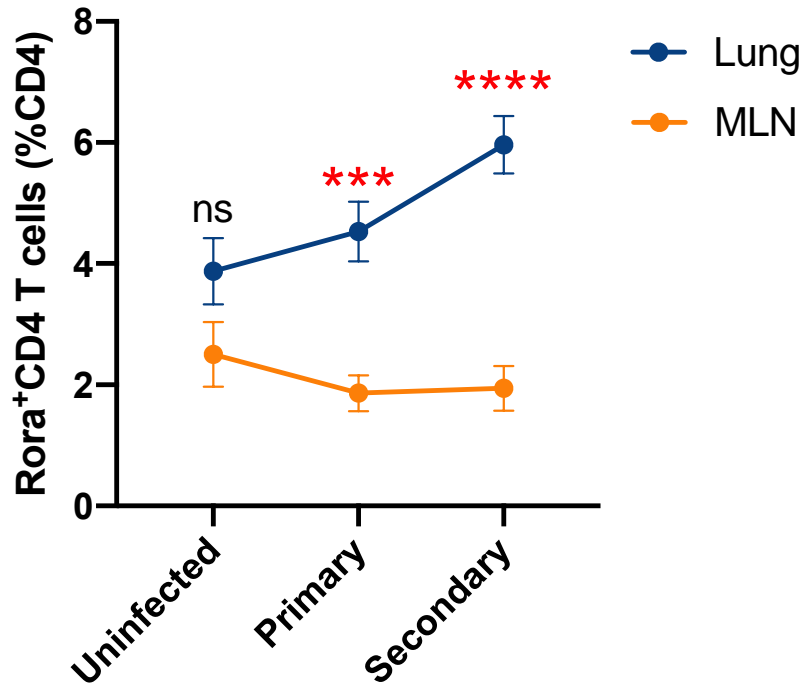


Figure 4.17: Increase in *Rora* expressing CD4 T cells in lung compared to MLN following *N. brasiliensis* infection. *Rora* reporter mice were either uninfected or infected with primary or secondary *N. brasiliensis* infection. Lungs and MLN were harvested and assessed by flow cytometry. Cells were gated as lymphocytes, single cells, live, CD4⁺ and *Rora*-YFP⁺. Differences indicated as two-tailed *p* values, as assessed by unpaired Student *t* test. ****p*<0.001, *****p*<0.0001. ns = non-significant. n = 4-6.

4.4 Discussion

In this chapter, I generated a *Rora* reporter mouse to explore *Rora* expressing cells by flow cytometry. We have recently used the *Rora* reporter mouse to show a role for ROR α expressing macrophages in adipose tissue (Hams et al., 2020). In this chapter, I utilised the *Rora* reporter mouse to explore the role of ROR α expressing cells during a type 2 immune response. Using tSNE analysis, an unsupervised clustering algorithm, it revealed a population of *Rora*-YFP expressing lung CD4 T cells. Indeed, CD4 T cells are known to express *Rora* (Yang et al., 2008, Van Dyken et al., 2016, Malhotra et al., 2018, Haim-Vilmovsky et al., 2020). Interestingly, the tSNE analysis also revealed a population of *Rora*-YFP expressing lung CD127 (IL7R α), SiglecF and CD19 cells. However, having previously reported that *Rora*^{sg/sg} mice and *Rora*^{sg/sg} BM chimera mice have a defect in CD4 T cells and GATA3⁺CD4 T cells, I utilised the *Rora* reporter mice to assess the role of *Rora* in CD4 T cells during a *N. brasiliensis* infection.

Interestingly, findings presented in this chapter revealed that, following *N. brasiliensis* infection there is an increase in the frequency of *Rora* expressing CD4 and GATA3⁺CD4 T (Th2) cells in the lung, and that *N. brasiliensis* infection increased expression of *Rora* mRNA in CD4 T cells. Indeed, there are other reports of mice challenged with papain and OVA having an increase in *Rora* expression in lung Th2 cells (Liu et al., 2015). Whilst RNA-sequencing data has also revealed that CD4 T cells isolated from the spleens of *N. brasiliensis* WT mice had increased *Rora* expression following infection (Haim-Vilmovsky et al., 2020). These data indicate that ROR α may have a role in GATA3⁺CD4 T cell (Th2) development. It has been reported that, following *N. brasiliensis* infection, there is an overlap of gene expression between *Rora*, *Gata3* and *Foxp3* in CD4 T cells (Haim-Vilmovsky et al., 2020). Indeed, following *N. brasiliensis* infection, there was an increase in the number of *Rora* expressing Foxp3⁺CD4 T cells, therefore, indicating the presence of a *Rora*-expressing population of Tregs in the lung. *Rora* has previously been reported to have a role in Treg function during skin inflammation, however, in that publication it was reported that *Rora* had no role in skin Treg development (Malhotra et al., 2018). Therefore, further studies are required to determine the precise role of ROR α in Treg cells both in the lung, and at distal sites. Furthermore, there is also a subset of Tregs that express GATA3 and is associated with enhanced function and tissue residency (Wohlfert et al., 2011, Halim et al., 2018). Results presented in this chapter show there was no significant difference in the frequency of *Rora* expressing GATA3⁺Foxp3⁺ CD4 T cells following *N. brasiliensis* infection, therefore, indicating ROR α had no role in GATA3⁺ Tregs during this model of immunity.

Interestingly, tSNE clustering analysis of the CD4 T cells revealed a population of *Rora* expressing activated CD4 T cells, based on expression of activation markers (CD44 and CD69), whilst there was no overlap of *Rora* expressing CD4 T cells with CD62L, a naïve CD4 T cell marker. This supports a recent publication that also reports *Rora* is expressed by activated CD4 T cells (Haim-Vilmovsky et al., 2020). Although it should be noted that Haim-Vilmovsky et al. (2020) used a *Rora* reporter mouse which was generated in Walker et al. (2019). In these publications, the *Rora* reporter mouse had T2A self-cleaving peptide and teal fluorescent protein inserted upstream of the *Rora* stop codon. Whereas in this thesis, I generated a *Rora* reporter mouse using Cre-Lox recombination technology by breeding a *Rora*Cre mice with *Rosa*^{YFP} mice, as previously described in

Malhotra et al. (2018). However, it is interesting to note that similar conclusions are reached. To expand on these observations, I further characterised *Rora* expressing CD4 T cells in the lung. Interestingly, the lungs were enriched with *Rora* expressing T_{EM} CD4 T cells (CD62L⁻CD44⁺), compared to T_N (CD62L⁻CD44⁺) and T_{CM} (CD62L⁺CD44⁺) CD4 T cells in uninfected mice, whilst following *N. brasiliensis* infection, there was an increase in *Rora* expressing T_{EM} CD4 T cells. In support, Miragaia et al. (2019) also reported *Rora* was expressed in NLT CD4 T memory cells. Therefore, suggesting that ROR α may have a role in T_{EM} CD4 T cell development. Furthermore, findings in this chapter also report that following *N. brasiliensis* infection there is an increase in frequency of *Rora* expressing activated (CD69⁺) and resident (CD103⁺) CD4 T cells. Therefore, indicating that in addition to the roles in GATA3⁺CD4 T cell development, *Rora* may have a role in activation, memory and resident CD4 T cells.

Lung-resident CD4 T cells are critical in mediating immunity against secondary *N. brasiliensis* infection (Harvie et al., 2010, Thawer et al., 2014). In **Chapter 3**, the absence of a functional ROR α , resulted in an increased worm count following primary and secondary *N. brasiliensis* infection, and a reduced frequency of lung CD4 T and GATA3⁺ CD4 T cells. In this chapter, I identified a population of *Rora* expressing lung GATA3⁺CD4 T cells, and *Rora* expressing activated, memory, resident CD4 T cells. Therefore, the significance of these findings may indicate a population of *Rora* expressing CD4 T cells, that are critical for immunity against *N. brasiliensis* infection.

There is an increasing understanding that T cells display tissue specific heterogeneity. There is also differential expression of *Rora* expression in CD4 T cells across tissues with highest expression in NLT tissues (Miragaia et al., 2019, Haim-Vilmsky et al., 2020). The findings presented in this chapter show that there is an increase in frequency of *Rora* expressing CD4 T cells in the lungs (NLT) compared to the MLN (LT). Whilst following *N. brasiliensis* infection, there is a further increase in *Rora* expressing CD4 T cells in the lungs, there was no significant difference in the frequency of *Rora* expressing CD4 T cells in the MLN. This indicates tissue specific heterogeneity of *Rora* expressing CD4 T cells. However, it remains unclear if the enrichment of *Rora* expressing CD4 T cells in the lungs (NLT) reflects its association with CD4 T cell activation and effector function (T_{EM}), and/or it may have a role in CD4 T cell migration to NLT. Therefore, further

studies are required to following migration of *Rora* expressing CD4 T cells during inflammation.

Figure 4.12 shows there is an increase in frequency and total lung *Rora* expressing CD4 T cells following *N. brasiliensis* infection, indicating that *Rora* has a role in CD4 T cell development. On further characterisation of these *Rora* expressing CD4 T cells (**Figure 4.13**), flow cytometry panel included CD4 T cell markers (GATA3 and Foxp3), and thus allowed for the identification *Rora* expressing GATA3⁺, Foxp3⁺ and GATA3⁺Foxp3⁺ CD4 T cells. The results show that there is an increased total *Rora* expressing GATA3⁺ expressing cells, whilst there is no significant difference between uninfected and following secondary infection in frequency of *Rora* expressing GATA3⁺CD4 T cells. It is important to note that percentage frequency is affected by the frequency of other immune cells (Frequency of Foxp3⁺, GATA3⁺Foxp3⁺ and GATA3⁻Foxp3⁻ CD4 T cells) and less affected in changes of total cells between conditions (Uninfected, primary and secondary *N. brasiliensis*). However, following a secondary *N. brasiliensis* infection, there are significantly more total lung cells, and CD4 T cells, compared to uninfected mice, and results can mask any biological differences if only considering the percentage frequency of cells, rather than total number of cells. Therefore, this is a reason why it is important to present both the frequency and total cell counts in an attempt to get a full understanding of the biology

In summary, using a *Rora* reporter mouse I have identified distinct populations of *Rora* expressing cells. Notably, there is a population of *Rora* expressing CD4 T cells in the lungs. Following *N. brasiliensis* infection there is an increase in frequency of lung *Rora* expressing CD4 T cells and GATA3⁺CD4 T cells, which are associated with an activated and T_{EM} CD4 T cell phenotype. Therefore, these results suggest that *Rora* has a role in the development and activation of lung CD4 T cells following *N. brasiliensis* infection. It is unclear if *Rora* expressing CD4 T cells migrate towards the lung or if *N. brasiliensis* infection induces expansion of tissue resident *Rora* expressing CD4 T cells. However, results show that in MLN there was no increase in *Rora* expressing CD4 T cells, whilst in the lungs there is an increase in frequency of *Rora* expressing CD103⁺ and T_{EM} CD4 T cells following *N. brasiliensis* infection. This may indicate that there is a population of tissue resident *Rora* expressing CD4 T cells which expands following *N. brasiliensis*

infection. Further research is required to establish the migration of *Rora* expressing CD4 T cells during a type 2 immune response.

In **Chapter 3** I identified that *Rora*^{sg/sg} mice and *Rora*^{sg/sg} BM chimera mice have a reduced frequency of lung CD4 T cells and GATA3⁺CD4 T cells following *N. brasiliensis* infection, indicating a role for ROR α in GATA3⁺CD4 T cell development. In this chapter, I identify a population of *Rora* expressing lung CD4 T cells and GATA3⁺CD4 T cells, and following *N. brasiliensis* infection the frequency of lung *Rora* expressing lung CD4 T cells and GATA3⁺CD4 T cells increases, further indicating a role for *Rora* in GATA3⁺CD4 T cell development during inflammation. I also report that *Rora* was associated with activated (CD69⁺), T_{EM} (CD44⁺CD62L⁻) and resident (CD103⁺) CD4 T cells, and the frequency of these *Rora* expressing cells increased following *N. brasiliensis* infection. This indicates that ROR α may also have a role in activation of CD4 T cells, and development of T_{EM} and resident CD4 T cells.

Chapter 5

**Determining the role of *Rora* in CD4 and
Il7ra expressing cells using *Rora*
conditional deleter mice**

Chapter 5

5.1 Introduction

In **Chapter 3**, *Rora*^{sg/sg} mice, which have a ubiquitous absence of functional ROR α , were shown to have an altered type 2 immune response to *N. brasiliensis* infection. In addition to the known absence of ILC2s, I observed that *Rora*^{sg/sg} mice had a reduced frequency of lung CD4 T cells, GATA3⁺CD4 T cells and eosinophils following *N. brasiliensis* infection compared to WT mice. To expand on these observations, *Rora*^{sg/sg} BM chimera mice were generated to circumvent the *Rora*^{sg/sg} mice phenotype and allow investigation of the role of *Rora* in cells of hematopoietic versus non-hematopoietic origin. In support of the findings in *Rora*^{sg/sg} mice, *Rora*^{sg/sg} BM chimera mice had a similar response to *N. brasiliensis* infection, characterised by delayed worm expulsion, reduced frequency of lung ILC2s, CD4 T cells, GATA3⁺CD4 T cells and eosinophils, indicative of an altered type 2 immune response. Although these are useful mouse models for exploring the role of ROR α , *Rora*^{sg/sg} mice have a ubiquitous absence of ROR α , whilst in *Rora*^{sg/sg} BM chimera mice, ROR α is absent in all cells of a haematopoietic origin. This can provide challenges in deciphering the exact role of *Rora* in specific immune cells. To further investigate the cellular expression of *Rora*, in **Chapter 4**, I generated a *Rora* reporter mouse which allows for the investigation of *Rora* expressing cells by flow cytometry. Using the *Rora* reporter mouse, I identified several populations of immune cells that express *Rora* in the lungs, including ILC2s, CD4 T cells and GATA3⁺CD4 T cells. Interestingly, following *N. brasiliensis* infection there was an increase in *Rora* expressing CD4 T cells and GATA3⁺CD4 T cells in the lung. The expression of *Rora* in CD4 T cells was associated with activated (CD69), resident (CD103) and T_{EM} phenotypes in the lung. Therefore, indicating that in addition to a role for *Rora* in development of GATA3⁺CD4 T cells, *Rora* may also have a role in activation and the generation or function of resident memory CD4 T cells.

The Cre-LoxP system is a method that enables researchers to generate site-specific deletions, insertions, translocations, and inversions in the DNA of cells (Sauer, 1998). This technology utilises the Cre recombinase protein and a DNA sequence called LoxP

sites from the bacteriophage P1. The LoxP sites work in pairs and are positioned to flank a target region of DNA. Cells that have LoxP sites in their genome and in the presence of Cre recombinase, result in a recombination event occurring between the two LoxP sites. The Cre recombinase binds to the first and last 13 bp regions on the LoxP sites forming a dimer. These dimers bind to a dimer on another LoxP site to form a tetramer. The DNA is then cut at both LoxP sites by the Cre recombinase and the DNA strands are re-joined by DNA ligase, resulting in excision of site-specific DNA sequence flanked by LoxP sites (**Chapter 2, Section 2.2**).

In this chapter I utilised the Cre-LoxP system to generate conditional deleter mice, with *Rora* deleted from specific cells. To delete *Rora* from specific cells using the Cre-LoxP system, *Rora^{fl/fl}* mice were generated by Lexicon Pharmaceuticals (NY, USA) (**Chapter 2, Section 2.1.4**). The *Rora^{fl/fl}* mice contain two LoxP sites flanking a genomic sequence in the *Rora* gene. In the presence of Cre recombinase, the LoxP sites excise the floxed *Rora* sequence, resulting in a dysfunctional Rora protein. In this chapter, two strains of mice expressing Cre recombinase were used (*CD4Cre* and *Il7raCre*). Therefore, Cre recombinase is expressed under the control of CD4 (Sawada et al., 1994) (**Chapter 2, Section 2.1.5**) and *Il7ra* (Schlenner et al., 2010) (**Chapter 2, Section 2.1.6**) gene expression. Using the Cre-Lox recombination technology, I generated *Rora^{fl/fl}CD4Cre* (Halim et al., 2018) (**Chapter 2, Section 2.4.1**) and *Rora^{fl/fl}Il7raCre* (Oliphant et al., 2014, Hams et al., 2020) (**Chapter 2, Section 2.4.2**) mice, where *Rora* is excised from CD4 and *IL7ra* expressing cells, respectively. The *Rora^{fl/fl}Il7raCre* mice strain has been extensively used as an ILC2-deficient mouse strain and will be used as a comparator to *Rora^{fl/fl}CD4Cre* mice. These conditional *Rora* knock-out mice will provide an insight to the role of ROR α in specific immune cells in a type 2 immune response.

5.2 Objectives

1. To investigate the role of the transcription factor ROR α in *N. brasiliensis* infection using conditional deleter mice, *Rora^{fl/fl}CD4Cre* and *Rora^{fl/fl}Il7raCre*
2. To investigate the role of the transcription factor ROR α in *in vitro* CD4 T cell polarisation using naïve CD4 T cells isolated from conditional deleter mice *Rora^{fl/fl}CD4Cre*

5.3 Results

5.3.1 *Rora^{fl/fl}Il7raCre* mice have delayed *N. brasiliensis* expulsion

In **Chapter 3**, it was observed that *Rora^{sg/sg}* mice had a higher worm count and *Rora^{sg/sg}* BM mice a delayed worm clearance in the small intestine, compared to WT mice. To specifically assess the role of *Rora* expression in CD4- and *Il7ra*-expressing cells during a type 2 response, I infected *Rora^{fl/fl}CD4Cre* and *Rora^{fl/fl}Il7raCre* mice with *N. brasiliensis*, using WT animals as a control. I assessed the worm count in the small intestine as a surrogate for the generation of a functional immune response in these mice.

There was no significant difference in worm count at day 3 and day 5 post-infection between WT, *Rora^{fl/fl}Il7raCre* and *Rora^{fl/fl}CD4Cre* mice, suggesting that there is no difference in worm migration to the small intestine (**Figure 5.1**). By day 10 post-infection there was complete worm expulsion in WT and *Rora^{fl/fl}CD4Cre* mice, however, as previously reported Oliphant et al. (2014), *Rora^{fl/fl}Il7raCre* mice had delayed expulsion of *N. brasiliensis* (**Figure 5.1**). This indicates that whilst deletion of *Rora* from *Il7ra*-expressing cells results in a reduced functionality of the type 2 response, this is not apparent in the absence of *Rora*-expressing CD4 cells, implying that these cells are not integral for the functionality of the type 2 response following primary infection.

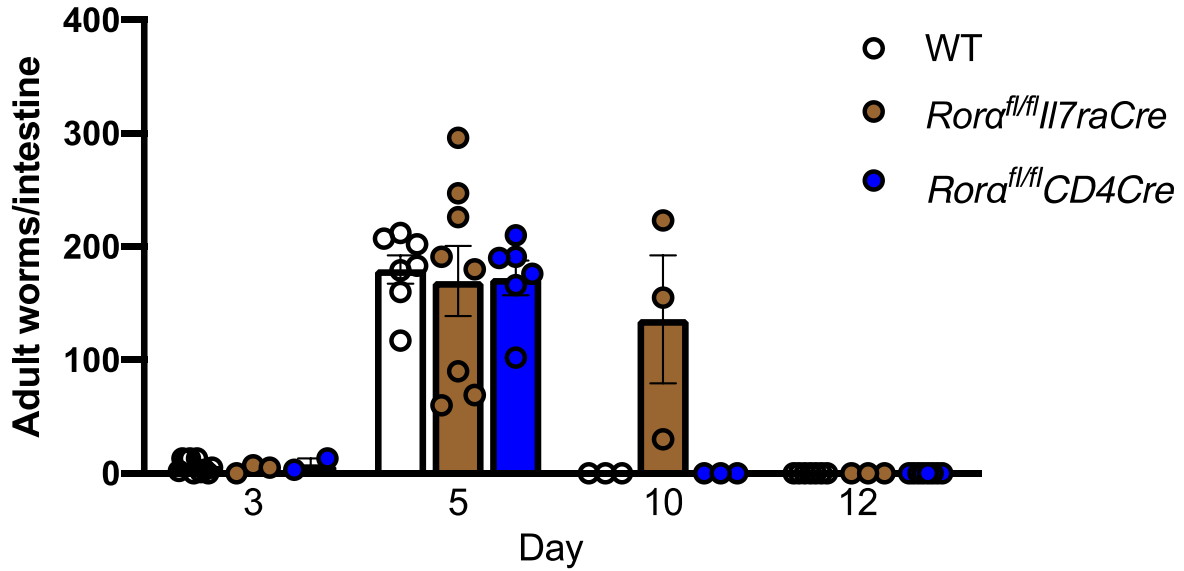


Figure 5.1: *Rora^{fl/fl}Il7raCre* mice have a delayed worm expulsion. WT, *Rora^{fl/fl}Il7raCre* and *Rora^{fl/fl}CD4Cre* mice were infected with 500 L3 *N. brasiliensis* subcutaneously. Small intestines were harvested at days 3, 5, 10 and 12 post-infection. Data is four independent experiments. n = 2-8.

5.3.2 *Rora^{fl/fl}CD4Cre* and *Rora^{fl/fl}Il7raCre* mice had comparable small intestine goblet cells in uninfected and following *N. brasiliensis* infection

Results show that deletion of *Rora* in CD4 T cells had no effect on worm expulsion, whilst deletion of *Rora* from *Il7ra* cells had a delayed worm expulsion (**Figure 5.1**). As worm expulsion is facilitated by small intestine goblet cell mucus secretion, to fully appraise the role of *Rora*-expressing CD4 cells and *Il7ra*-expressing cells, I assessed goblet cell hyperplasia in the small intestine in WT, *Rora^{fl/fl}CD4Cre* and *Rora^{fl/fl}Il7raCre* mice.

Following *N. brasiliensis* infection there is an increase in number of small intestine goblet cells in WT, *Rora^{fl/fl}CD4Cre* and *Rora^{fl/fl}Il7raCre* mice (**Figure 5.2**). Interestingly, there is comparable number of goblet cells between all mice in both uninfected and following *N. brasiliensis* infection (**Figure 5.2**). Therefore, deletion of *Rora* from CD4- and *Il7ra*-expressing cells had no significant impact on goblet cells in uninfected mice or at day 9 post-infection.

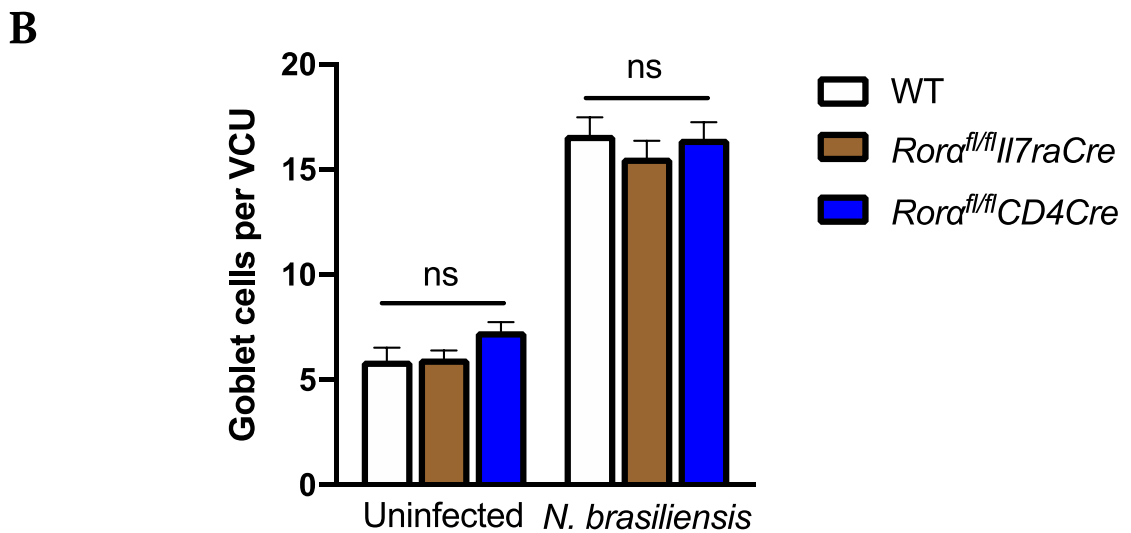
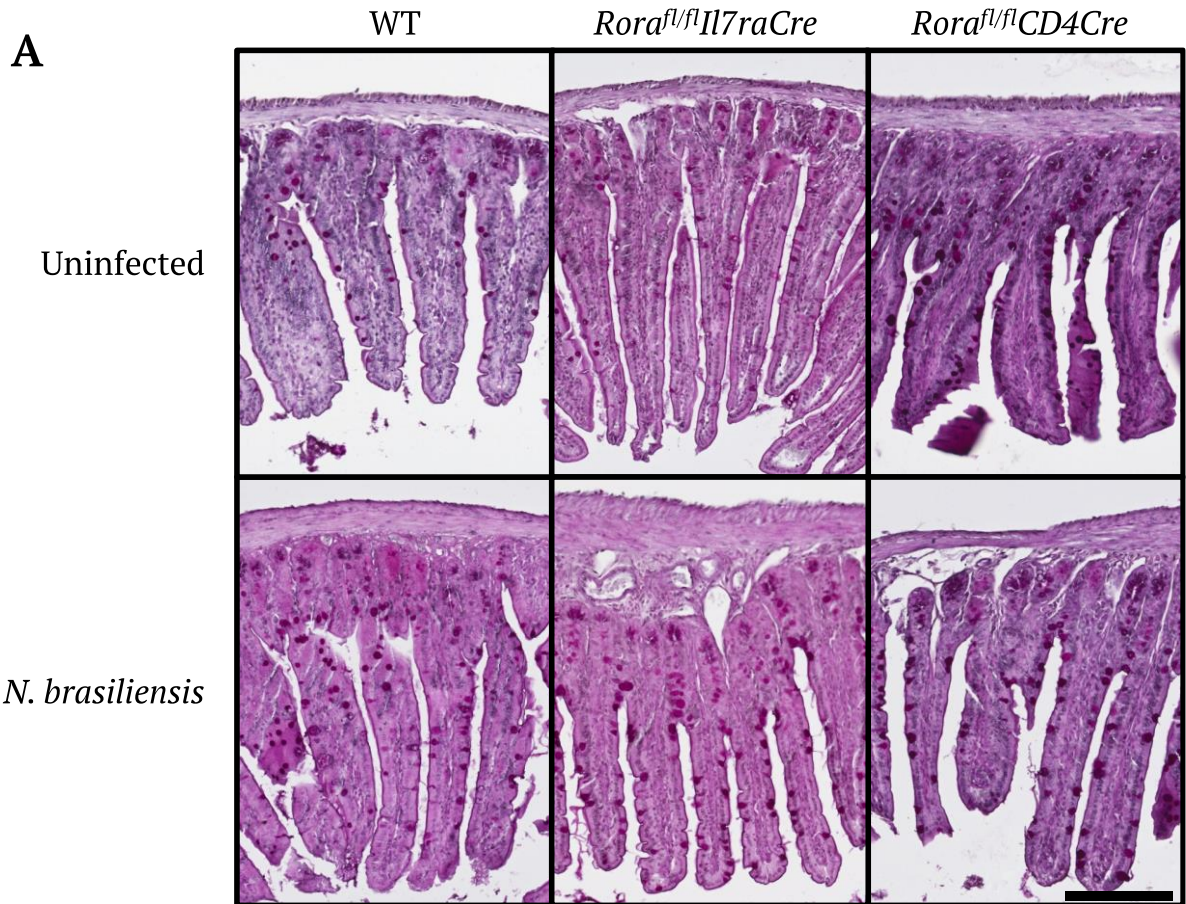


Figure 5.2: *Rora^{fl/fl}CD4Cre* and *Rora^{fl/fl}Il7raCre* mice had comparable number of goblet cells in the small intestine with WT mice. WT, *Rora^{fl/fl}Il7raCre* and *Rora^{fl/fl}CD4Cre* mice were infected with 500 L3 *N. brasiliensis* subcutaneously. Small intestine was isolated in uninfected mice and at day 9 post-infection. Representative histological sections of murine small intestine visualising goblet cell hyperplasia using PAS reagent staining. Magnification x10. Scale bar = 100 μ m. Data is representative of mean \pm SEM. Differences, indicated as two-tailed *p* values, as assessed by unpaired Student *t* test. ns = non-significant. n = 2-7.

5.3.3 *Rora^{fl/fl}Il7raCre* mice have reduced lung ILC2 cells, whilst *Rora^{fl/fl}CD4Cre* mice have comparable frequency of lung ILC2s to WT mice

In **Chapter 3**, I demonstrated that *Rora^{sg/sg}* mice and *Rora^{sg/sg}* BM chimera mice had reduced frequency of lung ILC2s. Using conditional deleter mice targeting *Il7ra*-expressing cells, it has previously been reported that *Rora^{fl/sg}Il7raCre* mice were deficient in ILC2s in the MLN following *N. brasiliensis* infection (Oliphant et al., 2014), and *Rora^{fl/fl}Il7raCre* mice were deficient in lung ILC2s at baseline and following infection with the natural mouse pathogen, Sendai virus (Wu et al., 2020). As *N. brasiliensis* migrates through the lung, there is a profound and prolonged type 2 immune response within the lungs. Therefore, I investigated the role of *Rora* in *Il7ra*- and CD4-expressing cells on frequency of lung ILC2s following *N. brasiliensis* infection.

There is comparable frequency of lung ILC2s between WT and *Rora^{fl/fl}CD4Cre* mice in both uninfected mice and following *N. brasiliensis* infection (**Figure 5.3**). Furthermore, following *N. brasiliensis* infection, WT and *Rora^{fl/fl}CD4Cre* mice have a comparable increase in frequency of lung ILC2s, indicating that deletion of *Rora* from CD4 expressing cells had no impact on the development of lung ILC2s. In contrast, *Rora^{fl/fl}Il7raCre* mice have a reduced frequency of lung ILC2s compared to WT mice, indicating that *Rora* in *Il7ra*-expressing cells is important for the development of lung ILC2s (**Figure 5.3**). These findings expand on previously published data that reported a deficiency of ILC2s in the MLN of *Rora^{fl/sg}Il7raCre* mice following *N. brasiliensis* infection (Oliphant et al., 2014) and in the lungs of *Rora^{fl/fl}Il7raCre* mice following infection with Sendai virus (Wu et al., 2020). These data taken in combination confirm that when *Rora* is not expressed in *Il7ra*-expressing cells, reduced ILC2s are generated either in naïve animals, or in response to stimuli.

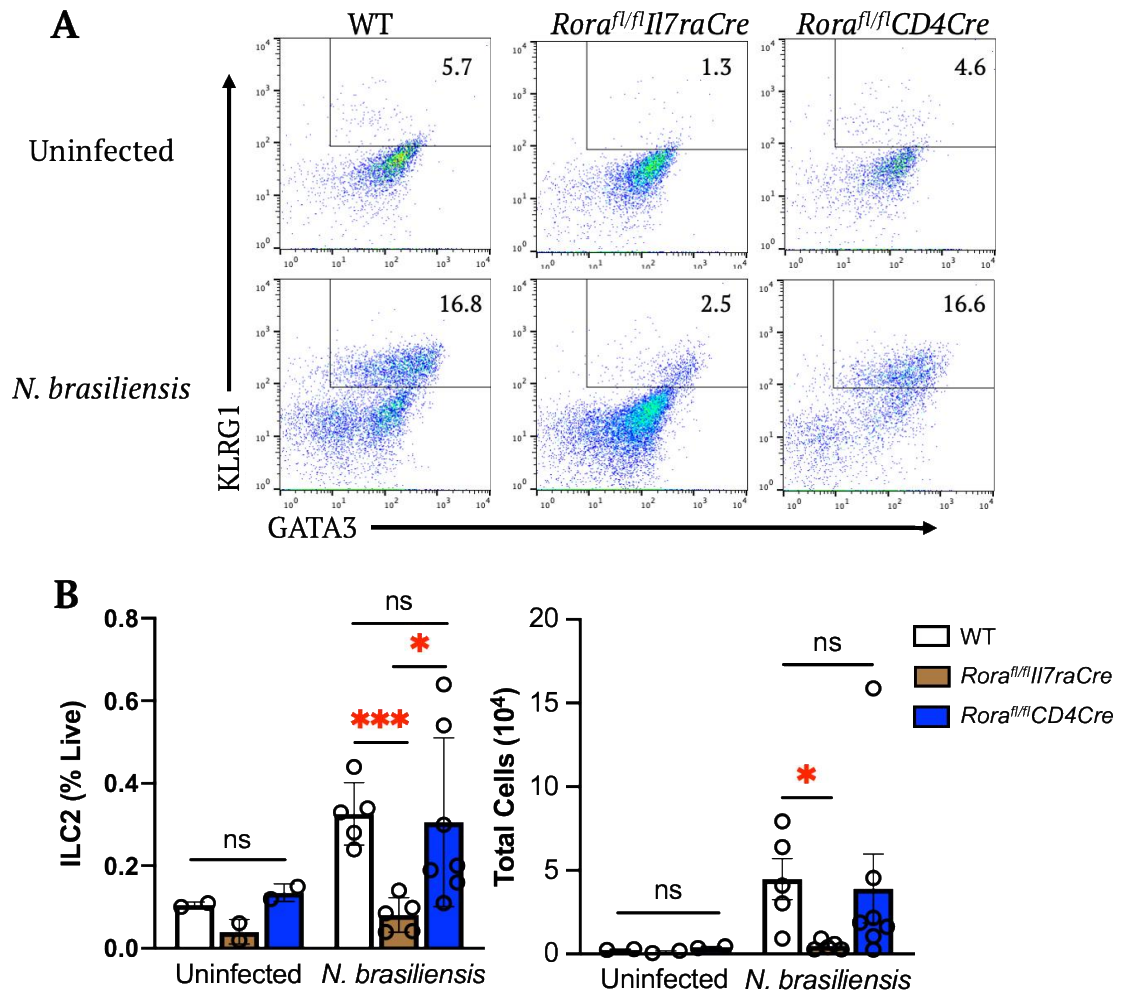


Figure 5.3: *Rora^{fl/fl}Il7raCre* mice have reduced frequency of lung ILC2s, whilst *Rora^{fl/fl}CD4Cre* mice had comparable frequency of lung ILC2s to WT mice. WT, *Rora^{fl/fl}Il7raCre* and *Rora^{fl/fl}CD4Cre* mice were infected with 500 L3 *N. brasiliensis* subcutaneously. Lungs were harvested at day 9 post *N. brasiliensis* infection and assessed by flow cytometry. **A**, ILC2s were gated as lymphocytes, single cells, live cells, CD45⁺, lineage negative (CD3, CD11b, CD11c, CD19, F4/80, FcER1, Gr-1 and γ TCR), KLRG1⁺ and GATA3⁺. The numbers on flow cytometry plots represents percentage of KLRG1⁺GATA3⁺ cells. **B**, Quantification of lung ILC2s. Data is representative of mean \pm SEM. Differences indicated as two-tailed *p* values, as assessed by unpaired Student *t* test. **p*<0.05, ****p*<0.001 ns = non-significant. n = 2-7.

5.3.4 Identification of *Rora* expressing *Il7ra* (CD127) CD4 T cells and ILC2 populations

In support of published literature, I have confirmed that *Rora^{fl/fl}Il7raCre* mice are an ILC2-deficient mouse strain (**Figure 5.3**) (Halim et al., 2018, Wu et al., 2020). However, *Il7ra* (CD127) is broadly expressed throughout the lymphoid system, with both ILC2s and CD4 T cells expressing *Il7ra* (Fry and Mackall, 2005, Schlenner et al., 2010, Spits et

al., 2013, Lev et al., 2019). Therefore, I assessed the expression of *Il7ra* in lung ILC2s and CD4 T cells by flow cytometry.

Flow cytometry analysis revealed that both lung ILC2s and CD4 T cells express *Il7ra* (**Figure 5.4A**). Furthermore, in **Chapter 4**, tSNE clustering analysis revealed a population of *Rora* expressing *Il7ra* (CD127) cells (**Figures 4.6 and 4.11**). Therefore, using the *Rora* reporter mouse, I investigated if there was a population of *Rora* expressing *Il7ra*⁺ILC2s, and *Rora* expressing *Il7ra*⁺CD4 T cells. Interestingly, flow cytometry analysis showed a population of *Rora* expressing *Il7ra*⁺ILC2s and *Rora* expressing *Il7ra*⁺CD4 T cells (**Figure 5.4B**). Whilst following *N. brasiliensis* infection, there was a significant ($p > 0.05$) increase in both *Rora* expressing *Il7ra*⁺ILC2s and *Rora* expressing *Il7ra*⁺CD4 T cells (**Figure 5.4C**), indicating ROR α may have a role in both *Il7ra* expressing ILC2s and CD4 T cells. Therefore, in addition to being ILC2-deficient, these findings indicate that in *Rora*^{fl/fl}*Il7ra*Cre mice, *Rora* may also be deleted from *Il7ra* expressing CD4 T cells and therefore may affect development of CD4 T cells.

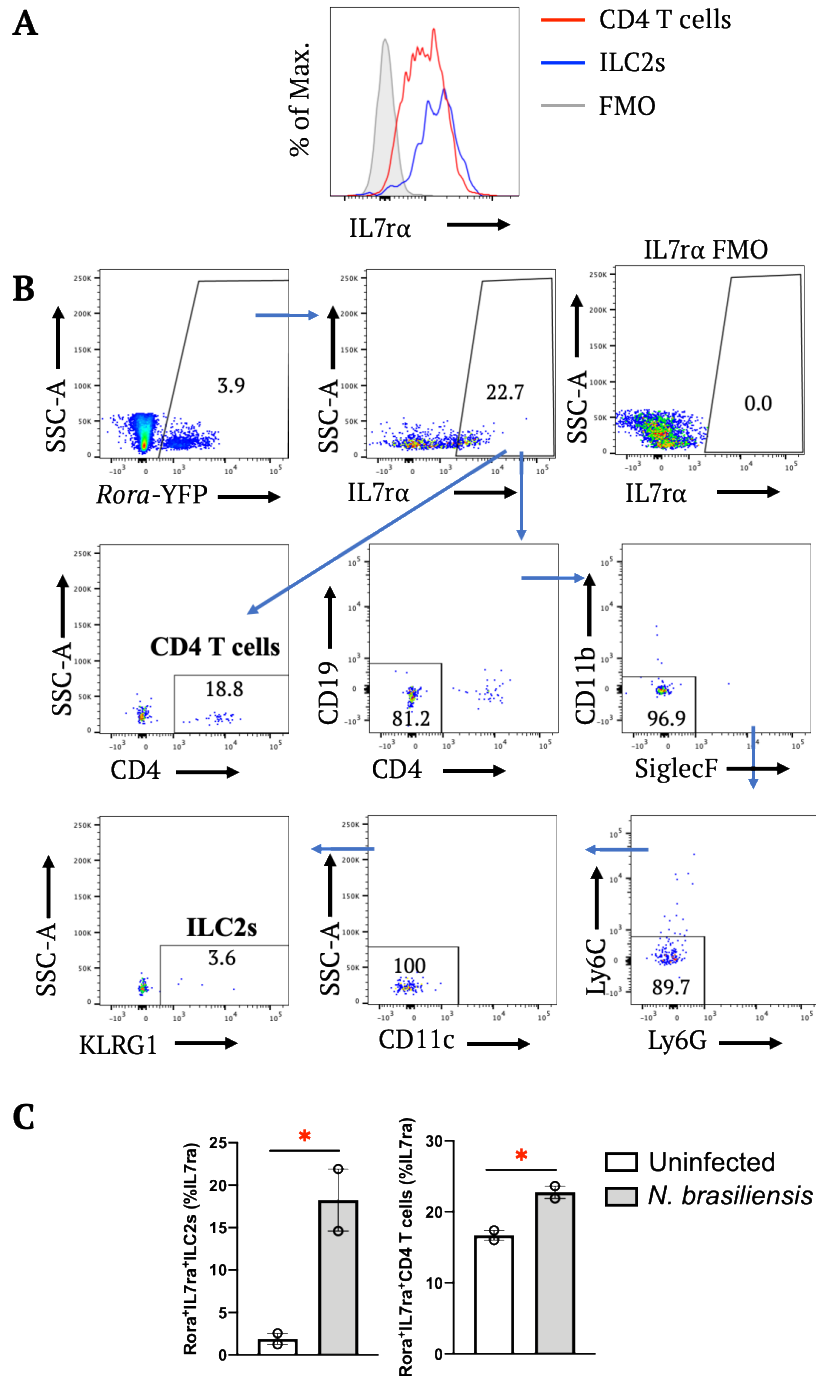


Figure 5.4: ILC2s and CD4 T cells express Il7ra (CD127). **A**, WT mice lungs were assessed by flow cytometry for Il7ra expression. CD4 T cells were identified as lymphocytes, single, live, CD45⁺ and CD4⁺. ILC2s were identified as lymphocytes, single, live, CD45⁺, lineage negative (CD4⁻, CD19⁻, CD11b⁻, SiglecF⁻, Ly6C⁻, Ly6G⁻, CD11c⁻) and KLRG1⁺. Red = CD4 T cells. Blue = ILC2s. Grey = Il7ra FMO. **B**, *Rora* reporter mice lungs were harvested from uninfected mice. Cell populations were pre-gated as lymphocytes, single cells, live, CD45⁺. Identification of *Rora* expressing Il-7ra⁺CD4 T cells and Il-7ra⁺ILC2s. **C**, *Rora* reporter mice were infected with 500 L3 *N. brasiliensis* subcutaneously. Lungs were harvested at day 7 post-infection for flow cytometry analysis. Quantification of lung *Rora* expressing Il-7ra⁺CD4 T cells and Il-7ra⁺ILC2s. Data representative of means \pm SEM. Differences indicated as two-tailed *p* values, as assessed by unpaired Student *t* test. **p*<0.05. n = 2.

5.3.5 *Rora^{fl/fl}CD4Cre* and *Rora^{fl/fl}Il7raCre* mice have a reduced frequency of lung CD4 T cells compared to WT mice following *N. brasiliensis* infection

In **Chapter 3** it was observed that *Rora^{sg/sg}* mice and *Rora^{sg/sg}* BM chimera mice have a reduced frequency of CD4 T cells following *N. brasiliensis* infection. In **Chapter 4**, there was an increase in frequency of *Rora*-expressing CD4 T cells following *N. brasiliensis* infection, indicating ROR α has a role in CD4 T cell development. Therefore, I assessed the frequency of lung CD4 T cells in *Rora^{fl/fl}CD4Cre* mice following *N. brasiliensis* infection. In addition, as I have previously identified that CD4 T cells express *Il7ra* (CD127) and there is a population of *Rora* expressing *Il7ra*⁺CD4 T cells (**Figure 5.4**), indicating that *Rora^{fl/fl}Il7raCre* mice may have *Rora* deleted from *Il7ra*⁺CD4 T cells, I also assessed the frequency of lung CD4 T cells in *Rora^{fl/fl}Il7raCre* mice.

As anticipated, in WT mice there is an increase in lung CD4 T cells following *N. brasiliensis* infection (**Figure 5.5**). Interestingly, however, there is significantly ($p>0.05$) reduced frequency of lung CD4 T cells in both *Rora^{fl/fl}Il7raCre* and *Rora^{fl/fl}CD4Cre* mice compared to WT mice following *N. brasiliensis* infection (**Figure 5.5**). There was no significant difference in the frequency of lung CD4 T cells between uninfected mice, indicating that *Rora* impacts CD4 T cells specifically during inflammation. Indeed, there is evidence that ILC2s communicate with CD4 T cells and influence Th2 cell polarisation and function (Oliphant et al., 2014, Mirchandani et al., 2014, Drake et al., 2014, Gold et al., 2014, Schwartz et al., 2017). Therefore, as having previously identified that *Rora^{fl/fl}Il7raCre* mice are ILC2-deficient (**Figure 5.3**), the reduced frequency of ILC2s could alter the frequency of lung CD4 T cells. However, the precise role of *Rora*-expressing cells in *Rora^{fl/fl}Il7raCre* mice is not fully clear, as I have highlighted there is a population of *Rora* expressing *Il7ra*⁺CD4 T cells (**Figure 5.4**), which implies that deletion of *Rora* from *Il7ra*-expressing cells may also impact CD4 T cell development directly. Interestingly, in *Rora^{fl/fl}CD4Cre* mice the frequency of lung ILC2s is comparable with WT mice (**Figure 5.3**), however these mice have reduced frequency of lung CD4 T cells in following *N. brasiliensis* infection, indicating that *Rora* has a role in CD4 T cell development which is ILC2 independent.

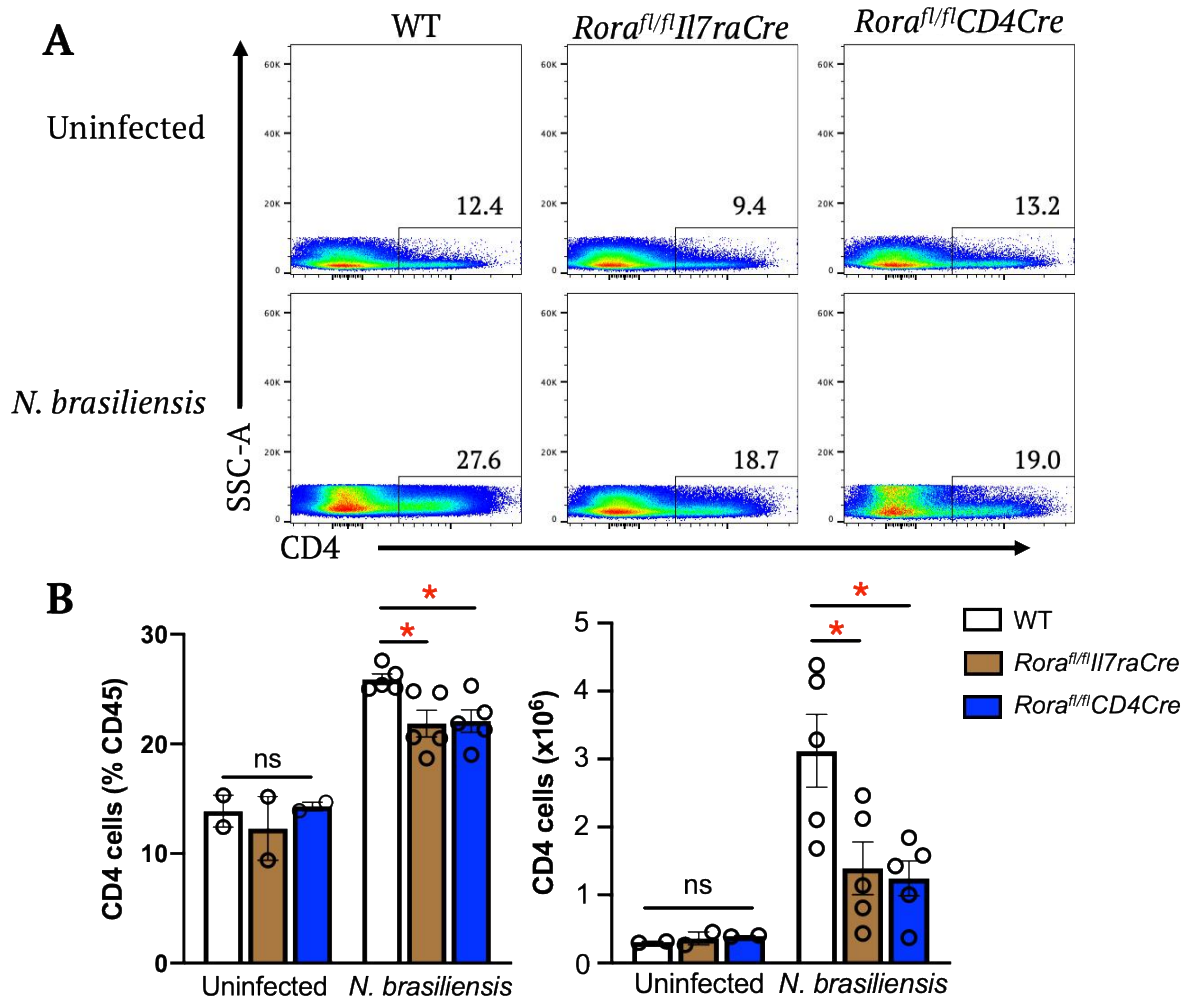


Figure 5.5: *Rora^{fl/fl}CD4Cre* and *Rora^{fl/fl}Il7raCre* mice have reduced frequency of lung CD4 T cells compared to WT mice in response to *N. brasiliensis*. WT, *Rora^{fl/fl}CD4Cre* and *Rora^{fl/fl}Il7raCre* mice were infected with 500 L3 *N. brasiliensis* subcutaneously. Lungs were harvested for flow cytometry at days 9 post-infection. **A**, Representative flow cytometry plots of gating strategy, cells were initially gated on lymphocytes, single cells, live cells, CD45⁺ and CD4⁺. **B**, Quantification of lung CD4 T cells. Data is representative of mean \pm SEM. Numbers on flow cytometry plots reflect percentage of CD4⁺ cells. Differences indicated as *p* values, as assessed by Student *t* Test **p*<0.05. ns = non-significant. n = 2-5.

5.3.6 *Rora^{fl/fl}CD4Cre* and *Rora^{fl/fl}Il7raCre* mice have a reduced frequency of lung GATA3⁺CD4 T cells compared to WT mice following *N. brasiliensis* infection

Having identified that *Rora^{fl/fl}Il7raCre* and *Rora^{fl/fl}CD4Cre* mice have a reduced frequency of lung CD4 T cells following *N. brasiliensis* infection (**Figure 5.5**), I characterized the CD4 T cell subsets in the lungs of *Rora^{fl/fl}Il7raCre* and *Rora^{fl/fl}CD4Cre*

mice. As previously discussed, *N. brasiliensis* infection induces conversion of Th1 and Th17 cells into Th2 cells (Panzer et al., 2012). Therefore, I investigated the role of deletion of *Rora* in *Il7ra* and CD4 T cell expressing cells on the frequency of lung GATA3⁺CD4 T cells following *N. brasiliensis* infection.

In WT mice there is an increase in frequency of lung GATA3⁺CD4 T cells following *N. brasiliensis* infection (**Figure 5.6**). However, both *Rora^{fl/fl}Il7raCre* and *Rora^{fl/fl}CD4Cre* mice have reduced lung GATA3⁺CD4 T cells compared to WT mice following *N. brasiliensis* infection (**Figure 5.6**). There was no significant difference in frequency of lung GATA3⁺CD4 T cells across all groups of uninfected mice (**Figure 5.6**). This data supports previously published literature, which reported *Rora^{fl/fl}Il7raCre* mice have reduced lung GATA3⁺CD4 T cells following *N. brasiliensis*, IL-33 and papain administration (Halim et al., 2018). *Rora^{fl/fl}Il7raCre* mice are ILC2-deficient, however, as I have demonstrated, there is a population of *Rora* expressing *Il7ra*⁺CD4 T cells, therefore, further studies are required to delineate the exact interplay between *Rora*-expressing *Il7ra*⁺ ILC2s and CD4 T cells on development of GATA3⁺CD4 T cells. In contrast, it was reported that *Rora^{fl/fl}CD4Cre* mice had comparable lung GATA3⁺CD4 T cells with control mice following i.n. IL-33 administration (Halim et al., 2018). However, it is important to note that this is a different mouse model, and the frequency of lung GATA3⁺CD4 T cells in *Rora^{fl/fl}CD4Cre* mice following *N. brasiliensis* infection has not previously been reported. The findings presented in this chapter indicate that *Rora^{fl/fl}CD4Cre* mice, which have comparable frequency of ILC2s with WT mice, have a reduced frequency of GATA3⁺CD4 T cells following *N. brasiliensis* infection. Therefore, indicating a role for ROR α in GATA3⁺CD4 T cell development, which is ILC2 independent.

to infection (**Figure 5.5**). To expand on these findings, I investigated the frequency of CD4 T cells in the blood of uninfected *Rora*^{fl/fl}*CD4Cre* mice to explore any systemic effects of *Rora* on CD4 T cell development.

There was no significant difference in the frequency of CD4 T cells in the blood of uninfected WT and *Rora*^{fl/fl}*CD4Cre* mice (**Figure 5.7**). Therefore, taken together with results presented in this chapter (**Figure 5.5**), and in support of results presented in Haim-Vilmovsky et al. (2020), these findings indicate that there is no role for *Rora* in generation of CD4 T cells in uninfected mice. However, the findings presented throughout this thesis, indicate that the absence of a functional ROR α impacts on the development of CD4 T cells following *N. brasiliensis* infection, rather than development of CD4 T cells as baseline. Therefore, it may be interesting to assess the frequency of CD4 T cells in the whole blood of *N. brasiliensis* infected WT and *Rora*^{fl/fl}*CD4Cre* mice in future.

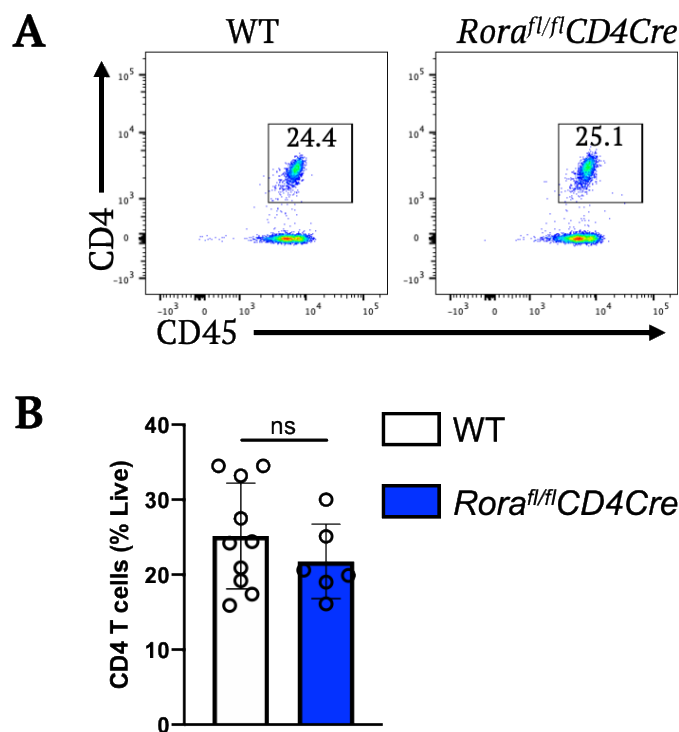


Figure 5.7: *Rora*^{fl/fl}*CD4Cre* mice have comparable frequency of CD4 T cells to WT mice in the whole blood in uninfected mice. Whole blood was isolated from WT and *Rora*^{fl/fl}*CD4Cre* mice. CD4⁺ T cells were determined by flow cytometry. **A**, Representative flow cytometry gating. Cells were gated as lymphocytes, single cells, live, CD45⁺ and CD4⁺. **B**, Quantification of CD4 T cells. Data is representative of mean \pm SEM. The numbers on flow cytometry plots reflect percentage of live cells. Differences assessed by unpaired Student *t* test. ns = non-significant. n = 6-10.

5.3.8 *Rora^{fl/fl}CD4Cre* mice have reduced frequency of lung GATA3⁺CD4 T cells compared to *Rora^{fl/fl}* mice in response to *N. brasiliensis* infection

There is a subset of Treg (Foxp3⁺) cells which express GATA3, which is associated with enhanced function and tissue-residency (Wohlfert et al., 2011, Halim et al., 2018). Following *N. brasiliensis* infection there is an increase in frequency of lung GATA3⁺, GATA3⁺Foxp3⁺ and GATA3⁻Foxp3⁺ in control animals (Halim et al., 2018). Furthermore, it has been reported that ROR α is important for Treg function and restraining allergic inflammation (Malhotra et al., 2018). Therefore, having identified that *Rora^{fl/fl}CD4Cre* mice have reduced lung GATA3⁺CD4 T cells following *N. brasiliensis* infection compared to WT mice (**Figure 5.6**), indicating that *Rora* is important for the development of lung GATA3⁺CD4 T cells, I further characterised the GATA3⁺CD4 T cells. I assessed the effect of deletion of *Rora* in CD4 expressing cells on the frequency of lung CD4 T cells subsets (GATA3⁺, GATA3⁺Foxp3⁺ and GATA3⁻Foxp3⁺) following *N. brasiliensis* infection.

Flow cytometry analysis showed that in uninfected mice there was no significant difference in the frequency of lung CD4 T cell subsets (GATA3⁺, GATA3⁺Foxp3⁺, GATA3⁻Foxp3⁺) between *Rora^{fl/fl}CD4Cre* and control (*Rora^{fl/fl}*) mice (**Figure 5.8**). Following *N. brasiliensis* infection there is an increase in frequency of lung GATA3⁺CD4 T cells in *Rora^{fl/fl}* mice. However, there was significantly ($p > 0.01$) reduced lung GATA3⁺CD4 T cells in *Rora^{fl/fl}CD4Cre* mice compared to control mice (**Figure 5.8**). These findings are consistent with previous results presented in this chapter (**Figure 5.6**), and indicate that deletion of *Rora* in CD4 T cells reduces frequency of GATA3⁺CD4 T cells following *N. brasiliensis* infection, independent of ILC2s. Interestingly, deletion of *Rora* from CD4 T cells had no impact on the frequency of lung Foxp3⁺ and GATA3⁺Foxp3⁺ CD4 T cell subsets in both uninfected mice and following *N. brasiliensis* infection (**Figure 5.8**). Therefore, indicating that *Rora* had no role in the frequency of lung Foxp3⁺ and GATA3⁺Foxp3⁺ cells in uninfected conditions and following *N. brasiliensis* infection. These results further indicate a role for *Rora* in GATA3⁺CD4 T (Th2) cell development following *N. brasiliensis* infection.

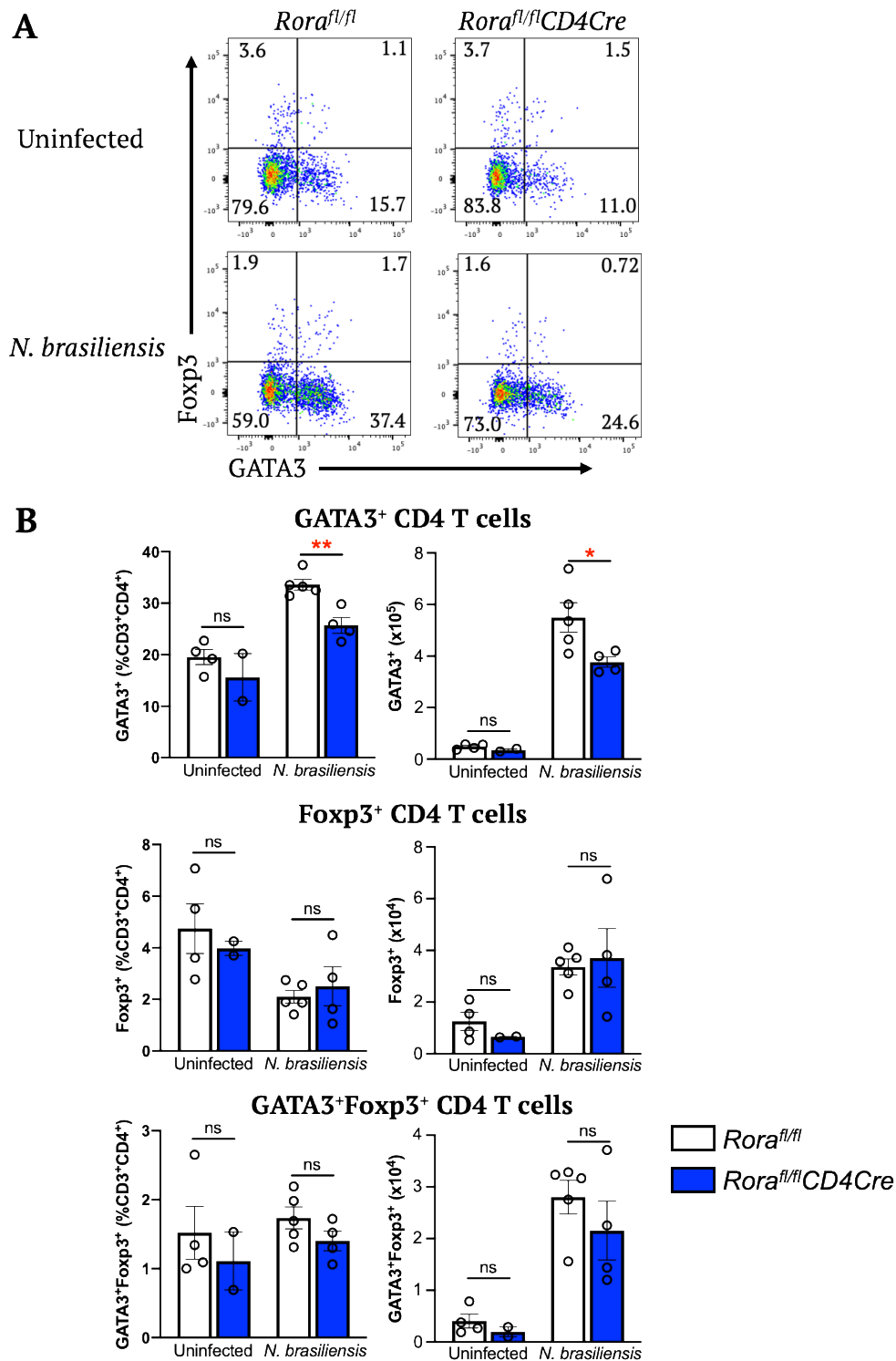


Figure 5.8: *Rora^{fl/fl}CD4Cre* have reduced frequency of lung GATA3⁺CD4 T cells following *N. brasiliensis* infection compared to *Rora^{fl/fl}* mice. *Rora^{fl/fl}* and *Rora^{fl/fl}CD4Cre* mice were infected with 500 L3 *N. brasiliensis* subcutaneously. Lungs were harvested at day 7 and assessed by flow cytometry. **A**, Cells gated as live, single, CD45⁺, CD3⁺, CD4⁺ and either GATA3⁺, GATA3⁺Foxp3⁺ or Foxp3⁺. The numbers on flow cytometry plots reflect percentage of CD3⁺CD4⁺ cells. **B**, Quantification of lung GATA3⁺, GATA3⁺Foxp3⁺ and Foxp3⁺ CD4 T cells. Data is representative of mean ± SEM. Differences indicated as two-tailed *p* values, as assessed by unpaired Student *t* test. **p*<0.05, ***p*<0.01. ns = Non-significant. n = 2-5.

5.3.9 *Rora^{fl/fl}CD4Cre* mice have a reduced frequency of proliferating (Ki67⁺) lung GATA3⁺CD4 T cells following *N. brasiliensis* infection compared to WT mice

Having identified that *Rora^{fl/fl}CD4Cre* mice have reduced frequency of lung GATA3⁺CD4 T cells following *N. brasiliensis* infection (**Figure 5.6** and **5.8**), indicating that ROR α had a role in GATA3⁺CD4 T cell development, I investigated the role of *Rora* in proliferation of GATA3⁺CD4 T cells. The proliferation was assessed by measuring the expression of the proliferation surface marker Ki67 on lung GATA3⁺CD4 T cells by flow cytometry.

Following *N. brasiliensis* infection, there is an increase in proliferating GATA3⁺CD4 T cells in *Rora^{fl/fl}* mice in the lungs (**Figure 5.9**). However, *Rora^{fl/fl}CD4Cre* have significantly ($p>0.05$) reduced proliferating GATA3⁺CD4 T cells in the lung following *N. brasiliensis* infection, compared to *Rora^{fl/fl}* mice (**Figure 5.9**). There was no significant difference in the proliferation of GATA3⁺CD4 T cells in uninfected *Rora^{fl/fl}CD4Cre* and *Rora^{fl/fl}* mice. Therefore, the reduced proliferation of GATA3⁺CD4 T cells occurs following *N. brasiliensis* infection. These findings suggest that ROR α may regulate the proliferation of GATA3⁺CD4 T cells, which may explain the reduced frequency of lung GATA3⁺CD4 T cells (**Figure 5.6** and **5.8**) in *Rora^{fl/fl}CD4Cre* mice.

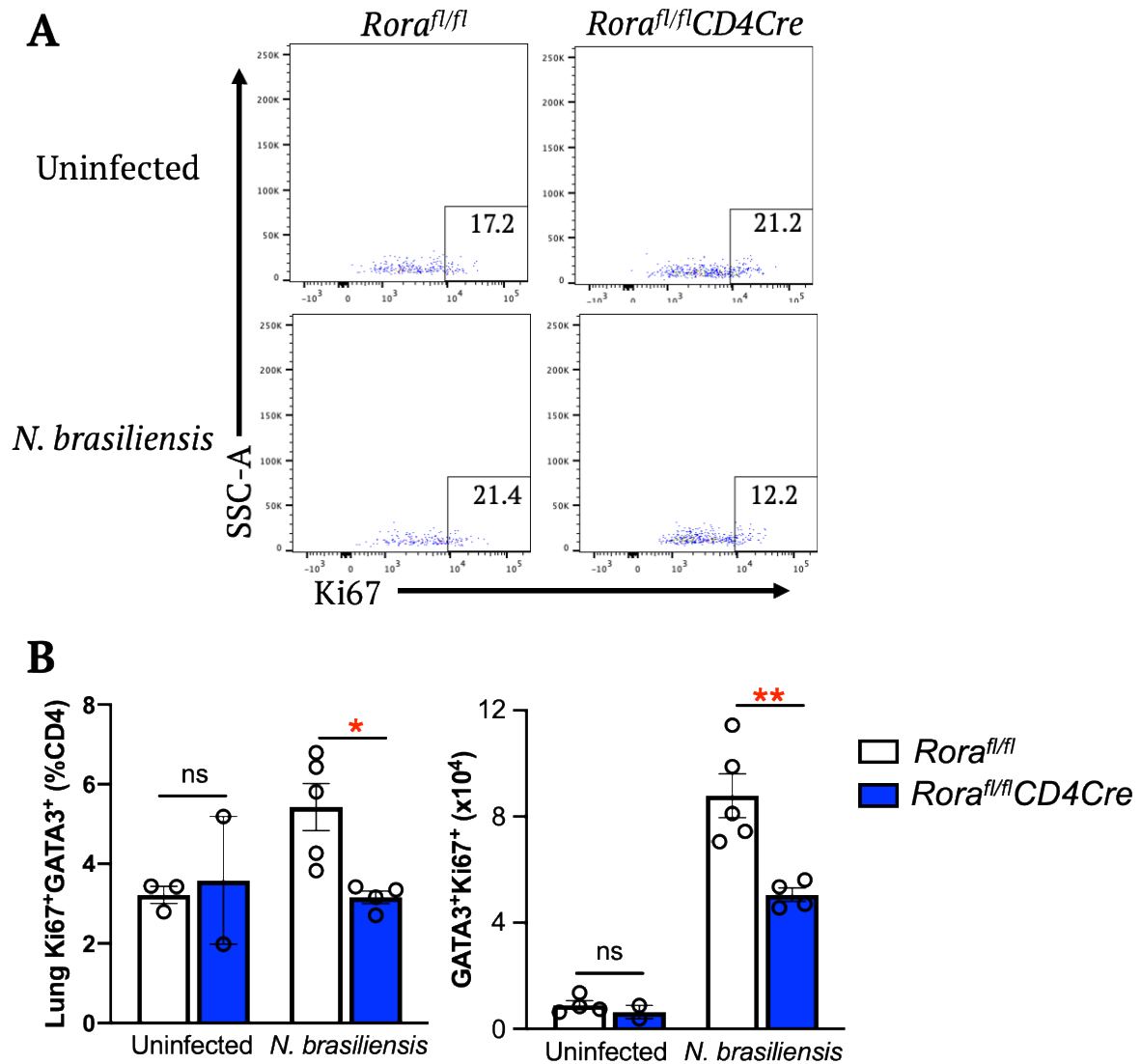


Figure 5.9: *Rora*^{fl/fl}CD4Cre mice have a reduced frequency of lung proliferating (Ki67⁺) GATA3⁺CD4 T cells compared to *Rora*^{fl/fl} mice following *N. brasiliensis* infection. *Rora*^{fl/fl} and *Rora*^{fl/fl}CD4Cre mice were infected with 500 L3 *N. brasiliensis* subcutaneously. Lungs were harvested at day 7 post *N. brasiliensis* infection. **A**, Cells gated as lymphocytes, single, live, CD3⁺, CD4⁺, GATA3⁺ and Ki67⁺. Numbers on flow cytometry plots reflect percentage of CD3⁺CD4⁺ cells. **B**, Quantification of lung Ki67⁺GATA3⁺ CD4 T cells. Data is representative of mean ± SEM. Differences indicated as *p* values, as assessed by Student *t* Test **p*<0.05. ns = non-significant. n = 2-5.

5.3.10 *Rora*^{fl/fl}CD4Cre mice have reduced frequency of MLN GATA3⁺CD4 T cells compared to *Rora*^{fl/fl} mice following *N. brasiliensis* infection

The primary focus of this thesis has been the immune response generated in the lung, a non-lymphoid tissue (NLT), following *N. brasiliensis* infection. At day 7 post *N. brasiliensis* infection, the worms have migrated to the small intestine eliciting another localised type 2 immune response. I therefore investigated the role of *Rora* in CD4 T cells within the intestinal draining lymph nodes, MLN.

There was no significant difference in frequency of GATA3⁺CD4 T cells between *Rora*^{fl/fl}CD4Cre and *Rora*^{fl/fl} mice in uninfected mice (**Figure 5.10**). However, following *N. brasiliensis* infection, *Rora*^{fl/fl}CD4Cre mice had a significantly ($p > 0.005$) reduced frequency of MLN GATA3⁺CD4 T cells compared to *Rora*^{fl/fl} mice (**Figure 5.10**). These findings are in support of the results presented in **Chapter 3** which showed *Rora*^{sg/sg} mice had reduced frequency of GATA3⁺CD4 T cells in MLN following *N. brasiliensis* infection. Therefore, indicating that GATA3⁺CD4 T cells are reduced in both NLT and LT in *Rora*^{fl/fl}CD4Cre mice following *N. brasiliensis* infection. Investigation of the frequency of GATA3⁺CD4 T cells in the mediastinal LN, which is the draining lymph node from the lungs, would be interesting in future, to determine if this disparity is observed in all lymphoid tissue.

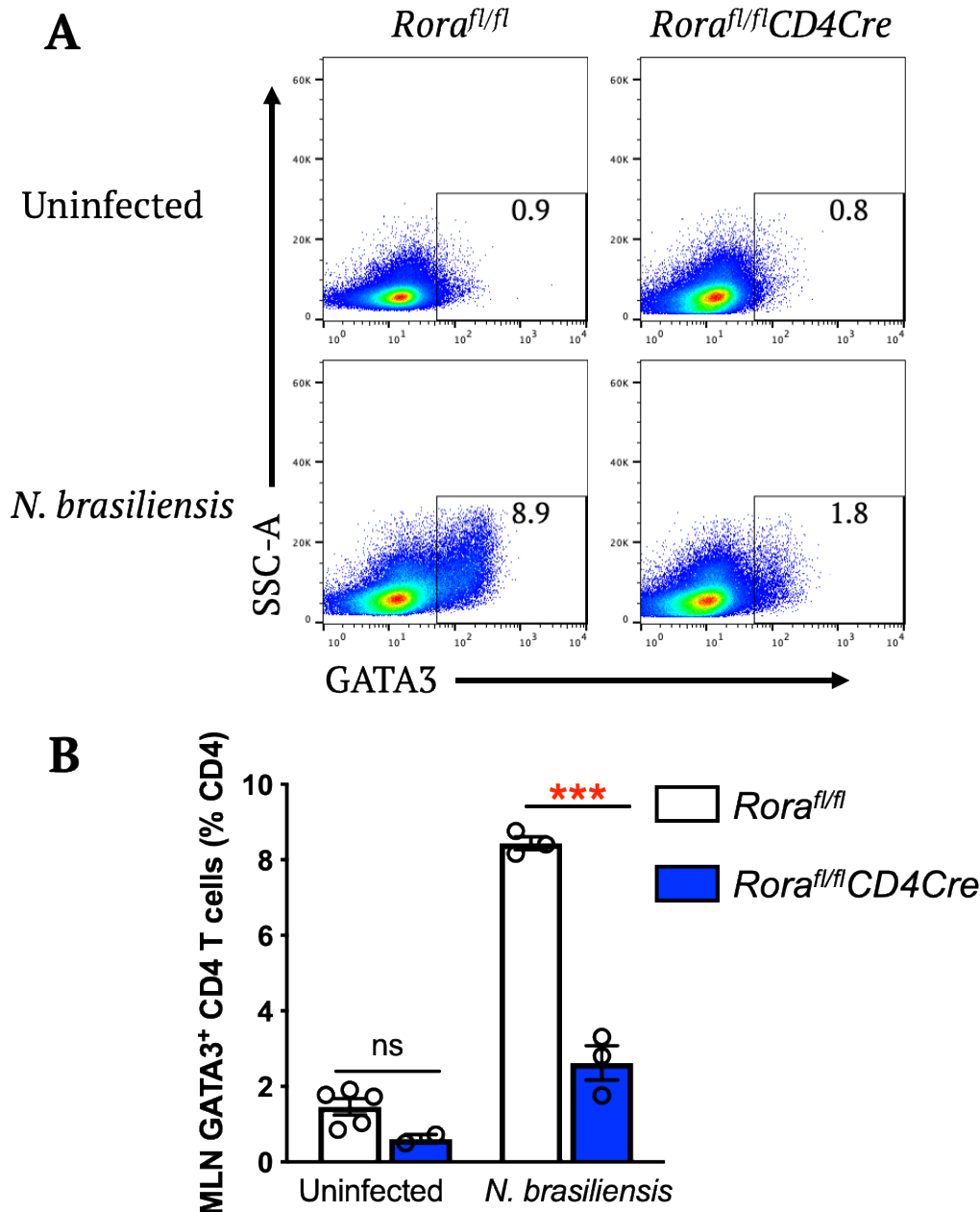


Figure 5.10: *Rora*^{fl/fl}CD4Cre mice have reduced frequency of MLN GATA3⁺CD4 T cells compared to *Rora*^{fl/fl} mice following *N. brasiliensis* infection. Mice were infected with 500 L3 *N. brasiliensis* subcutaneously. MLN were harvested at days 7 post-infection and assessed by flow cytometry. **A**, Cells gated as lymphocytes, single cells, live cells and CD4⁺ and GATA3⁺. **B**, Quantification of MLN GATA3⁺CD4 T cells. Data is representative of mean \pm SEM. Numbers on flow cytometry plots reflect percentage of CD4⁺ cells. Differences indicated as two-tailed *p* values, as assessed by unpaired Student *t* test. ****p*<0.005. ns = Non-significant. n = 2-5.

5.3.11 Naïve CD4 T cells isolated from *Rora*^{fl/fl}CD4Cre have reduced *in vitro* GATA3⁺ CD4 T cell polarisation compared to *Rora*^{fl/fl} naïve CD4 T cells

In this chapter, the role of ROR α in CD4 T cells during a type 2 immune response has been investigated using *N. brasiliensis* infection as an *in vivo* mouse model for type 2 immunity. It was observed that *Rora*^{fl/fl}CD4Cre mice have a reduced frequency of GATA3⁺CD4 T cells compared to control mice following *N. brasiliensis* infection, suggesting that ROR α is important for GATA3⁺CD4 T cell development. Therefore, to further investigate the role of ROR α in T cell development, I assessed the capacity of ROR α to impact on CD4 T cell polarisation *in vitro*. To explore this, I generated naïve CD4 T cells from splenocytes isolated from *Rora*^{fl/fl} and *Rora*^{fl/fl}CD4Cre (**Chapter 2, Section 2.18**) and induced polarisation into Th cell subsets (**Chapter 2, Section 2.19**). Following the culture of naïve CD4 T cells in the presence of specific cytokines and antibodies, CD4 T cell polarisation was determined by assessing classical Th cell transcription factors expression by flow cytometry (Th1 – Tbet, Th2 – GATA3, Th17 – Ror γ t, and Tregs – Foxp3).

Supporting the *in vivo* observations, naïve CD4 T cells isolated from *Rora*^{fl/fl}CD4Cre mice have significantly ($p < 0.01$) reduced GATA3⁺ (Th2) polarisation compared to those isolated from *Rora*^{fl/fl} mice (**Figure 5.11**). There was no significant difference between the polarisation of naïve CD4 T cells isolated from *Rora*^{fl/fl}CD4Cre and *Rora*^{fl/fl} mice towards Tbet (Th1), Ror γ t (Th17) or Foxp3 (Treg) CD4 T cells (**Figure 5.11**). It is known that ROR α is required for Th17 cell differentiation (Yang et al., 2008), therefore, it is surprising naïve CD4 T cells from *Rora*^{fl/fl}CD4Cre mice had comparable polarisation towards that Ror γ t⁺ (Th17) cells. However, it is possible that in naïve CD4 T cells from *Rora*^{fl/fl}CD4Cre mice were compensated for by the transcription factors, such as ROR γ t, which is also required for Th17 cell development (Ivanov et al., 2006). The comparable polarisation towards a Th1 or Treg phenotype in naïve CD4 T cells from *Rora*^{fl/fl} and *Rora*^{fl/fl}CD4Cre mice is unsurprising, as there are currently no known roles for ROR α in Th1 and Treg cell development. Therefore, the *in vitro* data presented here support the *in vivo* results, providing further indication that *Rora* has a role in development of GATA3⁺CD4 T cells.

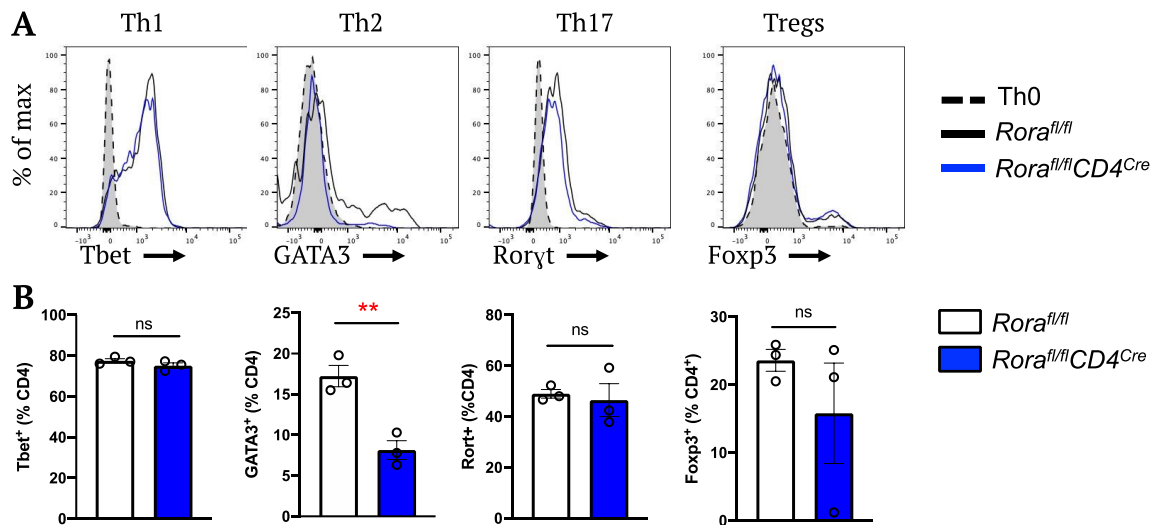


Figure 5.11: *Rora^{fl/fl}CD4Cre* naïve CD4 T cells have reduced ability for *in vitro* GATA3⁺ polarisation compared to *Rora^{fl/fl}* naïve CD4 T cells. Naïve CD4 T cells were isolated from *Rora^{fl/fl}CD4Cre* and *Rora^{fl/fl}* spleens using AutoMACS and cultured in T cell polarisation conditions. **A**, Expression of CD4 T cell subpopulation defining transcription factors in differentiated T cells. Tbet⁺ (Th1), GATA3⁺ (Th2), Roryt⁺ (Th17) and Foxp3⁺ (Tregs). **B**, Frequency of *in vitro* differentiated CD4 T cell subpopulations. Data is representative of mean ± SEM. Differences indicated as *p* values, as assessed by Student *t* Test. ***p*<0.01. ns = non-significant. n = 3.

The results presented in this chapter thus far have provided further support for a role of *Rora* in CD4 T cells following *N. brasiliensis* infection. In support of previously published data (Halim et al., 2018), *Rora^{fl/fl}Il7raCre* mice are demonstrated as ILC2-deficient and have delayed worm expulsion following *N. brasiliensis* infection. However, in this chapter, I have demonstrated that both ILC2s and CD4 T cells express *Il7ra*, and there are *Rora* expressing *Il7ra*⁺ILC2s and *Il7ra*⁺CD4 T cells, suggesting a potential role for *Il7ra*⁺CD4 T cells. Thus, in addition to being ILC2-deficient, *Rora^{fl/fl}Il7raCre* mice also had a reduced frequency of lung CD4 T cell and GATA3⁺CD4 T cells. This indicates a role for *Rora* beyond ILC2 development and suggests that *Rora* is also important for GATA3⁺CD4 T cell development. However, given that there is crosstalk between ILC2s and CD4 T cells, the complex interplay between *Rora*-expressing ILC2 and CD4 T cells is not fully understood and further studies are required.

There was no impact on the generation of a functional type 2 response in *Rora^{fl/fl}CD4Cre* mice, with these mice demonstrating a comparable frequency of lung ILC2s, and worm expulsion with WT mice. However, *Rora^{fl/fl}CD4Cre* mice had reduced lung CD4 T cells and GATA3⁺CD4 T cells following *N. brasiliensis* infection compared to control mice.

On further investigation, *Rora^{fl/fl}CD4Cre* mice had a reduced frequency of proliferating GATA3⁺CD4 T cells compared to control animals following *N. brasiliensis* infection. Therefore, as *Rora^{fl/fl}CD4Cre* mice had a comparable frequency of ILC2s with control mice, this indicates that the reduced frequency of GATA3⁺CD4 T cells in *Rora^{fl/fl}CD4Cre* mice is ILC2 independent, and ROR α has a role in CD4 T cell development. Furthermore, it was also observed that naïve CD4 T cells isolated from *Rora^{fl/fl}CD4Cre* mice had reduced capacity for *in vitro* GATA3⁺ (Th2) cell polarisation, supporting the *in vivo* observations in these mice. Therefore, data generated using the conditional deleter animals supports observations from studies presented in **Chapter 3** and **Chapter 4**, that *Rora* has a role in the development of GATA3⁺CD4 T cells during inflammation.

5.3.12 *Rora^{fl/fl}Il7raCre* mice have reduced frequency of lung eosinophils, whilst *Rora^{fl/fl}CD4Cre* mice had comparable lung eosinophils with WT mice following *N. brasiliensis* infection

In **Chapter 3**, I demonstrated that *Rora^{sg/sg}* mice and *Rora^{sg/sg}* BM chimera mice had a reduced frequency of lung eosinophils following *N. brasiliensis* infection, indicating that ROR α may have a direct or indirect role in the development or recruitment of eosinophils to the site of inflammation. Previously it has been reported that *Rora^{fl/fl}Il7raCre* mice have reduced lung eosinophils in response to papain challenge (Halim et al., 2018), which the authors commented was due to the ILC2 deficiency resulted in decreased release of the eosinophil chemoattractant IL-5, and therefore reduced recruitment of lung eosinophils. In this chapter, I have shown that *Rora^{fl/fl}Il7raCre* mice have a reduced lung ILC2s and GATA3⁺CD4 T cells following *N. brasiliensis* infection, whilst *Rora^{fl/fl}CD4Cre* mice have comparable frequency of ILC2s to control mice, but reduced GATA3⁺CD4 T cells following infection. Therefore, I sought to determine if the reduction in GATA3⁺CD4 T cells could impact eosinophil recruitment, in a similar manner to the reduction of ILC2 following primary *N. brasiliensis* infection.

As anticipated, *N. brasiliensis* infection drives the recruitment and expansion of lung eosinophils in the lung of WT mice (**Figure 5.12**). As previously reported, *Rora^{fl/fl}Il7raCre* mice have a reduced frequency of lung eosinophils compared to WT mice following *N. brasiliensis* infection (**Figure 5.12**). However, the frequency of lung

eosinophils was comparable between *Rora^{fl/fl}CD4Cre* mice and control mice in both the naïve state and following *N. brasiliensis* infection. This data suggests that while ILC2s are required for eosinophil recruitment, an absence of GATA3⁺CD4 T cells alone did not impact on recruitment or expansion of lung eosinophils during primary infection (**Figure 5.12**). These findings expand on those observed in *Rora^{sg/sg}* mice and *Rora^{sg/sg}* BM chimera mice, indicating a role for ILC2s in the recruitment and expansion of eosinophils in the lung in response to *N. brasiliensis* infection. Interestingly, eosinophils have a reported role in killing *N. brasiliensis* (Voehringer et al., 2006, Knott et al., 2007, Giacomini et al., 2008), and therefore the delayed worm expulsion observed in *Rora^{fl/fl}Il7raCre* mice may be partially due to the reduced frequency of eosinophils. However, further studies are required to fully understand the role of ROR α in eosinophil development, activation, and functionality within the context of helminth infection.

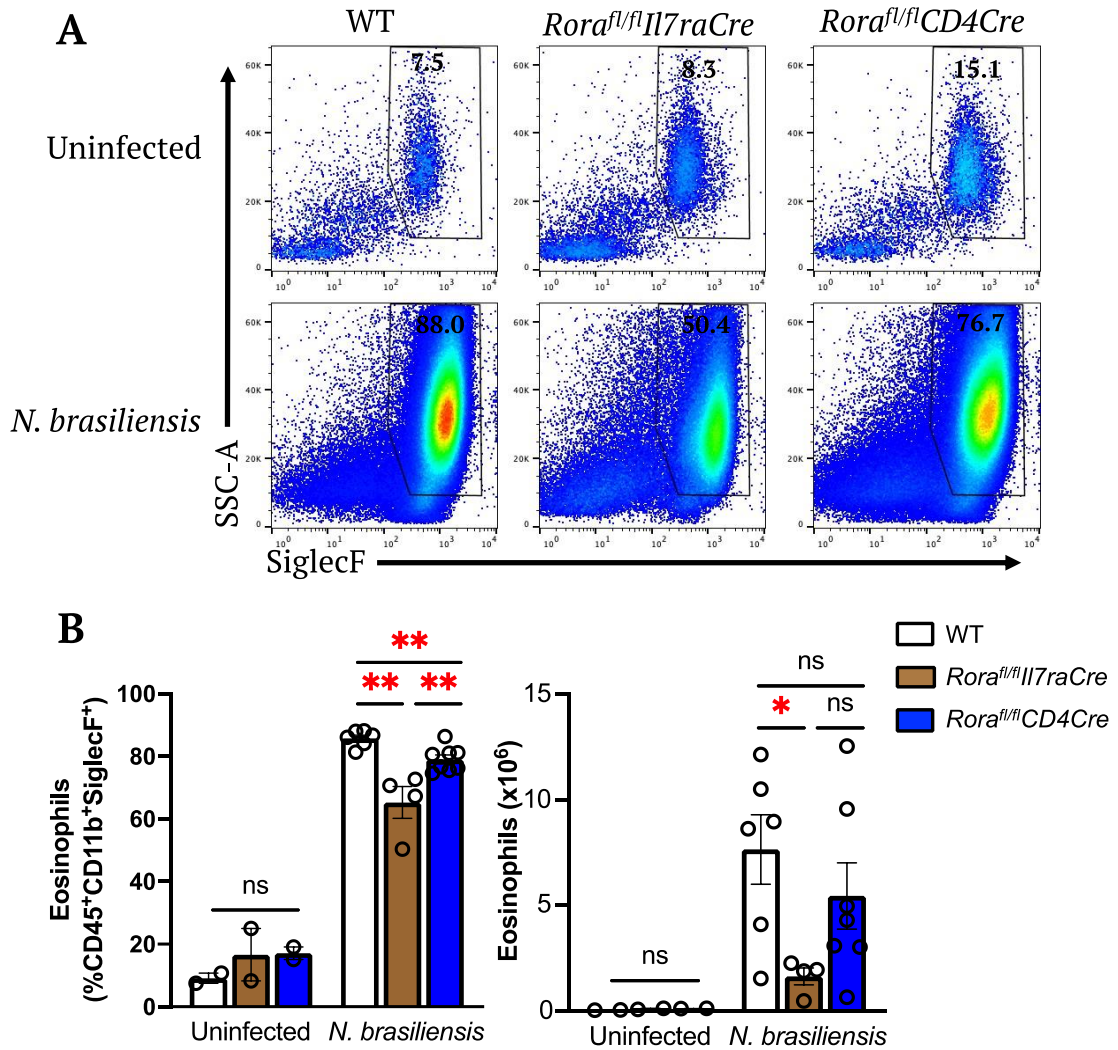


Figure 5.12: *Rora^{fl/fl}Il7raCre* mice have reduced lung eosinophils compared to WT and *Rora^{fl/fl}CD4Cre* mice in response to *N. brasiliensis*. WT, *Rora^{fl/fl}CD4Cre* and *Rora^{fl/fl}Il7raCre* mice were infected with 500 L3 *N. brasiliensis* subcutaneously. Lungs were harvested at day 9 post-infection and assessed by flow cytometry. **A**, Representative flow cytometry plots of gating strategy. Eosinophils were gated as CD45⁺SiglecF⁺CD11b⁺F4/80⁺CD11c⁻. **B**, Quantification of lung eosinophils. Data is representative of mean \pm SEM. The numbers on flow cytometry plots reflect the percentage of SiglecF⁺CD11b⁺ cells. Differences indicated as *p* values, as assessed by Student *t* Test **p*<0.05, ***p*<0.01. ns = non-significant. n = 2-7.

5.3.13 WT, *Rora^{fl/fl}Il7raCre* and *Rora^{fl/fl}CD4Cre* mice had comparable frequency of lung M2 macrophages in uninfected mice and following *N. brasiliensis* infection

The lifecycle of *N. brasiliensis* infection causes significant damage to epithelium and vasculature of the lungs as a result of worm penetration and migration. M2 macrophages play an important role in repairing this lung damage (Chen et al., 2012) (**Chapter 1, Section 1.5.1.3**). Interestingly, it has been reported that M2 macrophages increase expression of programmed death ligand 2 (PD-L2) following *N. brasiliensis* infection and participate in the inhibition of Th2 cell responses (Huber et al., 2010). Indeed, it is known that PD-L2 interacts with programmed death receptor 1 (PD-1) on T cells, resulting in regulation of T cells (Latchman et al., 2001). It was reported that the parasitic helminth, *Fasciola hepatica*, excretory-secretory products induced CD4 T cell anergy by upregulation of PD-L2 expression in macrophages (Guasconi et al., 2015). Therefore, to further delineate the potential impact of the previously observed reduced frequency of lung GATA3⁺CD4 T cells in both *Rora^{fl/fl}CD4Cre* and *Rora^{fl/fl}Il7raCre* mice following *N. brasiliensis*, I assessed the frequency of PD-L2 expressing M2 macrophages following *N. brasiliensis* in WT, *Rora^{fl/fl}CD4Cre* and *Rora^{fl/fl}Il7raCre* mice.

As anticipated, there is an increase in lung PD-L2 expressing M2 macrophages following *N. brasiliensis* infection in WT mice (**Figure 5.13**). Interestingly, this increase is also seen in both *Rora^{fl/fl}CD4Cre* and *Rora^{fl/fl}Il7raCre* mice, and there was no significant difference in frequency of lung M2 macrophages between WT, *Rora^{fl/fl}CD4Cre* and *Rora^{fl/fl}Il7raCre* mice in both uninfected conditions and following *N. brasiliensis* infection (**Figure 5.13**). Therefore, these findings indicate that the observed reduced frequency of lung GATA3⁺CD4 T cells in *Rora^{fl/fl}CD4Cre* and *Rora^{fl/fl}Il7raCre* mice is not due to an increased frequency of PD-L2 expressing M2 macrophages, leading to CD4 T cell anergy.

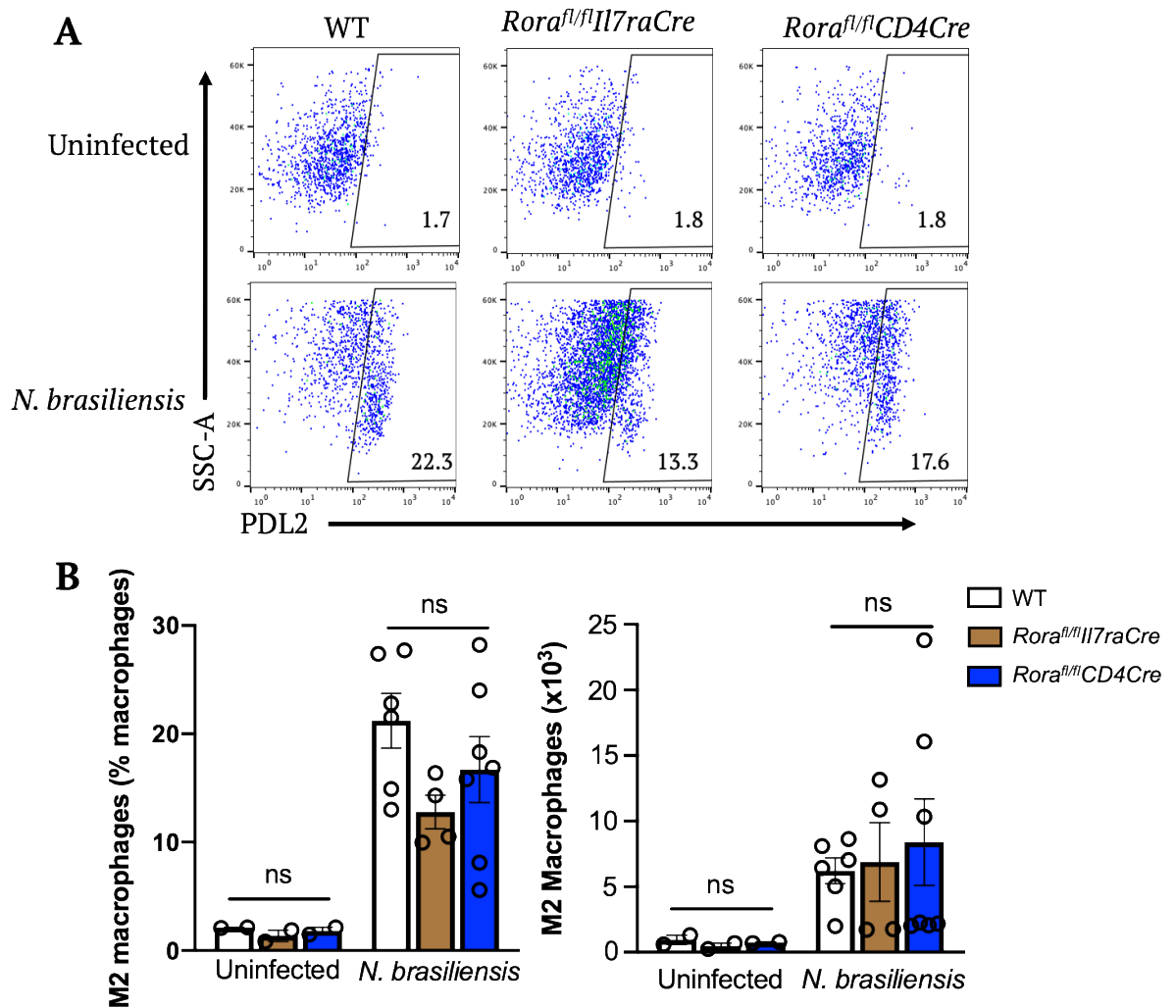


Figure 5.13: No significant difference in lung M2 macrophages in the naïve state and in response to *N. brasiliensis* between WT, $Rora^{fl/fl}CD4Cre$ and $Rora^{fl/fl}Il7raCre$ mice. WT, $Rora^{fl/fl}CD4Cre$ and $Rora^{fl/fl}Il7raCre$ mice were infected with 500 L3 *N. brasiliensis* subcutaneously. **A**, Lungs were harvested at day 9 post-infection and assessed by flow cytometry. M2 macrophages were gated as cells, single cells, live cells, $CD45^+SiglecF^+CD11b^+F4/80^+CD11c^+PDL2^+$. **B**, Quantification of M2 macrophages. Data is representative of mean \pm SEM. The number on flow cytometry plots reflect percentage of $SiglecF^+CD11b^+$ cells. Differences indicated as *p* values, as assessed by Student *t* Test. ns = non-significant. n = 2-7.

5.3.14 WT, *Rora*^{fl/fl}*Il7raCre* and *Rora*^{fl/fl}*CD4Cre* mice had comparable frequency of lung neutrophils in uninfected conditions and following *N. brasiliensis* infection

Neutrophils are innate immune cells that rapidly enter the sites of infection (**Chapter 1, Section 1.5.1.1**). Through phagocytosis, production of reactive oxygen species, release of granules containing toxic mediators, and neutrophil extracellular traps (NETs), neutrophils have been shown to have a role in killing *N. brasiliensis* (Sutherland et al., 2014, Bouchery et al., 2020). Indeed, neutrophil depletion resulted in more *N. brasiliensis* reaching the small intestine (Sutherland et al., 2014). Therefore, to expand on previous findings in this chapter that reported *Rora*^{fl/fl}*Il7raCre* mice delayed worm expulsion, I assessed the frequency of lung neutrophils in *Rora*^{fl/fl}*Il7raCre* and *Rora*^{fl/fl}*CD4Cre* mice following *N. brasiliensis* infection. Neutrophils were identified as being CD11b⁺Ly6G⁺, as previously described in Misharin et al. (2013).

Flow cytometry analysis revealed there was no significant difference in the frequency of lung neutrophils between WT, *Rora*^{fl/fl}*CD4Cre* and *Rora*^{fl/fl}*Il7raCre* mice in both uninfected conditions and following *N. brasiliensis* infection (**Figure 5.14**). Therefore, indicating that *Rora* deletion in CD4 T cells and *Il7ra* expressing cells had no impact on the frequency of lung neutrophils and therefore, was not implicated in the delayed worm clearance in *Rora*^{fl/fl}*Il7raCre* mice.

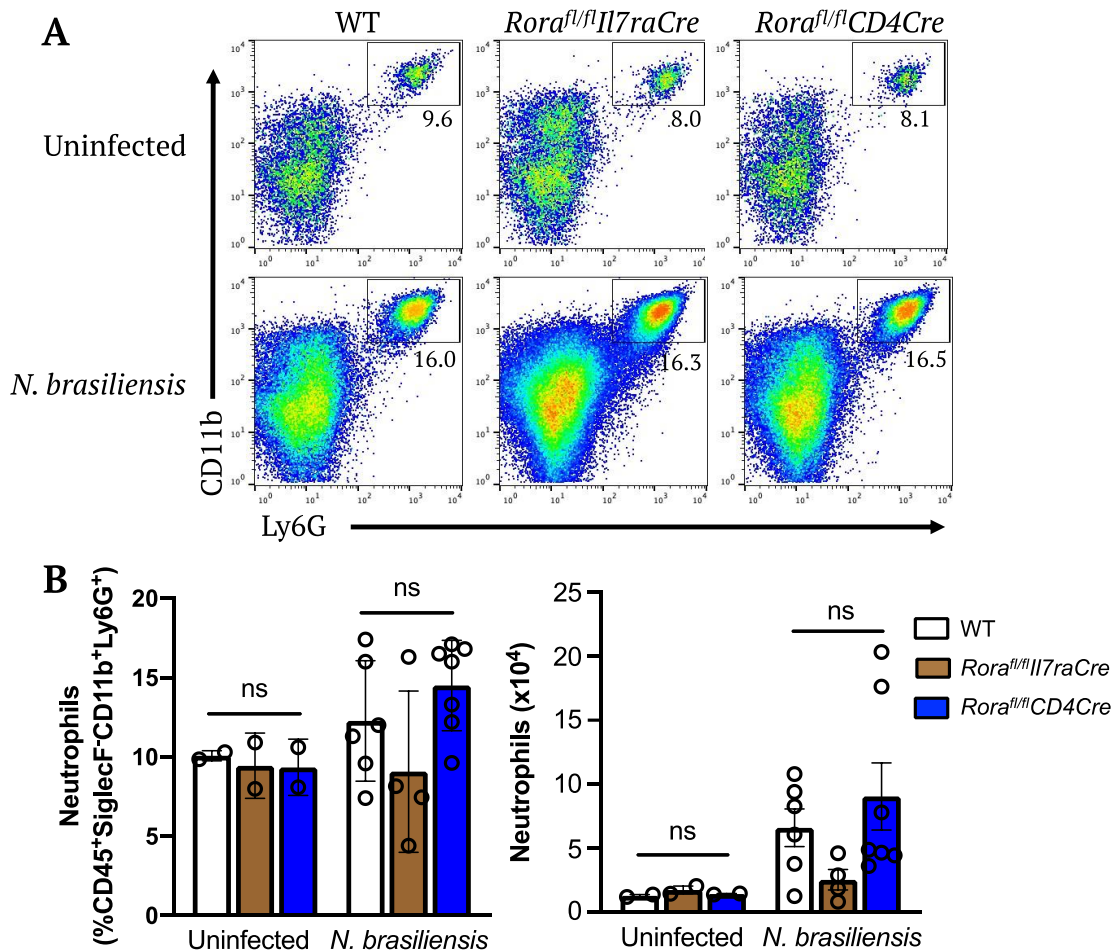


Figure 5.14: WT, $Rora^{fl/fl}Il7raCre$ and $Rora^{fl/fl}CD4Cre$ mice had comparable frequency of lung neutrophils in uninfected condition and following *N. brasiliensis* infection. WT, $Rora^{fl/fl}Il7raCre$ and $Rora^{fl/fl}CD4Cre$ mice were infected with 500 L3 *N. brasiliensis* subcutaneously. **A**, Lungs were harvested at day 9 post-infection and assessed by flow cytometry. Neutrophils gated as single cells, live cells, CD45⁺CD11b⁺Ly6G⁺. **B**, Quantification of lung neutrophils. Data is representative of mean \pm SEM. Differences indicated as p values, as assessed by Student t Test. ns = non-significant. n = 2-7.

5.3.15 $Rora^{fl/fl}CD4Cre$ mice had comparable serum IgE with $Rora^{fl/fl}$ mice

In this chapter I have observed a role for *Rora* in CD4 T cells following *N. brasiliensis* infection. $Rora^{fl/fl}CD4Cre$ mice have reduced lung GATA3⁺CD4 T cells when compared to control animals. Indeed, following helminth infection, ILC2s and Th2 (GATA3⁺CD4 T cells) secrete type 2 cytokines IL-4, IL-5 and IL-13, which drives B cell proliferation and Ig class switching to IgE (Walker and McKenzie, 2018). Therefore, having observed a reduced frequency GATA3⁺CD4 T cells in $Rora^{fl/fl}CD4Cre$ mice, I assessed the

concentration of serum IgE to explore if reduced frequency of GATA3⁺CD4 T cells impacted on the adaptive B cell humoral immune response.

There was no serum IgE detected in the uninfected mice of both *Rora*^{fl/fl} and *Rora*^{fl/fl}CD4Cre mice (**Figure 5.15**). This was anticipated and confirmed that there was no underlying immunological response in uninfected mice. Following *N. brasiliensis* infection there is a substantial increase in serum IgE in *Rora*^{fl/fl} and *Rora*^{fl/fl}CD4Cre mice. However, there was no significant difference in the concentration of serum IgE between *Rora*^{fl/fl} and *Rora*^{fl/fl}CD4Cre mice following *N. brasiliensis* infection (**Figure 5.15**). It is possible that, as *Rora*^{fl/fl}CD4Cre mice have a comparable frequency of ILC2s as WT mice, this may compensate for the reduction in GATA3⁺CD4 T cells with respect to B cell IgE secretion in these mice, during the primary infection. Therefore, these findings indicate that deletion of *Rora* from CD4 cells had no impact on the generation of an adaptive B cell humoral immune response as assessed by detection of serum IgE.

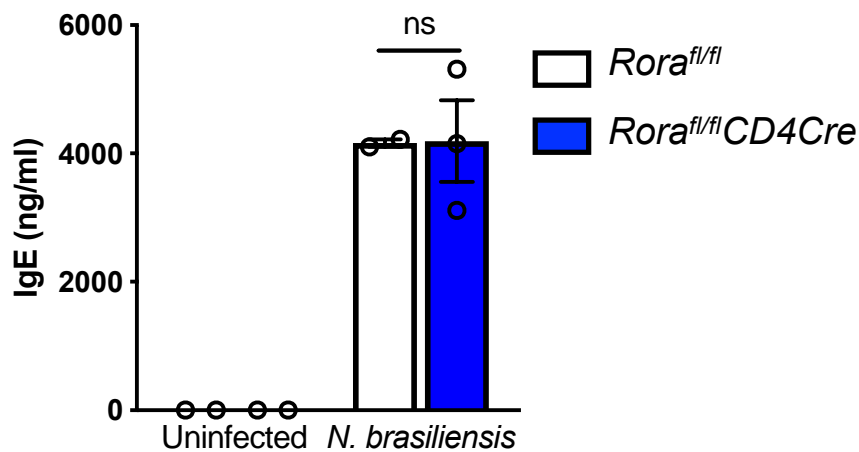


Figure 5.15: No significant difference in serum IgE between *Rora*^{fl/fl} and *Rora*^{fl/fl}CD4Cre in uninfected mice and at day 10 post *N. brasiliensis* infection. *Rora*^{fl/fl} and *Rora*^{fl/fl}CD4Cre mice were infected with 500 L3 *N. brasiliensis* subcutaneously. Serum was collected from uninfected mice and at day 10 post-infection. Data is representative of mean \pm SEM. Differences assessed by unpaired Student *t* test. ns = non-significant. n = 2-3.

5.4 Discussion

In **Chapter 3**, *Rora*^{sg/sg} mice and *Rora*^{sg/sg} BM chimera mice were used to investigate the role of *Rora* during *N. brasiliensis* infection. Although both are very useful mouse models for exploring the role of ROR α , as functional ROR α is absent ubiquitously in *Rora*^{sg/sg} mice, and in haematopoietic cells in *Rora*^{sg/sg} BM chimera mice, it is difficult to decipher the exact role of *Rora* in specific immune cells. In **Chapter 4**, it was observed that there was a population of *Rora*-expressing CD4 and Il7Ra⁺ (CD127) cells. *CD4Cre* and *Il7raCre* mice are used in the literature to delete specific floxed sequences in CD4 and Il7ra expressing cells, respectively. In this chapter *Rora*^{fl/fl}*CD4Cre* mice (Halim et al., 2018) and *Rora*^{fl/fl}*Il7raCre* mice (Oliphant et al., 2014) were used to investigate the role of ROR α following *N. brasiliensis* by site specific deletion of *Rora* in *CD4* and *Il7ra* cells, respectively.

In **Chapter 3**, I demonstrated that *Rora*^{sg/sg} mice and *Rora*^{sg/sg} BM chimera mice had delayed expulsion of *N. brasiliensis* worms in the intestine. In this chapter, I investigated the role of *Rora* in CD4 and Il7ra expressing cells on the expulsion of *N. brasiliensis*. In support of previously published data, *Rora*^{fl/fl}*Il7raCre* mice have a delayed worm expulsion compared to control mice (Oliphant et al., 2014), whilst *Rora*^{fl/fl}*CD4Cre* mice had comparable worm expulsion with control mice (Halim et al., 2018). On further investigation, *Rora*^{fl/fl}*Il7raCre*, *Rora*^{fl/fl}*CD4Cre* and WT mice had a comparable number small intestine goblet cells in both uninfected mice and following *N. brasiliensis* infection. There is a possibility that any differences in goblet cell hyperplasia may have been outside of the time point assessed, and therefore, to definitively assess the impact of an absence or *Rora*-expressing CD4 or Il7ra-expressing cells in goblet cell hyperplasia, a range of time points should be assessed in future studies.

Expanding on previously reported data (Oliphant et al., 2014), *Rora*^{fl/fl}*Il7raCre* mice had a reduced frequency of lung ILC2s in uninfected conditions and following *N. brasiliensis* infection. I also observed a population of *Rora* expressing lung Il7ra⁺CD4 T cells and therefore explored the frequency of CD4 T cells in *Rora*^{fl/fl}*Il7raCre* mice. Interestingly, *Rora*^{fl/fl}*Il7raCre* mice also had reduced frequency of lung CD4 T cells and GATA3⁺CD4 T cells following *N. brasiliensis* infection. This supports previously published data, that reported that *Rora*^{fl/fl}*Il7raCre* mice had reduced lung GATA3⁺CD4 T cells (Halim et al.,

2018). However, given the known direct communication between ILC2s and CD4 T cells (Drake et al., 2014, Mirchandani et al., 2014, Oliphant et al., 2014, Schwartz et al., 2017), the underlying mechanisms of ILC2 and GATA3⁺CD4 T cell reduction in these animals remains unclear. Therefore, further studies are required to confirm if the impact on CD4 T cells in these mice is solely due to the ILC2 deficiency, or if there is a standalone effect of *Rora* deletion in Il7ra expressing CD4 T cells.

To specifically address the impact of *Rora* expressing CD4 cells, without the confounding deletion of ILC2s, I utilised *Rora^{fl/fl}CD4Cre* mice. In support of previously published data (Haim-Vilmovsky et al., 2020), CD4 T cells were not altered in *Rora^{fl/fl}CD4Cre* mice from uninfected mice, indicating that ROR α is not required for CD4 T cell development in baseline conditions. However, in this chapter I observed that *Rora^{fl/fl}CD4Cre* mice had a reduced frequency of lung GATA3⁺CD4 T cells following *N. brasiliensis* infection, suggesting that *Rora* may be required for the development of GATA3⁺CD4 T cells during inflammation. These results are in support of those observed using *Rora^{sg/sg}* and *Rora^{sg/sg}* BM chimera mice. It has been reported that following papain challenge or IL-33 i.n. administration, *Rora^{fl/fl}CD4Cre* mice had comparable numbers of Th2 and Tregs to WT mice. However, it is important to note that these are different inflammatory conditions compared to *N. brasiliensis* infection and the role and requirement for CD4 T cells differs dependent on the model, and therefore ROR α may have different roles in CD4 T cells depending on the type of inflammation. In this chapter I also demonstrated that *Rora^{fl/fl}CD4Cre* mice had levels of lung ILC2s following infection comparable with WT mice, indicating that the impact of *Rora* in GATA3⁺CD4 T cell development is independent of ILC2. Furthermore, assessment of proliferation of GATA3⁺CD4 T cells in the lungs in response to *N. brasiliensis* infection, demonstrated decreased proliferation in *Rora^{fl/fl}CD4Cre*, indicating that *Rora* may be important for proliferation of these cells, which may partially explain the reduced frequency of GATA3⁺CD4 T cells observed in the lungs of *Rora^{fl/fl}CD4Cre* mice. In support of the *in vivo* results, *in vitro* CD4 T cell polarisation studies presented in this chapter showed that naïve CD4 T cells from *Rora^{fl/fl}CD4Cre* mice had reduced polarisation towards GATA3⁺ (Th2) compared to naïve CD4 T cells isolated from WT mice.

There is a population of Treg cells that express GATA3 (GATA3⁺Foxp3⁺) (Wohlfert et al., 2011, Halim et al., 2018). As ROR α has a role in Treg cell function in allergic skin

inflammation (Malhotra et al., 2018), the role of ROR α in Treg cells development was determined by assessing the frequency of lung Foxp3⁺ and GATA3⁺Foxp3⁺ CD4 T cells were assessed *Rora*^{fl/fl}*CD4Cre* mice following *N. brasiliensis* infection. There were comparable levels of lung Foxp3⁺ and GATA3⁺Foxp3⁺ CD4 T cells with control mice in both uninfected animals, and following *N. brasiliensis* infection. Therefore, indicating that *Rora* was important to the development GATA3⁺CD4 T cells following *N. brasiliensis* infection and had no roles in the development of lung Foxp3⁺ and GATA3⁺Foxp3⁺ CD4 T cells. The results in this chapter investigated the role of ROR α during a primary *N. brasiliensis* infection and identified that *Rora*^{fl/fl}*CD4Cre* mice have an altered GATA3⁺CD4 T cell development.

ILC2s are important cells at mediating expulsion of *N. brasiliensis* following primary infection (Fallon et al., 2006, Moro et al., 2010, Neill et al., 2010). This may explain why *Rora*^{fl/fl}*Il7raCre* mice, which are ILC2-deficient, have a delayed worm expulsion, and *Rora*^{fl/fl}*CD4Cre* mice, which have comparable frequency of ILC2s, have comparable worm expulsion to WT mice. Lung CD4 T cells are important at mediating protection following secondary *N. brasiliensis* infection (Harvie et al., 2010, Thawer et al., 2014, Bouchery et al., 2015). As *Rora*^{fl/fl}*CD4Cre* mice have a reduced frequency of lung GATA3⁺CD4 T cells, independent of ILC2s, following primary *N. brasiliensis* infection, it would be interesting for future studies to explore the functional role of ROR α in CD4 T cells following a secondary *N. brasiliensis* infection using *Rora*^{fl/fl}*CD4Cre* mice.

In **chapter 3**, it was also observed that *Rora*^{sg/sg} mice and *Rora*^{sg/sg} BM chimera mice had reduced frequency of lung eosinophils following *N. brasiliensis* infection. In this chapter it was observed that *Rora*^{fl/fl}*Il7raCre* mice had a reduced frequency of lung eosinophils, whilst *Rora*^{fl/fl}*CD4Cre* mice had comparable lung eosinophils with control mice. Therefore, given *Rora*^{fl/fl}*Il7raCre* mice have reduced ILC2s, this may explain the reduced lung eosinophils as ILC2s promote the control of homeostasis and eosinophilia (Nussbaum et al., 2013). However, I have not been able to study eosinophils in isolation, and therefore, cannot discount the possibility for an additional role for *Rora*-expression in eosinophils themselves. Future studies would be interesting to fully delineate the precise role of ROR α in eosinophils.

M2 macrophages have been shown to increase expression of programmed death ligand 2 (PD-L2) following *N. brasiliensis* infection and participate in the inhibition of Th2 cell responses (Huber et al., 2010). It has previously been reported that *Rora^{fl/fl}Il7raCre* mice have reduced M2 macrophages, based on intracellular staining for RELM α , in response to papain challenge (Halim et al., 2018), which would be anticipated due to the known role of ILC2 in promoting M2 macrophage polarisation. However, in contrast, results presented herein showed that both *Rora^{fl/fl}Il7raCre* and *Rora^{fl/fl}CD4Cre* mice had comparable lung M2 macrophages with control mice, both in a naïve state and following *N. brasiliensis* infection. Staining herein relied upon expression of PD-L2 as a marker for M2 macrophages, and as macrophages are an extremely heterogeneous population, it may be that this staining was not optimal for identifying M2 macrophages. It would be interesting to repeat this assessing a number of different marker combinations to determine if M2 macrophages are impacted by the absence of *Rora*-expressing CD4 and Il7ra-expressing cells.

In summary, results presented in **Chapters 3, 4 and 5** highlight a role for ROR α in a type 2 immune response beyond its known role in ILC2 development. More specifically, results indicate that ROR α is important for GATA3⁺CD4 T cells development following *N. brasiliensis* infection. Therefore, in **Chapter 6** I sought to investigate the role of ROR α in an additional model of type 2 immunity by treating *Rora^{sg/sg}* mice, *Rora^{sg/sg}* BM mice, *Rora* reporter mice, *Rora^{fl/fl}CD4Cre* and *Rora^{fl/fl}Il7raCre* mice with house dust mite, as a model for induced allergic airway inflammation.

Chapter 6

Determining the role of *Rora* in inflammatory responses to HDM using ubiquitous mutant *Rora* mice (*Rora*^{sg/sg}), *Rora* reporter mice and *Rora* CD4 and Il7ra conditional deleter mice

Chapter 6

6.1 Introduction

In this thesis I have investigated the role of ROR α utilising the parasitic helminth *N. brasiliensis* to elicit a type 2 immune response. In **Chapter 3**, *Rora*^{sg/sg} mice, which have a deficiency in a functional ROR α , were shown to be ILC2-deficient, and had a reduced frequency of lung GATA3⁺CD4 T cell and eosinophils compared to WT mice following *N. brasiliensis* infection. Therefore, indicating that in addition to the well-characterised role in the development of ILC2, ROR α may also play a role in the development or recruitment of lung GATA3⁺CD4 T cells and eosinophils. In **Chapter 4**, I generated a *Rora* reporter mouse to investigate the expression of *Rora* in immune cells implicated in type 2 immunity. Using these mice I demonstrated that, following *N. brasiliensis* infection, there was an increase in *Rora* expressing lung CD4 T cells and GATA3⁺CD4 T cells, suggesting a role for *Rora* in the development and function of these cells during inflammation. It was also observed that *Rora* expressing CD4 T cells were associated with co-expression of both activation markers, and those associated with a memory and resident CD4 T cell phenotype. In **Chapter 5**, I used conditional deleter mice, *Rora*^{fl/fl}*CD4Cre* and *Rora*^{fl/fl}*Il7raCre*, which have *Rora* excised from CD4 and *Il7ra* expressing cells, respectively, to expand upon the proposed role of *Rora* in the development and function of GATA3⁺CD4 T cells. As previously reported, *Rora*^{fl/fl}*Il7raCre* mice had reduced frequency of ILC2s (Oliphant et al., 2014), whilst *Rora*^{fl/fl}*CD4Cre* mice had a comparable frequency of lung ILC2s as WT mice. Interestingly, both *Rora*^{fl/fl}*CD4Cre* and *Rora*^{fl/fl}*Il7raCre* mice had reduced lung GATA3⁺CD4 T cells following *N. brasiliensis* infection, indicating that *Rora* has a role in GATA3⁺CD4 T cell development that is independent of ILC2s.

To further investigate the role of ROR α in type 2 immune cells, and to confirm that the results generated thus far were not specific to helminth infection, in this chapter I utilised an alternative type 2 inducing mouse model, using i.n. administration of HDM (**Chapter 2, Section 2.8.7**). The HDM mouse model induces allergic airway inflammation, characterised by pulmonary Th2, Th17, Th1 and Treg immune responses along with lung

eosinophilia, similar to that observed in the human disease asthma (Plantinga et al., 2013, Fallon and Schwartz, 2019, Branchett et al., 2020). Asthma is an inflammatory airway disorder affecting over 300 million people worldwide (Athari, 2019). HDM is one of the most common sources of aeroallergens worldwide, with over 50% of allergic patients sensitised to these allergenic molecules. Indeed, allergen-specific Th2 cells orchestrate allergic airway inflammation by secreting type 2 cytokines (IL-4, IL-5 and IL-13), which drives lung eosinophilia, mucus metaplasia and airway hyper-responsiveness (Rahimi et al., 2020).

ROR α has been shown to be associated with asthma (Moffatt et al., 2010, Ramasamy et al., 2012, Acevedo et al., 2013), with *RORA* expression being significantly upregulated in patients with therapy-resistant asthma (Persson et al., 2015). Interestingly, *RORA* was expressed in T cells of the airways in both the healthy control and asthma patients (Vieira Braga et al., 2019), indicating that ROR α may have a role in T cells during asthma, however, the exact role is not fully understood.

In this chapter, I sought to investigate the role of ROR α in immune cells, in a helminth-independent model for type 2 immunity by i.n. HDM challenge. With focus on the role of ROR α in lung CD4 T cells and eosinophils following HDM challenge by using the mice used throughout this thesis, namely *Rora*^{sg/sg}, *Rora* reporter, and *Rora*^{fl/fl}*CD4Cre* and *Rora*^{fl/fl}*Il7raCre* mice.

6.2 Chapter Objectives

1. To investigate the role of the transcription factor ROR α in lung immune cells following house dust mite (HDM) challenge using *Rora*^{sg/sg} mice
2. To investigate the role of the transcription factor ROR α in lung immune cells following HDM challenge using *Rora* reporter mice
3. To investigate the role of the transcription factor ROR α in lung immune cells following HDM challenge using *Rora*^{fl/fl}*CD4Cre* and *Rora*^{fl/fl}*Il7raCre* mice

6.3 Results

6.3.1 Determining the role of the transcription factor ROR α in lung immune cells in the HDM mouse model using *Rora*^{sg/sg} mice

6.3.1.1 *Rora*^{sg/sg} mice have a reduced frequency of lung GATA3⁺ and Ror γ t⁺ CD4 T cells in response to HDM challenge compared to WT mice

In **Chapter 3**, it was observed that *Rora*^{sg/sg} mice had a reduced frequency of lung GATA3⁺CD4 T cells following *N. brasiliensis* infection. To further investigate this, I assessed the frequency of lung GATA3⁺CD4 T cells following HDM challenge. As previously discussed, the HDM mouse model of immunity leads to the development of Th1, Th2, Th17 and Treg immune responses (Fallon and Schwartz, 2019). Therefore, given that there are no known roles for ROR α in the generation of Th1 cells (**Figure 3.18**), I focused on the frequency of lung GATA3⁺ (Th2) and Ror γ t⁺ (Th17) cells CD4 T cells in the lungs of *Rora*^{sg/sg} and WT mice following HDM challenge.

As anticipated, there is an increase in both lung GATA3⁺ and Ror γ t⁺ CD4 T cells in WT mice following HDM challenge, indicating that the HDM model induced lung inflammation (**Figure 6.1**). However, in *Rora*^{sg/sg} mice there was a significantly reduced percentage of lung GATA3⁺ ($p < 0.01$) and Ror γ t⁺ ($p < 0.05$) CD4 T cells compared to WT mice following HDM challenge (**Figure 6.1**). There is no significant difference in the percentage of lung GATA3⁺ and Ror γ t⁺ CD4 T cells in vehicle treated *Rora*^{sg/sg} and WT mice (**Figure 6.1**), suggesting that there are no basal differences in cell frequency due to the lack of functional ROR α , with the observed results of reduced lung GATA3⁺ and Ror γ t⁺ CD4 T cells in *Rora*^{sg/sg} mice occurring only following inflammatory insult. The reduction of lung Ror γ t⁺ (Th17) CD4 T cells in *Rora*^{sg/sg} mice, compared to WT mice, supports the known role of ROR α in Th17 cell development (Yang et al., 2008). Whilst the reduction in lung GATA3⁺CD4 T cells findings are consistent with the results presented in **Chapter 3**, which identified that *Rora*^{sg/sg} mice have reduced frequency of lung GATA3⁺CD4 T cells following *N. brasiliensis* infection. Therefore, this data indicates that ROR α has a role in lung GATA3⁺CD4 T cell development during two independent models of type 2 immunity.

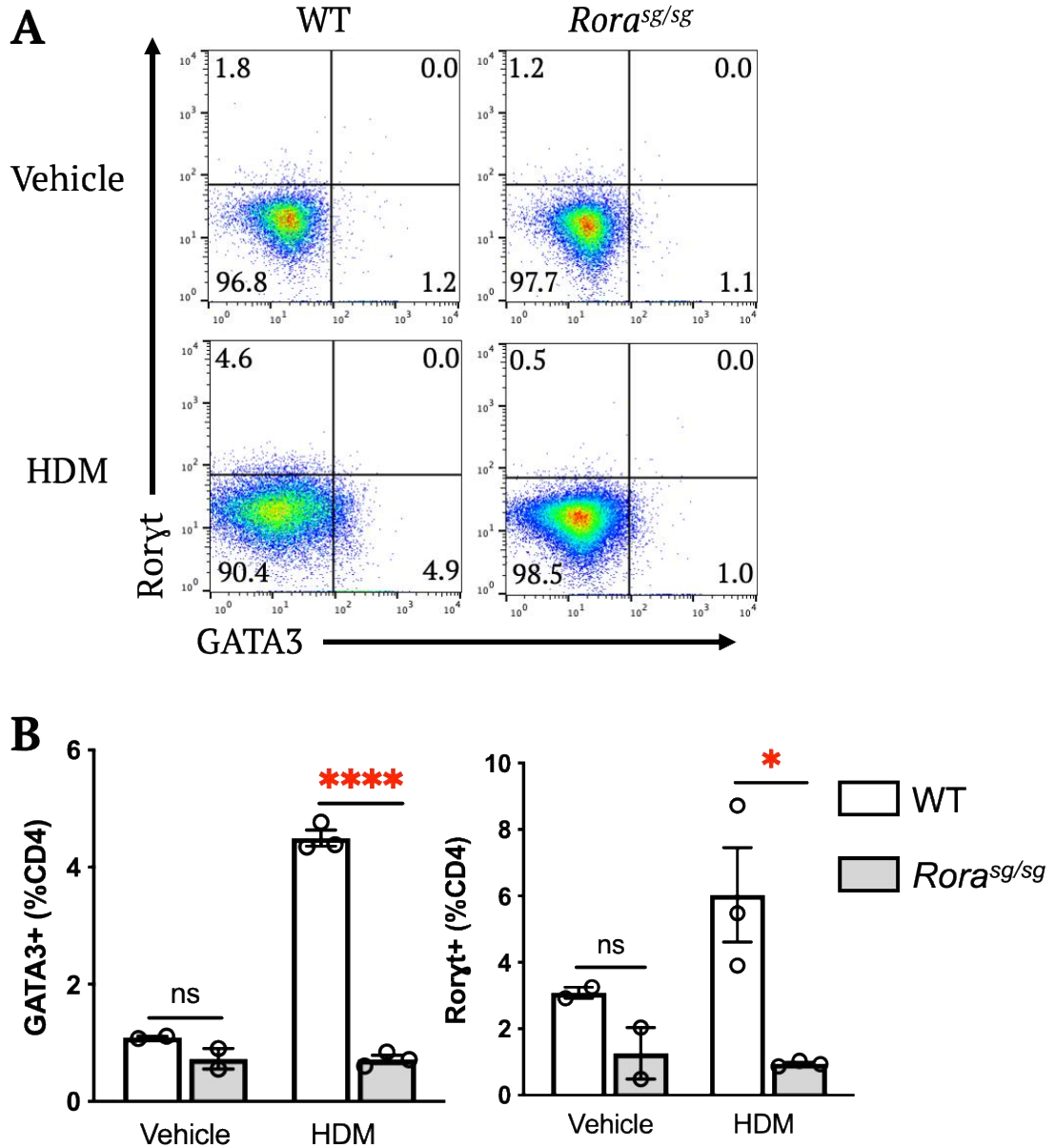


Figure 6.1: *Rora^{sg/sg}* mice have reduced lung GATA3⁺ and Roryt⁺ CD4 T cells following HDM challenge compared to WT mice. *Rora^{sg/sg}* and WT mice were challenged with HDM. Lungs were harvested for flow cytometry analysis. **A**, Representative flow cytometry plots of gating strategy. Cells pre-gated as lymphocytes, single cells, live cells and CD4⁺. CD4 T cell subpopulations were gated based on intracellular staining of GATA3⁺ and Roryt⁺ cells. **B**, Quantification of lung GATA3⁺ and Roryt⁺ CD4 T cell. Data is representative of mean \pm SEM. Differences indicated as two-tailed *p* values, as assessed by unpaired Student *t* test. **p*<0.05, *****p*<0.0001. ns = non-significant. n = 2-3.

6.3.1.2 *Rora*^{sg/sg} mice have reduced frequency of lung eosinophils in response to HDM challenge compared to WT mice

As previously alluded to, HDM induces lung eosinophilia (Fallon and Schwartz, 2019, Branchett et al., 2020). Therefore, having previously observed that *Rora*^{sg/sg} mice had reduced frequency of lung eosinophils following *N. brasiliensis* infection, I assessed the frequency of lung eosinophils in *Rora*^{sg/sg} and WT mice following HDM challenge, to explore if this was a helminth-specific observation.

As anticipated, there is a substantial increase in lung eosinophils in WT mice following HDM challenge, indicating that HDM challenge induced lung inflammation (**Figure 6.2**). Interestingly, however, *Rora*^{sg/sg} mice have reduced frequency of lung eosinophils in vehicle treated and when challenged with HDM compared to WT mice (**Figure 6.2**), although these results did not reach statistical significance. In contrast to WT mice, *Rora*^{sg/sg} mice did not have an increase in frequency of lung eosinophils following HDM challenge. These results support those in **Chapter 3**, which observed a reduced frequency of lung eosinophils in *Rora*^{sg/sg} mice following *N. brasiliensis* infection. Therefore, these findings indicate that there may be a role for *Rora* in eosinophil development during a type 2 immune response. However, as discussed in **Chapter 5**, eosinophils are induced by IL-5 which is secreted by ILC2s and CD4 T cells, which are both reduced in *Rora*^{sg/sg} mice, therefore further studies are required to fully understand the role of ROR α in eosinophil development, ideally with the use of a conditional knock out mice to delete *Rora* expression solely in eosinophils.

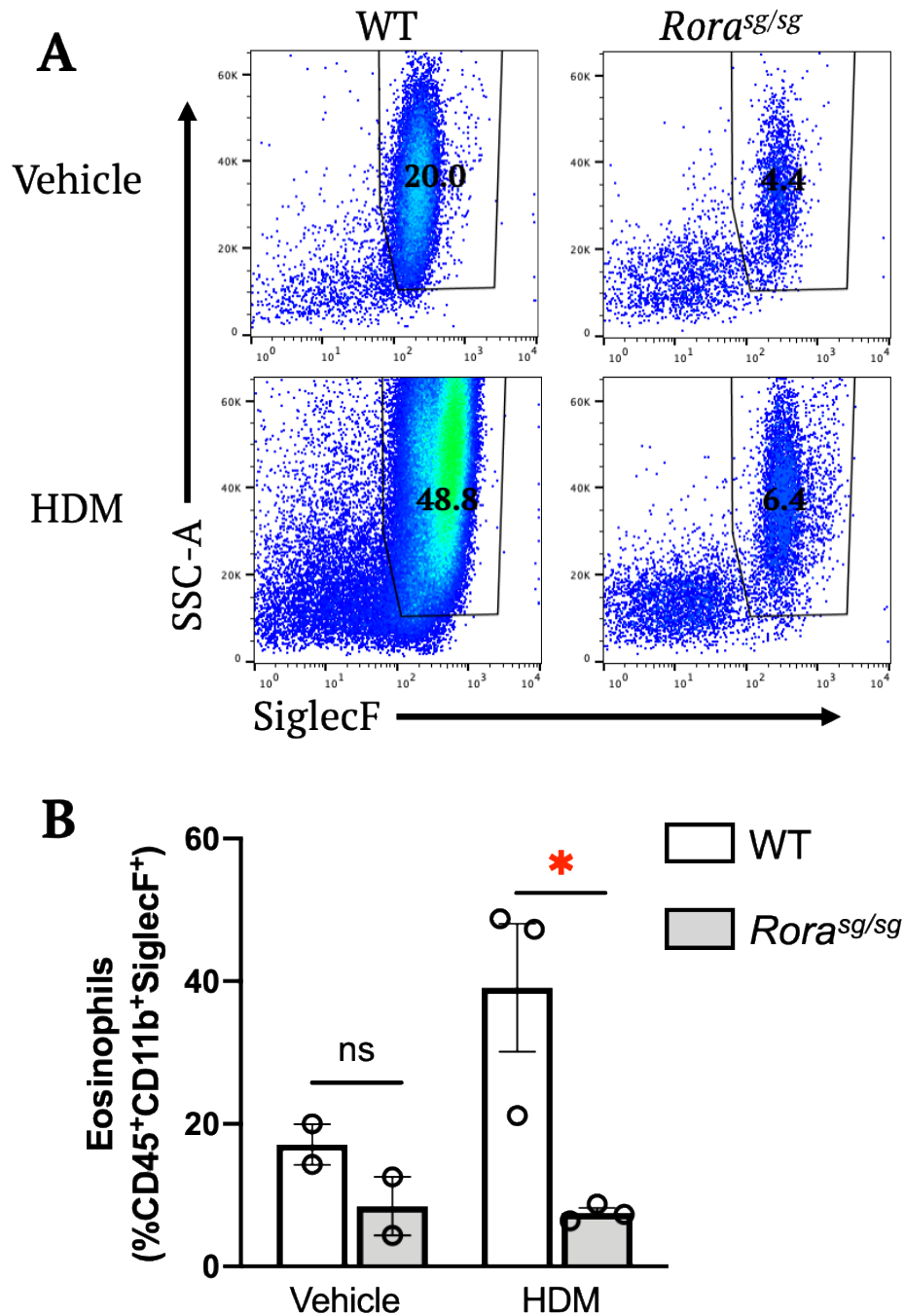


Figure 6.2: *Rora^{sg/sg}* mice have reduced frequency of lung eosinophils following HDM challenge compared to WT mice. *Rora^{sg/sg}* and WT mice were challenged with HDM. Lungs were harvested for flow cytometry analysis. **A**, Representative flow cytometry plots of gating strategy used for identifying lung eosinophils. Eosinophils were gated as single cells, live cells, CD45⁺CD11b⁺SiglecF⁺F4/80⁺CD11c⁻. The numbers in flow plots reflects percentage of CD11b⁺SiglecF⁺ cells. **B**, Quantification of lung eosinophils. Data is representative of mean \pm SEM. Differences indicated as two-tailed *p* values, as assessed by unpaired Student *t* test. **p*<0.05. ns = non-significant. n = 2-3.

6.3.2 Determining the role of the transcription factor ROR α in the lung immune cells in the HDM mouse model using *Rora* reporter mice

6.3.2.1 Increase in *Rora* expressing lung CD4 T cells following HDM

In **Chapter 4**, I observed that following *N. brasiliensis* infection, there was an increase in *Rora* expressing CD4 T in the lungs. This was also demonstrated following i.n. administration Ragweed pollen, where there was an increase in *Rora* expressing CD4 T cells in the lungs (Haim-Vilmovsky et al., 2020). Therefore, to further expand on these observations I assessed the frequency of *Rora* expressing CD4 T cells in the lungs following HDM challenge.

As anticipated, consistent with results presented in this thesis, there is a population of *Rora* expressing CD4 T cells in *Rora* reporter mice. Following HDM challenge, there is a significant ($p < 0.01$) increase in frequency of *Rora* expressing CD4 T cells in the lung compared to vehicle treatment *Rora* reporter mice (**Figure 6.3**). These results support Haim-Vilmovsky et al. (2020) which reported an increase in *Rora* expressing CD4 T cells following Ragweed pollen administration. These results also expand on those in **Chapter 4**, that observed following *N. brasiliensis* infection, there is an increase in frequency of *Rora* expressing CD4 T cells. Therefore, taken together, these findings indicate that *Rora* may have a role in lung CD4 T cell development that is consistent across a number of independent models of type 2 immunity.

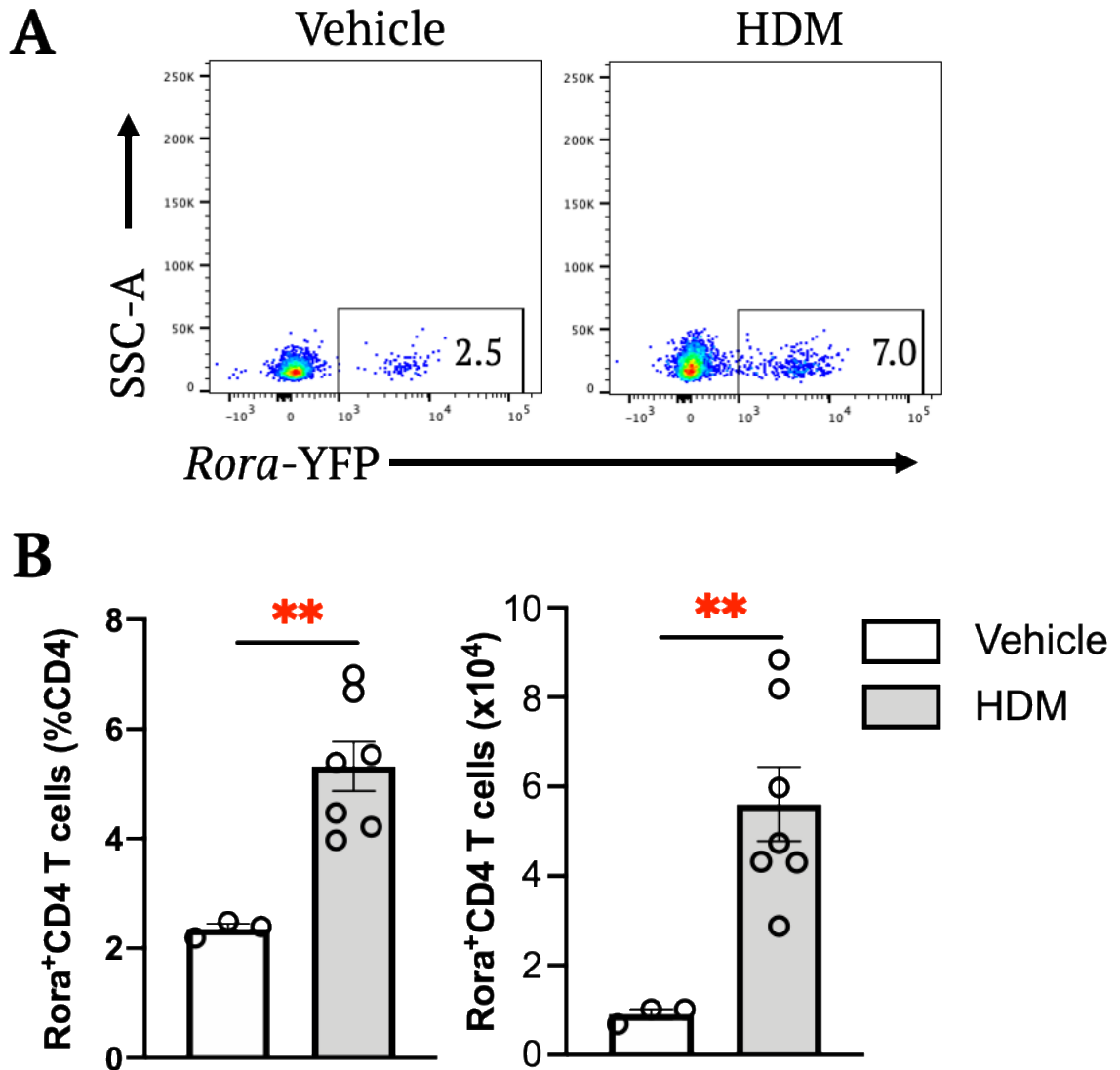


Figure 6.3 Increase in lung *Rora* expressing CD4 T cells following HDM challenge. *Rora* reporter mice were challenged with HDM. Lungs were harvested for flow cytometry analysis. **A**, Representative flow cytometry plots of gating strategy of lung in response to HDM challenge. Cells pre-gated as lymphocytes, single cells, live cells, CD4⁺ and *Rora*-YFP. **B**, Quantification of lung *Rora*-YFP CD4 T cells. Data is representative of mean \pm SEM. Differences indicated as two-tailed *p* values, as assessed by unpaired Student *t* test. ***p*<0.01. ns = non-significant. n = 3-7.

6.3.2.2 Increase in *Rora* expressing lung GATA3⁺ and Foxp3⁺ CD4 T cells following HDM challenge

In **Chapter 4**, I observed that following *N. brasiliensis* infection, there was an increase in *Rora* expressing GATA3⁺CD4 T cells in the lungs, indicating that *Rora* has a role in GATA3⁺CD4 T cell development. To expand on these observations, using the *Rora*

reporter mouse, I assessed the frequency of *Rora* expressing CD4 T cell subsets in response to i.n. HDM. As HDM challenge induces lung Th2, Th17 and Treg cell responses, I identified *Rora* expressing CD4 T cell subsets as per flow cytometry panel used in Halim et al. (2018) and CD4⁺ T cells were gated based on expression of GATA3⁺, Foxp3⁺, GATA3⁺Foxp3⁺ and Rorty⁺.

There is a significant ($p>0.005$) increase in the absolute number of *Rora* expressing GATA3⁺ CD4 T cells in the lungs following HDM treatment (**Figure 6.4**). These findings were consistent with the results presented in **Chapter 4**, which identified that following *N. brasiliensis* infection there was an increase in *Rora* expressing GATA3⁺CD4 T cells in the lungs. Therefore, indicating that these findings were not a helminth-specific observation. ROR α is known to have a role in Th17 cell development (Yang et al., 2008), and indeed there is a significant ($p>0.05$) increase in percentage of *Rora* expressing Rorty⁺ CD4 T cells following HDM challenge. The absolute number of *Rora* expressing Rorty⁺ CD4 T cells is also increased following HDM challenge, however, this did not reach statistical significance (**Figure 6.4**). There was also a significant ($p>0.01$) increase in the absolute number of *Rora* expressing Foxp3⁺CD4 T cells following HDM challenge (**Figure 6.4**). ROR α is known to have a role in Treg function, during skin inflammation (Malhotra et al., 2018), therefore, it is possible that ROR α has a role in lung Tregs during HDM challenge, however this was not apparent in response to *N. brasiliensis* infection. This would be interesting to dissect further to determine if this is apparent in another lung inflammation model. Furthermore, there was also a population of *Rora* expressing GATA3⁺Foxp3⁺ CD4 T cells in the lungs. However, there was no significant difference in frequency between vehicle and HDM treated mice, indicating that *Rora* had no role in GATA3⁺Foxp3⁺ CD4 T cell development following HDM treatment (**Figure 6.4**). Therefore, taken together, these findings support those in **Chapter 4**, that there is an increased frequency of *Rora* expressing GATA3⁺CD4 T cells following lung inflammation, and indicate a role for *Rora* in GATA3⁺CD4 T cell development.

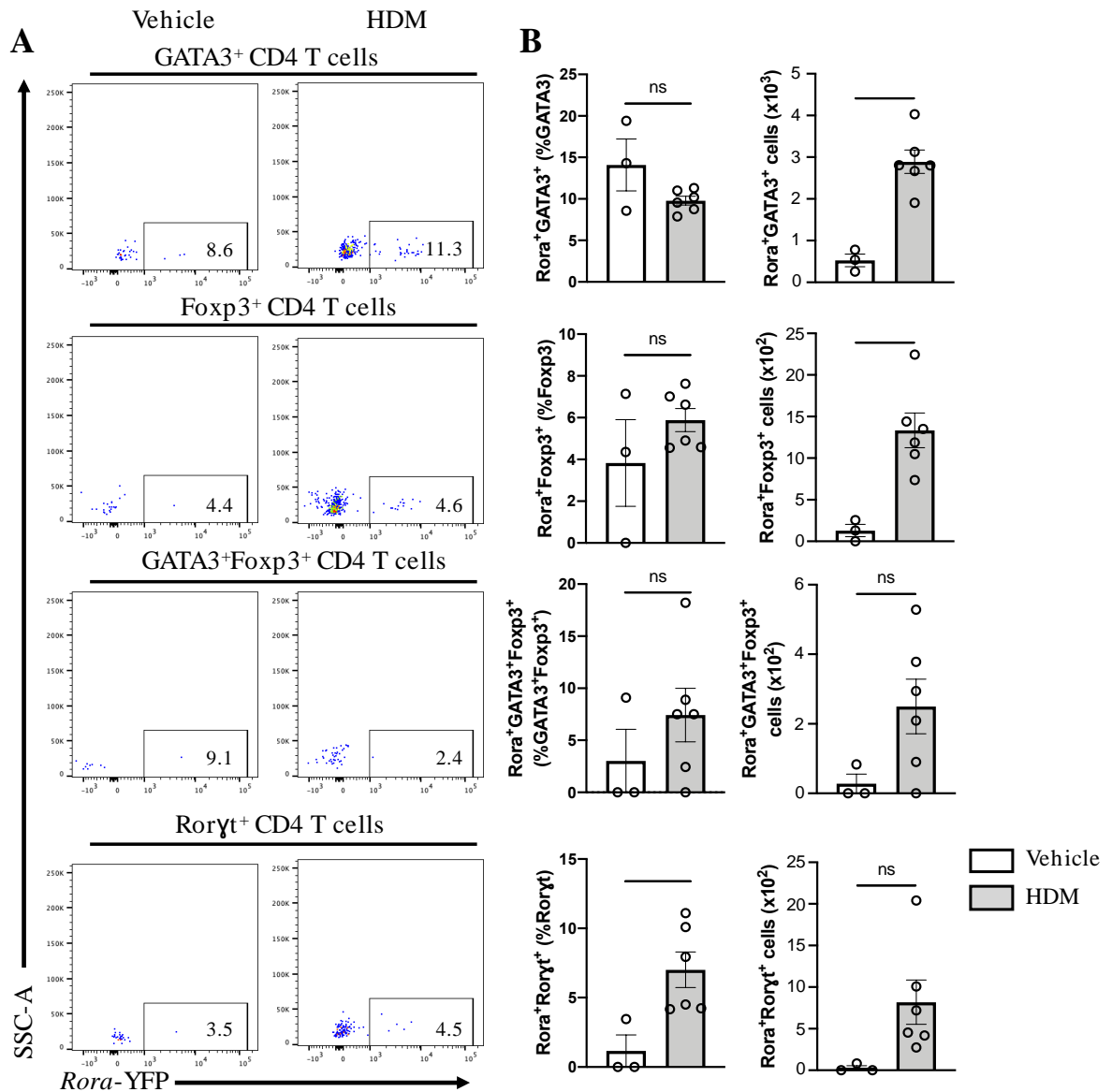


Figure 6.4: Increase in *Rora* expressing GATA3⁺ and Foxp3⁺ CD4 T cells in the lung following HDM challenge. *Rora* reporter mice were challenged with HDM. Lungs were harvested for flow cytometry analysis. **A**, Representative flow cytometry plots of gating strategy of lung in response to HDM challenge. Cells pre-gated as lymphocytes, single cells, live cells, CD4⁺, *Rora*-YFP and either GATA3⁺, Foxp3⁺, GATA3⁺Foxp3⁺ or Roryt⁺. **B**, Quantification of lung *Rora*-YFP CD4 T cells. Data is representative of mean \pm SEM. Differences indicated as two-tailed *p* values, as assessed by unpaired Student *t* test. **p*<0.05, ***p*<0.01, ****p*<0.005. ns = non-significant. n = 3-6.

6.3.2.3 *Rora* expressing lung CD4 T cells are associated T_{EM} CD4 T cells

In **Chapter 4**, it was observed that *Rora* expressing lung CD4 T cells were associated with a T_{EM} phenotype. It was also noticed that following *N. brasiliensis* infection there was an increase in frequency of *Rora* expressing T_{EM}, indicating that ROR α may have a role in development of effector memory lung CD4 T cells during inflammation. To expand on these findings, I investigated the association of lung *Rora* expressing CD4 T cells with T_N (CD62L⁺CD44⁻), T_{CM} (CD62L⁺CD44⁺) and T_{EM} (CD62L⁺CD44⁻) in vehicle and HDM challenged *Rora* reporter mice.

Flow cytometry analysis revealed that *Rora* expressing CD4 T cells were significantly ($p < 0.005$) increased in T_{EM} lung CD4 T cells compared to T_N and T_{CM} CD4 T cells in vehicle treated mice (**Figure 6.5**). Results are presented as a percentage of lung CD4 T cells, in contrast to presenting results as a percentage of T_N, T_{CM}, T_{EM}, respectively. This takes into account changes in frequency T_N, T_{CM}, T_{EM} following HDM, and therefore allows for comparison of *Rora* expressing T_N, T_{CM}, T_{EM} CD4 T cells. Interestingly, following HDM challenge, there is a significant increase in *Rora* expressing T_{EM} lung CD4 T cells compared to T_N and T_{CM} CD4 T cells. These findings support the results in **Chapter 4**, that following *N. brasiliensis* infection, there is an increase in *Rora* expressing T_{EM} CD4 T cells in the lungs compared to control conditions. Therefore, suggesting that *Rora* is associated with T_{EM} CD4 T cells and may have a role in the development during type 2 inflammation.

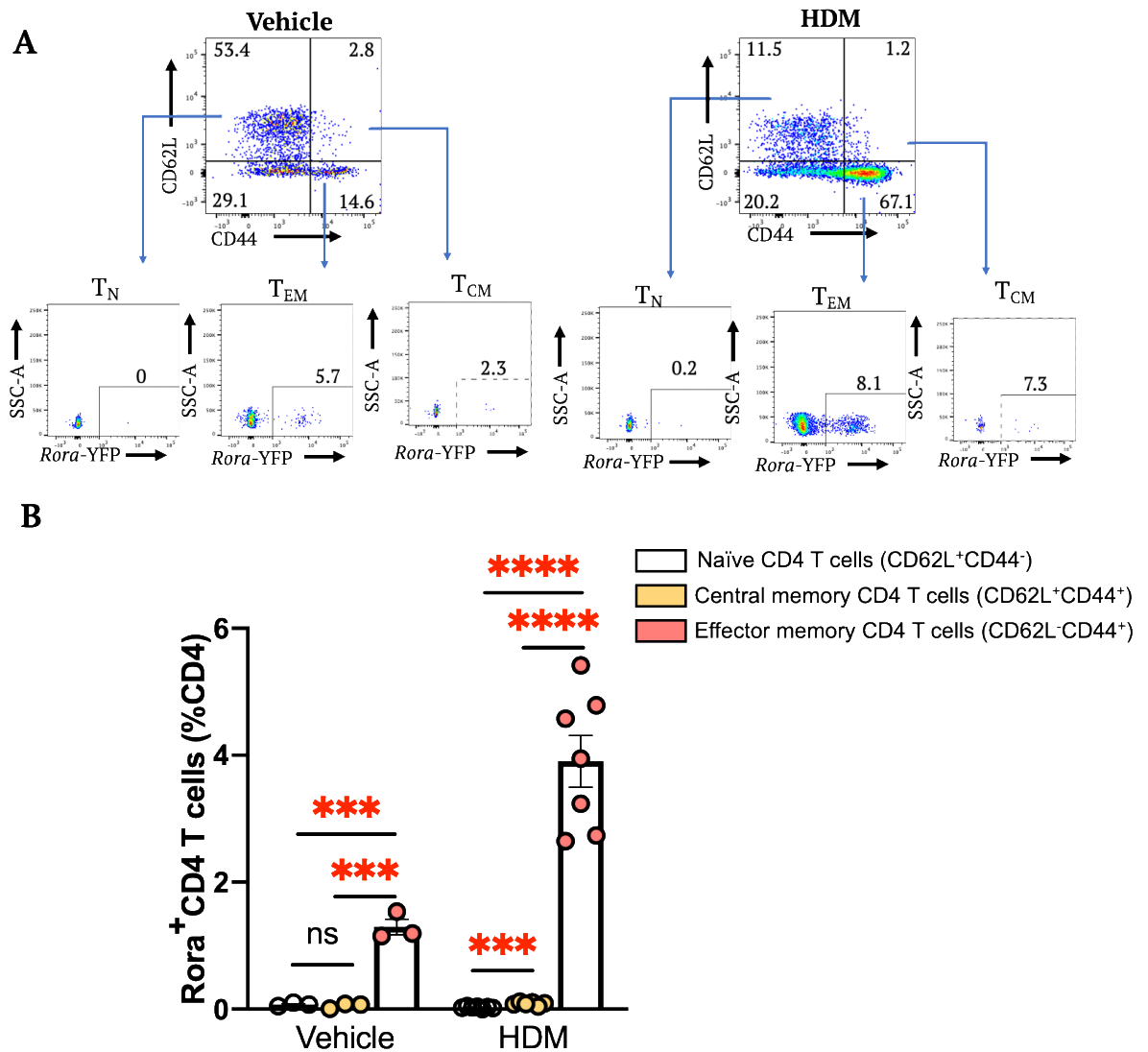


Figure 6.5: *Rora* expressing CD4 T cells are associated with T_{EM} CD4 T cells. *Rora* reporter mice were challenged with HDM. Lungs were harvested for flow cytometry analysis. **A**, Cell populations were gated as lymphocytes, single cells, live, CD45⁺, CD4⁺. Naïve CD4 T cells (T_N) were identified as CD62L⁺CD44⁻. Central memory CD4 T cells (T_{CM}) were identified as CD62L⁺CD44⁺. Effector memory CD4 T cells (T_{EM}) were identified as CD62L⁻CD44⁺. **B**, Quantification of lung *Rora*-YFP expressing naive and activated CD4 T cells. The numbers on flow cytometry plots represents percentage of parent gate. CD44 vs CD62L flow cytometry plot numbers represent percentage of CD4. *Rora*YFP flow cytometry plot numbers represent percentage of T_N, T_{EM}, and T_{CM}, respectively. Data representative of means ± SEM. Differences indicated as two-tailed *p* values, as assessed by unpaired Student *t* test. ns = non-significant. ****p* < 0.005, *****p* < 0.001. n = 3-7.

6.3.2.4 Increase in *Rora* expressing CD69⁺ and CD103⁺ CD4 T cells in the lungs following HDM challenge

In **Chapter 4**, I observed that *Rora* expressing CD4 T cells were associated with activated (CD69⁺) and resident (CD103⁺) markers in the lungs, and following *N. brasiliensis* infection there was an increase in the frequency of *Rora* expressing activated and resident CD4 T cells. Therefore, indicating that *Rora* had a role in activation and resident CD4 T cells during inflammation. To expand on these findings, I investigated the frequency of *Rora* activated and memory CD4 T cells in a helminth-independent model of type 2 immunity.

Consistent with the results presented in **Chapter 4**, there is a population of *Rora* expressing activated and resident CD4 T cells in control mice, with both populations increased following HDM challenge (**Figure 6.6**). These findings expands on a recent publication which reported that *Rora* is associated with activated CD4 T cells following *N. brasiliensis* infection, Ragweed pollen administration and SW1S peptide stimulation (Haim-Vilmovsky et al., 2020). Here, I expand these observations and report an association of *Rora* and activated lung CD4 T cells using the HDM model of type 2 immunity. Furthermore, it has also been recently reported that NLT memory T cells express *Rora* (Miragaia et al., 2019). This supports the findings here that show *Rora* is associated with CD103, a resident CD4 T cell marker. Therefore, taken together, these results provide further indication that *Rora* has a role in activation, memory and residency of CD4 T cells during inflammation.

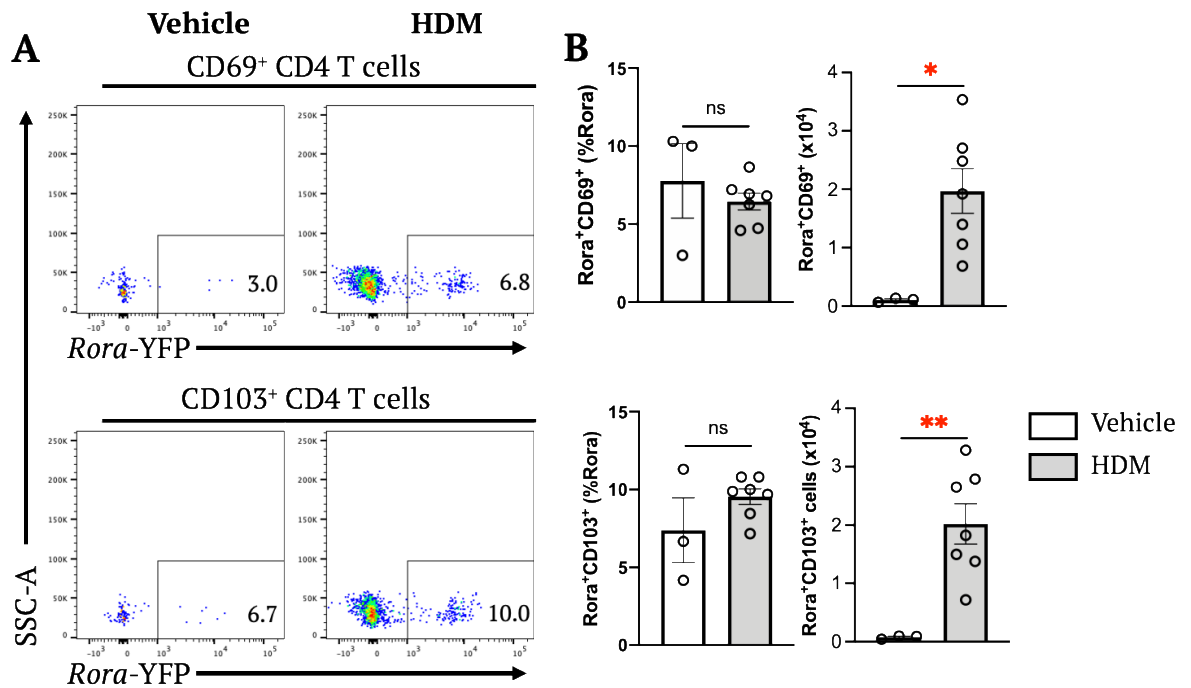


Figure 6.6: Increase in *Rora* expressing CD69⁺ and CD103⁺ CD4 T cells following HDM treatment. *Rora* reporter mice were challenged with HDM. Lungs were harvested for flow cytometry analysis. **A**, Cell populations were gated as lymphocytes, single cells, live, CD45⁺, CD4⁺ and either CD69⁺ or CD103⁺. **B**, Quantification of lung *Rora*-YFP expressing CD69⁺ or CD103⁺ CD4 T cells. Data representative of means \pm SEM. Differences indicated as two-tailed *p* values, as assessed by unpaired Student *t* test. ***p*<0.01. n = 3-7.

6.3.3 Determining the role of the transcription factor ROR α in lung immune cells in the HDM mouse model using *Rora* conditional deleter mice

6.3.3.1 *Rora*^{fl/fl}*CD4Cre* and *Rora*^{fl/fl}*Il7raCre* mice have reduced lung CD4⁺ T cell subsets compared to WT mice in response to HDM challenge

In **Chapter 5**, both *Rora*^{fl/fl}*CD4Cre* and *Rora*^{fl/fl}*Il7raCre* mice were used to investigate the role of *Rora* in CD4 and *Il7ra* expressing cells following *N. brasiliensis* infection. As mentioned, *Rora*^{fl/fl}*Il7raCre* mice are commonly used as a mouse model of ILC2-deficiency. However, in **Chapter 5**, in addition to ILC2s, there is a population of *Rora* expressing *Il7ra*⁺CD4 T cells, and *Rora*^{fl/fl}*Il7raCre* mice have reduced lung CD4 T cells and GATA3⁺CD4 T cells following *N. brasiliensis* infection. The precise interplay between a deficiency of ILC2 and role for ROR α in *Il7ra* expressing CD4 T cells remains unclear. However, in **Chapter 5**, I also observed that *Rora*^{fl/fl}*CD4Cre* mice had a reduced lung GATA3⁺CD4 T cells following *N. brasiliensis* infection, suggesting that in both mouse strains, *Rora* was implicated in the development of GATA3⁺CD4 T cells. Therefore, to expand on these findings, I investigated the frequency of lung CD4 T cell subsets (GATA3⁺, Foxp3⁺, GATA3⁺Foxp3⁺ and Ror γ ⁺) in *Rora*^{fl/fl}*Il7raCre* and *Rora*^{fl/fl}*CD4Cre* mice following HDM challenge.

There is an increase in all CD4 T cell subsets in WT mice following HDM challenge, indicating HDM induced lung inflammation (**Figure 6.7**). However, interestingly, *Rora*^{fl/fl}*Il7raCre* mice had reduced frequency of all lung CD4 T cell subsets (GATA3⁺, Foxp3⁺, Foxp3⁺GATA3⁺ and Ror γ ⁺ cells) in response to HDM treatment, compared to WT mice (**Figure 6.7**). It remains undetermined if this is due to a role of ROR α in *Il7ra* expressing CD4 T cells or due to the effect of ILC2-deficiency. Furthermore, *Rora*^{fl/fl}*CD4Cre* mice had significantly reduced lung GATA3⁺ and GATA3⁺Foxp3⁺ CD4 T cells following HDM treatment compared to WT mice (**Figure 6.7**), whilst comparable frequency of lung Foxp3⁺ and Ror γ ⁺ cells, indicating that *Rora* has a role in GATA3⁺ and GATA3⁺Foxp3⁺ CD4 T cell development, independent of ILC2s.

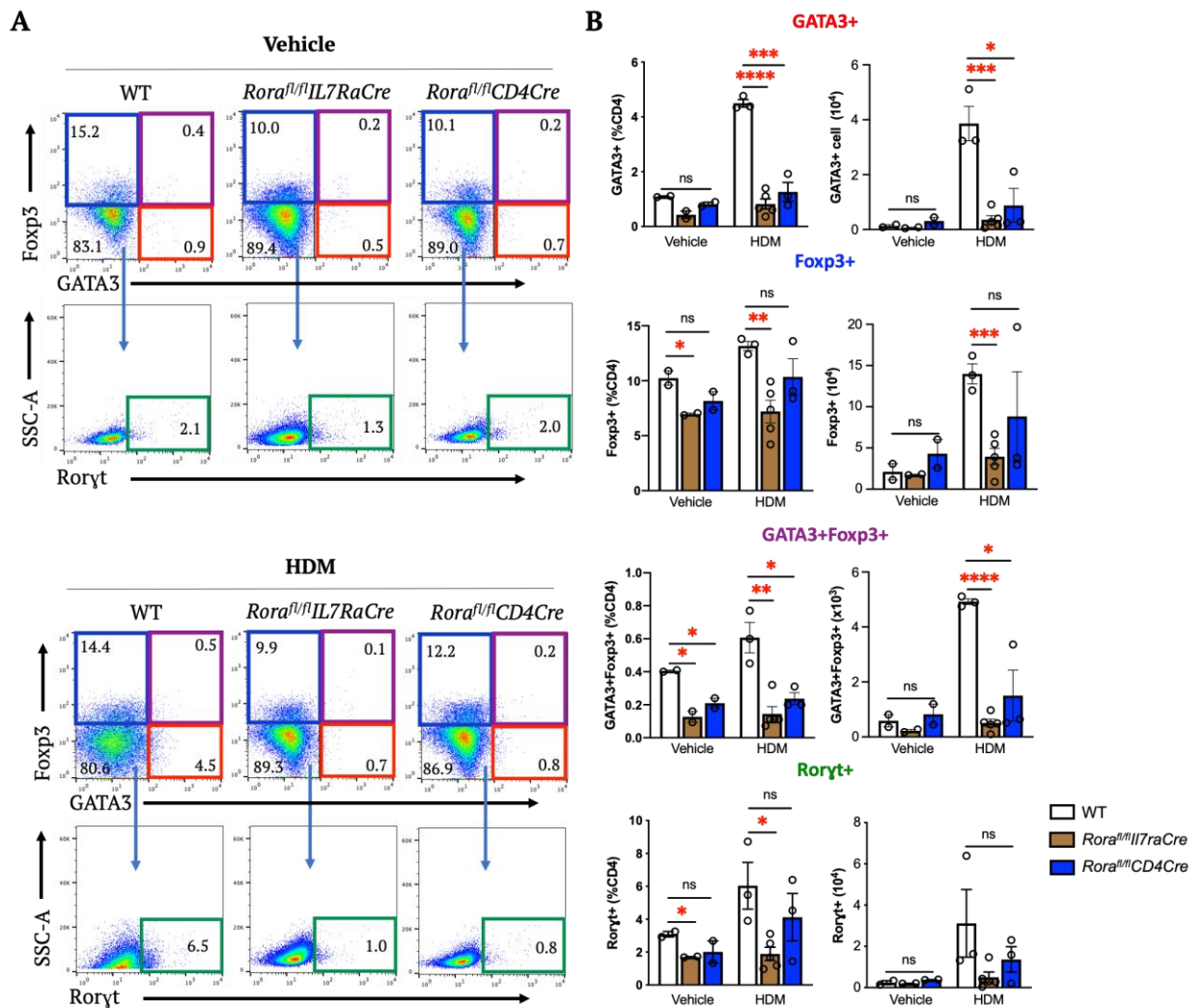


Figure 6.7: *Rora^{fl/fl}CD4Cre* and *Rora^{fl/fl}IL7raCre* mice have altered GATA3⁺ CD4 T cell recruitment in response to HDM challenge compared to WT mice. WT, *Rora^{fl/fl}IL7raCre* and *Rora^{fl/fl}CD4Cre* mice were administered HDM or vehicle treatment. **A**, Representative flow cytometry plots of lung gating strategy. Cells gated as live, single, CD4⁺. T cell subpopulations were gated as GATA3⁺, Foxp3⁺, Foxp3⁺GATA3⁺ and Roryt⁺. **B**, Quantification of lung CD4 T cell subsets. Data is representative of mean ± SEM. The numbers on the flow cytometry plots reflect percentage of CD45⁺ cells. Differences indicated as *p* values, as assessed by Student *t* Test **p*<0.05, ***p*<0.01, ****p*<0.005, *****p*<0.001. ns = non-significant. n = 2-5.

6.3.3.2 *Rora^{fl/fl}Il7raCre* mice have reduced lung eosinophils in response to HDM challenge

In **Chapter 5**, it was observed that *Rora^{fl/fl}Il7raCre* mice had a reduced frequency of lung eosinophils following *N. brasiliensis* infection, whilst *Rora^{fl/fl}CD4Cre* mice had comparable frequency of lung eosinophils with WT mice. To explore if these observations were helminth-specific, I assessed the frequency of lung eosinophils in *Rora^{fl/fl}Il7raCre* and *Rora^{fl/fl}CD4Cre* mice in response to HDM challenge.

There is an increase in lung eosinophils in HDM challenged WT mice (**Figure 6.8**), a hallmark of allergic airway inflammation. Whilst there was comparable frequency of lung eosinophils in *Rora^{fl/fl}CD4Cre* mice and WT mice in both vehicle and HDM challenged mice (**Figure 6.8**). However, *Rora^{fl/fl}Il7raCre* mice show reduced frequency of lung eosinophils in response to HDM (**Figure 6.8**). Therefore, the findings presented here, are consistent with those observed in response to *N. brasiliensis* infection, that *Rora^{fl/fl}CD4Cre* mice had no impact on the frequency of lung eosinophils, whilst *Rora^{fl/fl}Il7raCre* mice had a reduced frequency of lung eosinophils following inflammation. This suggests that the impact on localised eosinophilia in response to type 2 inflammatory challenge that is associated with a deficiency in *Rora* may be due to the decrease in ILC2, rather than as a direct effect of ROR α itself, or through the associated reduction in *Rora*-expressing CD4 T cells. However, further studies are required to understand the exact role of ROR α in ILC2s and CD4 T cells on eosinophil development.

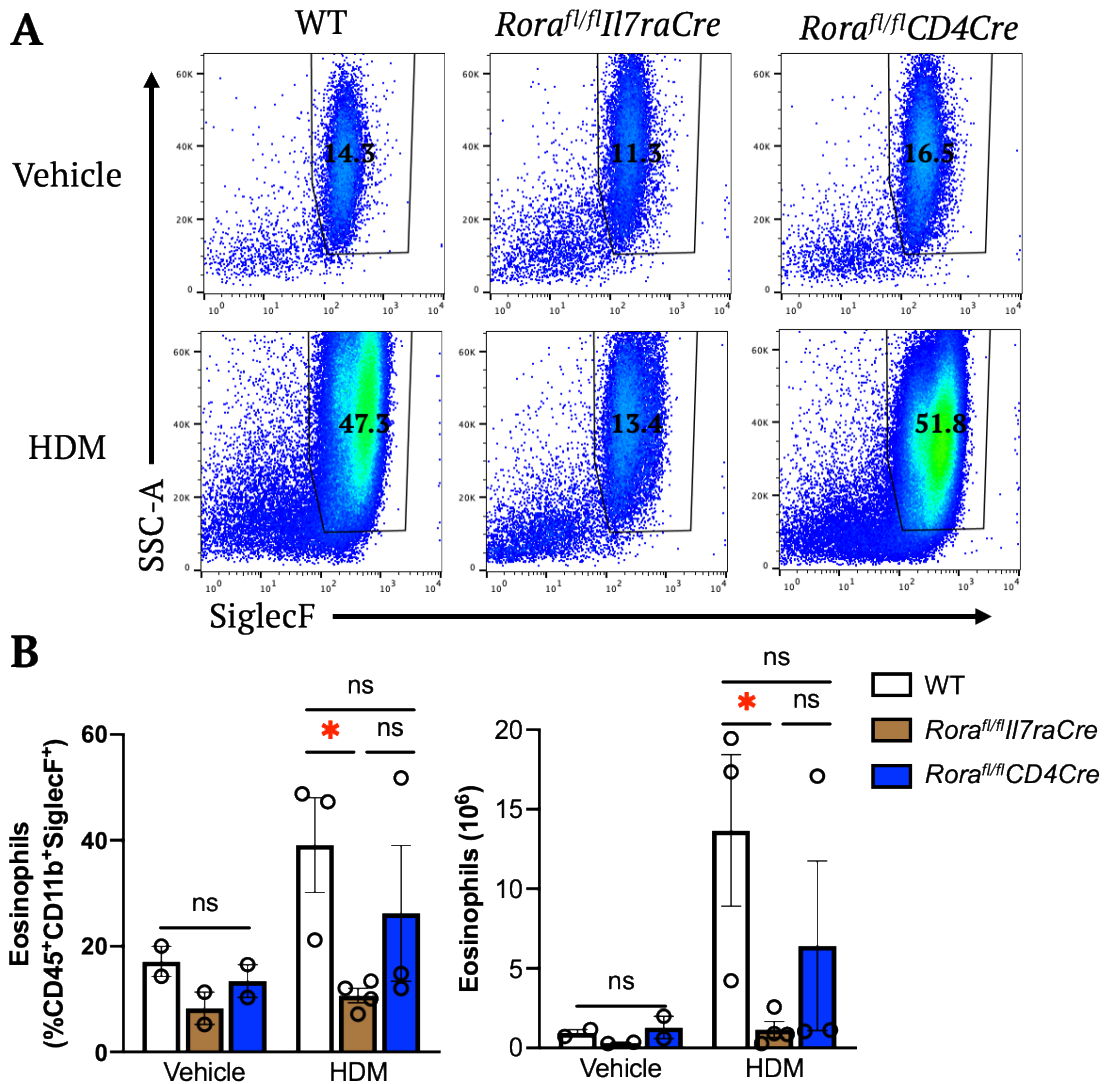


Figure 6.8: *Rora*^{fl/fl}*Il7raCre* mice have reduced lung eosinophils in response to HDM challenge. WT, *Rora*^{fl/fl}*Il7raCre* and *Rora*^{fl/fl}*CD4Cre* mice were administered with HDM or vehicle treatment. **A**, Eosinophils were gated as live cells, single, CD45⁺SiglecF⁺CD11b⁺F4/80⁺CD11c⁻. **B**, Quantification of lung eosinophils. Data is representative of mean ± SEM. Differences indicated as *p* values, as assessed by Student *t* Test. **p*<0.05. ns = non-significant. n = 2-4.

6.4 Discussion

In previous chapters of this thesis, *Rora*^{sg/sg} mice, *Rora* reporter mice, *Rora*^{fl/fl}*CD4Cre* and *Rora*^{fl/fl}*Il7raCre* mice, were used to explore the role of *Rora* during a helminth model of type 2 immunity. The prevailing results indicated a role for *Rora* in either the development, activation or recruitment of GATA3⁺CD4 T (Th2) cells during inflammation. In this chapter, I sought to confirm these observations in a helminth-independent model of type 2 immunity, using i.n. administration of HDM in *Rora*^{sg/sg}, *Rora* reporter, *Rora*^{fl/fl}*CD4Cre* and *Rora*^{fl/fl}*Il7raCre* mice. The HDM mouse model induces allergic airway inflammation, similar to that observed in the human disease asthma (Fallon and Schwartz, 2019). Indeed, ROR α has been associated with asthma, a common chronic inflammatory disease of the airways (Moffatt et al., 2010, Ramasamy et al., 2012, Acevedo et al., 2013, Persson et al., 2015). Furthermore, it was shown that *RORA* was expressed in T cells of the airways in both the healthy control and asthma patients (Vieira Braga et al., 2019), however, the impact of *RORA*-expressing T cells in the context of asthma is not fully understood.

In **Chapter 3**, I demonstrated that *Rora*^{sg/sg} mice had reduced GATA3⁺CD4 T cells following *N. brasiliensis* infection, therefore indicating that *Rora* may have a role in the development of GATA3⁺CD4 T cells. In support of these findings, in this chapter I observed that *Rora*^{sg/sg} mice had reduced lung GATA3⁺ CD4 T cells following HDM challenge, compared with WT mice. Consistent with results presented in this thesis, there was no difference in lung GATA3⁺CD4 T cells between *Rora*^{sg/sg} and WT mice in the control groups, either vehicle treated or uninfected mice. Therefore, indicating that the role of *Rora* in GATA3⁺CD4 T cell development is induced during inflammatory challenge. Using the HDM model, which, unlike *N. brasiliensis*, is associated with a Th17 response, I also observed that *Rora*^{sg/sg} mice had reduced Ror γ ⁺ CD4 T cells, which is in support of the known role of ROR α in Th17 (Ror γ ⁺) cell development (Yang et al., 2008). Furthermore, it was also observed that *Rora*^{sg/sg} mice had reduced lung eosinophils in response to HDM compared to WT mice, suggesting that *Rora* may have a role in eosinophil development during type 2 inflammation. Therefore, taken together, these findings support those presented in **Chapter 3**, that *Rora*^{sg/sg} mice have an altered repertoire of type 2 immune cells, indicating that these observations are not helminth-specific.

In **Chapter 4**, it was observed that following *N. brasiliensis* infection, there was an increase in *Rora* expressing CD4 T cells and GATA3⁺CD4 T cells in the lungs. Consistent with these findings, in this chapter it was observed that following HDM challenge there is an increase in *Rora* expressing CD4 T cells and GATA3⁺CD4 T cells in the lungs. In addition, it was also observed that following HDM challenge, there was an increase in *Rora* expressing Rorγt⁺ (Th17) and Foxp3⁺ (Treg) CD4 T cells. Indeed, RORα is critical for Th17 cell development (Yang et al., 2008), therefore, it was not a surprise to observe an increase in *Rora* expressing Rorγt⁺ (Th17) CD4 T cells. Whilst RORα is known to have a role in Treg cell function in allergic skin inflammation (Malhotra et al., 2018), there was no significant difference in the frequency of *Rora* expressing GATA3⁺Foxp3⁺ CD4 T cells between vehicle and HDM challenge. Therefore, indicating that in this model, *Rora* had no role in the development of GATA3⁺Foxp3⁺ CD4 T cells. Therefore, in corroboration with the *N. brasiliensis* data, following inflammation, there is an increase in *Rora* expressing lung GATA3⁺CD4 T cells, providing further evidence for a role for *Rora* in GATA3⁺CD4 T cell development.

It was also observed in this chapter that *Rora* expressing CD4 T cells were associated with T_{EM}, activated and resident CD4 T cells, whilst following HDM challenge there was an increase in *Rora* expressing T_{EM}, activated, memory and resident CD4 T cells. These findings are consistent with the results presented in **Chapter 4** using *N. brasiliensis* infection as a model of type 2 immunity. These results also expand on a recent publication that reported RORα is associated with activated CD4 T cells following *N. brasiliensis* infection, Ragweed pollen administration and SW1S peptide stimulation (Haim-Vilmovsky et al., 2020). Therefore, in addition to GATA3⁺CD4 T cell development, these results indicate that *Rora* has a role in activation and memory CD4 T cells during inflammation. These findings may indicate RORα could be a novel therapeutic target for mediating CD4 T cell responses (CD4 T cell activation, memory and Th2 cell development), providing benefit during allergic inflammation.

In **Chapter 5**, it was observed that *Rora^{fl/fl}CD4Cre* and *Rora^{fl/fl}Il7raCre* mice had a reduced frequency of lung GATA3⁺CD4 T cells following *N. brasiliensis* infection. Expanding on these observations, results presented in this chapter show that both *Rora^{fl/fl}CD4Cre* and *Rora^{fl/fl}Il7raCre* mice have a reduced frequency of lung GATA3⁺CD4

T cells following HDM challenge compared to WT mice. Therefore, similar results are observed in lung GATA3⁺CD4 T cells through using both the loss of functional *Rora* with Cre-Lox recombination and through a natural mutation (*Rora*^{sg/sg} mice). Both these mouse models of *Rora* manipulation result in reduced lung GATA3⁺CD4 T cells in two models of type 2 immunity. Furthermore, following HDM challenge there was also reduced GATA3⁺Foxp3⁺ CD4 T cells in *Rora*^{fl/fl}CD4Cre mice, indicating that *Rora* may have a role in GATA3⁺Foxp3⁺ CD4 T cell subset development. Interestingly, it was also observed that *Rora*^{fl/fl}Il7raCre mice had reduced frequency of lung Foxp3⁺, GATA3⁺Foxp3⁺ and Rorγt⁺ CD4 T cells compared to WT mice following HDM. It remains unclear if this is due to the interaction between ILC2s or the role of *Rora* in Il7ra expressing CD4 T cells.

Recently, it has been reported that RORα regulates Th2 cellular responses in allergic asthma (Lee et al., 2021). In this publication, it was reported that *Rora* deleted from CD4 T cells enhanced Th2 cellular responses, with increased IL-4/5/13 producing CD4 T cells following two models (Aspergillus/Ovalbumin and HDM) of allergy induced inflammation and *ex vivo* stimulation. This publication draws parallels with this thesis that *Rora* has a role in Th2 cells during a type 2 immune response. However, the focus of this publication highlights that *Rora* has a role in Th2 (Defined by IL-4⁺CD4 T cells) cytokine secretion (IL-5/IL-13). Whilst in this thesis I have identified *Rora* has a role in GATA3⁺ Th2 cellular development during inflammation. Future experiments should investigate the role of *Rora* in GATA3⁺CD4 T cell cytokine secretion.

In summary, the results generated in this chapter using HDM model, a helminth-independent model of type 2 immunity confirm those observed in response to infection with the helminth *N. brasiliensis*. One prevailing observation indicates a role for RORα in GATA3⁺CD4 T cell development and CD4 T cell activation during inflammation.

Chapter 7

Discussion and future directions

Discussion and future directions

Helminth infections and allergic diseases such as asthma are a major public concern. The hygiene hypothesis proposes that stimulation of the immune system by microbes protects from the development of inflammatory diseases. Whilst a reduction to exposure to infectious agents may lead to rise in allergic autoimmune diseases in industrialised countries (Yazdanbakhsh and Matricardi, 2004). Several studies have shown an inverse association between parasites and allergy, and parasite derived molecules to down-regulate immune responses control inflammation diseases such as allergies (Yazdanbakhsh and Matricardi, 2004). The type 2 immune response is central to anti-helminth immunity, allergic inflammation, and tissue homeostasis. ILC2s and CD4 T (Th2) cells are important immune cells that orchestrate a type 2 immune response, yet the complex interplay between the cells involved are not yet fully understood, with novel pathways and even cell types still being identified. Indeed, the innate lymphoid cells (ILCs) are a group of cells that were identified over the last 10 years, with ILC2 integral in the functionality of a type 2 immune response. ROR α , is a transcription factor that plays an important role in regulating inflammation and cellular development, was demonstrated to be critical for ILC2 development (Wong et al., 2012, Halim et al., 2012). The seminal studies which identified the role of *Rora* in ILC2 development utilised the type 2 immune model of *N. brasiliensis* infection (Wong et al., 2012). There is accumulating evidence to suggest a role for *Rora* in CD4 T cells during inflammation, beyond the role of ROR α in the development of Th17 cells (Yang et al., 2008, Liu et al., 2015, Van Dyken et al., 2016, Maggi et al., 2017, Malhotra et al., 2018, Miragaia et al., 2019, Haim-Vilmovsky et al., 2020), and the precise role of ROR α during a type 2 immune response beyond ILC2 development remains not fully understood. Therefore, in this thesis I have investigated the role that the transcription factor ROR α , has in a type 2 immune response.

In Chapter 3, I used *Rora*^{sg/sg} mice, which have a ubiquitous mutation in the *Rora* gene, resulting in translation of a non-functional ROR α protein in all cells, to investigate the role of *Rora* in the generation and maintenance of a type 2 immune response following *N. brasiliensis* infection. In support of previously published data I demonstrated an impaired type 2 response in *Rora*^{sg/sg} mice, exemplified by an increased small intestine

worm count, and reduced lung ILC2s in both uninfected mice and following *N. brasiliensis* infection compared to control mice (Wong et al., 2012, Halim et al., 2012). This data was confirmed using *Rora*^{sg/sg} BM chimeras, in which all cells of a haematopoietic origin have a non-functional ROR α protein, which also demonstrated delayed worm expulsion, as is indicative of decreased functionality of a type 2 response. These data suggest that the impact of ROR α is not due to the phenotypic disparity in *Rora*^{sg/sg} mice, which could potentially impact on the immune responses in these animals, as *Rora*^{sg/sg} BM chimeras are phenotypically comparable with WT animals. Furthermore, in *Rora*^{sg/sg} BM chimeras, cells of a non-haematopoietic origin express a fully functional ROR α , therefore suggesting that there is no apparent role for stromal cells in influencing a type 2 response in this model. Interestingly, it was also observed that both *Rora*^{sg/sg} mice and *Rora*^{sg/sg} BM mice had a reduced frequency of lung CD4 T cells and GATA3⁺CD4 T cells following *N. brasiliensis* infection compared to control mice. In support, a previous study have demonstrated that *Rora*^{sg/sg} BM chimera mice had fewer lung GATA3⁺CD4 T cells compared to WT BM chimera mice following papain challenge (Halim et al., 2014). There was no difference in lung CD4 T cells and GATA3⁺CD4 T cells in uninfected mice, therefore, indicating that *Rora* has a role in the *in vivo* development, activation or recruitment of lung GATA3⁺CD4 T cells during an inflammatory response.

Rora^{sg/sg} mice and *Rora*^{sg/sg} BM chimera mice provide a useful mouse model for exploring the role of ROR α , however, with a functional ROR α absent in every cell in *Rora*^{sg/sg} mice, and haematopoietic cells in *Rora*^{sg/sg} BM chimera mice it is difficult to decipher the precise role of ROR α in specific immune cells. Therefore, in Chapter 4, I generated a *Rora* reporter mouse to investigate *Rora* expressing immune cells implicated in type 2 immunity. As anticipated, I identified a population of *Rora* expressing ILC2s in the lungs of *Rora* reporter mice (Wong et al., 2012, Halim et al., 2012). The expression of *Rora* in ILC2, a population known to be reliant upon expression of ROR α , provided validation of the efficacy of the reporter mice to successfully detect *Rora* by flow cytometry. There is increasing evidence that *RORA/Rora* is expressed in Th2 cells (Van Dyken et al., 2016, Miragaia et al., 2019, Haim-Vilmovsky et al., 2020), and indeed, I identified a population of *Rora* expressing CD4 T cells. To further validate the specificity of the *Rora*-YFP reporter mouse, I confirmed that CD4 T cells expressing *Rora*-YFP also expressed *Rora* mRNA. Further analysis of the *Rora*-YFP expressing CD4 T cells demonstrated that a

subset of this population co-expressed the transcription factors *Gata3* and *Foxp3* mRNA, classical markers for Th2 and Treg cells, respectively. Therefore, indicating that *Rora* may have a role in *Gata3* (Th2) and *Foxp3* (Treg) in CD4 T cells. Indeed, *N. brasiliensis* infection was shown to drive an increase in both *Rora* expressing CD4 T cells and specifically *Rora*⁺GATA3⁺CD4 T cells in the lungs. Whilst analysis of CD4 T cells from the spleens of WT mice infected with *N. brasiliensis* had increased mRNA expression of *Rora*, *Gata3* and *Foxp3* mRNA compared to uninfected mice. These findings support published RNA-Seq analysis, which reported CD4 T cells isolated from the spleen of *N. brasiliensis* infected WT mice had increased *Rora* expression after infection (Haim-Vilmovsky et al., 2020). These data suggest that *Rora* expression is not limited to organs local to the site of inflammation. The data presented in this thesis has largely focused on the lungs, but it may also be apparent that *Rora* has systemic effects following infection. Whilst *in vivo* scRNA-Seq data revealed that *Rora* is elevated in Th2 cells compared to other Th subtypes and *Rora* was lowly expressed in naïve CD4 T cells (Haim-Vilmovsky et al., 2020). scRT-PCR analysis of activated Th2 cells following *N. brasiliensis* infection, showed a significant overlap of *Rora*, *Gata3* and *Foxp3* genes (Haim-Vilmovsky et al., 2020). In separate models of type 2 lung inflammation, following RWP administration, there was an increase in *Rora* expressing CD4 T cells in the lungs (Haim-Vilmovsky et al., 2020), whilst mice challenged with papain and OVA, also have an increased *Rora* expression in lung Th2 cells (Liu et al., 2015). Therefore, taken together with information generated in this thesis, this data suggests that *Rora* is expressed in GATA3⁺CD4 T (Th2) cells, and that these cells are increased during an inflammatory response.

In Chapter 4, it was also observed that *Rora* expressing CD4 T cells were associated with co-expression of both activation markers, and those associated with an effector memory and tissue resident phenotype. These findings presented in this thesis are supported by other studies that identified *Rora* regulates activated T helper cells during inflammation (Haim-Vilmovsky et al., 2020). It is important to note that Haim-Vilmovsky et al. (2020) generated a *Rora* reporter mouse strain which contained a T2A self-cleaving peptide and teal fluorescent protein inserted upstream of the *Rora* stop codon. Whilst in this thesis, a *Rora* reporter mouse was generated using Cre-Lox recombination technology by breeding a *Rora*Cre mice with *Rosa*^{YFP} mice, as previously described in Malhotra et al. (2018). However, it is interesting to note that similar conclusions were drawn from these two

different *Rora* reporter mice strains. I observed that *Rora* expressing CD4 T cells were associated with T_{EM} (CD44⁺CD62L⁻) compared to T_N (CD44⁻CD62L⁺) and T_{CM} (CD44⁺CD62L⁺) cells. Indeed, T_N cells have no prior exposure to the pathogen, T_{CM} are largely restricted to lymphoid organs and the blood, whilst T_{EM} cells are present in the blood and persist in peripheral organs (Gray et al., 2018). It is reported that peripheral effector memory CD4 T cells are important in coordinating host pulmonary immunity and contribute to controlling secondary *N. brasiliensis* infection, and there is redundancy for secondary lymphoid organs derived CD4 T cells following secondary *N. brasiliensis* infection (Thawer et al., 2014). Following *N. brasiliensis* infection, there is an increase in *Rora*⁺CD4 T cells expressing activation (CD69⁺) and resident (CD103⁺) cell markers. There was a further increase in *Rora* expressing CD4 T cells and an increase in *Rora* expressing activated and resident CD4 T cells following secondary *N. brasiliensis* infection. It has been reported that *Rora* is correlated with cytokine-releasing cells, indicating a role for *Rora* in effector cells (Haim-Vilmsky et al., 2020). Therefore, *Rora* may have a role in lung T_{EM} cells development and activation of CD4 T cells during inflammation. As T_{EM} cells have a role in mediating immunity to secondary *N. brasiliensis* infection (Thawer et al., 2014), it may provide a possible opportunity for targeting *Rora* for therapeutic benefit for helminth infections.

Miragaia et al. (2019) highlighted that non-lymphoid tissues (NLT) harbour a pool of adaptive immune cells that differ from LT, and that *Rora* expression was increased in memory T cells following LT to NLT tissue migration. In support of this data, Malhotra et al. (2018) reported an increase in *Rora* expressing Tregs in skin compared to draining lymph nodes, suggesting migration and/or expansion of *Rora* expressing Tregs in peripheral tissues. Haim-Vilmsky et al. (2020) also reported that there was differential expression of *Rora* in CD4 T cells across different tissues. In Chapter 4, I observed an increase in *Rora* expressing CD4 T cells in the lungs (NLT) compared to MLN (LT), suggesting tissue adaptation of *Rora* expressing CD4 T cells. Whilst following *N. brasiliensis* infection, there is an increase in *Rora* expressing CD4 T cells in the lung. However, in the MLN there was no significant difference in frequency of *Rora* expressing CD4 T cells. This suggests that there may be tissue restricted roles for *Rora* in CD4 T cells during inflammation. It has been reported that following Ragweed pollen challenge, there is an increase in frequency of *Rora* expressing CD4 T cells in the lung, but not in the mediastinal lymph nodes (Haim-Vilmsky et al., 2020). Therefore, indicating a role

for *Rora* in NLT CD4 T cells, compared LT. However, it remains to be determined whether circulating *Rora* expressing CD4 T cells are specifically attracted to the lungs or whether the lung environment drives *Rora* expression in CD4 T cells following *N. brasiliensis* infection. Although it has been reported that there is an enrichment of *Rora* expressing cells in peripheral tissues, which is mainly associated with NLT and activated T cells (Haim-Vilmovsky et al., 2020). This may reflect a role for ROR α in T cell activation and effector function, and/or a role in T cell migration to peripheral NLT tissue. It has also been reported that IL-33 leads to activation of Th2 cells and can induce *Rora* expression in Th2 cells (Haim-Vilmovsky et al., 2020). Indeed, the epithelial-derived cytokine IL-33, is critical for initiation of a type 2 immune response and has a pivotal role driving primary and secondary immunity against *N. brasiliensis* (Hung et al., 2013). Therefore, the increase in *Rora* expressing lung CD4 T cells following *N. brasiliensis*, may be mediated through epithelial derived IL-33 cytokine secretion. However, further work is required to delineate the precise role of *Rora* in GATA3⁺CD4 T cells between the lungs (NLT) and mediastinal lymph nodes (LT).

It is interesting to note that lung *Rora* expressing CD4 T cells associated with activated, tissue resident T cells. Therefore, it would be interesting for future experiments to explore the migration/expansion/activation of lung *Rora* expressing CD4 T cells following *N. brasiliensis* infection. To assess whether *Rora* expressing CD4 T cells are recruited from secondary lymphoid organs (SLO) or expand from tissue resident lung cells, experiments should look to block T cell migration from the lymph nodes using Fingolimod (FTY720), as per Thawer et al. (2014). FTY720 is an immunomodulator that acts as an agonist to Sphingosine-1-Phosphate receptor, including lymphopenia by blocking lymphocyte egress from SLO to peripheral sites. Therefore, using FTY720 in a *Rora* reporter mouse, this would identify if there were an increase in lung resident (CD103), activated (CD69) *Rora* expressing CD4 T cells or if these cells arrive by migration from draining lymph nodes following *N. brasiliensis* infection. It should be noted that not all CD69⁺ *Rora* expressing CD4 T cells co-express CD103, therefore possibly indicating distinct subsets of activated, tissue resident *Rora* expressing CD4 T cells. Furthermore, another method to explore migration/expansion of *Rora* expressing CD4 T cells, a *Rora* reporter mouse and a WT mouse could be surgically sutured together (Parabiosis), as per Rahimi et al. (2020). Therefore, following *N. brasiliensis* infection, *Rora*-YFP CD4 T cells expressed in the WT mice would indicate migration of *Rora*-YFP expressing cells through the joint

circulation. However, if there are no *Rora* expressing CD4 T cells detected in WT mice, this would indicate that *Rora* expressing CD4 T cells are tissue resident.

Having identified a possible role for ROR α in CD4 T cells, in Chapter 5, Cre-LoxP recombination technology was used to investigate the role of *Rora* in distinct immune cell populations. *Rora^{fl/fl}CD4Cre* (Halim et al., 2018) and *Rora^{fl/fl}Il7raCre* (Oliphant et al., 2014, Hams et al., 2020) mice were used to explore the role of deletion of *Rora* in CD4- and *Il7ra*-expressing cells, respectively. In support of previous publications, *Rora^{fl/fl}Il7raCre* mice had delayed worm expulsion after primary infection with *N. brasiliensis*, and had ILC2-deficiency (Oliphant et al., 2014). Whilst there was no impact on worm expulsion following primary infection in *Rora^{fl/fl}CD4Cre* mice (Halim et al., 2018). Furthermore, these mice had a comparable frequency of ILC2s with WT mice. *Il7ra* (CD127) is broadly expressed throughout the lymphoid system, with both ILC2s and CD4 T cells expressing *Il7ra* (Fry and Mackall, 2005, Schlenner et al., 2010, Spits et al., 2013, Lev et al., 2019). Expanding on this, I observed populations of *Rora* expressing *Il7ra*⁺CD4 T cells and *Il7ra*⁺ILC2s. Therefore, indicating that *Rora^{fl/fl}Il7raCre* mice have *Rora* excised from *Il7ra* expressing CD4 T cells, which may impact on CD4 T cell development. I observed that *Rora^{fl/fl}Il7raCre* mice had reduced lung GATA3⁺CD4 T cells following *N. brasiliensis* infection. This is consistent with a previous publication that reported *Rora^{fl/fl}Il7raCre* mice had reduced lung GATA3⁺CD4 T cells in response to IL-33 and *N. brasiliensis* infection (Halim et al., 2018). Therefore, indicating that *Rora^{fl/fl}Il7raCre* mice, which are commonly used as ILC2-deficient mouse, may also have altered development of CD4 T cells. However, given the known direct communication between ILC2s and CD4 T cells (Drake et al., 2014, Mirchandani et al., 2014, Oliphant et al., 2014, Schwartz et al., 2017), the underlying mechanisms of ILC2 and GATA3⁺CD4 T cell reduction in these animals remains unclear. Therefore, further studies are required to confirm if the impact on CD4 T cells in these mice is solely due to the ILC2 deficiency, or if there is a standalone effect of *Rora* deletion in *Il7ra* expressing CD4 T cells and if that affects the functionality of the type 2 immune response in these mice.

Rora^{fl/fl}CD4Cre mice were used to investigate the role of *Rora* specifically in CD4 T cells. In support of Haim-Vilmovsky et al. (2020), results presented in this thesis show that naïve *Rora^{fl/fl}CD4Cre* mice had no alterations in frequency of CD4 T cells, indicating that *Rora* had no role in CD4 T cell development in baseline conditions. However, the data

presented in this thesis shows that *Rora^{fl/fl}CD4Cre* mice had a reduced frequency of lung GATA3⁺CD4 T cells following *N. brasiliensis* infection. These results were consistent with the observations in both *Rora^{sg/sg}* mice and *Rora^{sg/sg}* BM chimera mice in Chapter 3. Indeed, there is evidence that shows ILC2s can directly influence Th cell polarisation, which could potentially explain the deficiency in both *Rora^{sg/sg}* and *Rora^{sg/sg}* BM chimera mice (Oliphant et al., 2014, Halim et al., 2016, Schwartz et al., 2017, Drake et al., 2014). However, as *Rora^{fl/fl}CD4Cre* mice have a comparable frequency of ILC2s with control mice, this indicates that the reduced frequency of GATA3⁺CD4 T cells in *Rora^{fl/fl}CD4Cre* is due to role of *Rora* in CD4 T cells, rather than ILC2s influencing Th cell polarisation. It was also observed that *Rora^{fl/fl}CD4Cre* mice had a reduction in proliferating lung GATA3⁺CD4 T cells compared to control mice. This may explain the reduced frequency of GATA3⁺CD4 T cells and may indicate that *Rora* has a role in cellular proliferation. It has previously been reported that *Rora^{fl/fl}CD4Cre* mice had a comparable frequency of GATA3⁺CD4 T cells with control (*Rora^{fl/fl}*) mice following i.n. IL-33 and papain administration (Halim et al., 2018). However, it should be noted that these are different models of immunity to those presented in this thesis, and the frequency of lung GATA3⁺CD4 T cells in *Rora^{fl/fl}CD4Cre* mice following *N. brasiliensis* infection has previously not been reported. Therefore, it may be possible that the role of *Rora* in GATA3⁺CD4 T cells is dependent on the inflammatory model utilised. Indeed, it is widely accepted that ILC2 mediates expulsion of *N. brasiliensis* following primary infection (Fallon et al., 2006, Moro et al., 2010, Neill et al., 2010), whilst CD4 T cells (memory Th2 cell) in the lungs are important at mediating protection following secondary *N. brasiliensis* infection (Harvie et al., 2010, Thawer et al., 2014, Bouchery et al., 2015). Therefore, having identified that *Rora^{fl/fl}CD4Cre* mice have a reduced frequency of lung GATA3⁺CD4 T cells, independent of ILC2s, following primary *N. brasiliensis* infection, future studies should explore the functional role of reduced lung GATA3⁺CD4 T cells in *Rora^{fl/fl}CD4Cre* mice following secondary *N. brasiliensis* infection. Recently, it has also been shown that following *N. brasiliensis* infection, *Rora^{fl/fl}CD4Cre* mice have a higher emphysema score in the lungs compared to infected control mice (Haim-Vilmovsky et al., 2020). Therefore, suggesting that *Rora^{fl/fl}CD4Cre* mice have reduced resolution and repair of lung tissue damage caused by migrating helminths. Therefore, having shown in this thesis that *Rora* has a role GATA3⁺CD4 T (Th2) cellular development, future experiments should investigate the lung pathology and a possible role of *Rora* expressing CD4 T cells in tissue repair

In Chapter 6, I sought to confirm the results generated in other chapters, using a helminth-independent model of type 2 immunity by i.n. HDM challenge. The HDM mouse model induces allergic airway inflammation, similar to that observed in asthma seen in humans (Fallon and Schwartz, 2019). Interestingly, GWAS studies have identified an association of ROR α with asthma (Moffatt et al., 2010, Ramasamy et al., 2012, Acevedo et al., 2013). Furthermore, *RORA* is expressed in T cells of the airways in both the healthy control and asthma patients (Vieira Braga et al., 2019), whilst *RORA* expression was significantly upregulated in patients with therapy-resistant asthma (Persson et al., 2015), suggesting that ROR α may have a role in asthma. However, whilst ROR α is certainly implicated in the pathogenesis of asthma, the precise roles are not yet fully understood. Interestingly, in support of data observed using the helminth model of immunity, *Rora*^{sg/sg} mice had reduced frequency of lung GATA3⁺CD4 T cell following HDM challenge, compared to WT mice. Whilst using the *Rora* reporter mouse, I observed that there was an increase in frequency of *Rora* expressing CD4 T cells and GATA3⁺CD4 T cells in the lungs following HDM challenge. Therefore, these data support the findings in earlier chapters, that *Rora* is required for lung GATA3⁺CD4 T cell development during an inflammatory response. There was also an increase in *Rora* expressing T_{EM} and *Rora* expressing activated (CD69) and resident (CD103) CD4 T cells in the lungs following HDM challenge, indicating that *Rora* may be important for T_{EM} and CD4 T cell activation and memory during inflammation. Furthermore, *Rora*^{fl/fl}*CD4Cre* and *Rora*^{fl/fl}*Il7raCre* mice had reduced lung GATA3⁺CD4 T cells following HDM challenge compared to control mice, further indicating a role for *Rora* in GATA3⁺CD4 T cell development. There was no difference in frequency of lung GATA3⁺CD4 T cells in vehicle treated *Rora*^{sg/sg} mice, *Rora*^{fl/fl}*CD4Cre* and *Rora*^{fl/fl}*Il7raCre* mice, with their respective control mice, indicating that the role of *Rora* in Th2 cells development occurs during an inflammatory response, and is not as a result of a pre-existing disparity in naïve animals. Therefore, these findings indicate that *Rora* has a role in lung GATA3⁺CD4 T cell development and activation during two independent models of type 2 immunity, which is important when this data is compared with data already in the public domain.

To support the findings from the *in vivo* mouse models used in this thesis, I assessed the potential impact of ROR α on T cell polarisation *in vitro*. Analysis of naïve CD4 T cells isolated from *Rora*^{sg/sg} mice and *Rora*^{fl/fl}*CD4Cre* mice demonstrated reduced polarisation

towards a Th2 (GATA3⁺) phenotype compared to control mice. These results support the data generated *in vivo* and provide further indication that *Rora* has a role in GATA3⁺ (Th2) CD4 T cell development. Indeed, it is reported that *RORA* is expressed in *in vitro* expanded human Th2 cells (Maggi et al., 2017), therefore, suggesting that these results may translate to humans, which is interesting given the association of *RORA* with human asthma. However, further studies are required to fully understand the role of ROR α in human Th2 cells, both in the context of health and disease.

The transcription factor GATA3 is classically termed the “master” regulator of Th2 cells (Zhu et al., 2006a), and GATA3 has also been shown to control the differentiation, maintenance and function of ILC2s (Hoyler et al., 2012, Mjosberg et al., 2012). The transcriptional and epigenetic status of lung Th2 and ILC2 cells shares a high degree of similarity, including expression of transcription factors *Rora* and *Gata3* (Van Dyken et al., 2016). Whilst the transcriptional and chromatin landscapes of lung Th2 cells from *N. brasiliensis* infected mice are more closely related to lung ILC2s, compared to naïve CD4 T cells and Th2 cells from the lymph nodes (Shih et al., 2016). In this thesis, using GATA3 as a marker for Th2 cells, and using several mouse strains and mouse models, I report that a deficiency in functional ROR α results in a reduced frequency of GATA3⁺CD4 T cells during inflammation. Indeed, it is reported that GATA3 binds to *Rora* (Yagi et al., 2014), however, *Rora* transcription is not regulated by GATA3 (Mjosberg et al., 2012). In addition to the direct interaction of ROR α and GATA3, ROR α can regulate Peroxisome proliferators-activated receptor gamma (*Pparg*) (Kim et al., 2017) and Basic helix-loop-helix 40 (*Bhlhe40*) (Ozaki et al., 2012) genes. The transcription factors *Pparg* and *Bhlhe40* are part of the core regulatory network governing Th2 cell differentiation (Chen et al., 2017, Henriksson et al., 2019). *Pparg* and *Bhlhe40* are upstream transcription factors that functionally overlap with the central Th2 genes GATA3, BAFT and IRF4 (Henriksson et al., 2019), and PPAR family members can also influence T cell activation and differentiation (Choi and Bothwell, 2012). It has also been shown that Th2 cells were dependent on PPAR- γ for their differentiation into IL-5 and IL-13 producing effector cells (Chen et al., 2017). Therefore, ROR α may have a role in Th2 cell development and activation through regulating *Pparg* and *Bhlhe40* gene expression. Further research is required to fully understand the precise protein-protein

interaction between ROR α and other transcription factors in Th2 cell development during inflammation.

ROR α is known to play an important role in metabolism, and can regulate the metabolism of glucose and lipids (Lau et al., 2008, Kadiri et al., 2015). Indeed, in a separate project to the work reported in this thesis, we have reported a role for ROR α -expressing macrophages in the adipose tissue in altering the metabolic state of mice fed a high-fat diet (Hams et al., 2020). Furthermore, the cellular metabolism of macrophages is altered in the absence of *Rora*, with *Rora*-deficient macrophages increasing oxidative phosphorylation (Hams et al., 2021). In these publications, we generated *Rora^{fl/fl}LysMCre* mice, which do not express *Rora* in myeloid cells. There was no apparent role for *Rora* in myeloid cells during *N. brasiliensis* infection. Th2 cellular differentiation is also associated with a metabolic change, and as an energy-intensive process and requires a switch from oxidative phosphorylation to aerobic glycolysis (Walker and McKenzie, 2018). Therefore, as we have demonstrated that ROR α impacts on cellular metabolism in macrophages, it may also play a role in Th2 cell differentiation through regulating metabolism. This would be an interesting area for further research building upon the findings presented herein and in our recent publications focused on ROR α .

In this thesis, the primary focus was the role of *Rora* in CD4 T cells, however, there was also a significant impact on other immune cells in the absence of functional *Rora*. Of note, the frequency of lung eosinophils was reduced in ILC2-deficient mice (*Rora^{sg/sg}* mice, *Rora^{sg/sg}* BM chimera and *Rora^{fl/fl}Il7raCre* mice) following *N. brasiliensis* infection and HDM challenge. This observation is supported by published literature, which reported following administration of papain, *Rora^{sg/sg}* BM chimera mice and *Rora^{fl/fl}Il7raCre* mice had reduced lung eosinophils compared to control mice (Halim et al., 2014, Halim et al., 2018). However, it remains unclear if the reduced frequency of eosinophils is due to the interaction between ILC2s or if there is a direct impact of ROR α expression in eosinophils. Therefore, further research is required to understand the exact role of ROR α in eosinophil development, which would be particularly interesting given the association of ROR α with allergic lung diseases, which are often associated with significant eosinophilia. Future experiments should look to use an eosinophil specific Cre mice, such as *EpxCre* mice and cross breed these with *Rora^{fl/fl}* mice. This will generate

an eosinophil specific deletion of *Rora* and will allow identification of any intrinsic role of *Rora* in eosinophils. In particular, the role of *Rora* in eosinophil development following *N. brasiliensis* infection. As the observed reduced frequency of eosinophils in *Rora*^{sg/sg}, *Rora*^{sg/sg} BM chimera and *Rora*^{fl/fl}*I17raCre* mice indicates *Rora* may have a role in eosinophil development. Or a possible explanation may be the reduced eosinophils in *Rora*^{sg/sg}, *Rora*^{sg/sg} BM chimera and *Rora*^{fl/fl}*I17raCre* mice is due to reduced frequency of ILC2s and CD4 T cells, and therefore reduced IL-5. Using an eosinophil specific deletion of *Rora* mice will help identify any intrinsic role of *Rora* in eosinophil development.

Table 7.1 outlines the differences in lung immune cells (ILC2s, CD4, GATA3⁺CD4 T cells and eosinophils) in mouse strains used within this thesis following *N. brasiliensis* infection.

Cell type	Mouse strain			
	<i>Rora</i> ^{sg/sg}	<i>Rora</i> ^{sg/sg} BM chimera	<i>Rora</i> ^{fl/fl} <i>I17raCre</i>	<i>Rora</i> ^{fl/fl} <i>CD4Cre</i>
ILC2s	Decreased	Decreased	Decreased	Same
CD4 T cells	Decreased	Decreased	Decreased	Decreased
GATA3 ⁺ CD4 T (Th2) cells	Decreased	Decreased	Decreased	Decreased
Eosinophils	Decreased	Decreased	Decreased	Same
Control	WT	WT BM Chimera	<i>Rora</i> ^{fl/fl}	<i>Rora</i> ^{fl/fl}

Table 7.1: Summary of lung immune cell populations in the different mouse strains used in this thesis following *N. brasiliensis* infection as compared to control mice. Same = same frequency of population as compared to control mice. Decreased = decreased frequency of population as compared to controls.

All experiments in this thesis were conducted in mice or using murine-derived cells. Animal models are a valuable tool enabling us to investigate complex processes and diseases, which may translate to human conditions. Indeed, murine *Rora* is a homologue of human *Rora*, and *RORA/Rora* is expressed in Th2 cells in humans and mice respectively (Van Dyken et al., 2016, Miragaia et al., 2019, Haim-Vilmovsky et al., 2020). However, it should be acknowledged that studies in mice have limitations. For instance, *N. brasiliensis* is a natural rodent helminth which does not naturally infect humans, however, the lifecycle and immune responses elicited by *N. brasiliensis*

resemble that of the human hookworm, therefore a useful mouse model. Furthermore, mice do not develop asthma spontaneously, so the disease has to be artificially induced in the airways by i.n. administration of HDM. This model mimics the airway lung inflammation observed in asthma. Therefore, while both these models allow for the understanding of the role of ROR α in a type 2 immunity in mice, care must be taken when assessing the translatability to human conditions. Nevertheless, mouse models are often used to identify potential therapeutic targets for human conditions, such as allergic diseases including asthma. It is important to note that when developing therapeutic drugs targeting ROR α , it has many roles including cerebellum development, circadian rhythm, metabolism, cancer and cellular development. Therefore, considerations of possible off-target effects on metabolism, cerebellum and cellular development should be considered and the precise targeting of ROR α may be tissue- and time-of-day-dependent.

Rora^{sg/sg} mice contain a 6.4kb intragenic deletion that removes the 122-bp fifth exon, encoding the start of the LBD. Northern blot analysis revealed >10 fold reduction in *Rora* relative to *Gapdh*, consistent with degradation of the mutated RNA through nonsense-mediated decay pathway (Hamilton et al., 1996, Gold et al., 2007). Two independent *Rora*^{-/-} mice were created by gene targeting produced identical phenotype to *Rora*^{sg/sg} mice (Dussault et al., 1998, Steinmayr et al., 1998). However, it should be noted a possible limitation of using *Rora*^{sg/sg} mice could be that as the Rora protein is truncated, it has an intact DBD. Therefore, if nonsense-mediated decay does not occur, it may be possible this the truncated Rora protein could act as a competitor for DNA binding on RORE and interfere with co-regulator functions required for the activity of other nuclear receptors. Therefore, this should be considered when using *Rora*^{sg/sg} mice.

To investigate the role of ROR α in Th2 cells and ILC2s further, we are currently cross breeding *Rora*^{fl/fl} mice with *CD4CreER*^{T2} and *ID2CreER*^{T2} mice to generate *Rora*^{fl/fl}*CD4CreER*^{T2} and *Rora*^{fl/fl}*ID2CreER*^{T2} mice, respectively. These mice have an inducible Cre knockout of *Rora* in CD4 and ID2 (ILC) expressing cells. Therefore, treatment with tamoxifen binds to CreER^{T2} to induce Cre activity, allowing the inducible knockout of *Rora* in CD4 and ID2 cells. Using these mice, we will be able to further understand the role of *Rora* in CD4 and ID2 expressing cells during different stages of inflammation. Future experiments should also explore adoptive transfer of naïve CD4 T cells from *Rora*^{fl/fl} and *Rora*^{fl/fl}*CD4Cre* mice into *Rag1*^{-/-} mice to further examine the role

of *Rora* in GATA3⁺CD4 T cell development and if *Rora* has a functional role in CD4 T cells during in helminth infection. In addition, CD4 T cells could be pre-labelled with CFSE prior to transfer to investigate the role of *Rora* on proliferation during inflammation. Furthermore, having generated a *Rora* reporter mouse, it would be interesting adoptively transfer *Rora* expressing CD4 T cells into WT mice and investigate the migration, recruitment and proliferation of *Rora* expressing CD4 T cells during inflammation. Further studies should also investigate the role of ROR α in Th2 cell metabolism. By assessing the oxygen consumption rate (OCR) and extracellular acidification rate (ECAR) of cultured Th2 cells it is possible to generate a metabolic profile of Th2 cells from *Rora*^{sg/sg} and *Rora*^{fl/fl}CD4Cre mice. Additionally, there has been a significant advancement of single cell technology over the last few years. Indeed, flow cytometers can now analyse 30+ parameters and Mass Cytometry (CyTOF Fluidigm™), which uses antibodies conjugated with heavy metal ion tags, can analyse 40+ parameters per single cell. Whilst advances in single cell RNA-sequencing would allow for exploring the expression profile of single *Rora* expressing cells. Therefore, these advances in single cell technologies would be beneficial to further understand the precise role of *Rora* in immune cells during a type 2 immune response.

In summary, in this thesis I have identified a role for *Rora* in Th2 cells during type 2 inflammation. Initial results identified that *Rora*^{sg/sg} mice and *Rora*^{sg/sg} BM chimera mice have delayed *N. brasiliensis* expulsion, ILC2-deficiency and had a reduced frequency of lung CD4 T cell and GATA3⁺CD4 T cells following *N. brasiliensis* infection. In support of these findings, *Rora*^{sg/sg} mice had reduced lung GATA3⁺CD4 T cells following HDM challenge. Supporting these observations, using a *Rora* reporter mouse, I identified a population of *Rora* expressing CD4 T cells in the lungs in uninfected conditions, with increases in populations of *Rora* expressing CD4 T and GATA3⁺CD4 T cells in the lung following induction of two separate models of type 2 immunity (*N. brasiliensis* and HDM). Following secondary *N. brasiliensis* infection, *Rora*^{sg/sg} BM chimera mice failed to develop resistance to reinfection, compared to WT BM chimera mice, indicating an altered adaptive type 2 immune response. Furthermore, I also show that there is an association of *Rora* expressing CD4 T cells co-expressing T_{EM}, activated and memory cell markers and following models of type 2 immunity (*N. brasiliensis* infection and HDM), there was an increase in *Rora* expressing T_{EM}, activated and memory CD4 T cells, indicating that ROR α has a role in T_{EM}, activation and memory CD4 T cells. Therefore,

having identified that *Rora* may have a role in CD4 T and GATA3⁺CD4 T cells development during inflammatory insult, I used *Rora*^{fl/fl}*CD4Cre* mice, in which *Rora* is deleted in CD4 cells, to further investigate the role of ROR α in CD4 T cells. Indeed, consistent with the results observed in *Rora*^{sg/sg} mice and *Rora*^{sg/sg} BM chimera mice, following *N. brasiliensis* infection and HDM challenge, *Rora*^{fl/fl}*CD4Cre* mice had a reduced frequency of lung GATA3⁺CD4 T cells. Whilst *Rora*^{fl/fl}*CD4Cre* mice had comparable frequency of ILC2s with WT mice, in uninfected mice and following *N. brasiliensis* infection, therefore indicating that the reduced GATA3⁺CD4 T cells was ILC2 independent. In addition, I observed that *Rora*^{fl/fl}*CD4Cre* mice had reduced frequency of proliferating GATA3⁺CD4 T cells, which may explain the reduced frequency of lung GATA3⁺CD4 T cell following *N. brasiliensis* infection. Whilst in support of the *in vivo* results, naïve CD4 T cells from *Rora*^{sg/sg} mice and *Rora*^{fl/fl}*CD4Cre* mice had reduced *in vitro* polarisation towards GATA3⁺ (Th2) cells. Therefore, the data presented in this thesis, cumulatively indicate that *Rora* is required for full GATA3⁺CD4 T (Th2) cell development and activation during type 2 inflammation.

In conclusion, I report a role for ROR α in CD4 T cell activation and Th2 development during type 2 immunity (**Figure 7.1**). These cells are important for orchestrating type 2 immunity. Therefore, these results may provide a possible opportunity for targeting *Rora* for therapeutic benefit in allergic disorders such as asthma, or other type 2 inflammatory conditions.

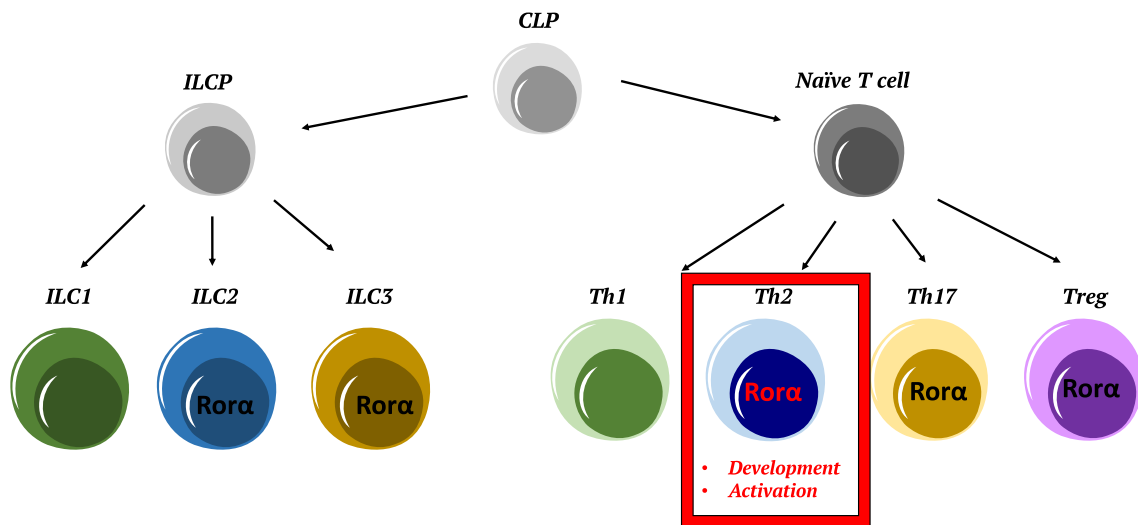


Figure 7.1: Overview of ROR α role in lymphoid cells. The results presented in this thesis indicates that *Rora* contributes to GATA3⁺CD4 (Th2) cellular development and activation during inflammation.

Appendices

7.1 Appendix I

DNA sequence: *Rora^{fl/fl}* mice

...GCAGAAAGCCTATGACAAGGCCAAGGTCTTCAAGTCTCTGAATCCACCATACTTCCAGCA
GTCTTGTGGCTTTGCAAAGCCTCTCTCCTCCATCCCCTGGGGCACAAACACAGGCGGTTTCC
ATCTTCTTAGCTATACAAAGGAAACCAAATGTCAGCACATTGCTTTAAGTGAGTTGCTTTTT
AAGGGCCGCTCTAGAGGCCATAGCGGCCGGCCATAACTTCGTATAGCATAACATTATACGAA
GTTATGGCGCGCCGTGGATGACACCGGCAGAAGAGTATTATTGGCTCCTAAAATAACGTGG
CTGTTTCATGGTCGTGATCTCCTGTTTTCTCCCCAGAACACCTTGCCCAGAACATATCCAAATC
CCACCTGGAACCTGCCAGTACTTGCGGGAAGAGCTCCAGCAGATAACGTGGCAGACCTTC
CTGCAGGAGGAGATTGAAAACCTACCAGAACAAGGTAGAGTTGGAGGACTTTCTCTTCCCAC
CGAGGCAACATTGGGTGGGGGTGGGAGAAGGGCATTCAAGAGTCCAGACAGACAGCGCG
CGCCCTCGAGCTTTCGGAAGTTCCTATTCGGAAGTTCCTATTCTCTAGAAAGTATAGGAACTT
CTCGAGATCCGATATCGAATTCGCCGCCAGCTGGTTCTTCCGCCTCAGAAGCCATAG
AGCCCACCGCATCCCCAGCATGCCTGCTATTGTCTTCCCAATCCTCCCCCTTGCTGTCTGCTGCC
CCACCCACCCCCAGAATAGAATGACACCTACTCAGACAATGCGATGCAATTCCTCATTT
TATTAGGAAAGGACAGTGGGAGTGGCACCTTCCAGGGTCAAGGAAGGCACGGGGGAGGGG
CAAACAACAGATGGCTGGCAACTAGAAGGCACAGTCGAGGCTGATCAGCGAGCTCTAGAGA
ATTGATCCCCTCAGAAGAAGTTCGTCAAGAAGGCGATAGAAGGCGATGCGCTGCGAATCGGG
AGCGGCGATACCGTAAAGCACGAGGAAGCGGTCAGCCATTCGCCGCCAAGCTCTTCAGCA
ATATCACGGGTAGCCAACGCTATGTCCTGATAGCGATCCGCCACACCCAGCCGGCCACAGTC
GATGAATCCAGAAAAGCGGCCATTTTCCACCATGATATTCGGCAAGCAGGCATCGCCATGG
GTCACGACGAGATCCTCGCCGTCGGGCATGCGCGCCTTGAGCCTGGCGAACAGTTCGGCTGG
CGCGAGCCCCTGATGCTCTTCGTCCAGATCATCCTGATCGACAAGACCGGCTTCCATCCGAG
TACGTGCTCGCTCGATGCGATGTTTTCGCTTGGTGGTTCGAATGGGCAGGTAGCCGGATCAAGC
GTATGCAGCCGCCGATTGCATCAGCCATGATGGATACTTTCTCGGCAGGAGCAAGGTGAG
ATGACAGGAGATCCTGCCCGGCACTTCGCCCAATAGCAGCCAGTCCCTTCCCGCTTCAGTG
ACAACGTTCGAGCACAGCTGCGCAAGGAACGCCCGTTCGTGGCCAGCCACGATAGCCGCGCTG
CCTCGTCTGCAGTTCATTCAAGGCACCGGACAGGTTCGGTCTTGACAAAAAGAACCGGGCG
CCCCTGCGCTGACAGCCGGAACACGGCGGCATCAGAGCAGCCGATTGTCTGTTGTGCCCAGT
CATAGCCGAATAGCCTCTCCCAAGGCGGCCGGAGAACCCTGCGTGCAATCCATCTTGTTCAAT
GGCCGATCCCATTATGACCTGCAGGTCGAAAGGCCCGGAGATGAGGAAGAGGAGAACAGC
GCGGCAGACGTGCGCTTTTGAAGCGTGCAGAATGCCGGGCTCCGGAGGACCTTCGCGCCCG
CCCCGCCCTGAGCCCGCCCTGAGCCCGCCCCGGACCCACCCCTTCCAGCCTCTGAGCC
CAGAAAGCGAAGGAGCCAAGCTGCTATTGGCCGCTGCCCAAAGGCCTACCCGCTTCCATT
GCTCAGCGGTGCTGTCCATCTGCACGAGACTAGTGAGACGTGCTACTTCCATTTGTCACGTC
CTGCACGACGCGAGCTGCGGGGCGGGGGGAACCTTCTGACTAGGGGAGGAGTAGAAGGT
GGCGCGAAGGGGCCACCAAAGAAGGGAGCCGGTGGCGCTACCGGTGGATGTGGAATGTGT
GCGAGGCCAGAGGCCACTTGTGTAGCGCCAAGTGCCAGCGGGGCTGCTAAAGCGCATGCTC
CAGACTGCCTTGGGAAAAGCGCCTCCCCTACCCGGTAGGGCGCGGGAATTCGATATCGAATT
CGAGCTCGGTACCCGGGGATCGAAGTTCCTATTTCGGAAGTTCCTATTCTCTAGAAAAGTATAG
GAACTTCTCGACCTGCAGGCATGCAAGCTGATCCGGCGCGTATAACTTCGTATAGCATAACAT
TATACGAAGTTATCCTCAGGCCAGCGAGGCCGGTACCCAATTTCGCCCTATAGCAAGGCTGAC
TGTCCTGCATCAGAGCTCAAGTCTCTGATCAGGATCTTACAGCCAGAGCTTTGTTGTCTTCT
GAGATGCTAGCGTGTGAAAGTTCAGCTGGAACAAAGTTTATTGTGTTTCGTAAGTCTTCTCT
TTGTGCCAGTTGGGATAACTGGATCGGG...

Yellow = LoxP sequences

Grey = 30 and 31 Primers

Underlined = Loxp5 and Loxp3 primers

7.2 Appendix II

Genotyping Reagents

DreamTaq Green Buffer (Fermentas)

dNTPs (dATP, dCTP, dGCTP, dTTP) (Promega, USA)

Primers (Sigma, UK)

Dream Taq DNA Polymerase (ThermoScientific)

Distilled Water (DNase/RNase Free) (Invitrogen)

Genotyping Protocols

CD4Cre

Step	Temp (°C)	Time	Note	Process
1	94	3 min		Hot start
2	94	30 sec		Denaturation
3	64	1 min		Annealing
4	72	1 min	Repeat steps 2-4 for 35 times	Elongation
5	72	2 min		Elongation
6	10	Hold		Hold

Il7raCre

Step	Temp (°C)	Time	Note	Process
1	94	2 min		Hot start
2	94	30 sec		Denaturation
3	55	30 sec		Annealing
4	72	30 sec	Repeat steps 2-4 for 30 times	Elongation
5	4	Hold		Elongation

Rora^{fl/fl}

Step	Temp (°C)	Time	Note	Process
1	94	15 sec		Denaturation
2	65	30 sec	Decrease by 1°C every cycle	Annealing
3	72	40 sec	Repeat steps 1-3 for 10 times	Elongation
4	94	15 sec		Denaturation
5	55	30 sec		Annealing
6	72	40 sec	Repeat steps 4-6 for 30 times	Elongation
7	4	Hold		Hold

Rora^{sg/sg}

Step	Temp (°C)	Time	Note	Step
1	94	3 min		Hot start
2	94	20 sec		Denaturation
3	54	1 min		Annealing
4	72	1 min	Repeat steps 2-4 for 35 times	Elongation
5	72	2 min		Elongation
6	10	Hold		Hold

RoraCre

Step	Temp (°C)	Time	Note	Step
1	94	4 min		Hot start
2	94	30 sec		Denaturation
3	53	35 sec		Annealing
4	72	1 min 15 sec	Repeat steps 2-4 for 35 times	Elongation
5	72	7 min		Elongation
6	10	Hold		Hold

RosaYFP

Step	Temp (°C)	Time	Note	Step
1	94	2 min		Hot start
2	94	20 sec		Denaturation
3	65	15 sec	Decrease by 0.5°C every cycle	Annealing
4	68	10 sec	Repeat steps 2-4 for 10 times	Elongation
5	94	15 sec		Denaturation
6	60	15		Annealing
7	72	15 sec	Repeat steps 5-7 for 28 times	Elongation
8	72	2 min		Elongation
9	4	Hold		Hold

7.3 Appendix III

qPCR Probes

All probes were purchased from Thermo Fisher Scientific.

Murine gene	Assay Code
<i>Rora</i>	Mm00443103_m1
<i>Gata3</i>	Mm00484683_m1
<i>Foxp3</i>	Mm00475162_m1
<i>Tbet</i>	Mm00450960_m1
<i>Rorgt</i>	Mm01261022_m1
<i>18S</i>	4318839

7.4 Appendix IV

Flow Cytometry Antibodies

Antibody	Fluorochrome	Clone	Company
CD3	FITC	17A2	eBioscience
CD3	APC	17A2	eBioscience
CD3	eFluor 450	17A2	eBioscience
CD3e	PE-eFluor 610	145-2C11	eBioscience
CD4	PerCP-Cy5.5	RM4-5	eBioscience
CD4	APC	RM4-5	BD Biosciences
CD4	APC-eFluor 780	RM4-5	eBioscience
CD8	APC-eFluor 780	53-6.7	Invitrogen
CD11b	PerCP-Cy5.5	M1/70	eBioscience
CD11b	eFluor 450	M1/70	eBioscience
CD11c	PE	HL3	BD Biosciences
CD11c	eFluor 450	N418	eBioscience
CD19	APC	1D3	BD Biosciences
CD19	PerCP-Cy5.5	1D3	BD Biosciences
CD19	eFluor 450	eBio1D3	eBioscience
CD25	APC-eFluor 780	PC61.5	eBioscience
CD38	PE-Cy7	90	Invitrogen
CD44	PerCP-Cy5.5	IM7	BD Biosciences
CD44	PE	IM7	BD Biosciences
CD45.1	FITC	A20	BD Biosciences
CD45.1	PE	A20	BD Biosciences
CD45.2	PerCP-Cy5.5	30-F11	eBioscience
CD45.2	V450	104	BD Biosciences
CD62L	V450	MEL-14	BD Biosciences
CD69	PE	H1.2F3	eBioscience
CD103	PE-CF594	M290	BD Biosciences
CD206	PE-Cy7	C068C2	Biologend
F4/80	eFluor 450	BM8	eBioscience
F4/80	FITC	BM8	Biologend
FOXP3	Pe-Cy7	FJK-16s	eBioscience
FOXP3	PE-CF594	MF23	BD Biosciences
GATA3	PE	TWAJ	Invitrogen
GATA3	eF660	TWAJ	Invitrogen
Gr-1 (Ly-6G/Ly-6C)	APC-Cy7	RB6-8C5	Biologend
KLRG1	PE-eFluor 610	2F1	Invitrogen
KLRG1	BV421	2F1	BD Biosciences
Ly6C	FITC	HK1.4	Biologend
Ly6C	PerCP	HK1.4	Biologend
Ly6G (Gr1)	eFluor 450	RB6-8C5	eBioscience
NK1.1	PE-Cy7	PK136	eBioscience
PD-L2 (CD273, B7-DC)	FITC	122	eBioscience

Rorgt	BV421	Q31-378	BD Biosciences
Sca-1/Ly-6A/E	PE-Cy7	D7	BD Biosciences
SiglecF	PE	E50-2440	BD Biosciences
T1/ST2	FITC	DJ8	MD Bioproducts
TBET	AF647	O4-46	BD Biosciences
TER-119	eFluor 450	TER-119	eBioscience
$\gamma\delta$ TCR	eFluor 450	eBioGL3	eBioscience

References

- Abel, A. M., Yang, C., Thakar, M. S. & Malarkannan, S. 2018. Natural Killer Cells: Development, Maturation, and Clinical Utilization. *Front Immunol*, 9, 1869.
- Acevedo, N., Saaf, A., Soderhall, C., Melen, E., Mandelin, J., Pietras, C. O., Ezer, S., Karisola, P., Vendelin, J., Gennas, G. B., Yli-Kauhaluoma, J., Alenius, H., Von Mutius, E., Doekes, G., Braun-Fahrlander, C., Riedler, J., Van Hage, M., D'amato, M., Scheynius, A., Pershagen, G., Kere, J. & Pulkkinen, V. 2013. Interaction between retinoid acid receptor-related orphan receptor alpha (RORA) and neuropeptide S receptor 1 (NPSR1) in asthma. *PLoS One*, 8, e60111.
- Ahyi, A. N., Chang, H. C., Dent, A. L., Nutt, S. L. & Kaplan, M. H. 2009. IFN regulatory factor 4 regulates the expression of a subset of Th2 cytokines. *J Immunol*, 183, 1598-606.
- Akashi, M. & Takumi, T. 2005. The orphan nuclear receptor RORalpha regulates circadian transcription of the mammalian core-clock Bmal1. *Nat Struct Mol Biol*, 12, 441-8.
- Allan, R. S., Zueva, E., Cammas, F., Schreiber, H. A., Masson, V., Belz, G. T., Roche, D., Maison, C., Quivy, J. P., Almouzni, G. & Amigorena, S. 2012. An epigenetic silencing pathway controlling T helper 2 cell lineage commitment. *Nature*, 487, 249-53.
- Allen, J. E. & Maizels, R. M. 2011. Diversity and dialogue in immunity to helminths. *Nat Rev Immunol*, 11, 375-88.
- Allen, J. E. & Sutherland, T. E. 2014. Host protective roles of type 2 immunity: parasite killing and tissue repair, flip sides of the same coin. *Semin Immunol*, 26, 329-40.
- Amin, K. 2012. The role of mast cells in allergic inflammation. *Respir Med*, 106, 9-14.
- Anthony, R. M., Urban, J. F., Jr., Alem, F., Hamed, H. A., Rozo, C. T., Boucher, J. L., Van Rooijen, N. & Gause, W. C. 2006. Memory T(H)2 cells induce alternatively activated macrophages to mediate protection against nematode parasites. *Nat Med*, 12, 955-60.
- Athari, S. S. 2019. Targeting cell signaling in allergic asthma. *Signal Transduct Target Ther*, 4, 45.
- Auffray, C., Fogg, D. K., Narni-Mancinelli, E., Senechal, B., Trouillet, C., Saederup, N., Leemput, J., Bigot, K., Campisi, L., Abitbol, M., Molina, T., Charo, I.,

- Hume, D. A., Cumano, A., Lauvau, G. & Geissmann, F. 2009. CX3CR1+ CD115+ CD135+ common macrophage/DC precursors and the role of CX3CR1 in their response to inflammation. *J Exp Med*, 206, 595-606.
- Aviello, G., Corr, S. C., Johnston, D. G., O'Neill, L. A. & Fallon, P. G. 2014. MyD88 adaptor-like (Mal) regulates intestinal homeostasis and colitis-associated colorectal cancer in mice. *Am J Physiol Gastrointest Liver Physiol*, 306, G769-78.
- Besnard, S., Heymes, C., Merval, R., Rodriguez, M., Galizzi, J. P., Boutin, J. A., Mariani, J. & Tedgui, A. 2002. Expression and regulation of the nuclear receptor RORalpha in human vascular cells. *FEBS Lett*, 511, 36-40.
- Bitsch, F., Aichholz, R., Kallen, J., Geisse, S., Fournier, B. & Schlaeppli, J. M. 2003. Identification of natural ligands of retinoic acid receptor-related orphan receptor alpha ligand-binding domain expressed in Sf9 cells--a mass spectrometry approach. *Anal Biochem*, 323, 139-49.
- Björklund Å, K., Forkel, M., Picelli, S., Konya, V., Theorell, J., Friberg, D., Sandberg, R. & Mjösberg, J. 2016. The heterogeneity of human CD127(+) innate lymphoid cells revealed by single-cell RNA sequencing. *Nat Immunol*, 17, 451-60.
- Bouchery, T., Kyle, R., Camberis, M., Shepherd, A., Filbey, K., Smith, A., Harvie, M., Painter, G., Johnston, K., Ferguson, P., Jain, R., Roediger, B., Delahunty, B., Weninger, W., Forbes-Blom, E. & Le Gros, G. 2015. ILC2s and T cells cooperate to ensure maintenance of M2 macrophages for lung immunity against hookworms. *Nat Commun*, 6, 6970.
- Bouchery, T., Moyat, M., Sotillo, J., Silverstein, S., Volpe, B., Coakley, G., Tsourouktsoglou, T. D., Becker, L., Shah, K., Kulagin, M., Guiet, R., Camberis, M., Schmidt, A., Seitz, A., Giacomini, P., Le Gros, G., Papayannopoulos, V., Loukas, A. & Harris, N. L. 2020. Hookworms Evade Host Immunity by Secreting a Deoxyribonuclease to Degrade Neutrophil Extracellular Traps. *Cell Host Microbe*, 27, 277-289.e6.
- Bouchery, T., Volpe, B., Shah, K., Lebon, L., Filbey, K., Legros, G. & Harris, N. 2017. The Study of Host Immune Responses Elicited by the Model Murine Hookworms *Nippostrongylus brasiliensis* and *Heligmosomoides polygyrus*. *Curr Protoc Mouse Biol*, 7, 236-286.
- Branchett, W. J., Stölting, H., Oliver, R. A., Walker, S. A., Puttur, F., Gregory, L. G., Gabryšová, L., Wilson, M. S., O'garra, A. & Lloyd, C. M. 2020. A T cell-

- myeloid IL-10 axis regulates pathogenic IFN- γ -dependent immunity in a mouse model of type 2-low asthma. *J Allergy Clin Immunol*, 145, 666-678.e9.
- Califano, D., Cho, J. J., Uddin, M. N., Lorentsen, K. J., Yang, Q., Bhandoola, A., Li, H. & Avram, D. 2015. Transcription Factor Bcl11b Controls Identity and Function of Mature Type 2 Innate Lymphoid Cells. *Immunity*, 43, 354-68.
- Camberis, M., Le Gros, G. & Urban, J., Jr. 2003. Animal model of *Nippostrongylus brasiliensis* and *Heligmosomoides polygyrus*. *Curr Protoc Immunol*, Chapter 19, Unit 19.12.
- Caminati, M., Pham, D. L., Bagnasco, D. & Canonica, G. W. 2018. Type 2 immunity in asthma. *World Allergy Organ J*, 11, 13.
- Carrega, P. & Ferlazzo, G. 2012. Natural killer cell distribution and trafficking in human tissues. *Front Immunol*, 3, 347.
- Castro, G., Liu, X., Ngo, K., De Leon-Tabaldo, A., Zhao, S., Luna-Roman, R., Yu, J., Cao, T., Kuhn, R., Wilkinson, P., Herman, K., Nelen, M. I., Blevitt, J., Xue, X., Fourie, A. & Fung-Leung, W. P. 2017. ROR γ and ROR α signature genes in human Th17 cells. *PLoS One*, 12, e0181868.
- Cephus, J. Y., Stier, M. T., Fuseini, H., Yung, J. A., Toki, S., Bloodworth, M. H., Zhou, W., Goleniewska, K., Zhang, J., Garon, S. L., Hamilton, R. G., Poloshukin, V. V., Boyd, K. L., Peebles, R. S., Jr. & Newcomb, D. C. 2017. Testosterone Attenuates Group 2 Innate Lymphoid Cell-Mediated Airway Inflammation. *Cell Rep*, 21, 2487-2499.
- Charlier, J., Van Der Voort, M., Kenyon, F., Skuce, P. & Vercruyse, J. 2014. Chasing helminths and their economic impact on farmed ruminants. *Trends Parasitol*, 30, 361-7.
- Chen, F., Liu, Z., Wu, W., Rozo, C., Bowdridge, S., Millman, A., Van Rooijen, N., Urban, J. F., Jr., Wynn, T. A. & Gause, W. C. 2012. An essential role for TH2-type responses in limiting acute tissue damage during experimental helminth infection. *Nat Med*, 18, 260-6.
- Chen, L. & Flies, D. B. 2013. Molecular mechanisms of T cell co-stimulation and co-inhibition. *Nat Rev Immunol*, 13, 227-42.
- Chen, T., Tibbitt, C. A., Feng, X., Stark, J. M., Rohrbeck, L., Rausch, L., Sedimbi, S. K., Karlsson, M. C. I., Lambrecht, B. N., Karlsson Hedestam, G. B., Hendriks, R. W., Chambers, B. J., Nylén, S. & Coquet, J. M. 2017. PPAR- γ promotes type 2 immune responses in allergy and nematode infection. *Sci Immunol*, 2.

- Chen, X. R., Heck, N., Lohof, A. M., Rochefort, C., Morel, M. P., Wehrlé, R., Doulazmi, M., Marty, S., Cannaya, V., Avci, H. X., Mariani, J., Rondi-Reig, L., Vodjdani, G., Sherrard, R. M., Sotelo, C. & Dusart, I. 2013. Mature Purkinje cells require the retinoic acid-related orphan receptor- α (ROR α) to maintain climbing fiber mono-innervation and other adult characteristics. *J Neurosci*, 33, 9546-62.
- Choi, J. M. & Bothwell, A. L. 2012. The nuclear receptor PPARs as important regulators of T-cell functions and autoimmune diseases. *Mol Cells*, 33, 217-22.
- Chopra, A. R., Louet, J. F., Saha, P., An, J., Demayo, F., Xu, J., York, B., Karpen, S., Finegold, M., Moore, D., Chan, L., Newgard, C. B. & O'malley, B. W. 2008. Absence of the SRC-2 coactivator results in a glycogenopathy resembling Von Gierke's disease. *Science*, 322, 1395-9.
- Chou, S. J., Babot, Z., Leingartner, A., Studer, M., Nakagawa, Y. & O'leary, D. D. 2013. Geniculocortical input drives genetic distinctions between primary and higher-order visual areas. *Science*, 340, 1239-42.
- Cook, D. N., Kang, H. S. & Jetten, A. M. 2015. Retinoic Acid-Related Orphan Receptors (RORs): Regulatory Functions in Immunity, Development, Circadian Rhythm, and Metabolism. *Nucl Receptor Res*, 2.
- Cox, M. A., Kahan, S. M. & Zajac, A. J. 2013. Anti-viral CD8 T cells and the cytokines that they love. *Virology*, 435, 157-69.
- Craig, J. M. & Scott, A. L. 2014. Helminths in the lungs. *Parasite Immunol*, 36, 463-74.
- Delerive, P., Monte, D., Dubois, G., Trottein, F., Fruchart-Najib, J., Mariani, J., Fruchart, J. C. & Staels, B. 2001. The orphan nuclear receptor ROR alpha is a negative regulator of the inflammatory response. *EMBO Rep*, 2, 42-8.
- Devanna, P. & Vernes, S. C. 2014. A direct molecular link between the autism candidate gene RORa and the schizophrenia candidate MIR137. *Sci Rep*, 4, 3994.
- Doulazmi, M., Capone, F., Frederic, F., Bakouche, J., Lemaigre-Dubreuil, Y. & Mariani, J. 2006. Cerebellar purkinje cell loss in heterozygous rora $^{+/-}$ mice: a longitudinal study. *J Neurogenet*, 20, 1-17.
- Drake, L. Y., Iijima, K. & Kita, H. 2014. Group 2 innate lymphoid cells and CD4 $^{+}$ T cells cooperate to mediate type 2 immune response in mice. *Allergy*, 69, 1300-7.

- Duran-Struuck, R. & Dysko, R. C. 2009. Principles of bone marrow transplantation (BMT): providing optimal veterinary and husbandry care to irradiated mice in BMT studies. *J Am Assoc Lab Anim Sci*, 48, 11-22.
- Dussault, I., Fawcett, D., Matthyssen, A., Bader, J. A. & Giguere, V. 1998. Orphan nuclear receptor ROR alpha-deficient mice display the cerebellar defects of staggerer. *Mech Dev*, 70, 147-53.
- Dvorak, A. M., Nabel, G., Pyne, K., Cantor, H., Dvorak, H. F. & Galli, S. J. 1982. Ultrastructural identification of the mouse basophil. *Blood*, 59, 1279-85.
- Dzhagalov, I., Giguere, V. & He, Y. W. 2004. Lymphocyte development and function in the absence of retinoic acid-related orphan receptor alpha. *J Immunol*, 173, 2952-9.
- Eberl, G., Colonna, M., Di Santo, J. P. & McKenzie, A. N. 2015. Innate lymphoid cells. Innate lymphoid cells: a new paradigm in immunology. *Science*, 348, aaa6566.
- Eftekharian, M. M., Noroozi, R., Sayad, A., Sarrafzadeh, S., Toghi, M., Azimi, T., Komaki, A., Mazdeh, M., Inoko, H., Taheri, M. & Mirfakhraie, R. 2016. RAR-related orphan receptor A (RORA): A new susceptibility gene for multiple sclerosis. *J Neurol Sci*, 369, 259-262.
- Fallon, P. G., Ballantyne, S. J., Mangan, N. E., Barlow, J. L., Dasvarma, A., Hewett, D. R., McIlgorm, A., Jolin, H. E. & McKenzie, A. N. 2006. Identification of an interleukin (IL)-25-dependent cell population that provides IL-4, IL-5, and IL-13 at the onset of helminth expulsion. *J Exp Med*, 203, 1105-16.
- Fallon, P. G. & Schwartz, C. 2019. The high and lows of Type 2 asthma and mouse models. *J Allergy Clin Immunol*.
- Finkelman, F. D., Morris, S. C., Orekhova, T., Mori, M., Donaldson, D., Reiner, S. L., Reilly, N. L., Schopf, L. & Urban, J. F., Jr. 2000. Stat6 regulation of in vivo IL-4 responses. *J Immunol*, 164, 2303-10.
- Fry, T. J. & Mackall, C. L. 2005. The many faces of IL-7: from lymphopoiesis to peripheral T cell maintenance. *J Immunol*, 174, 6571-6.
- Fu, R. D., Qiu, C. H., Chen, H. A., Zhang, Z. G. & Lu, M. Q. 2014. Retinoic acid receptor-related receptor alpha (RORalpha) is a prognostic marker for hepatocellular carcinoma. *Tumour Biol*, 35, 7603-10.
- Galvan-Pena, S. & O'Neill, L. A. 2014. Metabolic reprogramming in macrophage polarization. *Front Immunol*, 5, 420.

- Gause, W. C., Wynn, T. A. & Allen, J. E. 2013. Type 2 immunity and wound healing: evolutionary refinement of adaptive immunity by helminths. *Nat Rev Immunol*, 13, 607-14.
- Germain, R. N. 2002. T-cell development and the CD4-CD8 lineage decision. *Nat Rev Immunol*, 2, 309-22.
- Ghaedi, M., Shen, Z. Y., Orangi, M., Martinez-Gonzalez, I., Wei, L., Lu, X., Das, A., Heravi-Moussavi, A., Marra, M. A., Bhandoola, A. & Takei, F. 2020. Single-cell analysis of ROR α tracer mouse lung reveals ILC progenitors and effector ILC2 subsets. *J Exp Med*, 217.
- Giacomin, P. R., Gordon, D. L., Botto, M., Daha, M. R., Sanderson, S. D., Taylor, S. M. & Dent, L. A. 2008. The role of complement in innate, adaptive and eosinophil-dependent immunity to the nematode *Nippostrongylus brasiliensis*. *Mol Immunol*, 45, 446-55.
- Giguere, V. 1999. Orphan nuclear receptors: from gene to function. *Endocr Rev*, 20, 689-725.
- Giguere, V., Beatty, B., Squire, J., Copeland, N. G. & Jenkins, N. A. 1995. The orphan nuclear receptor ROR alpha (RORA) maps to a conserved region of homology on human chromosome 15q21-q22 and mouse chromosome 9. *Genomics*, 28, 596-8.
- Giguere, V., Tini, M., Flock, G., Ong, E., Evans, R. M. & Otulakowski, G. 1994. Isoform-specific amino-terminal domains dictate DNA-binding properties of ROR alpha, a novel family of orphan hormone nuclear receptors. *Genes Dev*, 8, 538-53.
- Godfrey, D. I. & Zlotnik, A. 1993. Control points in early T-cell development. *Immunol Today*, 14, 547-53.
- Gold, D. A., Baek, S. H., Schork, N. J., Rose, D. W., Larsen, D. D., Sachs, B. D., Rosenfeld, M. G. & Hamilton, B. A. 2003. RORalpha coordinates reciprocal signaling in cerebellar development through sonic hedgehog and calcium-dependent pathways. *Neuron*, 40, 1119-31.
- Gold, D. A., Gent, P. M. & Hamilton, B. A. 2007. ROR alpha in genetic control of cerebellum development: 50 staggering years. *Brain Res*, 1140, 19-25.
- Gold, M. J., Antignano, F., Halim, T. Y., Hirota, J. A., Blanchet, M. R., Zaph, C., Takei, F. & McNagny, K. M. 2014. Group 2 innate lymphoid cells facilitate

- sensitization to local, but not systemic, TH2-inducing allergen exposures. *J Allergy Clin Immunol*, 133, 1142-8.
- Gray, J. I., Westerhof, L. M. & Macleod, M. K. L. 2018. The roles of resident, central and effector memory CD4 T-cells in protective immunity following infection or vaccination. *Immunology*, 154, 574-81.
- Gu, H., Zou, Y. R. & Rajewsky, K. 1993. Independent control of immunoglobulin switch recombination at individual switch regions evidenced through Cre-loxP-mediated gene targeting. *Cell*, 73, 1155-64.
- Guan, H., Nagarkatti, P. S. & Nagarkatti, M. 2009. Role of CD44 in the differentiation of Th1 and Th2 cells: CD44-deficiency enhances the development of Th2 effectors in response to sheep RBC and chicken ovalbumin. *J Immunol*, 183, 172-80.
- Guasconi, L., Chiapello, L. S. & Masih, D. T. 2015. Fasciola hepatica excretory-secretory products induce CD4⁺T cell anergy via selective up-regulation of PD-L2 expression on macrophages in a Dectin-1 dependent way. *Immunobiology*, 220, 934-9.
- Guillaumond, F., Dardente, H., Giguere, V. & Cermakian, N. 2005. Differential control of Bmal1 circadian transcription by REV-ERB and ROR nuclear receptors. *J Biol Rhythms*, 20, 391-403.
- Guilliams, M., De Kleer, I., Henri, S., Post, S., Vanhoutte, L., De Prijck, S., Deswarte, K., Malissen, B., Hammad, H. & Lambrecht, B. N. 2013. Alveolar macrophages develop from fetal monocytes that differentiate into long-lived cells in the first week of life via GM-CSF. *J Exp Med*, 210, 1977-92.
- Gurram, R. K. & Zhu, J. 2019. Orchestration between ILC2s and Th2 cells in shaping type 2 immune responses. *Cell Mol Immunol*.
- Haim-Vilmovsky, L., Henriksson, J., Walker, J. A., Miao, Z., Natan, E., Kar, G., Clare, S., Barlow, J. L., Charidemou, E., Mamanova, L., Chen, X., Proserpio, V., Pramanik, J., Woodhouse, S., Protasio, A. V., Efremova, M., Griffin, J. L., Berriman, M., Dougan, G., Fisher, J., Marioni, J. C., Mckenzie, A. N. & Teichmann, S. A. 2020. Rora regulates activated T helper cells during inflammation. *bioRxiv*, 709998.
- Halim, T. Y., Hwang, Y. Y., Scanlon, S. T., Zaghouani, H., Garbi, N., Fallon, P. G. & Mckenzie, A. N. 2016. Group 2 innate lymphoid cells license dendritic cells to potentiate memory TH2 cell responses. *Nat Immunol*, 17, 57-64.

- Halim, T. Y., Maclaren, A., Romanish, M. T., Gold, M. J., McNagny, K. M. & Takei, F. 2012. Retinoic-acid-receptor-related orphan nuclear receptor alpha is required for natural helper cell development and allergic inflammation. *Immunity*, 37, 463-74.
- Halim, T. Y., Steer, C. A., Matha, L., Gold, M. J., Martinez-Gonzalez, I., McNagny, K. M., Mckenzie, A. N. & Takei, F. 2014. Group 2 innate lymphoid cells are critical for the initiation of adaptive T helper 2 cell-mediated allergic lung inflammation. *Immunity*, 40, 425-35.
- Halim, T. Y. F., Rana, B. M. J., Walker, J. A., Kerscher, B., Knolle, M. D., Jolin, H. E., Serrao, E. M., Haim-Vilmovsky, L., Teichmann, S. A., Rodewald, H. R., Botto, M., Vyse, T. J., Fallon, P. G., Li, Z., Withers, D. R. & Mckenzie, A. N. J. 2018. Tissue-Restricted Adaptive Type 2 Immunity Is Orchestrated by Expression of the Costimulatory Molecule OX40L on Group 2 Innate Lymphoid Cells. *Immunity*, 48, 1195-1207.e6.
- Hamilton, B. A., Frankel, W. N., Kerrebrock, A. W., Hawkins, T. L., Fitzhugh, W., Kusumi, K., Russell, L. B., Mueller, K. L., Van Berkel, V., Birren, B. W., Kruglyak, L. & Lander, E. S. 1996. Disruption of the nuclear hormone receptor RORalpha in staggerer mice. *Nature*, 379, 736-9.
- Hams, E., Roberts, J., Bermingham, R. & Fallon, P. G. 2021. Functions for Retinoic Acid-Related Orphan Receptor Alpha (ROR α) in the Activation of Macrophages During Lipopolysaccharide-Induced Septic Shock. *Frontiers in Immunology*, 12.
- Hams, E., Roberts, J., Bermingham, R., Hogan, A. E., O'shea, D., O'Neill, L. & Fallon, P. G. 2020. Role for Retinoic Acid-Related Orphan Receptor Alpha (ROR α) Expressing Macrophages in Diet-Induced Obesity. *Frontiers in Immunology*, 11.
- Han, Y. H., Kim, H. J., Na, H., Nam, M. W., Kim, J. Y., Kim, J. S., Koo, S. H. & Lee, M. O. 2017. RORalpha Induces KLF4-Mediated M2 Polarization in the Liver Macrophages that Protect against Nonalcoholic Steatohepatitis. *Cell Rep*, 20, 124-135.
- Han, Y. H., Shin, K. O., Kim, J. Y., Khadka, D. B., Kim, H. J., Lee, Y. M., Cho, W. J., Cha, J. Y., Lee, B. J. & Lee, M. O. 2019. A maresin 1/RORalpha/12-lipoxygenase autoregulatory circuit prevents inflammation and progression of nonalcoholic steatohepatitis. *J Clin Invest*, 130, 1684-1698.
- Harris, N. & Gause, W. C. 2011. To B or not to B: B cells and the Th2-type immune response to helminths. *Trends Immunol*, 32, 80-8.

- Harris, N. L., Watt, V., Ronchese, F. & Le Gros, G. 2002. Differential T cell function and fate in lymph node and nonlymphoid tissues. *J Exp Med*, 195, 317-26.
- Harvie, M., Camberis, M. & Le Gros, G. 2013. Development of CD4 T Cell Dependent Immunity Against *N. brasiliensis* Infection. *Front Immunol*, 4, 74.
- Harvie, M., Camberis, M., Tang, S. C., Delahunt, B., Paul, W. & Le Gros, G. 2010. The lung is an important site for priming CD4 T-cell-mediated protective immunity against gastrointestinal helminth parasites. *Infect Immun*, 78, 3753-62.
- Hashimoto, D., Chow, A., Noizat, C., Teo, P., Beasley, M. B., Leboeuf, M., Becker, C. D., See, P., Price, J., Lucas, D., Greter, M., Mortha, A., Boyer, S. W., Forsberg, E. C., Tanaka, M., Van Rooijen, N., García-Sastre, A., Stanley, E. R., Ginhoux, F., Frenette, P. S. & Merad, M. 2013. Tissue-resident macrophages self-maintain locally throughout adult life with minimal contribution from circulating monocytes. *Immunity*, 38, 792-804.
- Hasnain, S. Z., Evans, C. M., Roy, M., Gallagher, A. L., Kindrachuk, K. N., Barron, L., Dickey, B. F., Wilson, M. S., Wynn, T. A., Grencis, R. K. & Thornton, D. J. 2011. Muc5ac: a critical component mediating the rejection of enteric nematodes. *J Exp Med*, 208, 893-900.
- Heinen, A. P., Wanke, F., Moos, S., Attig, S., Luche, H., Pal, P. P., Budisa, N., Fehling, H. J., Waisman, A. & Kurschus, F. C. 2014. Improved method to retain cytosolic reporter protein fluorescence while staining for nuclear proteins. *Cytometry A*, 85, 621-7.
- Hennings, J. M., Uhr, M., Klengel, T., Weber, P., Putz, B., Touma, C., Czamara, D., Ising, M., Holsboer, F. & Lucae, S. 2015. RNA expression profiling in depressed patients suggests retinoid-related orphan receptor alpha as a biomarker for antidepressant response. *Transl Psychiatry*, 5, e538.
- Henriksson, J., Chen, X., Gomes, T., Ullah, U., Meyer, K. B., Miragaia, R., Duddy, G., Pramanik, J., Yusa, K., Lahesmaa, R. & Teichmann, S. A. 2019. Genome-wide CRISPR Screens in T Helper Cells Reveal Pervasive Crosstalk between Activation and Differentiation. *Cell*, 176, 882-896.e18.
- Hoyler, T., Klose, C. S., Souabni, A., Turqueti-Neves, A., Pfeifer, D., Rawlins, E. L., Voehringer, D., Busslinger, M. & Diefenbach, A. 2012. The transcription factor GATA-3 controls cell fate and maintenance of type 2 innate lymphoid cells. *Immunity*, 37, 634-48.

- Hu, V. W., Sarachana, T., Sherrard, R. M. & Kocher, K. M. 2015. Investigation of sex differences in the expression of RORA and its transcriptional targets in the brain as a potential contributor to the sex bias in autism. *Mol Autism*, 6, 7.
- Huang, P., Chandra, V. & Rastinejad, F. 2010. Structural overview of the nuclear receptor superfamily: insights into physiology and therapeutics. *Annu Rev Physiol*, 72, 247-72.
- Huang, Y., Guo, L., Qiu, J., Chen, X., Hu-Li, J., Siebenlist, U., Williamson, P. R., Urban, J. F., Jr. & Paul, W. E. 2015. IL-25-responsive, lineage-negative KLRG1(hi) cells are multipotential 'inflammatory' type 2 innate lymphoid cells. *Nat Immunol*, 16, 161-9.
- Huang, Y. & Paul, W. E. 2016. Inflammatory group 2 innate lymphoid cells. *Int Immunol*, 28, 23-8.
- Huber, S., Hoffmann, R., Muskens, F. & Voehringer, D. 2010. Alternatively activated macrophages inhibit T-cell proliferation by Stat6-dependent expression of PD-L2. *Blood*, 116, 3311-20.
- Hung, L. Y., Lewkowich, I. P., Dawson, L. A., Downey, J., Yang, Y., Smith, D. E. & Herbert, D. R. 2013. IL-33 drives biphasic IL-13 production for noncanonical Type 2 immunity against hookworms. *Proc Natl Acad Sci U S A*, 110, 282-7.
- Ino, H. 2004. Immunohistochemical characterization of the orphan nuclear receptor ROR alpha in the mouse nervous system. *J Histochem Cytochem*, 52, 311-23.
- Ito, I., Bhopale, K. K., Kobayashi, M., Finnerty, C. C., Herndon, D. N. & Suzuki, F. 2017. Lamina propria group 2 innate lymphoid cells impair the antibacterial defense of burned mice to enterococcal translocation. *J Leukoc Biol*, 102, 1451-1460.
- Ivanov, Ii, Mckenzie, B. S., Zhou, L., Tadokoro, C. E., Lepelley, A., Lafaille, J. J., Cua, D. J. & Littman, D. R. 2006. The orphan nuclear receptor RORgammat directs the differentiation program of proinflammatory IL-17+ T helper cells. *Cell*, 126, 1121-33.
- Jafri, S., Moore, S. D., Morrell, N. W. & Ormiston, M. L. 2017. A sex-specific reconstitution bias in the competitive CD45.1/CD45.2 congenic bone marrow transplant model. *Sci Rep*, 7, 3495.
- Janmaat, S., Akwa, Y., Doulazmi, M., Bakouche, J., Gautheron, V., Liere, P., Eychenne, B., Pianos, A., Luiten, P., Groothuis, T., Baulieu, E. E., Mariani, J., Sherrard, R. M. & Frederic, F. 2011. Age-related Purkinje cell death is steroid

- dependent: RORalpha haplo-insufficiency impairs plasma and cerebellar steroids and Purkinje cell survival. *Age (Dordr)*, 33, 565-78.
- Jaradat, M., Stapleton, C., Tilley, S. L., Dixon, D., Erikson, C. J., Mccaskill, J. G., Kang, H. S., Angers, M., Liao, G., Collins, J., Grissom, S. & Jetten, A. M. 2006. Modulatory role for retinoid-related orphan receptor alpha in allergen-induced lung inflammation. *Am J Respir Crit Care Med*, 174, 1299-309.
- Jetten, A. M. 2009. Retinoid-related orphan receptors (RORs): critical roles in development, immunity, circadian rhythm, and cellular metabolism. *Nucl Recept Signal*, 7, e003.
- Jetten, A. M. 2011. Immunology: A helping hand against autoimmunity. *Nature*, 472, 421-2.
- Jia, L. & Wu, C. 2014. The biology and functions of Th22 cells. *Adv Exp Med Biol*, 841, 209-30.
- Kadiri, S., Monnier, C., Ganbold, M., Ledent, T., Capeau, J. & Antoine, B. 2015. The nuclear retinoid-related orphan receptor-alpha regulates adipose tissue glyceroneogenesis in addition to hepatic gluconeogenesis. *Am J Physiol Endocrinol Metab*, 309, E105-14.
- Kallen, J., Schlaeppli, J. M., Bitsch, F., Delhon, I. & Fournier, B. 2004. Crystal structure of the human RORalpha Ligand binding domain in complex with cholesterol sulfate at 2.2 Å. *J Biol Chem*, 279, 14033-8.
- Kallen, J. A., Schlaeppli, J. M., Bitsch, F., Geisse, S., Geiser, M., Delhon, I. & Fournier, B. 2002. X-ray structure of the hRORalpha LBD at 1.63 Å: structural and functional data that cholesterol or a cholesterol derivative is the natural ligand of RORalpha. *Structure*, 10, 1697-707.
- Kaplan, M. H. 2013. Th9 cells: differentiation and disease. *Immunol Rev*, 252, 104-15.
- Kaplan, M. H., Schindler, U., Smiley, S. T. & Grusby, M. J. 1996. Stat6 is required for mediating responses to IL-4 and for development of Th2 cells. *Immunity*, 4, 313-9.
- Kapsenberg, M. L. 2003. Dendritic-cell control of pathogen-driven T-cell polarization. *Nat Rev Immunol*, 3, 984-93.
- Kawamura, S. & Ohteki, T. 2018. Monopoiesis in humans and mice. *Int Immunol*, 30, 503-509.
- Kim, H., Lee, J. M., Lee, G., Bhin, J., Oh, S. K., Kim, K., Pyo, K. E., Lee, J. S., Yim, H. Y., Kim, K. I., Hwang, D., Chung, J. & Baek, S. H. 2011. DNA damage-

- induced RORalpha is crucial for p53 stabilization and increased apoptosis. *Mol Cell*, 44, 797-810.
- Kim, J. I., Ho, I. C., Grusby, M. J. & Glimcher, L. H. 1999. The transcription factor c-Maf controls the production of interleukin-4 but not other Th2 cytokines. *Immunity*, 10, 745-51.
- Kim, K., Boo, K., Yu, Y. S., Oh, S. K., Kim, H., Jeon, Y., Bhin, J., Hwang, D., Kim, K. I., Lee, J. S., Im, S. S., Yoon, S. G., Kim, I. Y., Seong, J. K., Lee, H., Fang, S. & Baek, S. H. 2017. RORalpha controls hepatic lipid homeostasis via negative regulation of PPARgamma transcriptional network. *Nat Commun*, 8, 162.
- Klose, C. S. N., Mhlaköiv, T., Moeller, J. B., Rankin, L. C., Flamar, A. L., Kabata, H., Monticelli, L. A., Moriyama, S., Putzel, G. G., Rakhilin, N., Shen, X., Kostenis, E., König, G. M., Senda, T., Carpenter, D., Farber, D. L. & Artis, D. 2017. The neuropeptide neuromedin U stimulates innate lymphoid cells and type 2 inflammation. *Nature*, 549, 282-286.
- Knott, M. L., Matthaei, K. I., Giacomini, P. R., Wang, H., Foster, P. S. & Dent, L. A. 2007. Impaired resistance in early secondary *Nippostrongylus brasiliensis* infections in mice with defective eosinophilopoiesis. *Int J Parasitol*, 37, 1367-78.
- Kopmels, B., Mariani, J., Delhay-Bouchaud, N., Audibert, F., Fradelizi, D. & Wollman, E. E. 1992. Evidence for a hyperexcitability state of staggerer mutant mice macrophages. *J Neurochem*, 58, 192-9.
- Kottorou, A. E., Antonacopoulou, A. G., Dimitrakopoulos, F. I., Tsamandas, A. C., Scopa, C. D., Petsas, T. & Kalofonos, H. P. 2012. Altered expression of NFY-C and RORA in colorectal adenocarcinomas. *Acta Histochem*, 114, 553-61.
- Koyasu, S., Moro, K., Tanabe, M. & Takeuchi, T. 2010. Natural helper cells: a new player in the innate immune response against helminth infection. *Adv Immunol*, 108, 21-44.
- Lai, Y. C., Kao, C. F., Lu, M. L., Chen, H. C., Chen, P. Y., Chen, C. H., Shen, W. W., Wu, J. Y., Lu, R. B. & Kuo, P. H. 2015. Investigation of associations between NR1D1, RORA and RORB genes and bipolar disorder. *PLoS One*, 10, e0121245.
- Langers, I., Renoux, V. M., Thiry, M., Delvenne, P. & Jacobs, N. 2012. Natural killer cells: role in local tumor growth and metastasis. *Biologics*, 6, 73-82.

- Latchman, Y., Wood, C. R., Chernova, T., Chaudhary, D., Borde, M., Chernova, I., Iwai, Y., Long, A. J., Brown, J. A., Nunes, R., Greenfield, E. A., Bourque, K., Boussiotis, V. A., Carter, L. L., Carreno, B. M., Malenkovich, N., Nishimura, H., Okazaki, T., Honjo, T., Sharpe, A. H. & Freeman, G. J. 2001. PD-L2 is a second ligand for PD-1 and inhibits T cell activation. *Nat Immunol*, 2, 261-8.
- Lau, P., Fitzsimmons, R. L., Pearen, M. A., Watt, M. J. & Muscat, G. E. 2011. Homozygous staggerer (sg/sg) mice display improved insulin sensitivity and enhanced glucose uptake in skeletal muscle. *Diabetologia*, 54, 1169-80.
- Lau, P., Fitzsimmons, R. L., Raichur, S., Wang, S. C., Lechtken, A. & Muscat, G. E. 2008. The orphan nuclear receptor, RORalpha, regulates gene expression that controls lipid metabolism: staggerer (SG/SG) mice are resistant to diet-induced obesity. *J Biol Chem*, 283, 18411-21.
- Lau, P., Tuong, Z. K., Wang, S. C., Fitzsimmons, R. L., Goode, J. M., Thomas, G. P., Cowin, G. J., Pearen, M. A., Mardon, K., Stow, J. L. & Muscat, G. E. 2015. Roralpha deficiency and decreased adiposity are associated with induction of thermogenic gene expression in subcutaneous white adipose and brown adipose tissue. *Am J Physiol Endocrinol Metab*, 308, E159-71.
- Lee, J. E., Choi, G., Cho, M., Kim, D., Lee, M. O. & Chung, Y. 2021. A critical regulation of Th2 cell responses by ROR α in allergic asthma. *Sci China Life Sci*, 64, 1326-1335.
- Lee, J. M., Kim, I. S., Kim, H., Lee, J. S., Kim, K., Yim, H. Y., Jeong, J., Kim, J. H., Kim, J. Y., Lee, H., Seo, S. B., Kim, H., Rosenfeld, M. G., Kim, K. I. & Baek, S. H. 2010. RORalpha attenuates Wnt/beta-catenin signaling by PKCalpha-dependent phosphorylation in colon cancer. *Mol Cell*, 37, 183-95.
- Lee, P. P., Fitzpatrick, D. R., Beard, C., Jessup, H. K., Lehar, S., Makar, K. W., Perez-Melgosa, M., Sweetser, M. T., Schlissel, M. S., Nguyen, S., Cherry, S. R., Tsai, J. H., Tucker, S. M., Weaver, W. M., Kelso, A., Jaenisch, R. & Wilson, C. B. 2001. A critical role for Dnmt1 and DNA methylation in T cell development, function, and survival. *Immunity*, 15, 763-74.
- Lev, A., Simon, A. J., Barel, O., Eyal, E., Glick-Saar, E., Nayshool, O., Birk, O., Stauber, T., Hochberg, A., Broides, A., Almashanu, S., Hendel, A., Lee, Y. N. & Somech, R. 2019. Reduced Function and Diversity of T Cell Repertoire and Distinct Clinical Course in Patients With IL7RA Mutation. *Front Immunol*, 10, 1672.

- Li-Weber, M., Giaisi, M., Baumann, S., Palfi, K. & Krammer, P. H. 2004. NF-kappa B synergizes with NF-AT and NF-IL6 in activation of the IL-4 gene in T cells. *Eur J Immunol*, 34, 1111-8.
- Liu, B., Lee, J. B., Chen, C. Y., Hershey, G. K. & Wang, Y. H. 2015. Collaborative interactions between type 2 innate lymphoid cells and antigen-specific CD4+ Th2 cells exacerbate murine allergic airway diseases with prominent eosinophilia. *J Immunol*, 194, 3583-93.
- Liu, Q., Kreider, T., Bowdridge, S., Liu, Z., Song, Y., Gaydo, A. G., Urban, J. F., Jr. & Gause, W. C. 2010. B cells have distinct roles in host protection against different nematode parasites. *J Immunol*, 184, 5213-23.
- Liu, X., Nurieva, R. I. & Dong, C. 2013. Transcriptional regulation of follicular T-helper (Tfh) cells. *Immunol Rev*, 252, 139-45.
- Liu, Y., Chen, Y., Zhang, J., Liu, Y., Zhang, Y. & Su, Z. 2017. Retinoic acid receptor-related orphan receptor alpha stimulates adipose tissue inflammation by modulating endoplasmic reticulum stress. *J Biol Chem*, 292, 13959-13969.
- Lo, B. C., Canals Hernaez, D., Scott, R. W., Hughes, M. R., Shin, S. B., Underhill, T. M., Takei, F. & McNagny, K. M. 2019. The Transcription Factor RORalpha Preserves ILC3 Lineage Identity and Function during Chronic Intestinal Infection. *J Immunol*.
- Lo, B. C., Gold, M. J., Hughes, M. R., Antignano, F., Valdez, Y., Zaph, C., Harder, K. W. & McNagny, K. M. 2016. The orphan nuclear receptor ROR alpha and group 3 innate lymphoid cells drive fibrosis in a mouse model of Crohn's disease. *Sci Immunol*, 1.
- Logue, M. W., Baldwin, C., Guffanti, G., Melista, E., Wolf, E. J., Reardon, A. F., Uddin, M., Wildman, D., Galea, S., Koenen, K. C. & Miller, M. W. 2013. A genome-wide association study of post-traumatic stress disorder identifies the retinoid-related orphan receptor alpha (RORA) gene as a significant risk locus. *Mol Psychiatry*, 18, 937-42.
- Luckheeram, R. V., Zhou, R., Verma, A. D. & Xia, B. 2012. CD4(+)T cells: differentiation and functions. *Clin Dev Immunol*, 2012, 925135.
- Lumeng, C. N., Delproposto, J. B., Westcott, D. J. & Saltiel, A. R. 2008. Phenotypic switching of adipose tissue macrophages with obesity is generated by spatiotemporal differences in macrophage subtypes. *Diabetes*, 57, 3239-46.

- Maggi, L., Montaini, G., Mazzoni, A., Rossetini, B., Capone, M., Rossi, M. C., Santarlasci, V., Liotta, F., Rossi, O., Gallo, O., De Palma, R., Maggi, E., Cosmi, L., Romagnani, S. & Annunziato, F. 2017. Human circulating group 2 innate lymphoid cells can express CD154 and promote IgE production. *J Allergy Clin Immunol*, 139, 964-976.e4.
- Majewska, A., Gajewska, M., Dembele, K., Maciejewski, H., Prostek, A. & Jank, M. 2016. Lymphocytic, cytokine and transcriptomic profiles in peripheral blood of dogs with atopic dermatitis. *BMC Vet Res*, 12, 174.
- Malhotra, N., Leyva-Castillo, J. M., Jadhav, U., Barreiro, O., Kam, C., O'Neill, N. K., Meylan, F., Chambon, P., Von Andrian, U. H., Siegel, R. M., Wang, E. C., Shivdasani, R. & Geha, R. S. 2018. RORalpha-expressing T regulatory cells restrain allergic skin inflammation. *Sci Immunol*, 3.
- Mamontova, A., Seguret-Mace, S., Esposito, B., Chanial, C., Bouly, M., Delhaye-Bouchaud, N., Luc, G., Staels, B., Duverger, N., Mariani, J. & Tedgui, A. 1998. Severe atherosclerosis and hypoalphalipoproteinemia in the staggerer mouse, a mutant of the nuclear receptor RORalpha. *Circulation*, 98, 2738-43.
- Martin, R. K., Damle, S. R., Valentine, Y. A., Zellner, M. P., James, B. N., Lownik, J. C., Luker, A. J., Davis, E. H., Demeules, M. M., Khandjian, L. M., Finkelman, F. D., Urban, J. F., Jr. & Conrad, D. H. 2018. B1 Cell IgE Impedes Mast Cell-Mediated Enhancement of Parasite Expulsion through B2 IgE Blockade. *Cell Rep*, 22, 1824-1834.
- Matsuoka, H., Shima, A., Kuramoto, D., Kikumoto, D., Matsui, T. & Michihara, A. 2015. Phosphoenolpyruvate Carboxykinase, a Key Enzyme That Controls Blood Glucose, Is a Target of Retinoic Acid Receptor-Related Orphan Receptor alpha. *PLoS One*, 10, e0137955.
- Mccoy, K. D., Stoel, M., Stettler, R., Merky, P., Fink, K., Senn, B. M., Schaer, C., Massacand, J., Odermatt, B., Oettgen, H. C., Zinkernagel, R. M., Bos, N. A., Hengartner, H., Macpherson, A. J. & Harris, N. L. 2008. Polyclonal and specific antibodies mediate protective immunity against enteric helminth infection. *Cell Host Microbe*, 4, 362-73.
- Melen, E., Kho, A. T., Sharma, S., Gaedigk, R., Leeder, J. S., Mariani, T. J., Carey, V. J., Weiss, S. T. & Tantisira, K. G. 2011. Expression analysis of asthma candidate genes during human and murine lung development. *Respir Res*, 12, 86.

- Metzger, D. & Feil, R. 1999. Engineering the mouse genome by site-specific recombination. *Curr Opin Biotechnol*, 10, 470-6.
- Miller, H. R. 1987. Gastrointestinal mucus, a medium for survival and for elimination of parasitic nematodes and protozoa. *Parasitology*, 94 Suppl, S77-100.
- Miller, M. W., Wolf, E. J., Logue, M. W. & Baldwin, C. T. 2013. The retinoid-related orphan receptor alpha (RORA) gene and fear-related psychopathology. *J Affect Disord*, 151, 702-8.
- Miragaia, R. J., Gomes, T., Chomka, A., Jardine, L., Riedel, A., Hegazy, A. N., Whibley, N., Tucci, A., Chen, X., Lindeman, I., Emerton, G., Krausgruber, T., Shields, J., Haniffa, M., Powrie, F. & Teichmann, S. A. 2019. Single-Cell Transcriptomics of Regulatory T Cells Reveals Trajectories of Tissue Adaptation. *Immunity*, 50, 493-504.e7.
- Mirchandani, A. S., Besnard, A. G., Yip, E., Scott, C., Bain, C. C., Cerovic, V., Salmond, R. J. & Liew, F. Y. 2014. Type 2 innate lymphoid cells drive CD4+ Th2 cell responses. *J Immunol*, 192, 2442-8.
- Misharin, A. V., Morales-Nebreda, L., Mutlu, G. M., Budinger, G. R. & Perlman, H. 2013. Flow cytometric analysis of macrophages and dendritic cell subsets in the mouse lung. *Am J Respir Cell Mol Biol*, 49, 503-10.
- Mjosberg, J., Bernink, J., Golebski, K., Karrich, J. J., Peters, C. P., Blom, B., Te Velde, A. A., Fokkens, W. J., Van Drunen, C. M. & Spits, H. 2012. The transcription factor GATA3 is essential for the function of human type 2 innate lymphoid cells. *Immunity*, 37, 649-59.
- Moffatt, M. F., Gut, I. G., Demenais, F., Strachan, D. P., Bouzigon, E., Heath, S., Von Mutius, E., Farrall, M., Lathrop, M. & Cookson, W. 2010. A large-scale, consortium-based genomewide association study of asthma. *N Engl J Med*, 363, 1211-1221.
- Montaldo, E., Juelke, K. & Romagnani, C. 2015. Group 3 innate lymphoid cells (ILC3s): Origin, differentiation, and plasticity in humans and mice. *Eur J Immunol*, 45, 2171-82.
- Moro, K., Yamada, T., Tanabe, M., Takeuchi, T., Ikawa, T., Kawamoto, H., Furusawa, J., Ohtani, M., Fujii, H. & Koyasu, S. 2010. Innate production of T(H)2 cytokines by adipose tissue-associated c-Kit(+)/Sca-1(+) lymphoid cells. *Nature*, 463, 540-4.

- Mosmann, T. R., Cherwinski, H., Bond, M. W., Giedlin, M. A. & Coffman, R. L. 1986. Two types of murine helper T cell clone. I. Definition according to profiles of lymphokine activities and secreted proteins. *J Immunol*, 136, 2348-57.
- Mukherjee, A. B. & Zhang, Z. 2011. Allergic asthma: influence of genetic and environmental factors. *J Biol Chem*, 286, 32883-9.
- Mukherji, A., Kobiita, A., Ye, T. & Chambon, P. 2013. Homeostasis in intestinal epithelium is orchestrated by the circadian clock and microbiota cues transduced by TLRs. *Cell*, 153, 812-27.
- Na, H., Cho, M. & Chung, Y. 2016. Regulation of Th2 Cell Immunity by Dendritic Cells. *Immune Netw*, 16, 1-12.
- Nakagawa, Y. & O'leary, D. D. 2003. Dynamic patterned expression of orphan nuclear receptor genes RORalpha and RORbeta in developing mouse forebrain. *Dev Neurosci*, 25, 234-44.
- Neill, D. R., Wong, S. H., Bellosi, A., Flynn, R. J., Daly, M., Langford, T. K., Bucks, C., Kane, C. M., Fallon, P. G., Pannell, R., Jolin, H. E. & Mckenzie, A. N. 2010. Nuocytes represent a new innate effector leukocyte that mediates type-2 immunity. *Nature*, 464, 1367-70.
- Ng, L. G., Ostuni, R. & Hidalgo, A. 2019. Heterogeneity of neutrophils. *Nat Rev Immunol*, 19, 255-265.
- Nguyen, A., Rauch, T. A., Pfeifer, G. P. & Hu, V. W. 2010. Global methylation profiling of lymphoblastoid cell lines reveals epigenetic contributions to autism spectrum disorders and a novel autism candidate gene, RORA, whose protein product is reduced in autistic brain. *Faseb j*, 24, 3036-51.
- Nono, J. K., Ndlovu, H., Abdel Aziz, N., Mpotje, T., Hlaka, L. & Brombacher, F. 2017. Interleukin-4 receptor alpha is still required after Th2 polarization for the maintenance and the recall of protective immunity to Nematode infection. *PLoS Negl Trop Dis*, 11, e0005675.
- Nussbaum, J. C., Van Dyken, S. J., Von Moltke, J., Cheng, L. E., Mohapatra, A., Molofsky, A. B., Thornton, E. E., Krummel, M. F., Chawla, A., Liang, H. E. & Locksley, R. M. 2013. Type 2 innate lymphoid cells control eosinophil homeostasis. *Nature*, 502, 245-8.
- O'shea, J. J. & Paul, W. E. 2010. Mechanisms underlying lineage commitment and plasticity of helper CD4+ T cells. *Science*, 327, 1098-102.

- Odawara, H., Iwasaki, T., Horiguchi, J., Rokutanda, N., Hirooka, K., Miyazaki, W., Koibuchi, Y., Shimokawa, N., Iino, Y., Takeyoshi, I. & Koibuchi, N. 2009. Activation of aromatase expression by retinoic acid receptor-related orphan receptor (ROR) alpha in breast cancer cells: identification of a novel ROR response element. *J Biol Chem*, 284, 17711-9.
- Ogongo, P., Porterfield, J. Z. & Leslie, A. 2019. Lung Tissue Resident Memory T-Cells in the Immune Response to Mycobacterium tuberculosis. *Front Immunol*, 10, 992.
- Okoye, I. S., Czieso, S., Ktistaki, E., Roderick, K., Coomes, S. M., Pelly, V. S., Kannan, Y., Perez-Lloret, J., Zhao, J. L., Baltimore, D., Langhorne, J. & Wilson, M. S. 2014. Transcriptomics identified a critical role for Th2 cell-intrinsic miR-155 in mediating allergy and antihelminth immunity. *Proc Natl Acad Sci U S A*, 111, E3081-90.
- Oliphant, C. J., Hwang, Y. Y., Walker, J. A., Salimi, M., Wong, S. H., Brewer, J. M., Englezakis, A., Barlow, J. L., Hams, E., Scanlon, S. T., Ogg, G. S., Fallon, P. G. & McKenzie, A. N. 2014. MHCII-mediated dialog between group 2 innate lymphoid cells and CD4(+) T cells potentiates type 2 immunity and promotes parasitic helminth expulsion. *Immunity*, 41, 283-95.
- Omata, Y., Frech, M., Primbs, T., Lucas, S., Andreev, D., Scholtysek, C., Sarter, K., Kindermann, M., Yremenko, N., Baeten, D. L., Andreas, N., Kamradt, T., Bozec, A., Ramming, A., Kronke, G., Wirtz, S., Schett, G. & Zaiss, M. M. 2018. Group 2 Innate Lymphoid Cells Attenuate Inflammatory Arthritis and Protect from Bone Destruction in Mice. *Cell Rep*, 24, 169-180.
- Otsuka, A. & Kabashima, K. 2015. Mast cells and basophils in cutaneous immune responses. *Allergy*, 70, 131-40.
- Ozaki, N., Noshiro, M., Kawamoto, T., Nakashima, A., Honda, K., Fukuzaki-Dohi, U., Honma, S., Fujimoto, K., Tanimoto, K., Tanne, K. & Kato, Y. 2012. Regulation of basic helix-loop-helix transcription factors Dec1 and Dec2 by ROR α and their roles in adipogenesis. *Genes Cells*, 17, 109-21.
- Ozaki, T. & Nakagawara, A. 2011. Role of p53 in Cell Death and Human Cancers. *Cancers (Basel)*, 3, 994-1013.
- Panzer, M., Sitte, S., Wirth, S., Drexler, I., Sparwasser, T. & Voehringer, D. 2012. Rapid in vivo conversion of effector T cells into Th2 cells during helminth infection. *J Immunol*, 188, 615-23.

- Persson, H., Kwon, A. T., Ramilowski, J. A., Silberberg, G., Soderhall, C., Orsmark-Pietras, C., Nordlund, B., Konradsen, J. R., De Hoon, M. J., Melen, E., Hayashizaki, Y., Hedlin, G., Kere, J. & Daub, C. O. 2015. Transcriptome analysis of controlled and therapy-resistant childhood asthma reveals distinct gene expression profiles. *J Allergy Clin Immunol*, 136, 638-48.
- Plantinga, M., Guillems, M., Vanheerswyngheles, M., Deswarte, K., Branco-Madeira, F., Toussaint, W., Vanhoutte, L., Neyt, K., Killeen, N., Malissen, B., Hammad, H. & Lambrecht, B. N. 2013. Conventional and monocyte-derived CD11b(+) dendritic cells initiate and maintain T helper 2 cell-mediated immunity to house dust mite allergen. *Immunity*, 38, 322-35.
- Potten, C. S. 1970. Radiation depigmentation of mouse hair: effect of the hair growth cycle on the sensitivity. *J Invest Dermatol*, 55, 410-8.
- Price, A. E., Liang, H. E., Sullivan, B. M., Reinhardt, R. L., Eisle, C. J., Erle, D. J. & Locksley, R. M. 2010. Systemically dispersed innate IL-13-expressing cells in type 2 immunity. *Proc Natl Acad Sci U S A*, 107, 11489-94.
- Pua, H. H., Steiner, D. F., Patel, S., Gonzalez, J. R., Ortiz-Carpena, J. F., Kageyama, R., Chiou, N. T., Gallman, A., De Kouchkovsky, D., Jeker, L. T., Mcmanus, M. T., Erle, D. J. & Ansel, K. M. 2016. MicroRNAs 24 and 27 Suppress Allergic Inflammation and Target a Network of Regulators of T Helper 2 Cell-Associated Cytokine Production. *Immunity*, 44, 821-32.
- Pullan, R. L., Smith, J. L., Jasrasaria, R. & Brooker, S. J. 2014. Global numbers of infection and disease burden of soil transmitted helminth infections in 2010. *Parasit Vectors*, 7, 37.
- Quirion, M. R., Gregory, G. D., Umetsu, S. E., Winandy, S. & Brown, M. A. 2009. Cutting edge: Ikaros is a regulator of Th2 cell differentiation. *J Immunol*, 182, 741-5.
- Raabe, B. M., Artwohl, J. E., Purcell, J. E., Lovaglio, J. & Fortman, J. D. 2011. Effects of weekly blood collection in C57BL/6 mice. *J Am Assoc Lab Anim Sci*, 50, 680-5.
- Rahimi, R. A., Nepal, K., Cetinbas, M., Sadreyev, R. I. & Luster, A. D. 2020. Distinct functions of tissue-resident and circulating memory Th2 cells in allergic airway disease. *J Exp Med*, 217.
- Rajput, C., Cui, T., Han, M., Lei, J., Hinde, J. L., Wu, Q., Bentley, J. K. & Hershenson, M. B. 2017. RORalpha-dependent type 2 innate lymphoid cells are required and

- sufficient for mucous metaplasia in immature mice. *Am J Physiol Lung Cell Mol Physiol*, 312, L983-1993.
- Ramasamy, A., Kuokkanen, M., Vedantam, S., Gajdos, Z. K., Couto Alves, A., Lyon, H. N., Ferreira, M. A., Strachan, D. P., Zhao, J. H., Abramson, M. J., Brown, M. A., Coin, L., Dharmage, S. C., Duffy, D. L., Haahtela, T., Heath, A. C., Janson, C., Kahonen, M., Khaw, K. T., Laitinen, J., Le Souef, P., Lehtimaki, T., Madden, P. A., Marks, G. B., Martin, N. G., Matheson, M. C., Palmer, C. D., Palotie, A., Pouta, A., Robertson, C. F., Viikari, J., Widen, E., Wjst, M., Jarvis, D. L., Montgomery, G. W., Thompson, P. J., Wareham, N., Eriksson, J., Jousilahti, P., Laitinen, T., Pekkanen, J., Raitakari, O. T., O'connor, G. T., Salomaa, V., Jarvelin, M. R. & Hirschhorn, J. N. 2012. Genome-wide association studies of asthma in population-based cohorts confirm known and suggested loci and identify an additional association near HLA. *PLoS One*, 7, e44008.
- Reece, J. J., Siracusa, M. C., Southard, T. L., Brayton, C. F., Urban, J. F., Jr. & Scott, A. L. 2008. Hookworm-induced persistent changes to the immunological environment of the lung. *Infect Immun*, 76, 3511-24.
- Roberts, J., Fallon, P. & Hams, E. 2019. The pivotal role of macrophages in metabolic distress. In: BHAT, D. K. H. (ed.) *MACROPHAGE AT THE CROSSROADS OF INNATE AND ADAPTIVE IMMUNITY*. IntechOpen.
- Romera-Hernandez, M., Matha, L., Steer, C. A., Ghaedi, M. & Takei, F. 2019. Identification of Group 2 Innate Lymphoid Cells in Mouse Lung, Liver, Small Intestine, Bone Marrow, and Mediastinal and Mesenteric Lymph Nodes. *Curr Protoc Immunol*, 125, e73.
- Rosales, C. 2018. Neutrophil: A Cell with Many Roles in Inflammation or Several Cell Types? *Front Physiol*, 9, 113.
- Rose, H., Rinaldi, L., Bosco, A., Mavrot, F., De Waal, T., Skuce, P., Charlier, J., Torgerson, P. R., Hertzberg, H., Hendrickx, G., Vercruyse, J. & Morgan, E. R. 2015. Widespread anthelmintic resistance in European farmed ruminants: a systematic review. *Vet Rec*, 176, 546.
- Rosenberg, H. F., Dyer, K. D. & Foster, P. S. 2013. Eosinophils: changing perspectives in health and disease. *Nat Rev Immunol*, 13, 9-22.
- Saenz, S. A., Siracusa, M. C., Perrigoue, J. G., Spencer, S. P., Urban, J. F., Jr., Tocker, J. E., Budelsky, A. L., Kleinschek, M. A., Kastelein, R. A., Kambayashi, T.,

- Bhandoola, A. & Artis, D. 2010. IL25 elicits a multipotent progenitor cell population that promotes T(H)2 cytokine responses. *Nature*, 464, 1362-6.
- Salimi, M., Barlow, J. L., Saunders, S. P., Xue, L., Gutowska-Owsiak, D., Wang, X., Huang, L. C., Johnson, D., Scanlon, S. T., Mckenzie, A. N., Fallon, P. G. & Ogg, G. S. 2013. A role for IL-25 and IL-33-driven type-2 innate lymphoid cells in atopic dermatitis. *J Exp Med*, 210, 2939-50.
- Sarachana, T. & Hu, V. W. 2013. Genome-wide identification of transcriptional targets of RORA reveals direct regulation of multiple genes associated with autism spectrum disorder. *Mol Autism*, 4, 14.
- Sarachana, T., Xu, M., Wu, R. C. & Hu, V. W. 2011. Sex hormones in autism: androgens and estrogens differentially and reciprocally regulate RORA, a novel candidate gene for autism. *PLoS One*, 6, e17116.
- Sato, T. K., Panda, S., Miraglia, L. J., Reyes, T. M., Rudic, R. D., Mcnamara, P., Naik, K. A., Fitzgerald, G. A., Kay, S. A. & Hogenesch, J. B. 2004. A functional genomics strategy reveals Rora as a component of the mammalian circadian clock. *Neuron*, 43, 527-37.
- Sauer, B. 1998. Inducible gene targeting in mice using the Cre/lox system. *Methods*, 14, 381-92.
- Sawada, S., Scarborough, J. D., Killeen, N. & Littman, D. R. 1994. A lineage-specific transcriptional silencer regulates CD4 gene expression during T lymphocyte development. *Cell*, 77, 917-29.
- Sayad, A., Noroozi, R., Omrani, M. D., Taheri, M. & Ghafouri-Fard, S. 2017. Retinoic acid-related orphan receptor alpha (RORA) variants are associated with autism spectrum disorder. *Metab Brain Dis*, 32, 1595-1601.
- Schiering, C., Krausgruber, T., Chomka, A., Frohlich, A., Adelman, K., Wohlfert, E. A., Pott, J., Griseri, T., Bollrath, J., Hegazy, A. N., Harrison, O. J., Owens, B. M. J., Lohning, M., Belkaid, Y., Fallon, P. G. & Powrie, F. 2014. The alarmin IL-33 promotes regulatory T-cell function in the intestine. *Nature*, 513, 564-568.
- Schlenner, S. M., Madan, V., Busch, K., Tietz, A., Laufle, C., Costa, C., Blum, C., Fehling, H. J. & Rodewald, H. R. 2010. Fate mapping reveals separate origins of T cells and myeloid lineages in the thymus. *Immunity*, 32, 426-36.
- Schmidt, S., Hoving, J. C., Horsnell, W. G., Mearns, H., Cutler, A. J., Brombacher, T. M. & Brombacher, F. 2012. Nippostrongylus-induced intestinal

- hypercontractility requires IL-4 receptor alpha-responsiveness by T cells in mice. *PLoS One*, 7, e52211.
- Schoenberger, S. P. 2012. CD69 guides CD4+ T cells to the seat of memory. *Proc Natl Acad Sci U S A*, 109, 8358-9.
- Schwartz, C., Eberle, J. U. & Voehringer, D. 2016. Basophils in inflammation. *Eur J Pharmacol*, 778, 90-5.
- Schwartz, C., Hams, E. & Fallon, P. G. 2018. Helminth Modulation of Lung Inflammation. *Trends Parasitol.*
- Schwartz, C., Khan, A. R., Floudas, A., Saunders, S. P., Hams, E., Rodewald, H. R., Mckenzie, A. N. J. & Fallon, P. G. 2017. ILC2s regulate adaptive Th2 cell functions via PD-L1 checkpoint control. *J Exp Med*, 214, 2507-2521.
- Schwartz, C., Turqueti-Neves, A., Hartmann, S., Yu, P., Nimmerjahn, F. & Voehringer, D. 2014. Basophil-mediated protection against gastrointestinal helminths requires IgE-induced cytokine secretion. *Proc Natl Acad Sci U S A*, 111, E5169-77.
- Sckisel, G. D., Mirsoian, A., Minnar, C. M., Crittenden, M., Curti, B., Chen, J. Q., Blazar, B. R., Borowsky, A. D., Monjazebe, A. M. & Murphy, W. J. 2017. Differential phenotypes of memory CD4 and CD8 T cells in the spleen and peripheral tissues following immunostimulatory therapy. *J Immunother Cancer*, 5, 33.
- Seita, J. & Weissman, I. L. 2010. Hematopoietic stem cell: self-renewal versus differentiation. *Wiley Interdiscip Rev Syst Biol Med*, 2, 640-53.
- Sharpe, C., Thornton, D. J. & Grencis, R. K. 2018. A sticky end for gastrointestinal helminths; the role of the mucus barrier. *Parasite Immunol*, 40, e12517.
- Shen, F. W., Saga, Y., Litman, G., Freeman, G., Tung, J. S., Cantor, H. & Boyse, E. A. 1985. Cloning of Ly-5 cDNA. *Proc Natl Acad Sci U S A*, 82, 7360-3.
- Shih, H. Y., Sciume, G., Mikami, Y., Guo, L., Sun, H. W., Brooks, S. R., Urban, J. F., Jr., Davis, F. P., Kanno, Y. & O'shea, J. J. 2016. Developmental Acquisition of Regulomes Underlies Innate Lymphoid Cell Functionality. *Cell*, 165, 1120-1133.
- Sidman, R. L., Lane, P. W. & Dickie, M. M. 1962. Staggerer, a new mutation in the mouse affecting the cerebellum. *Science*, 137, 610-2.
- Sieweke, M. H. & Allen, J. E. 2013. Beyond stem cells: self-renewal of differentiated macrophages. *Science*, 342, 1242974.

- Simpson, L. J., Patel, S., Bhakta, N. R., Choy, D. F., Brightbill, H. D., Ren, X., Wang, Y., Pua, H. H., Baumjohann, D., Montoya, M. M., Panduro, M., Remedios, K. A., Huang, X., Fahy, J. V., Arron, J. R., Woodruff, P. G. & Ansel, K. M. 2014. A microRNA upregulated in asthma airway T cells promotes TH2 cytokine production. *Nat Immunol*, 15, 1162-70.
- Slominski, A. T., Kim, T. K., Hobrath, J. V., Oak, A. S. W., Tang, E. K. Y., Tieu, E. W., Li, W., Tuckey, R. C. & Jetten, A. M. 2017. Endogenously produced nonclassical vitamin D hydroxy-metabolites act as "biased" agonists on VDR and inverse agonists on RORalpha and RORgamma. *J Steroid Biochem Mol Biol*, 173, 42-56.
- Slominski, A. T., Kim, T. K., Takeda, Y., Janjetovic, Z., Brozyna, A. A., Skobowiat, C., Wang, J., Postlethwaite, A., Li, W., Tuckey, R. C. & Jetten, A. M. 2014. RORalpha and ROR gamma are expressed in human skin and serve as receptors for endogenously produced noncalcemic 20-hydroxy- and 20,23-dihydroxyvitamin D. *Faseb j*, 28, 2775-89.
- Solt, L. A. & Burris, T. P. 2012. Action of RORs and their ligands in (patho)physiology. *Trends Endocrinol Metab*, 23, 619-27.
- Spits, H., Artis, D., Colonna, M., Diefenbach, A., Di Santo, J. P., Eberl, G., Koyasu, S., Locksley, R. M., McKenzie, A. N., Mebius, R. E., Powrie, F. & Vivier, E. 2013. Innate lymphoid cells--a proposal for uniform nomenclature. *Nat Rev Immunol*, 13, 145-9.
- Srinivas, S., Watanabe, T., Lin, C. S., Williams, C. M., Tanabe, Y., Jessell, T. M. & Costantini, F. 2001. Cre reporter strains produced by targeted insertion of EYFP and ECFP into the ROSA26 locus. *BMC Dev Biol*, 1, 4.
- Stapleton, C. M., Jaradat, M., Dixon, D., Kang, H. S., Kim, S. C., Liao, G., Carey, M. A., Cristiano, J., Moorman, M. P. & Jetten, A. M. 2005. Enhanced susceptibility of staggerer (RORalpha^{sg}) mice to lipopolysaccharide-induced lung inflammation. *Am J Physiol Lung Cell Mol Physiol*, 289, L144-52.
- Steinbach, K. H., Schick, P., Trepel, F., Raffler, H., Dohrmann, J., Heilgeist, G., Heltzel, W., Li, K., Past, W., Van Der Woerd-De Lange, J. A., Theml, H., Fliedner, T. M. & Begemann, H. 1979. Estimation of kinetic parameters of neutrophilic, eosinophilic, and basophilic granulocytes in human blood. *Blut*, 39, 27-38.

- Steinmayr, M., Andre, E., Conquet, F., Rondi-Reig, L., Delhay-Bouchaud, N., Auclair, N., Daniel, H., Crepel, F., Mariani, J., Sotelo, C. & Becker-Andre, M. 1998. staggerer phenotype in retinoid-related orphan receptor alpha-deficient mice. *Proc Natl Acad Sci U S A*, 95, 3960-5.
- Stritesky, G. L., Muthukrishnan, R., Sehra, S., Goswami, R., Pham, D., Travers, J., Nguyen, E. T., Levy, D. E. & Kaplan, M. H. 2011. The transcription factor STAT3 is required for T helper 2 cell development. *Immunity*, 34, 39-49.
- Su, J., Su, B., Xia, H., Liu, F., Zhao, X., Li, J., Zhang, J., Shi, Y., Zeng, Y., Zeng, X., Ling, H., Wu, Y. & Su, Q. 2019. RORalpha Suppresses Epithelial-to-Mesenchymal Transition and Invasion in Human Gastric Cancer Cells via the Wnt/beta-Catenin Pathway. *Front Oncol*, 9, 1344.
- Summers, C., Rankin, S. M., Condliffe, A. M., Singh, N., Peters, A. M. & Chilvers, E. R. 2010. Neutrophil kinetics in health and disease. *Trends Immunol*, 31, 318-24.
- Sun, Y., Liu, C. H., Sangiovanni, J. P., Evans, L. P., Tian, K. T., Zhang, B., Stahl, A., Pu, W. T., Kamenecka, T. M., Solt, L. A. & Chen, J. 2015. Nuclear receptor RORalpha regulates pathologic retinal angiogenesis by modulating SOCS3-dependent inflammation. *Proc Natl Acad Sci U S A*, 112, 10401-6.
- Sutherland, T. E., Logan, N., Ruckerl, D., Humbles, A. A., Allan, S. M., Papayannopoulos, V., Stockinger, B., Maizels, R. M. & Allen, J. E. 2014. Chitinase-like proteins promote IL-17-mediated neutrophilia in a tradeoff between nematode killing and host damage. *Nat Immunol*, 15, 1116-25.
- Thawer, S. G., Horsnell, W. G., Darby, M., Hoving, J. C., Dewals, B., Cutler, A. J., Lang, D. & Brombacher, F. 2014. Lung-resident CD4(+) T cells are sufficient for IL-4Ralpha-dependent recall immunity to *Nippostrongylus brasiliensis* infection. *Mucosal Immunol*, 7, 239-48.
- Townsend, J. M., Fallon, G. P., Matthews, J. D., Smith, P., Jolin, E. H. & McKenzie, N. A. 2000. IL-9-deficient mice establish fundamental roles for IL-9 in pulmonary mastocytosis and goblet cell hyperplasia but not T cell development. *Immunity*, 13, 573-83.
- Trenkner, E. & Hoffmann, M. K. 1986. Defective development of the thymus and immunological abnormalities in the neurological mouse mutation "staggerer". *J Neurosci*, 6, 1733-7.

- Trifari, S., Kaplan, C. D., Tran, E. H., Crellin, N. K. & Spits, H. 2009. Identification of a human helper T cell population that has abundant production of interleukin 22 and is distinct from T(H)-17, T(H)1 and T(H)2 cells. *Nat Immunol*, 10, 864-71.
- Truong, T., Liquet, B., Menegaux, F., Plancoulaine, S., Laurent-Puig, P., Mulot, C., Cordina-Duverger, E., Sanchez, M., Arveux, P., Kerbrat, P., Richardson, S. & Guenel, P. 2014. Breast cancer risk, nightwork, and circadian clock gene polymorphisms. *Endocr Relat Cancer*, 21, 629-38.
- Tumes, D. J., Onodera, A., Suzuki, A., Shinoda, K., Endo, Y., Iwamura, C., Hosokawa, H., Koseki, H., Tokoyoda, K., Suzuki, Y., Motohashi, S. & Nakayama, T. 2013. The polycomb protein Ezh2 regulates differentiation and plasticity of CD4(+) T helper type 1 and type 2 cells. *Immunity*, 39, 819-32.
- Van Dyken, S. J., Nussbaum, J. C., Lee, J., Molofsky, A. B., Liang, H. E., Pollack, J. L., Gate, R. E., Haliburton, G. E., Ye, C. J., Marson, A., Erle, D. J. & Locksley, R. M. 2016. A tissue checkpoint regulates type 2 immunity. *Nat Immunol*, 17, 1381-1387.
- Vieira Braga, F. A., Kar, G., Berg, M., Carpaij, O. A., Polanski, K., Simon, L. M., Brouwer, S., Gomes, T., Hesse, L., Jiang, J., Fasouli, E. S., Efremova, M., Vento-Tormo, R., Talavera-Lopez, C., Jonker, M. R., Affleck, K., Palit, S., Strzelecka, P. M., Firth, H. V., Mahbubani, K. T., Cvejic, A., Meyer, K. B., Saeb-Parsy, K., Luinge, M., Brandsma, C. A., Timens, W., Angelidis, I., Strunz, M., Koppelman, G. H., Van Oosterhout, A. J., Schiller, H. B., Theis, F. J., Van Den Berge, M., Nawijn, M. C. & Teichmann, S. A. 2019. A cellular census of human lungs identifies novel cell states in health and in asthma. *Nat Med*, 25, 1153-1163.
- Voehringer, D., Reese, T. A., Huang, X., Shinkai, K. & Locksley, R. M. 2006. Type 2 immunity is controlled by IL-4/IL-13 expression in hematopoietic non-eosinophil cells of the innate immune system. *J Exp Med*, 203, 1435-46.
- Voehringer, D., Shinkai, K. & Locksley, R. M. 2004. Type 2 immunity reflects orchestrated recruitment of cells committed to IL-4 production. *Immunity*, 20, 267-77.
- Vu-Dac, N., Gervois, P., Grotzinger, T., De Vos, P., Schoonjans, K., Fruchart, J. C., Auwerx, J., Mariani, J., Tedgui, A. & Staels, B. 1997. Transcriptional regulation of apolipoprotein A-I gene expression by the nuclear receptor RORalpha. *J Biol Chem*, 272, 22401-4.

- Walker, J. A., Barlow, J. L. & McKenzie, A. N. 2013. Innate lymphoid cells--how did we miss them? *Nat Rev Immunol*, 13, 75-87.
- Walker, J. A., Clark, P. A., Crisp, A., Barlow, J. L., Szeto, A., Ferreira, A. C. F., Rana, B. M. J., Jolin, H. E., Rodriguez-Rodriguez, N., Sivasubramaniam, M., Pannell, R., Cruickshank, J., Daly, M., Haim-Vilmovsky, L., Teichmann, S. A. & McKenzie, A. N. J. 2019. Polychromic Reporter Mice Reveal Unappreciated Innate Lymphoid Cell Progenitor Heterogeneity and Elusive ILC3 Progenitors in Bone Marrow. *Immunity*, 51, 104-118.e7.
- Walker, J. A. & McKenzie, A. N. J. 2018. TH2 cell development and function. *Nat Rev Immunol*, 18, 121-133.
- Walker, J. A., Oliphant, C. J., Englezakis, A., Yu, Y., Clare, S., Rodewald, H. R., Belz, G., Liu, P., Fallon, P. G. & McKenzie, A. N. 2015. Bcl11b is essential for group 2 innate lymphoid cell development. *J Exp Med*, 212, 875-82.
- Wang, N. S., Mcheyzer-Williams, L. J., Okitsu, S. L., Burris, T. P., Reiner, S. L. & Mcheyzer-Williams, M. G. 2012. Divergent transcriptional programming of class-specific B cell memory by T-bet and ROR α . *Nat Immunol*, 13, 604-11.
- Wang, Y., Kumar, N., Crumbley, C., Griffin, P. R. & Burris, T. P. 2010a. A second class of nuclear receptors for oxysterols: Regulation of ROR α and ROR γ activity by 24S-hydroxycholesterol (cerebrosterol). *Biochim Biophys Acta*, 1801, 917-23.
- Wang, Y., Kumar, N., Solt, L. A., Richardson, T. I., Helvering, L. M., Crumbley, C., Garcia-Ordenez, R. D., Stayrook, K. R., Zhang, X., Novick, S., Chalmers, M. J., Griffin, P. R. & Burris, T. P. 2010b. Modulation of retinoic acid receptor-related orphan receptor alpha and gamma activity by 7-oxygenated sterol ligands. *J Biol Chem*, 285, 5013-25.
- Weger, M., Diotel, N., Dorsemans, A. C., Dickmeis, T. & Weger, B. D. 2017. Stem cells and the circadian clock. *Dev Biol*, 431, 111-123.
- Who 2020. Fact sheet: Soil-transmitted helminth infections. <https://www.who.int/news-room/fact-sheets/detail/soil-transmitted-helminth-infections>: World Health Organisation.
- Wohlfert, E. A., Grainger, J. R., Bouladoux, N., Konkel, J. E., Oldenhove, G., Ribeiro, C. H., Hall, J. A., Yagi, R., Naik, S., Bhairavabhotla, R., Paul, W. E., Bosselut, R., Wei, G., Zhao, K., Oukka, M., Zhu, J. & Belkaid, Y. 2011. GATA3 controls

- Foxp3⁺ regulatory T cell fate during inflammation in mice. *J Clin Invest*, 121, 4503-15.
- Wong, S. H., Walker, J. A., Jolin, H. E., Drynan, L. F., Hams, E., Camelo, A., Barlow, J. L., Neill, D. R., Panova, V., Koch, U., Radtke, F., Hardman, C. S., Hwang, Y. Y., Fallon, P. G. & McKenzie, A. N. 2012. Transcription factor RORalpha is critical for nuocyte development. *Nat Immunol*, 13, 229-36.
- Wu, C. S., Zhu, J., Wager-Miller, J., Wang, S., O'leary, D., Monory, K., Lutz, B., Mackie, K. & Lu, H. C. 2010. Requirement of cannabinoid CB(1) receptors in cortical pyramidal neurons for appropriate development of corticothalamic and thalamocortical projections. *Eur J Neurosci*, 32, 693-706.
- Wu, K., Wang, X., Keeler, S. P., Gerovac, B. J., Agapov, E. V., Byers, D. E., Gilfillan, S., Colonna, M., Zhang, Y. & Holtzman, M. J. 2020. Group 2 Innate Lymphoid Cells Must Partner with the Myeloid-Macrophage Lineage for Long-Term Postviral Lung Disease. *J Immunol*, 205, 1084-1101.
- Xiong, G., Wang, C., Evers, B. M., Zhou, B. P. & Xu, R. 2012. RORalpha suppresses breast tumor invasion by inducing SEMA3F expression. *Cancer Res*, 72, 1728-39.
- Yagi, R., Zhong, C., Northrup, D. L., Yu, F., Bouladoux, N., Spencer, S., Hu, G., Barron, L., Sharma, S., Nakayama, T., Belkaid, Y., Zhao, K. & Zhu, J. 2014. The transcription factor GATA3 is critical for the development of all IL-7Ralpha-expressing innate lymphoid cells. *Immunity*, 40, 378-88.
- Yang, X. O., Pappu, B. P., Nurieva, R., Akimzhanov, A., Kang, H. S., Chung, Y., Ma, L., Shah, B., Panopoulos, A. D., Schluns, K. S., Watowich, S. S., Tian, Q., Jetten, A. M. & Dong, C. 2008. T helper 17 lineage differentiation is programmed by orphan nuclear receptors ROR alpha and ROR gamma. *Immunity*, 28, 29-39.
- Yasuda, K., Muto, T., Kawagoe, T., Matsumoto, M., Sasaki, Y., Matsushita, K., Taki, Y., Futatsugi-Yumikura, S., Tsutsui, H., Ishii, K. J., Yoshimoto, T., Akira, S. & Nakanishi, K. 2012. Contribution of IL-33-activated type II innate lymphoid cells to pulmonary eosinophilia in intestinal nematode-infected mice. *Proc Natl Acad Sci U S A*, 109, 3451-6.
- Yazdanbakhsh, M. & Matricardi, P. M. 2004. Parasites and the hygiene hypothesis: regulating the immune system? *Clin Rev Allergy Immunol*, 26, 15-24.

- Yona, S., Kim, K. W., Wolf, Y., Mildner, A., Varol, D., Breker, M., Strauss-Ayali, D., Viukov, S., Guilliams, M., Misharin, A., Hume, D. A., Perlman, H., Malissen, B., Zelzer, E. & Jung, S. 2013. Fate mapping reveals origins and dynamics of monocytes and tissue macrophages under homeostasis. *Immunity*, 38, 79-91.
- Yu, F., Sharma, S., Edwards, J., Feigenbaum, L. & Zhu, J. 2015a. Dynamic expression of transcription factors T-bet and GATA-3 by regulatory T cells maintains immunotolerance. *Nat Immunol*, 16, 197-206.
- Yu, Y., Wang, C., Clare, S., Wang, J., Lee, S. C., Brandt, C., Burke, S., Lu, L., He, D., Jenkins, N. A., Copeland, N. G., Dougan, G. & Liu, P. 2015b. The transcription factor Bcl11b is specifically expressed in group 2 innate lymphoid cells and is essential for their development. *J Exp Med*, 212, 865-74.
- Zanjani, H. S., Mariani, J., Delhaye-Bouchaud, N. & Herrup, K. 1992. Neuronal cell loss in heterozygous staggerer mutant mice: a model for genetic contributions to the aging process. *Brain Res Dev Brain Res*, 67, 153-60.
- Zeng, B., Shi, S., Ashworth, G., Dong, C., Liu, J. & Xing, F. 2019. ILC3 function as a double-edged sword in inflammatory bowel diseases. *Cell Death Dis*, 10, 315.
- Zhang, Y., Luo, X. Y., Wu, D. H. & Xu, Y. 2015. ROR nuclear receptors: structures, related diseases, and drug discovery. *Acta Pharmacol Sin*, 36, 71-87.
- Zhang, Z., Burch, P. E., Cooney, A. J., Lanz, R. B., Pereira, F. A., Wu, J., Gibbs, R. A., Weinstock, G. & Wheeler, D. A. 2004. Genomic analysis of the nuclear receptor family: new insights into structure, regulation, and evolution from the rat genome. *Genome Res*, 14, 580-90.
- Zhu, J. 2015. T helper 2 (Th2) cell differentiation, type 2 innate lymphoid cell (ILC2) development and regulation of interleukin-4 (IL-4) and IL-13 production. *Cytokine*, 75, 14-24.
- Zhu, J., Cote-Sierra, J., Guo, L. & Paul, W. E. 2003. Stat5 activation plays a critical role in Th2 differentiation. *Immunity*, 19, 739-48.
- Zhu, J., Yamane, H., Cote-Sierra, J., Guo, L. & Paul, W. E. 2006a. GATA-3 promotes Th2 responses through three different mechanisms: induction of Th2 cytokine production, selective growth of Th2 cells and inhibition of Th1 cell-specific factors. *Cell Res*, 16, 3-10.
- Zhu, Y., Mcavoy, S., Kuhn, R. & Smith, D. I. 2006b. RORA, a large common fragile site gene, is involved in cellular stress response. *Oncogene*, 25, 2901-8.